STEREOLOGY

Proceedings of the Second International Congress
for STEREOLOGY, Chicago—April 8-13, 1967

Edited by

HANS ELIAS

Department of Anatomy
Chicago Medical School

Sponsored by: The National Science Foundation
and the
International Society for Stereology

Title No. 1450

NEWLY ELECTED OFFICERS

OF THE

INTERNATIONAL SOCIETY FOR STEREOLOGY

President:

Ewald R. Weibel
Anatomisches Institut
Universität Bern
Bühlstrasse 26
3000 Bern, Switzerland

Vice President:

Ervin E. Underwood
Lockheed Georgia Company
Department 72-14, Zone 402
Marietta, Georgia, 30060

Treasurer:

(having also the functions of executive secretary)
Hellmut Fischmeister
Chalmers Technical University
Department of Engineering Materials
Gothenburg, Sweden

Secretary:

Arnold Lazarow
Department of Anatomy
University of Minnesota
Minneapolis, Minnesota

Assistant Secretary:

(with the function of Editor of STEREOLOGIA,
Bulletin of the International Society for Stereology)
John E. Hilliard
Northwestern University
Department of Materials Sciences
Evanston, Illinois

KEYNOTE SPEAKERS

Guenter Bach
Department of Mathematics
Institute of Technology
Braunchweig, Germany

Robert T. DeHoff
Department of Metallurgical and Materials Engineering
University of Florida
Gainesville, Florida, USA

Hellmut F. Fischmeister
Department of Metallurgy
Chalmers University of Technology
Goeteborg, Sweden

R. Buckminster Fuller
Department of Architecture
Southern Illinois University
Carbondale, Illinois, USA

Herbert Haug
Department of Anatomy
University of Hamburg
Hamburg, Germany

Erling S. Hegre
Department of Anatomy
Medical College of Virginia
Richmond, Virginia, USA

August Hennig
Department of Anatomy
University of Muenchen
Muenchen, Germany

(continued)

John E. Hilliard
Department of Materials Science
Northwestern University
Evanston, Illinois, USA

Clara S. Hires
Mistaire Laboratories
Millburn, New Jersey, USA

Wendell J. S. Krieg
Department of Anatomy
Northwestern University Medical College
Chicago, Illinois, USA

Frederick N. Rhines
Department of Metallurgical and Materials Engineering
University of Flordia
Gainesville, Flordia, USA

Sarkis A. Saltikov
Department of Metallurgy
Polytechnical Institute
Erevan, Armenia, USSR

Cyril S. Smith
Massachusetts Institute of Technology
Cambridge, Massachusetts, USA

Ervin E. Underwood
Lockheed Georgia Company
Marietta, Georgia, USA

Ewald R. Weibel
Department of Anatomy
University of Bern
Bern, Switzerland

PREFACE

The Second International Congress for Stereology, again, has brought together scientists from very diverse disciplines for discussion of problems concerning the recognition of three-dimensional structure, problems which confront those who study materials, rocks, biological systems or heavenly bodies. The program was organized into sessions each dealing with a special type of structural problem regardless of systems in the study of which these problems occur. Since all natural sciences have similar structural questions to investigate, discourses among biologists, metallurgists etc. were intense. Subject areas were not separated during the Congress. No concurrent sessions were held. Each participant had the opportunity to hear every paper. This resulted in an unusually high attendance. During the last session, after five and a half days of intense work almost half the participants were still present in the lecture hall.

Each of us was fascinated with what he was able to learn from fellow-stereologists who studied different sectors of nature. Friendships were established across oceans and across disciplinary boundaries.

Each session was introduced by a key-note lecture didactical, methodological and theoretical in nature. These key-note lectures can be recognized in this volume by their greater length, 12 pages being allotted to each key-note speaker. Collectively they constitute almost a textbook of stereology.

Contributed papers in each problem category deal with applications. One exception to this rule is the paper on curvature determination by Dr. DeHoff, whose concept, although fundamental in nature, had been developed so recently that it was administratively not possible to give it a key-note position.

It is hoped that the scientific community as a whole will derive benefit from this volume.

APOLOGY

The editor herewith apologizes and hopes that you will pardon him for mistakes of grammar, spelling and style. His excuses are the following: He was forced to put this symposium together in a very brief period of time; and he had no assistance except his very able typist, Mrs. Rebecca Collen, who helped with this work most efficiently. Because of pressure and time limits, he could read every manuscript only once. He expects that many mistakes, particularly in his own contributions, have escaped detection.

Further: All these manuscripts have been typed on different typewriters for which at our office no matching type-face is available. Therefore in many cases detected mistakes had to be left as they were. Only in very few cases was the typing done so poorly that the entire manuscript had to be re-typed completely.

The editor also wishes to thank Professor Hilliard for editing and re-writing Professor Saltikov's contributions. No change in content has occurred in this process, only linguistic matters were improved.

Finally the editor in the name of the officers of the International Society for Stereology expresses thanks to Springer Verlag for its willingness to undertake the production and publication of this volume. Springer-Verlag has just published the symposium "Quantitative Methods in Morphology" organized by the International Society for Stereology during the 8th International Congress of Anatomists in Wiesbaden. This is a beautifully printed and bound volume done in letter press (typography). Its production was very time consuming and expensive. Therefore it has been decided to use a more economic method this time. But this method leads, of course, to deficiencies for which, again, we beg your pardon.

<div align="right">

Hans Elias
Chicago, Illinois
May 1967

</div>

LIST OF CONTRIBUTORS

ABRAHAMSON, DEAN E., Department of Anatomy, University of Minnesota, Minneapolis, Minnesota

ATKINSON, RALPH H., Department of Metallurgy, Stevens Institute of Technology, Hoboken, New Jersey

BACH, GUNTER, Technische Hochshule, Braunschweig, Germany

BARTLEY, M.H., Department of Anatomy, University of Utah, College of Medicine, Salt Lake City, Utah

BLÜMCKE, SIGURD, Institute of Pathology, Münster, West Germany

BOCKSTIEGEL, GERHARD, Höganäs AB, Hoganas, Sweden

BRIESE, FRANKLIN W., Biometry Division and Department of Anatomy, University of Minnesota, Minneapolis, Minnesota

CARPENTER, ANNA-MARY, Department of Anatomy, University of Minnesota Medical School, Minneapolis, Minnesota

COUDERC, HENRI, Laboratoire de Biologie Vegetale SPCN, Bt 490, Essone, France

DE HOFF, ROBERT, Department of Metallurgy, College of Engineering, University of Florida, Gainesville, Florida

DÖRFLER, GERHARD, Analytisches Institut der Universität Wein, Vienna, Austria

EBBESSON, SVEN O.E., Laboratory of Perinatal Physiology, NINDB, Puerta de Tierra, Puerto Rico

EICHNER, DIETRICH, Department of Anatomy, University of Münster

ELIAS, HANS, Department of Anatomy, University of Chicago Medical School, Chicago, Illinois

FISCHER, WOLFGANG, Frauenklinik, Universitaet Hamburg, Hamburg, Germany

FISCHMEISTER, HELMUTT, Department of Metallurgy, Chalmers University of Technology, Goteborg S., Sweden

FISHER, COLIN, Metals Research Limited, Cam-
   bridge, England

FLINN, J.E., Argonne National Laboratory, Ar-
   gonne, Illinois

FULLER, R. BUCKMINSTER, Carbondale, Illinois

GANDER, R.H., Wild-Heerbrugg, Heerbrugg, Switz-
   erland

GIGER, HANS, University of Bern, Bern, Switzer-
   land

GORENFLOT, ROBERT, Laboratoire de Biologie Veg-
   etale Bt 490, Essone, France

GURLAND, JOSEPH, School of Engineering, Brown
   University, Providence, Rhode Island

HAUG, HERBERT, Anatomisches Institut der Univ-
   ersitaet Hamburg, Hamburg, Germany

HEGRE, ERLING S., Department of Anatomy, Med-
   ical College of Virginia, Richmond, Virginia

HENNIG, AUGUST, Anatomisches Institut der Univ-
   ersität München, München, Germany

HILLIARD, JOHN E., Department of Materials Sci-
   ences, Institute of Technology, Northwestern
   University, Evanston, Illinois

HIRES, CLARA S., Milstaire Laboratories, Mill-
   burn, New Jersey

JANKE, HELMUT, Universität Göttingen, Göttingen,
   Germany

JEE, W.S.S., Department of Anatomy, University
   of Utah, College of Medicine, Salt Lake City,
   Utah

KOLODNY, STEVEN, Department of Anatomy, Chicago
   Medical School, Chicago, Illinois

KRIEG, WENDELL, Northwestern University, Med-
   ical School, Chicago, Illinois

KRONSBEIN, J., Department of Metallurgy, Univ-
   ersity of Florida, Gainesville, Florida

LAZAROW, ARNOLD, Department of Anatomy, Univer-
   sity of Minnesota, Minneapolis, Minnesota

LEYDOLPH, WALTER K., Institute for Bio-Photo-
   grammetry, Göttingen, Germany

LOUD, ALDEN V., Department of Pathology, Colum-
   bia University, New York, New York

MARTINO, LUIGI, Instituto di Anatomia Umana Nor-
  male della Universita, Bari, Italy

MERCKX, KENNETH R., Battelle Northwest, Richland,
  Washington

MILLHOUSE, EDWARD W., Chicago Medical School,
  Chicago, Illinois

MILLS, ROY, Department of Biological Sciences,
  Lilly Hall of Life Sciences, Purdue Univer-
  sity, Lafayette, Indiana

deMONTEBELLO, ROGER L., RLM Research Corporation,
  Yonkers, New York

MOORE, GEORGE A., National Bureau of Standards,
  Washington, D.C.

MORGENROTH, KONRAD M., Institute of Pathology,
  Muenster, West Germany

MÜLLER, GERHARD A., Department of Anatomy, Univ-
  ersity of Mainz, Mainz, Germany

MYERS, EDWARD J., Air Force Institute of Tech-
  nology, Wright-Patterson Air Force Base, Ohio

NICHOLSON, WESLEY L., Battelle Northwest, Rich-
  land, Washington

OHTA, YOSHIKUNI, Department of Anatomy, Osaka
  Dental College, Osaka, Japan

OSBORN, J.W., Department of Anatomy Guy's Hos-
  pital Medical School, London Bridge, England

PEDLER, C.M.H., Department of Anatomy, Institute
  of Opthalmology, London, England

PHILOFSKY, E.M., Department of Materials Science,
  Northwestern University, Evanston, Illinois

POSTLETHWAIT, SAMUEL N., Department of Biologi-
  cal Sciences, Lilly Hall of Life Sciences,
  Purdue University, Lafayette, Indiana

PYSH, JOSEPH J., Department of Anatomy, North-
  western University, Medical School, Chicago,
  Illinois

RHINES, FREDERICK N., Department of Metallurgy,
  College of Engineering, University of Florida,
  Gainesville, Florida

ROSENOW, ULF F., Radiation Department, Univer-
  sitäts Frauenklinik, Göttingen, Germany

ROSSI, FRANCO, Engis Equipment Company, Morton
  Grove, Illinois

SALTIKOV, SARKIS A., Erevan, Armenia, USSR

SCHWARTZ, DAVID, Department of Anatomy, Chicago
    Medical School, Chicago, Illinois

SEAMANS, S., Department of Anatomy, University
    of Utah, College of Medicine, Salt Lake City,
    Utah

SMITH, CYRIL S., Massachusetts Institute of
    Technology, Cambridge, Massachusetts

STEELE, J.H., Department of Metallurgy, Univer-
    sity of Florida, Gainesville, Florida

TARGONSKI, S., Jarrel-Ash Company, Waltham, Mas-
    sachusetts

TANG, DOUGLAS B., Walter Reed Army Institute
    of Research, Washington, D.C.

TILLY, R., Department of Anatomy, Institute of
    Opthalmology, London, England

UNDERWOOD, ERVIN E., Lockheed Georgia Company,
    Marietta, Georgia

WEIBEL, EWALD, Anatomisches Institut der Univ-
    ersitaet, Bern, Switzerland

WERNICKE, ECKART H., Frauenklinik, Universitaet
    Hamburg, Hamburg, Germany

WOLFF, JOACHIM R., Forschungsabteilung für Elek-
    tronenmikroskopie der Freien Universität,
    Berlin, Germany

TABLE OF CONTENTS

STEREOSCOPY, PHOTOGRAMMETRY

AFTER DINNER TALK

SIZE DETERMINATION

INTRODUCTION:
PROBLEMS OF STEREOLOGY

HANS ELIAS

Department of Anatomy, Chicago Medical School, Chicago, Illinois

Stereology is three-dimensional interpretation of flat images or ex-
trapolation from two to three-dimensional space.

Such extrapolation is often necessary because many materials or or-
ganisms which we study are opaque or complex in their internal struc-
ture. The best method by which the composition of such objects can
be studied without distortion or rearrangement of parts is sectioning.
If the object is entirely opaque such as a metal, a section through it
after it is polished is a true mathematical plane. Biological and geo-
logical objects are translucent to various degrees; and "sections"
through them are, as a rule, slices of finite thickness. In both cases,
the image to be analysed results from uniaxial viewing and therefore
is, in essence, two-dimensional.

Heavenly objects present themselves as projections on the inner sur-
face of a sphere circumscribed around the observer, and, in practice,
are studied on two-dimensional photographs.

In all these cases the structures about whose three dimensional pro-
perties we desire to gain information are inaccessible to direct man-
ipulation, inspection or measurement.

It is the function of stereology to analyse these two dimensional im-
ages and to draw from them conclusions concerning the properties of
the structures in space. The chief methods of stereology are statistico-
geometrical; and they are applicable to the analysis of structures of
similar shape numerously present in a specimen. In order to be tract-
able by mathematical stereology the structures under investigation
should be randomly arranged in space; or it should be possible to
create random distribution by proper methods of sampling.

When only a single specimen of a structure is present or when this
structure is complicated in shape mathematical methods will no long-
er be applicable. Reconstruction from serial sections and serial sec-
tion cinematography will be preferred methods in such cases.

1

The basic problems and concepts of stereology shall now be enume-
rated. Their sequence in this introduction is not the same as the
sequence of their presentation during the Congress. But in the main
body of the volume all papers are printed in their original succession
so that the readers can gain an insight into the actual organization
of the Congress.

Before beginning to enumerate the basic problems of stereology, the
editor wishes to apologize for the fact that he must select examples
from the realm of his personal experience, that is from microscopic
anatomy and from a field in which he is but an amateur, namely
astronomy. Readers from other disciplines will be able to find ex-
amples from their own fields of endeavor.

Stereology as a formal science is very young; so is the word "stereo-
logy"; but it has been practiced by a few investigators in isolation
for more than a century. The following brief history of the Inter-
national Society for Stereology is reprinted from the Congress Pro-
gram.

By a chance meeting on a pleasure boat sailing around Manhattan
Island, one American and one European who were attending the
International Congress of Anatomists in New York, 1960, discovered,
during their conversation, that both were using statistico-geometrical
methods to obtain information on three-dimensional structure from
sections. They decided to call a gathering of persons interested in
three-dimensional interpretation of flat images. An announcement
in a few journals brought 11 scientists together on the Feldberg
Mountain in the Black Forest 11-12 May, 1961. The word stereology
was then coined and the International Society for Stereology was
founded and incorporated as a non-profit organization in Neustadt,
Schwarzwald.

The Society was subsequently incorporated as a non-profit organiza-
tion in Stuttgart, 1962; Vienna, 1963; and Deerfield, Illinois, 1964.

1. SHAPE AND NUMBER

Shape, often contemptuously considered a merely qualitative property and hence not worthy of a scientist's attention, may be of great functional importance. Let us think of the difference between a fiber and a membrane. Let the fiber be represented by a rope attached to the ceiling and to the floor of a room. You can walk around it and hold on to it for support. The membrane may be represented by a sheet attached to ceiling, walls and floor of a room. This sheet can divide the room into two parts, fully separated from one another, while the rope cannot divide it. In certain "sections", a fiber may not be distinguishable from the trace of a membrane.

In a single section, a follicle (closed bag) may not be distinguishable from an alveolus (hollow ball open on one side) or from a tubule. Yet these three shapes are functionally very different from each other: A follicle is closed on all sides. Only by diffusuion or active transport can substances pass from its interior to the outside. An alveolus, however, opens into a duct; and its contents can flow away freely. A tubule, also open, offers its lining epithelium (wall made of cells) an opportunity to act upon the content while the content slowly streams from the dead end to the opening.

Thus we see that shape is physiologically as important as size and number.

Also in certain materials, the shape of particles contained in them has great bearing on their strength. Bone would be brittle did it not contain long fibers of organic material which add toughness to hardness. Or let us consider plaster of Paris. If a plaster model is expected to be exposed to frequent impacts, jute or hemp fibers are often mixed into the plaster. It is chiefly the shape of these fibers, i.e. the great ratio of length to thickness which imparts strength to the material in both cases.

Stereology offers means for the determination of the shape of particles, if only all particles are similar in shape. In nature, this condition is usually fulfilled. Any human organ must necessarily be composed of similar parts; for only parts which resemble each other can function harmoniously together.

In rocks, composed of different minerals, the particles are similar in size and shape because they all originated simultaneously under identical conditions. The same holds true for many artifical mixtures such as alloys.

When metal tubing is drawn, the grains within the wall of the tube are subjected to mechanical stresses which impart an anisodiametric shape to them. And this shape has, in turn, a bearing on the strength of the tube (see the paper by Philofsky and Flinn).

By classifying the profiles of the cut particles by their axial ratios

$$Q = \frac{L}{W} \quad (\text{Length} / \text{Width})$$

their shape can easily be determined (see Dr. August Hennig's keynote lecture).

If, in spite of what we just said about the importance of shape for physiological efficiency and for the strength of materials, a reader may still persist in not being interested in shape, I will point out that even if we were interested only in the number of particles per unit volume, it would still be necessary to determine the shape of the particles before their number can be determined.

For the generally used formula for N_V, i.e., the number of particles per unit volume, contains a number $\bar{D}$, which is the average diameter if the particles are spherical. But if the particles are anisodiametric, $\bar{D}$ is the "average caliper diameter" or the average distance between tangent planes, also known as altitude, a figure which can be calculated only after the range of particle shape is known. (pp 211-215!)

Determination of curvature of surfaces from random sections is a problem of shape. This has been attacked for the first time by Dr. DeHoff.

Solids having or approximating the shapes of ellipsoids, both rotatory (prolate and oblate) and tri-axial, are very common in nature. Among them are nuclei of various kinds of cells, the glomeruli (filtering units) of the kidney, certain extragalactic nebulae etc. Sections through them or projections of them are ellipses. If all the objects under investigations are of equal shape and randomly arranged in space, distribution curves for the axial ratios of these profiles can be given for any specific ellipsoid, disk or cylinder (see Dr. Hennig's key-note address).

In nature we seldom have identical shapes. But we have ranges of shapes.

The so called elliptical nebulae, for example, range in shape from spheres to prolate ellipsoids. An individual image of such a nebula can not yield information on its shape, except when the nebula is seen in exact profile (when the earth is located in its equatorial plane). But statistical analysis of the distribution of axial ratios of

4

projected images of hundreds of these objects has revealed the fact that they have the above mentioned range of shape. In this case, Hubble interpreted this range as indicating an evolutionary process, the spherical nebulae thought to be younger, the flat lenses thought to be older.

In the case of chondrocytes (cartilage cells) the reverse would seem to be true: flat, lenticular cells being young, spherical ones older.

In practice, one plots a curve from observed values; and one can assume a range of shapes to exist in space between the two standard curves which delimit the area in which the experimental points are scattered.

We have emphasized the problem of shape out of proportion to its prominence during the Congress simply because its importance is frequently overlooked.

2. VOLUME

Volumes and volume fractions are parameters most easily handled by the most primitive stereological method, namely by counting points of a grid superimposed upon the image. The ratio of the number of points which "hit" the various component phases in a specimen equals their volume ratio.

3. SIZE

The diameter of a sectional circle through a spherical particle depends on the distance of the cut from the center of the particle. If all particles were of the same size, the diameters of approximately 13% of sectional circles would be smaller than the radius of the spherical particles, about 87% would be larger. If one finds this size distribution in a section through a sample, equality of size of particles in space is assured, except that the "small" circles are in practice less numerous than 13%, because they may fall out of the slice or are too thin to be recognizable.

If "small" circles are present in excess of 13%, a range of sizes of spherical particles must exist in space. In practice, one places sectional circles into size classes and attempts to compute from the distributions thus obtained, the size distribution of spheres in space. A pioneer in this field is A. S. Saltykov who, unfortunately, was unable to attend the Congress, but whose key-note address was read by Dr. Hilliard. This time he offered a new approach, namely classification of circles by area rather than diameter. In spite of many efforts, the

determination of size ranges is still offering great difficulties.

Since size determination is so important, a second key-note lecture was devoted to it: Dr. Bach presented an analytical approach to this problem, previously attacked by most investigators by simple algebraic procedures.

The difficulties increase when the particles are not spherical and become very great indeed when they possess concave facets.

4. SURFACE AREA

The importance, from the standpoint of physics and biology, of determining the area of interphases between components of a specimen or of the external surface area of objects is so obvious that it does not need to be stressed. Stereologically the process of area determination is extremely simple. It can be done by counting points of intersection with test lines of given length.

5. LENGTH

It is often interesting to learn how long a tube or a fiber is of which only sections can be seen in slides. For example, the total length of the nephron, the combined length of the seminiferous tubules or the combined length of capillaries in a bulky organ may present a problem of physiologic interest. In former times, such problems were studied by maceration and teasing out of the long objects, stretching them out on a glass plate and measuring them with a yardstick. This method presents, often unsurmountable, technical obstacles. However, using the technique of Alexander the Great, the histologist, instead of untying the Gordian knot, cuts it. Counting the number of intersected elements per unit area, he very easily obtains reliable results.

In mineralogy, metallurgy, cytology and crystallography, the total edge length along the edges of the polyhedral elements is of interest.

An extremely interesting example was presented by Dr. Haug who showed that the combined length of myelinated nerve fibers in the cortex of the brain is 152 $^m/mm^3$. And these are just the myelinated fibers which conduct impulses over long distances. They constitute only a fraction of the totel fiber length in gray matter.

6

6. ANISOTROPY

When a sample contains anisodiametrical particles, they frequently are arranged so that their long axes (if they are prolate) or their short axes (if they are oblate) or both (if they are triaxial) have preferred orientations. Dr. Hilliard, in a key-note speech, gave a lucid explanation on the determination of preferred directions and of the degree of dominance of the preferred orientation over randomness.

7. SAMPLING

Basic stereological procedures begin with the assumption of random arrangement of parts within a sample. But if anisotropy exists in an object or if there is a gradient of structure within it, the stereologist must treat his object of study with greatest care. Several examples were presented during the Congress where parts exhibited preferred orientation; or where particles were present in various regional condensations or layers. Two similar examples from micro-anatomy shall be cited: In the cortex of the brain, there exist cells of various sizes. These are arranged in hazily defined layers with almost cell free layers between. In each such layer a certain size class prevails. As far as the nerve fibers are concerned, they have strongly preferential orientations.

The kidney possesses strong anisotropy: Collecting tubules and "loop" tubules run parallel within bundles, and these bundles themselves are curved with great regularity. The "convoluted" tubules are irregularly arranged, yet exhibit a slight but noticeable, preferred orientation. The glomeruli are located in the cortex of the kidney in broad, very loosely defined layers, which layers gradually blend with zones free of glomeruli. In addition, there is a gradient of size, smaller glomeruli prevailing toward the outside of the organ and larger ones being dominant more centrally.

Dr. DeHoff's key-note paper summarized masterfully, methods by which such difficulties of density and size gradients as well as directional anisotropy can be controlled.

8. TOPOLOGY

It is less easy, by the ordinary stereological procedures of measuring and counting, to investigate topological properties of a specimen, although questions of connectivity, continuity, contiguity, separation and the topological genus of a structure are vitally important to those

interested in structure. Some beginning has been made in quantita-
tive stereology for the determination, from random sections, on the
probability of hollow balls to be open into one another and on the
probabity of contact between spherical particles. But this work, very
recently published in Mikroskopie (21:32-36, 1966) was not presented
at the Congress.

Dr. Rhines gave the audience a comprehensive view of topology and
stated the strong interrelationships of the two fields in a key-note
address.

9. SERIAL SECTION CINEMATOGRAPHY

The topological properties of an object can be revealed most success-
fully by serial section cinematography, a technique which involves
photography of the exposed, cut surface of a specimen on successive
frames of a motion picture film, while the slices, cut away by a mic-
rotome, are discarded. Dr. Hegre's and Dr. Postlethwait's presenta-
tions demonstrated these possibilities beautifully. Since successive
levels of a specimen differ in outline and position from each other,
the impression of motion is often created on the flat screen, while in
three-dimensional space, the specimen is motionless. This effect of
apparent motion when viewing successive levels of sectioning through
a stationary solid was utilized by Elias in an attempt to explain the
rigid rotation of barred and spiral nebulae assumming the universe to
be a hypersphere expanding within a four-dimensional space and
sectioning, as it expands, successive levels of certain hypersolids
which control the shapes, from moment to moment,of observable gal-
axies. These therefore appear to rotate when observed from a merely
three-dimensional view point.

10. RECONSTRUCTION FROM SERIAL SECTIONS

When an object exists in the singular only or if its internal structure
is very complex, it is intractable by quantitative stereology. In such
cases the very old method of disassembling it into serial sections and
putting them together again with internal detail reveiled and mag-
nified is still the best procedure available today. Dr. Krieg gave a
excellent review of the principles and history of this indispensible
technique.

11. STEREOSCOPY AND PHOTOGRAMMETRY

Biaxial viewing and parallax often give direct information on the
three-dimensional properties of solids. These techniques are particul-

arly useful for the study of surface sculpture and for the measurement
of specific, individual structures. Several papers and instruments
were presented on this aspect of stereology.

12. INSTRUMENTATION

Quantitative stereology depends on the collection of very numerous
data. It is therefore natural that one attempts to devise instruments
which can take some of the tedium out of stereological work. Auto-
matic scanning and counting devices, the former often depending on
photometry and spectrophotometry, the latter linked with computers
were presented.

Another aim of instrumentation is to eliminate human bias from sam-
pling. The unbiased selection of test areas in microscopic fields has
presented, in the past, great difficulties; these observational fields
can be randomized and their selection made independent of human
choice. Three types of mechanical stage, two motor driven and one
to be advanced by hand, but over pre-set distances were demonstrated.

Finally, it was pointed out that only in cases where great optical
contrast exists in a specimen, or where it can be created by differ-
ential staining or etching can a fully automatic scanning device be
used. It is especially with biological objects (though not all) that
an experienced human observer is indispensible, a person able to re-
cognize and to identify structures. For among many biological ob-
jects, such as different kinds of cells the differences are as delicate
as the differences between the faces of two brothers; and only living
persons who have seen such objects thousands of times can identify
them.

But for these living persons it is still easier to push buttons than to
record events in writing.

13. TERMINOLOGY, SYMBOLISM AND NOMENCLATURE

There has been proposed, a few years ago by a group of our members,
notably by Dr. Rhines and Dr. De Hoff, a system of symbols for temp-
orary use in stereology. To their list, a few new terms and express-
ions have been added. This preliminary symbolism was sent to Con-
gress participants in advance of the Congress in order to acchieve a
certain degree of uniformity and mutual understanding.

During the Congress several proposals for alterations and expansion
of the system were proposed; but action on them has been deferred.

To facilitate reading of this volume, the old preliminary list of ex-

pressions, definitions and symbols is given below:

Morphometry. Measurement of structure. This science deals with the dimensions of real, three-dimensional objects regardless of the method by which the measurements have been obtained. It is the end-result of quantitative investigation of structure.

Stereology. A system of methods to obtain information about three-dimensional structure from two-dimensional images, be they sections or projections. Stereological methods are statistico-geometrical procedures, reconstruction from serial sections, serial section cinematography and related techniques. Stereology can lead to morphometric results. It can also give information on three-dimensional shape and orientation of objects in space.

TERMS:

section	= cut or polished surface of an opaque object
slice	= a histological or mineralogical "section" of finite thickness through a translucent object
profile	= section through an individual component of a material
trace	= section of a two-dimensional structure, such as a membrane, a surface or an interface. This section would appear as a line
intercept	= length of that segment of a testline which coincides with the area of a profile
intersection	= point of crossing of a test line with a trace
axial ratio	= quotient of length over width of a profile

MEASURED AND COUNTED QUANTITIES IN SECTIONS:

P_P = number of points falling on profiles of a component divided by total number of test points

P_L = average number of intersections per length of test line

N_A = average number of profiles per test area

L_L = average length of intercept per length of test line

Q = axial ratio of profile

d = diameter of profile (average distance between parallel tangent lines)

QUANTITIES IN SPACE

V_V = volume fraction of a component

S_V = surface area per unit volume

L_V = length of linear structure per unit volume

10

T   = thickness of a sheet in space

t   = thickness of slice or average distance between cutting planes

D   = average distance between parallel tangent planes (diameter) of an individual pebble, corpuscle, follicle, grain etc.

List of retired officers who were in office until April 11, 1967:

President: Hans Elias, Chicago, Illinois, USA
Vice President: Herbert Haug, Hamburg, Germany
Secretary: Ewald R. Weibel, Bern, Switzerland
Treasurer: Ervin E. Underwood, Marietta, Georgia, USA
Assistant Secretary: Werner Treff, Tuebingen, Germany
Editor of Stereologia: Robert T. DeHoff, Gainesville, Flordia, USA

OPENING SESSION

STRUCTURE IN SPACE AND ITS APPEARANCE ON SECTIONS

Ewald R. Weibel

Department of Anatomy, University of Bern, Bern

Space in its most general sense means an indefinite
frame within which an indefinite number of events
can happen at any indefinite place. But with the
terms "event" and "place" we have already introdu-
ced the need for somehow limiting this indefinite
space. For, as scientists investigating specific
events we wish to focus on them; that is, we wish
to define their time and place, their expanse and
confinement, their course and interaction. We will
thus be mostly studying events taking place in some
specifiable compartment of space.

Structures, on the other hand, are discrete porti-
ons of space, which are set off from their sur-
roundings by some specified and differing proper-
ties. They are thus compartments of space, and if
properly defined, may be those compartments which
we demanded above for a characterization of events
taking place in space.

By what criteria can we define structures, or com-
partments of space? Since "structures" in this
sense are discrete objects they can first be defi-
ned by their dimensions; in a most general sense
by their content or volume, by their surface or
boundary with adjacent spaces or by linear dimen-
sions; furthermore by their shape, by their connec-
tivity or topological properties (Fig. 1).

These are characteristics of individual structures.
We are, however, mostly dealing with aggregates of
structures, i.e. with compounded compartments which
make up a structural system, and here we must con-
sider some general characteristics of the mode and
degree of association of elements.

The dimensional properties of aggregates are con-
viently defined by the densities of the various
structures. With respect to the degree of associ-
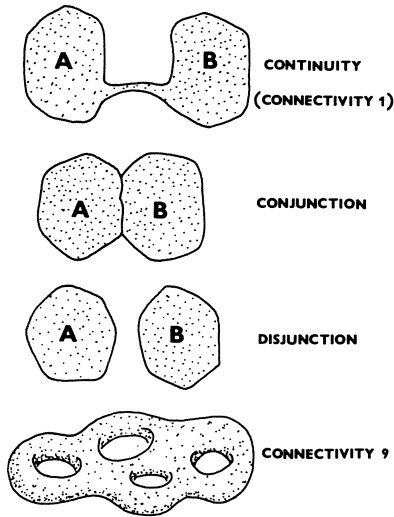
Fig. 1: Association of structures

ation of compounded compartments we may have to distinguish between continuous, conjoint, and disjoint compartments (Fig.1). Continuous compartments are only seemingly separated, since it is possible to move from any internal point to any other point without crossing the boundary. Conjoint compartments are separate but have common boundaries, while disjoint compartments remain separated by some intermediate structure. It may often be a matter of functional definition, or of resolution of the optical system, whether a given complex must be regarded as conjoint or disjoint.

This may be illustrated by a few examples taken from biology. In the lung, e.g., all 300 million alveoli are continuous structures, since they are all simple evaginations of one continuous airway system (Fig.2). Likewise, the interior of all blood vessels, is continuous (Fig.3). However, while the airway system is a simple topological structure of connectivity 1, the blood vessels form a threedimensional network of connectivity of the order of 10^{11}.

Airways and blood vessels are disjoint compartments since they remain separated by a continuous tissue layer (Fig.4). On the other hand air and tissue, as well as tissue and blood are in direct contact and may thus be defined as conjoint.

As further example, the numerous branches and synaptic bulbs of one unit of the nervous system, the neuron, are continuous with their nerve cell and with each other, although some nerve fibres may be up to one meter long. Demonstration of this continuity is one of the most difficult and most important problems in biologic morphology. The ner-

16
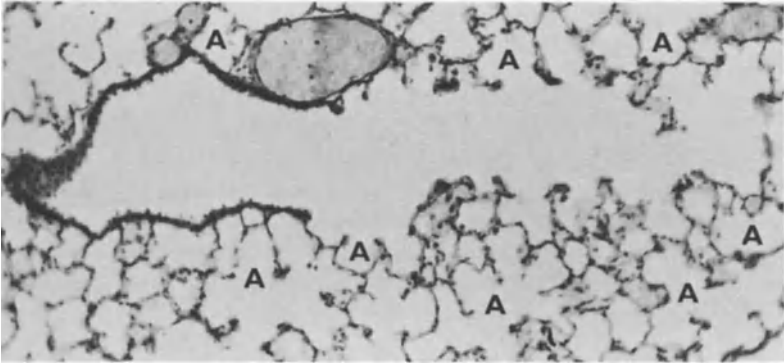
Fig. 2: Lung section; air spaces (alveoli A) appear separate but are continuous.
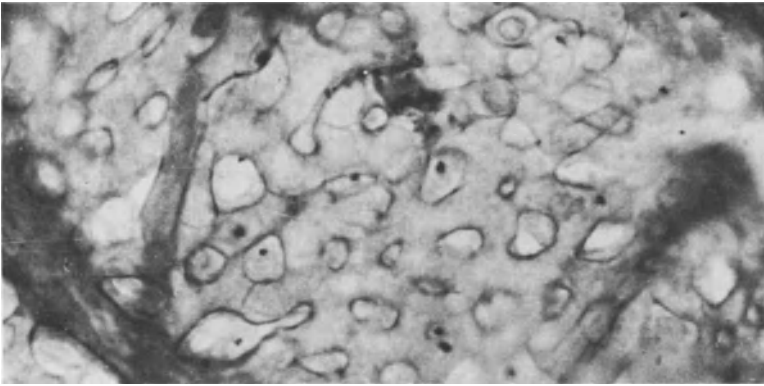
Fig. 3: Lung capillary network
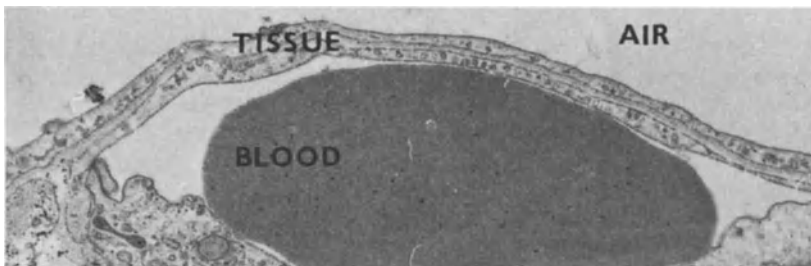
Fig. 4: Electron micrograph of tissue barrier separating air and blood in lung.

vous system of man consists of millions of neurons each with hundreds of branches, and its proper functioning depends on correct conjunction of some neurons, and disjunction of others.

Role of compartmentalization of organisms

At this point it may be appropriate to ask <u>why</u> space needs to be compartmentalized. Here, of course, I will put forth arguments from my own field of biology, arguments which may not hold true for the inorganic sciences.

A biological organism is a dynamic and vastly self-sufficient system which can keep up its activity, can grow, repair damages, and communicate with the external world, as long as some rather simple environmental conditions are fulfilled. This requires very complex functions, which must be highly coordinated. And this is achieved by segregation of specific partial functions into separate compartments which are associated with other compartments to form highly polarized systems. Establishment of <u>polarities</u> is thus the essential result of compartmentalization of biological organisms. Maintenance of this high degree of spatial order is one of the fundamental requirements for maintenance of life. In all ranges of magnitude partial functions are segregated into separate compartments and then re-associated according to specific schemes. For the morphologist, the biological organism is thus a compartmentalized space or an aggregate of associated structures. It is thus one of the systems which we may subject to stereologic analysis.

It is clear to everyone in this audience that such complex structural systems as biologic organisms must be opened by some method for analysis of inner construction. Among the various methods available, sectioning is the preferred method when material is to be studied microscopically, for it provides good lateral resolution.

Definition of "section"

Let us now try to arrive at a good and general definition of what a section is, so that we may derive some likewise general features of traces

18
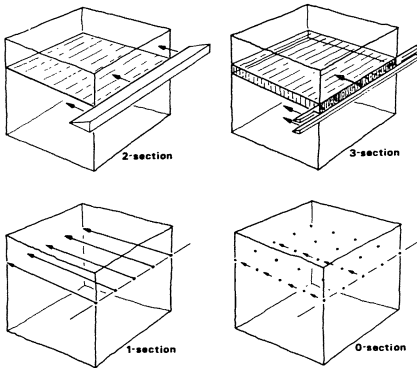
Fig. 5: Sectioning

of structures on sec-
tions (Fig. 5). Our com-
mon understanding of the
term "section" implies
a solid being cut open,
in other words, a plane
or 2-dimensional space
intersecting with a so-
lid or 3-dimensional
space. A "section" might
thus be redefined as the
intersection between two
spaces.

With this general definition it is obvious that
we may distinguish several degrees of sectioning.
Looking at solid structures we may obtain three-
dimensional sections or slices if the space inter-
secting the solid is itself 3-dimensional. We may
obtain a 2-dimensional section - a true section -
if a plane or 2-space intersects the solid, or we
may obtain a 1-dimensional section, if a line or
1-space intersects the solid. In further reduc-
tion of this scheme we may even consider a point
or a set of points as forming a 0-dimensional sec-
tion with the solid, if the points or 0-spaces
are introduced into the solid from outside.

To illustrate this concept we must briefly look
at the procedure by which we generate a section
(Fig. 5). Following the common understanding we
consider a section to be the trace left by the
edge of a microtome knife pushed through the tis-
sue along a straight line course more or less per-
pendicular to the knife edge. The section thus is
a plane, since the knife edge itself is a straight
line too. To obtain a histological section a se-
cond identical operation is necessary: the knife
edge is lowered by a certain small distance and
again pushed through the tissue. If we would have
the means to perform both cuts simultaneousely
the two parallel knife edges would be the edges
of a narrow plane strip which is pushed through
the tissue along a normal to this plane, thus ge-
nerating a 3-dimensional section or slice.

But what is the knife edge or line? Nothing else

than an infinite number of points linearly arran-
ged. If we now pick out a discrete number of points
and slide them through the tissue we obtain what
we have defined as a 1-dimensional section. And if,
instead of continuously sliding them through the
tissue, we let them jump by discrete intervals we
deposit a set of points inside the tissue and ob-
tain a 0-dimensional section.

What have we done? We have sent some _probes_ into
the tissue and these probes have picked out some
sample of the interior, on which we hope to gain
insight into the internal construction of the
tissue. And we may have chosen the dimension of
our probe for convenience.

Interaction of "section" and "structure"

Let us assume that a cube of tissue contains one
solid structure, characterised by its content or
volume V and by its surface S; one lineal element;
and a number of point objects (Fig. 6).
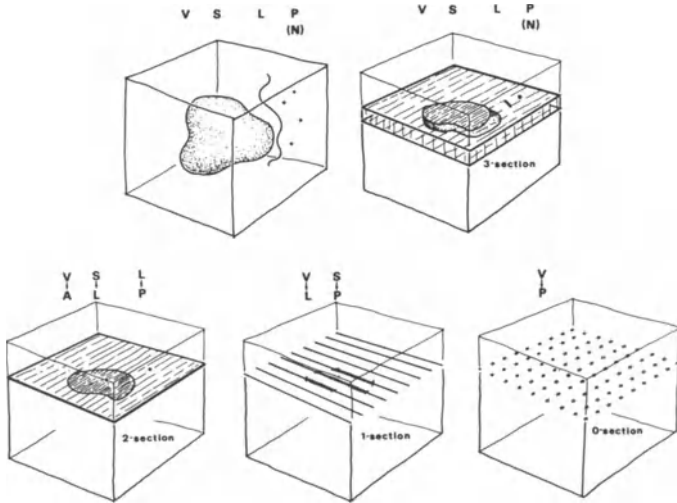
Fig. 6: Effect of sectioning on structures

A 3-section cuts out a volume and a strip of sur-
face of the solid, a stretch of the lineal ele-
ment and may also contain one of the point objects.
The dimensions of the traces of these structures

20

in this slice are preserved. In a 2-section, how-
ever, the dimensions of corresponding traces have
been reduced by 1 : volumes become areas, surfa-
ces lines and lines points; but point objects can-
not be represented on a 2-section; they are lost.
Linear probes or 1-sections provide traces of
structures, whose dimensions are reduced by 2 :
point objects and lineal elements are lost.

And finally, point lattices
or 0-sections are only able
to reflect volumes, while
surfaces, lineal elements
and point objects are lost.
With every step of dimensio-
nal reduction of sections
one degree of information is
lost (Table I).

TABLE I

do →

	3	2	1	0
dp 3	3	2	1	0
2	2	1	0	
1	1	0		
0	0			

dt

This can be summarised in
general form. Let the di-
mension of the object be d_o
and that of the section or
probe d_p, then the dimension of traces of the ob-
jects on these sections is

$$d_t = d_o + d_p - 3.$$

And since the dimension of the trace can never be
smaller than 0, it follows immediately that

$$d_o + d_p \geqq 3.$$

should a structure not be lost.

These rules apply specifically to 3-dimensional
systems, that is to objects contained in 3-space.
These rules can, however, be generalized to apply
to any system of dimension d_s : We find

$$d_t = d_o + d_p - d_s$$

$$d_o + d_p \geqq d_s$$

to be the general relations between dimensions of
system, objects, probe and trace.

We may draw a few conclusions from these conside-
rations. One of them, perhaps the most important,
relates to the impossibility of particle counting
on sections of lower dimension than d_s. When coun-

21

ting or enumerating structures we regard them as
dimensionless objects; we are mentally compressing
each structure into one point, say its center of
gravity. And it has been clearly demonstrated that
point objects $(d_o = 0)$ are only represented in sec-
tions of dimension d_s, but lost in any section of
lower order.

The second conclusion relates to the convenience
of stereologic work and its dependence on the di-
mension of the probe used for "measuring" objects.
The process of "measuring" is basically a compa-
rison of the objects with a basic unit which is
defined by independent means. Usually we will tend
to obtain a fraction of the standard unit small
enough that it is contained a large number of times
in the object, and we will count the number of
units we can fit into the objects. In the last
analysis our "measuring" will thus always be a
procedure of enumeration of units or points. We
conclude from this that we attain the highest de-
gree of operational convenience when we can reduce
the traces of objects on "sections" to points,
that is when

$$d_t = 0.$$

And this condition can be reached when

$$d_o + d_p = d_s .$$

Shape and topological properties

We now have to discuss the effect of sectioning on
those characteristics of structures which deter-
mine shape and topological properties, as well as
to the functionally most important problem of ana-
lysing the degree of association between compart-
ments. These aspects must be treated together,
since seemingly separate compartments may in re-
ality be either continuous of varying order of con-
nectivity, or may be conjoint, or even disjoint.
So, evidently, association, shape, and topological
features are closely related properties of struc-
tures.

As a general rule we can state that any degree of
sectioning introduces uncertainty into the analy-
sis of association. Relatively thin 3-sections and

2-sections destroy or mask continuity of all struc-
tures that are not simple convex bodies. As an ex-
ample take the intestine of a fetus, which is a
single coiled cylindrical tube (Fig. 7). A trans-
verse section of the abdomen presents about a
dozen sections of intestinal loops (Fig. 8). Who
will dare to state that these traces derive from
one continuous structure without knowing it from
other independent sources of information? In an
electron micrograph of an endothelial cell (Fig.
9) one may observe a group of elliptic sections
of a peculiar organelle. It is cylindrical and
apparently rather long. But are we here looking
at traces of a single coiled long structure or at
sections of many short rods? It cannot be decided
from a single section. Sections of brain tissue
show billions of disconnected bits of nerve fib-
res; how many of them belong to one and the same
neuron? This is one of the most difficult pro-
blems of biology.

Study of component association on sections

Let us examine the possibility of studying on
sections the degree of association between dis-
continuous compartments; we had distinguished bet-
ween conjunction and disjunction. 3-sections may
often show an erroneous conjunction of structures
due to overlap. In a 2-section as well as in a
1-section conjunction can be unambiguously deter-
mined; it is usually characterized as a direct
phase transition. To gain insight into the mode
and the properties of a conjunction it is neces-
sary to section it. The type of synapses between
two nerve cells in the brain can thus be deter-
mined.

This is an interesting statement which raises a
few questions. A conjunction is a 2-dimensional
feature and we appear to be able to analyse it
only on 1-dimensional traces. Shape and connecti-
vity are 3-dimensional features, and we can only
study them by looking at the surface of the unda-
maged body, that is by studying a 2-dimensional
trace. There may perhaps be a general principle
at the basis of these remarks.

The observation of discontinuous traces on sec-

23

Fig. 7 and 8: Intestinal loops (7) of human embryo appear as multiple discontinuous traces on section (8).
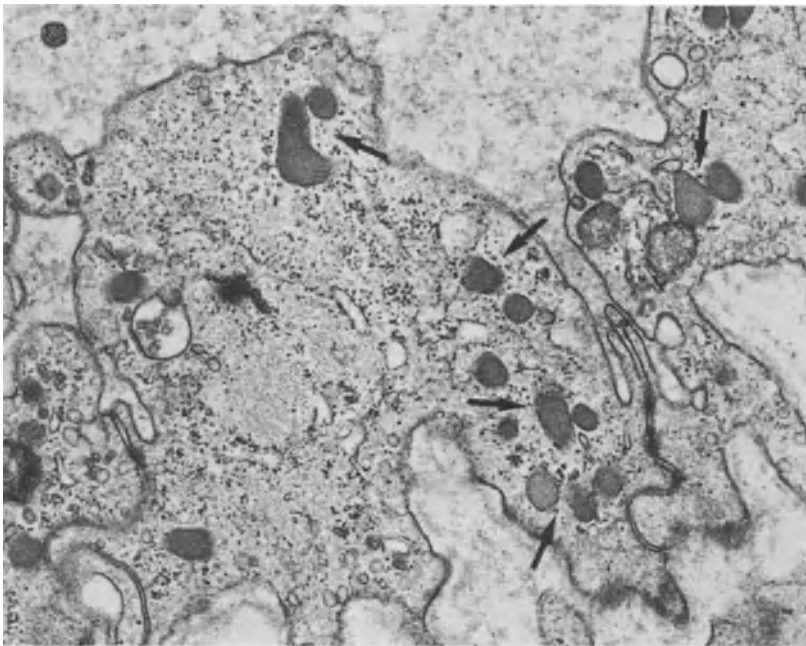
Fig. 9: Electron micrograph of endothelial cell of blood vessel. Are the traces of organelles (arrows) continuous or discontinuous?

tions does not preclude conjunction or even con-
tinuity of the two compartments in other regions
of the tissue. It is important to stress that, in
biology, functionally highly significant conjunc-
tions may occupy only a very small fraction of
the structural surface. It is therefore easy to
miss them in section analysis.

If we finally consider the value of 0-sections
or point lattices in the study of association of
compartments, it is evident that they cannot fur-
nish any information at all. Association of com-
partments presupposes as a necessary condition
continuity of space points. To study properties
of this continuous point set a sample is required
which is itself continuous at least in one di-
mension. But 0-sections, as we have defined them,
are discontinuous in all directions.

Orientation of structures

Last, but not least, we must give brief conside-
ration to one additional feature of associated
structures, namely to that of orientation. We had
remarked that the biological significance of com-
partmentalization of space was a segregation of
related functions to specific compartments. This
also implies that functionally related compart-
ments or structures must be topically related,
and this often leads to preferential orientation
of equivalent structures. Such anisotropic systems
yield misleading traces on sections, so that pro-
per care must be taken to determine anisotropy
and to orient sections accordingly.

Summary and Conclusions

We have defined structures as discrete homogenous
compartments of space, whereby homogeneity must
be naturally defined in relation to the specific
condition investigated. These structures are as-
sociated to form a compactly aggregated organized
system, which is space-filling. By aggregation,
however, deep structures are hidden and must be
made accessible for direct investigation by some
destructive method; this is unavoidable.

Sections, in the stereologic sense, are samples
of such aggregated systems obtained by some well-

controlled procedure which is essentially inde-
pendent of the structures in the system. According
to the definition used here, sections may be 3-,
2-, 1- or 0-dimensional.

When sections ineract with the system, the struc-
tures leave traces on the section, and by proper
choice of the sectioning procedure it is possible
to control the dimension of traces so as to attain
highest possible operational convenience in stere-
ologic work.

However, with each degree of sectioning one order
of information is sacrificed, and we are thus fa-
ced with a serious dilemma: In aggregated systems,
the degree of association of compartments can only
be investigated on sections: the compartments must
be opened if we want to determine whether they are
continuous or conjoint. Looking at the compartments
from outside gives us no information on whether
they may be internally continuous. But by the very
process of sectioning we destroy continuity; we
may find disjunction where highly significant con-
junction is present at another level. How can we
overcome the great difficulties arising from the
necessity of analysing internal relations on sec-
tions, while these sections destroy precisely the
relations sought? They cannot be overcome direct-
ly. However, we must remain aware that section
analysis, true stereology, is an extremely power-
ful tool, but that it cannot furnish all infor-
mation necessary for a full definition of closed
functional systems. Stereologic information must
needs be supplemented by information derived from
other independent methods. This will allow us to
approach truth and reality step by step.

THE TETRAHEDRON AS A UNIT OF VOLUMETRIC MEASUREMENT

R. BUCKMINSTER FULLER

Department of Architecture, Southern Illinois University, Carbondale, Illinois

(Professor Fuller did not submit a manuscript for his two-hour lecture originally entitled FUNDAMENTAL STRUCTURING. The editor took notes and is herewith presenting a very brief version of the part of Professor Fuller's talk which he considers of greatest interest to stereologists.)

Universities have departments of various subjects. But nature is not departmentalized. It is one. Therefore, a congress such as the present is of great significance, since scientists are coming together here to discuss one common aspect of nature, namely structure.

When the sides of a polygon are considered as rigid rods and the corners as flexible joints, then the triangle is the only stable polygon in a plane. Similarly the tetrahedron is the only stable polyhedron in space. Professor Fuller demonstrates these basic facts by using rods which he can hold together by means of rubber joints. He constructs a quadrilateral figure and deforms it at will, and shows that it can be bent even out of a plane. Then he constructs a cube out of 12 sticks; and it collapses. But the tetrahedron constructed of 6 rods is stable.

The tetrahedron has other, interesting properties. One of them is that it could, conveniently, serve as a unit of measurement for volumes. Customarily, volumes are measured by multiples of cubes. They could also be measured by multiples ot tetrahedra.

We may begin with the two-dimensional analogue, comparing "squaring" with "triangling" as shown in figure 1.

2 x 2 = 4   2 x 2 = 4

3 x 3 = 9
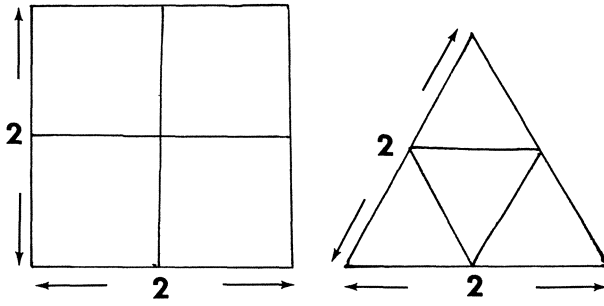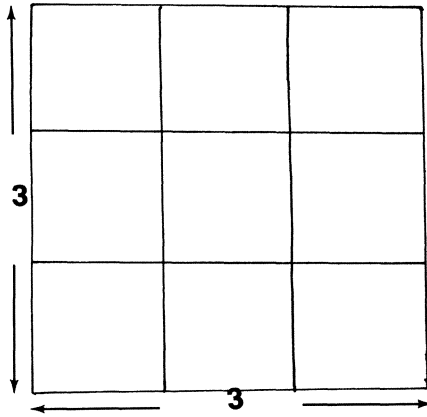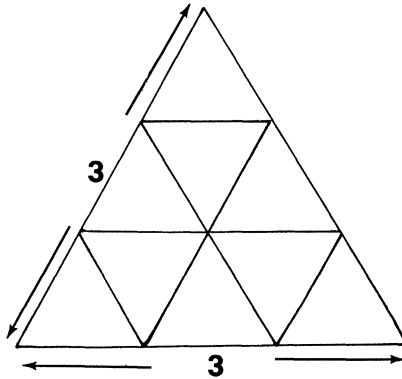
3 x 3 = 9

FIGURE 1.

How this process can be extended to three-dimensional space is shown in figure 2. Instead of "cubing" we perform "tetrahedron-ing".

2 x 2 x 2 = 8   2 x 2 x 2 = 8
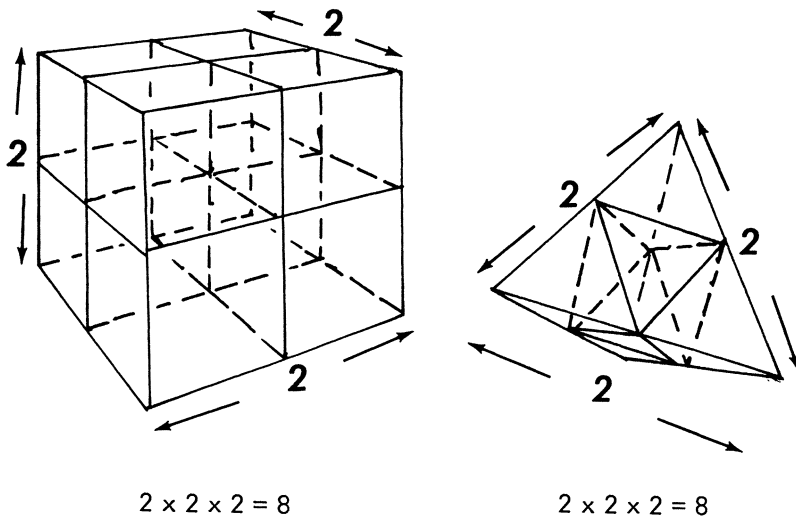
FIGURE 2.

If this process is carried to higher and higher numbers and to more complex polyhedra, interesting numerical relationships develop.

SPECIAL LECTURE

SECTIONED TEXTURES IN THE DECORATIVE ARTS

CYRIL STANLEY SMITH

Massachusetts Institute of Technology, Cambridge, Massachusetts

Although the quantitative interpretation of three-dimensional structures from two-dimensional sections is recent, the use of such sections in understanding matter and in enjoying it is old. The first action of a curious person in studying a stone or a stick or a piece of metal is to break it in two. Yet fracture is not a section, and the structural science of materials did not begin until the artisan's fracture test was replaced by Sorby's careful polished sections which presented the structure without distortion, though accepting the differences between a plane section and three-dimensional reality.

It is no accident that the first stereological analysis of any kind (done by Delesse in 1848) was on stone . Cut and polished rocks -- fossils in limestone, pebbles in conglomerates, large crystals in a porphyry, granite or basalt, and varicolored veins in marble -- all these, sectioned, provided decorative detail to be enjoyed in Roman times and much earlier. The finer detail of polished opal, agate or other gemstones had been admired for millennia, and three-dimensional variation in stone was exploited in carving cameos. In East Asia the subtle relationship between surface and substance in jade invokes profound, almost religious, admiration. Sculptors everywhere have sought to find the texture of their stone or wood and relate it to the shapes of their vision, and even the humble carpenter takes pride in the beauty of the grain disclosed by his plane.

All art involves abstraction of some kind, and just as two-dimensional paintings or drawings suggest multi-dimensional images so also do decorative sections of solid materials owe some of their aesthetic qualities to the hint that they convey of a three-dimensional reality. The viewer may not always be conscious of this, but the creating artist can hardly help but be.

The main skills required in the use of natural materials lie in the selection of the mass and the orientation

of the surfaces for the desired effect. In stone, orientation may be of minor importance (though super-patterns are regularly produced by mounting adjacent slices of stone together to give an artificial symmetry based on the near repetition of some feature), but in wood much of the beauty comes from the relation between the directionality in the material itself and the cut surface. The Chinese have exploited the simplicity of the grain of bamboo to marvellous effect (Fig. 1), but most uses of wood grain depend on its irregularity. The natural surface of a debarked log has knots and other distortions from a true cylinder and is totally unlike the sectioned grain seen on the geometrical surfaces produced by planing or especially by turning. Sheets of veneer are sliced spirally with the surface nearly concentric with the growth rings in the tree so that irregularities are intersected at a small angle and the texture is exaggerated. The Japanese have exploited this in producing modern woodblock prints (Fig. 2) with common plywood that would have been possible only with the rarest pieces of sawn timber. The texture transferred from plywood forms to cement is used by architects all over the world today.

Mosaics and Inlay. The earliest artificial material surfaces produced for decoration were probably IV millennium B.C. mosaics formed of shaped pieces of contrasting materials -- stone, shell, bitumen and plaster. Persian mosaic tile is the apogee of this technique, and anyone who has compared the north and south sides of the great gate of the Shah's mosque in Isfahan (early XVII century A.D.) knows the superiority of a tile with a cut outline over a painted glaze in the same design and color. Mosaics that are built up of rectangular tessarae are at their best when they are not adjusted to a plane surface and hence are beyond our topic, though floors of polished mosaic as well as terrazzo use the quality of a section for their effect.

On a smaller scale, colored stones were inlaid in bronze and gold jewelry and polished to a flat surface. This technique, which began early in the II millennium B.C., eventually led to cloisonné, champlevé and basse taille enamel, as well as niello and the inlaid ceramics (most magnificently those of Koryu dynasty, Korea). All of these owe their aesthetic qualities to local changes in quality or color in a single smoothly finished surface on a heterogeneous body.

In metal, true inlay first appears before 2200 B.C. in Anatolia (electrum in bronze) and was used superbly by Mycenaen smiths. No inlay in metal surpasses that of the Kaga

1. Carved bamboo brush pot. Chinese, XIX cent. (National Museum, Taiwan).

2. Print by Kiyoshi Saito, 1960, showing use of plywood grain. 52 x 38 cm.

3. Mosaic glass bowl, with heads. Roman, probably made in Alexandria, 100 B.C. to 100 A.D. (Corning Museum of Glass).

school of Japanese swordguard-makers (XVIII and XIX centuries). In the difference between true three-dimensional inlay and "false inlay" or damascening (in which the design is achieved by superficial attachment of gold or silver onto a mechanically roughen surface) lies the artistic counterpart of the scientific principles of stereology.

Some of the earliest glass vessels were molded from threads of glass wound over a sand core and then ground and partly polished to a smooth surface. Both in the Middle East and in China a few centuries B.C., simple rods of white and colored glass composed in intentionally imperfect cylinders were transversely sectioned and polished to make beads, sometimes so constructed as to represent eyes. Around the first century B.C. in both Rome and Alexandria, interesting effects were produced by grouping rods of glass of different colors together into designs of various degrees of intricacy and drawing these into canes, which were then sliced into flat slabs, assembled into mosaics in the form of a dish or vase, fused together and finally ground to shape (Fig. 3). Rods of incredibly complicated but controlled structure were assembled, showing on their sections portraits and other pictorial effects. The principle is used to this day, but now only in extruded candy.

A similar principle of producing decorative units for mosaic work is hatam-bandi inlay made in Shiraz and elsewhere in Persia. Long uniform rods of dark and light woods, bone and metal are prepared within the appropriate cross sections to fill space, assembled and glued together into rectangular rods. These are planed and again assembled into large rectangular rods which are transversely sawn into thin slices for final assembly as a decorative surface on boxes, picture frames, and the like. Far more sophisticated is the wood inlay (intarsia) of fifteenth-century Italy, in which the color and texture of selected wood pieces were used to represent pictorial details, and the even more skilled use of stone texture in the same way in both Russia and Italy (Fig. 5).

Oriental Lacquer and Ceramics. The makers of Chinese and Japanese lacquer have for centuries used inserted pieces of metal and other materials which appear like inlay on the finished surface. In the present connection, the most interesting ware is negoro-nuri in which layers of lacquer of different color are successively applied and the surface locally abraded or worn down to expose irregular areas of differing color. In guri-bori, thick parallel layers of

4. Lacquer box in *guri-bori*. Chinese, ca. 1600 A.D. (Coll. Hsien C. Tseng).
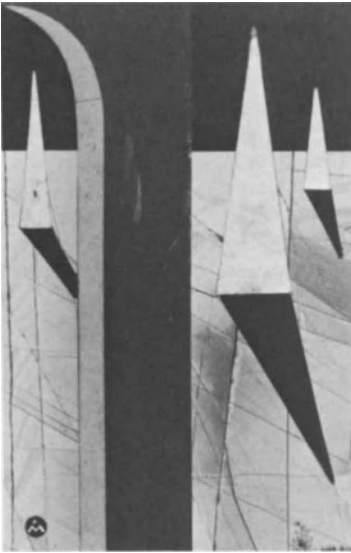
5. Stone inlay panel. By Richard Blow, Florence, 1951. 10 x 6 cm.

6. Merovingian pattern-welded sword, VI cent. A.D. Repolished and etched. 4.0 cm wide.

alternating red and black lacquer are built up to a consid-
erable thickness, and grooves are deeply incised to expose
colored lines on their sides (Fig. 4).

The working of plastic material from a crude mass to a
finished shape involves complex distortion, and if the sub-
stance is heterogeneous pleasant flow lines will be visible
in the final object: this produces the most interesting
class of surface textures. (It is curious that they are
often referred to as "marbleized," for in origin, geometry
and detailed appearance such textures are quite unlike mar-
ble. Chinese potters in the Tang and Sung dynasties pro-
duced some remarkable effects of this kind by the use of
slabs of white and dark clays repeatedly rolled together to
get thin laminae and then irregularly worked and cut into
the final shape (Fig. 7).

Textured Steel. Any iron made before the invention of
melting processes was heterogeneous because of local varia-
tions in slag and carbon content, and after the piled or
faggotted blooms were welded and forged (in La Tène times or
earlier), easily visible textures became unavoidable if the
surfaces were properly finished. An Etruscan lancehead of
the IV to III centuries B.C. has clearly intentional layers
of meteoric iron incorporated in it.[4] Consciously contrived
patterns appear in the pattern-welded sword,[3,5,6] used in
western Europe from the II to X centuries A.D. and made
famous by the Vikings and their sagas. Strips of iron and
steel were welded together, twisted, and the resulting bars
welded side by side to make the center of the blade. Final
polishing produced a surface that cut through the helical
structure and exposed the pattern (Fig. 6). Initially the
technique undoubtedly arose because a suitable pattern was
a guarantee of adequate forging in the metal, though it
seems to have been continued more for aesthetic than practi-
cal reasons, and did not die out on the shores of the Baltic
until the XIV century.[1]

The texture in the "Damascus" steel sword -- the Sword
of Islam -- is more famous. There is no archaeological evi-
dence for the texture prior to a description of it in an
early VI century poem, though they may have been a few cen-
turies old at that time. Several different kinds of texture
are subsumed under the name "Damascus," and there has been
disagreement on their origin.[4,6,8] Some swords, and all
"Damascus" gunbarrels (Fig. 8), were made from welded com-
posite faggots of iron and steel which were heavily twisted
or otherwise contorted, then forged to strips and, for the

barrels, helically coiled and hammer-welded. The texture
was developed by chemical etching. Other swords were made
by "brazing" together plates of wrought iron with molten
cast iron and forging out the resulting laminate. The best
blades owe their texture entirely to a coarse metallurgical
structure in a unique Indian steel known as "wootz." This
was of high-carbon content (1.5 to 1.8 percent), and had
been melted and slowly solidified. The pattern partly arises
from segregation, which reveals a dendritic pattern in the
crystallized steel, and partly from the precipitation of
cementite, Fe_3C, in plates which, after forging at a low
temperature, leave carbide particles in laminar groupings.
Regardless of whether the steel was initially welded or cast,
the laminations result from local variations of carbon con-
tent, and are approximately parallel to the sword surface
but with enough rumpling so that they are intersected in
pleasant irregularity. The shape and disposition of the fi-
nal hammer blows before grinding and polishing the sword
must determine much of the characteristics of its pattern.
Sometimes traces of dendrites remain visible in the texture
(Fig. 9); some appear granular (Fig. 10); while in others,
certainly the welded ones and perhaps others, have irregular
concentric markings reminiscent of waves on water. In the
prized form known as "Mohammed's ladder" there are cross-
markings, superimposed on the main pattern (Fig. 11), which
result from localized indentations in the surface before
final grinding.[4]

    The first kris produced in the Malayan Archipelago were
made of simple textured steel, but by the XVIII century
gaudy contrived patterns had developed, often using meteoric
iron (or in the XIX century nickel and in the XX stainless
steel) interleaved with steel. By a self-conscious process
of welding laminated metal, forging, locally cutting and re-
forging, and then making the finished surface by filing or
abrading so that it intersected the laminations, very elabo-
rate designs were produced (Fig. 13). These are not a nat-
ural texture resulting in the flow of the material during
forging, but can be reproduced at will by the smith. A
French smith named Clouet[2] studied such textures as part of
an attempt to duplicate Damascus steel in 1793 and gives
several illustrations, including these:
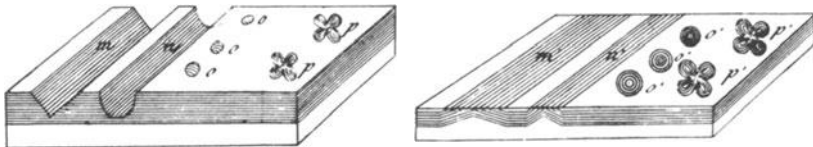
Towering over all other products of the smith is the
Japanese sword. This owes its effectiveness mainly to a
controlled carbon content and differential hardening of the
edge, but the welding, folding, and forging that were done
to make the steel homogeneous left a visible texture (Fig.
12) on the finely honed surface of the finished blade which
is much appreciated by connoisseurs.[7] The furniture of the
Japanese sword also provided an excuse for extremely sophis-
ticated work in both ferrous and nonferrous metals. Some of
them are of what is called mokumé (lit. wood grain) in which
the surface texture arises in heterogeneity in the metal re-
vealed by etching. Though some of these are rather self-
consciously forged, others have natural flow lines originat-
ing directly in the steelmaking and forging processes (Fig.
14). Nonferrous metal mokumé -- first made in the XVIII
century -- was produced by soldering together plates of var-
ious copper alloys (mainly those with silver and with gold),
which take on contrasting patination when appropriately
pickled, and hammering out the resulting composite with
enough localized or general cutting and hammering to produce
an interesting texture when the final surface is cut, pol-
ished and etched (Fig. 15). Most of these have a simple ir-
regular wood grain effect, but some tsuba-makers contrived
to superimpose thereon a specific design. Fig. 16 shows one
of the most remarkable of these. Sometimes nearly parallel
lamellae of iron and steel or of the nonferrous metals were
welded or soldered together and, after shaping, carved to
give an effect like guri-bori lacquer.

Damascene Geometry.   Patterns that are essentially
isotropic, such as the microcrystalline grains in a metal
casting and the filled-in fractures in rocks are not highly
sensitive to the angle of sectioning, and the section repre-
sents fairly well the three-dimensional structure. Interest-
ing textures appear only when many features are intersected
at low angles. The fundamental relationship between the
width or spacing of a lamellar feature as seen on a section
(W) and its true thickness or spacing (d) measured normal to
the lamella surface is, of course, simply that $W/d = 1/\sin\theta$,
where θ is the inclination between the lamella surface and
that of the section. The true thickness is seen only in a
section at $90°$ and is magnified by a factor of 2 at $30°$, 10
at $5.57°$, 50 at $1.15°$, 100 at $0.57°$, and 1,000 at $0.06°$.
Cabinet-makers know that a solid wooden board -- as distinct
from plywood -- will have a good grain only if it had been
cut from the outer part of a large tree, for the angle of
section is otherwise too high except where a growth accident
has produced local irregularity.

$$\theta = \tan^{-1}\frac{\pi nd}{\lambda}\sin\frac{2\pi c}{\lambda}$$

$$W = \frac{d}{\sin\theta}$$

For small angles this becomes

$$W = \frac{\lambda^2}{\pi^2 nc}$$

$$\frac{W}{d} = \frac{1}{\sin\theta} = \frac{R}{c} = \frac{R_0+nd}{c} = \frac{R_0+nd}{\sqrt{nd(2R_0+nd)}}$$
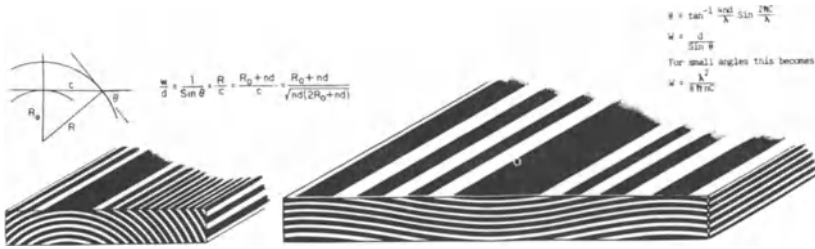
A [left]. The relation of wood-grain width to the location of the section. B [right]. Grain in sinusoidal laminae. (W is apparent width, d the true thickness of the laminae, C the lateral displacement to ring n, counted from point of tangency.)

In a plane surface cut through a cylindrical tree, the apparent width of the growth rings rapidly decreases away from the point of tangency (see eq. in Fig. A). Because the more interesting textures involve only slight rumpling of a nearly plane laminate, a better model (though still highly idealized) is that of a sinusoidal lamination (Fig. B).

There is an interesting identity between the topology and the geometry typical of the concentric rings and reversals on the Damascus texture of a laminated material, that of a contour map of rolling terrain, and that of the rings of interference colors seen on oily water. (It should be noticed that in neither case is it possible to tell a convex or a concave feature from the rings alone, unless there should be an identifiable polarity to the laminae or patterns of connectivity in the hills and valleys.) The moiré effects in watered silk and the patterns on "marbleized" paper are quite different: these involve no interplay between dimensionalities, though they often possess the same general appearance as a sectioned laminate.

In artificial laminates, a feature of the same width can result from a high-angle section of wide plates or a small-angle section of a thin one, but there are striking differences in physical appearance. Much of the charm of the textures that we have discussed comes from the fact that in adjacent areas on the surface similar structures are intersected at angles that produce widely different lateral magnification. Since the interfaces between the different laminae have small irregularities arising from differences in local deformability due to grain orientation or to local variations in composition or (in clay) to thixotropic memory, the surfaces that remain connected have an aesthetically pleasing irregularity enhanced by the variable

41

magnification.   Much of the pleasing quality of Damascus
steel or Japanese _mokumé_ arises from the fact that the sec-
tioned lamellae are very thin and are only slightly rumpled
from a plane surface: normal sections of them show almost
straight parallel lines. It requires considerable extension
of the raw material to achieve this, yet this is not enough.
The last stages of irregular local working of the surface
have far more effect on the texture than does twisting or
contortion of heavier sections.   Rolling a flat sheet from
an irregular composite will not give good texture.

⬛━━━━━━━━━━━━━⬛

The sweeping patterns of the main features in the tex-
tures discussed above are all subject to topological and
geometric restraints that arise in the physical nature of
the system and the mathematics of sectioning, but there are
enough irregularities to prevent unpleasant symmetry. The
local variations of scale produce a visual sensation com-
bining that of a resolvable abstract design with that of
pure texture.   These facts have long been appreciated in the
Orient, but they merit more attention than they have received
from craftsmen and scientists in the West.   The superiority
of the Damascus sword was related to its pleasing texture:
perhaps modern industry, as it returns to composite mate-
rials for engineering uses, might also benefit by a glance
at aesthetics.

BIBLIOGRAPHY

1.   A. Antiens, "In Lettland gefundene Schwerter mit damas-
zierten Klingen ... ," Proc. XI International Congress of
the History of Science (Poland, 1965) (in press).
2.   - Clouet, "Instruction sur la fabrication des lames fi-
gurées, ou des lames dites Damas," Journal des Mines, Ann.
12 [1803/4], 15, 421-35.
3.   Herbert Maryon, "Pattern-welding and Damascening of
sword-blades," Studies in Conservation, 1960, 5, 25-60.
4.   Carlo Panseri, "Damascus steel in legend and in reality,"
Gladius, 1965, 3, 5-66.
5.   Edouard Salin, La Civilisation Mérovingienne.   IIIᵉ
Partie: Les Techniques (Paris, 1957).
6.   C. S. Smith, A History of Metallography (Chicago, 1960).
7.   C. S. Smith, "A metallographic examination of some Jap-
anese sword blades," Doc. e Contrib. per la Storia della
Metallurgia (Milan), 1957, 2, 41-68.
8.   B. Zschokke, "Du Damassé et des lames de damas," Revue
de Métallurgie, 1924, 21, 635-69.

7. Model of a coffer in "marbleized" ceramic. Chinese, T'ang dynasty. 5.5 x 12.0 x 9.1 cm (Museum of Fine Arts, Boston).

8. Turkish gun barrel of welded "Damascus" steel. XVIII cent. (Victoria & Albert Museum).
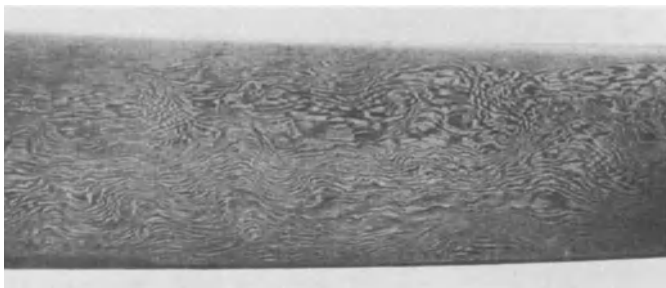
9. Persian sword, early XVII cent. Detail.

10. Persian sword, late XVII cent. Detail. (Wallace Coll.).
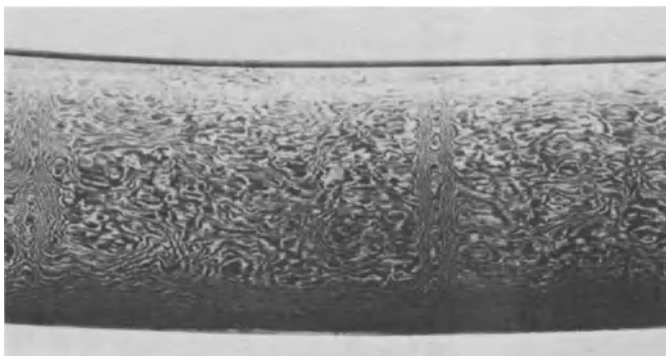
11. Persian sword showing cross-markings known as "Mohammed's ladder" (H. Maryon).
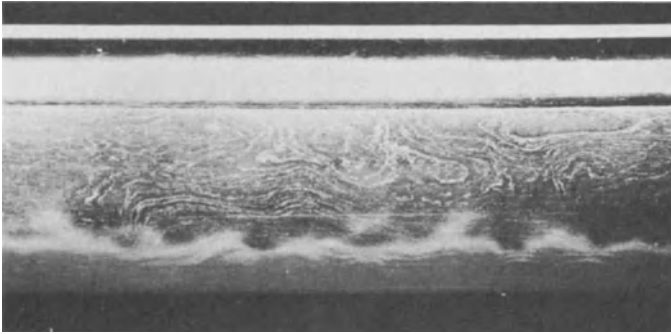
12. Japanese sword blade by Kanemitsu of Bizen. Detail.
3.6 cm wide (A. D. E. Craig).

13. Blades of three Malayan kris (H. Maryon). Nat'l. size.

14. Japanese swordguard of iron mokumé. Signed Kei of Kii Province. Ca. 1840. 8.6 cm. high.

16. Swordguard in nonferrous metal mokumé. Detail showing floating cherry blossoms. X2. XIX cent.(Museum of Fine Arts, Boston).

15. Swordguard in nonferrous metal mokumé. Ca. 1800 (Victoria & Albert Museum).

GENERAL   QUANTITATIVE   STEREOLOGY

QUANTITATIVE EVALUATION OF
SECTIONED MATERIAL

ERVIN E. UNDERWOOD

Research Laboratory, Lockheed-Georgia Company, Marietta, Georgia

Many of the basic equations of quantitative stereology are
known and are being utilized to an increasing extent.
However, the complete scope of current developments is
neither widely disseminated nor available. Consequently,
full utilization of the basic concepts is not always
realized.

Because of their essentially geometrical nature, the basic
equations and methods apply to any material. Thus, it is
possible, with the same equations, to describe quantita-
tively the microstructure of a metal, ceramic, or tissue.
Microstructures may be defined in terms of their features,
seen directly on prepared microsections or as projections
from a thin foil, at magnifications accessible to optical
and electron microscopy. By "features", we mean any of the
point, lineal, areal, or volume elements that make up the
microstructure. The features are referred to simply in
terms of their dimensionality (i.e., as objects with zero,
one, two, or three dimensions), and are described by their
magnitude, number, orientations, spacings, etc. This geo-
metrical emphasis can thus achieve great generality.

The true strength of quantitative stereological methods
(particularly in research work and theoretical treatments)
lies in the further manipulation of the basic equations.
What is frequently required are quantitative parameters of
the microstructure that have significance with regard to
the measured property, and these parameters must generally
be derived or combined from the basic expressions.

BASIC SYMBOLS

Table I gives a list of the basic symbols and their defini-
tions (Underwood, 1964). Note that P is used for <u>points</u>,
and N for <u>objects</u>. Both A and S pertain to two-dimensional
surfaces, but in deference to widespread usage, A is re-
served primarily for flat surfaces and S for curved surfaces

TABLE I
List of Basic Symbols and Their Definitions

Symbol	Dimensions	Definition
P	–	Number of point elements or test points
P_P	–	Point fraction. Number of points (in areal feature) per test point
P_L	mm^{-1}	Number of points (intersections) per unit length of test line
P_A	mm^{-2}	Number of points per unit test area
P_V	mm^{-3}	Number of points per unit test volume
L	mm	Length of lineal elements or test line
L_L	mm/mm	Lineal fraction. Length of lineal intercepts per unit length of test line
L_A	mm/mm^2	Length of lineal elements per unit test area
L_V	mm/mm^3	Length of lineal elements per unit test volume
A	mm^2	Planar area of intercepted features or test area
S	mm^2	Surface or interface area (not necessarily planar)
A_A	mm^2/mm^2	Area fraction. Area of intercepted features per unit test area
S_V	mm^2/mm^3	Surface area per unit test volume
V	mm^3	Volume of three-dimensional features or test volume
V_V	mm^3/mm^3	Volume fraction. Volume of features per unit test volume
N		Number of features (as opposed to points)
N_L	mm^{-1}	Number of features intersected per unit length of test line
N_A	mm^{-2}	Number of features intersected per unit test area
N_V	mm^{-3}	Number of features per unit test volume
$\bar{L}$	mm	Average lineal intercept, L_L/N_L
$\bar{A}$	mm^2	Average areal intercept, A_A/N_A
$\bar{S}$	mm^2	Average surface area, S_V/N_V
$\bar{V}$	mm^3	Average volume, V_V/N_V

Additional subscripts may be employed, if, for example, one wishes to distinguish between α and β phases.

The compound symbols represent fractional quantities. For example, P_L is equivalent to P/L. P_P means P/P, where the upper P refers to points (of a grid) that fall over the areas of interest in the microstructure. This might be the α-phase, for example. The lower P represents the number of points in the grid, and is a test quantity. The number of points in the α-phase, divided by the total number of points in the grid, gives the point fraction, and thus the volume fraction of the α-phase.

Both P_P and P_L represent simple counting measurements. Another useful quantity obtained by counting is N_A, the

50

number of objects per unit area. In a single-phase poly-
crystalline structure, a simple way to obtain N_A (for ex-
ample, number of grains/unit area) is to count triple
points (where 3 grain-boundary traces meet at a point),
according to the equation

$$N = (1/2) \, P + 1. \tag{1}$$

Dividing by the chosen test area gives N_A, of course.
Occasionally, a non-equilibrium 4-rayed junction will be
found -- this should be counted as <u>two</u> triple points. Use
of the above equation eliminates the need for determining
and counting the edge grains separately, as in other me-
thods.

BASIC EQUATIONS

Presented next are the basic equations for determining the
magnitude of lineal, areal, and volume elements from
measurements made on a test section (the plane of polish).

$$V_V = A_A = L_L = P_P \tag{2}$$

$$S_V = (4/\pi)L_A = 2P_L \qquad mm^{-1} \tag{3}$$

$$L_V = 2P_A \qquad mm^{-2} \tag{4}$$

$$P_V = (\tfrac{1}{2})L_V S_V = 2P_A P_L \qquad mm^{-3} \tag{5}$$

Dimensions are indicated arbitrarily in millimeters in or-
der to emphasize the dimensionality of the symbols used in
the equations. The basic equations in Line (2) state the
equality of the volume ratio, areal ratio, lineal ratio,
and point ratio of a particular phase as seen on random
sections through a microstructure. The equations in Line
(3) relate the surface area per unit volume of the micro-
structure to L_A and P_L as measured on a section through the
microstructure. Similarly, in Line (4) the equation re-
lates the length of random linear elements in three-dimen-
sional space to the two-dimensional point density, P_A, ob-
tained from sections through the system of lines. Equa-
tions in Line (5) pertain to the points in space generated
by the intersections of a system of surfaces with a system
of lines. The measurable values, P_A and P_L, are obtained
from the sectioning plane and are related to the system of
lines and to intersections of the test line with the system
of surfaces, respectively.

It is important to emphasize that all these equations are
exact, in the sense that no simplifying assumptions are

required as to size, shape, spacing, etc. of features in
the microstructure. There is a requirement, however, that
the measurements are made randomly or with statistical
uniformity and that the test sections are representative of
the entire sample. Then, the calculated quantity can be
obtained as precisely as desired, depending on the number
of measurements taken.

TABLE II

Relationship of Measured (○) to Calculated (□) Quantities

Dimensions of Symbols
(Arbitrarily expressed in terms of millimeters)

Microstructural Feature	mm^0	mm^{-1}	mm^{-2}	mm^{-3}
Points	P_P	$P_L \longrightarrow P_A \longrightarrow P_V$		
Lines	L_L	$L_A \longrightarrow L_V$		
Surfaces	A_A	S_V		
Volumes	V_V			
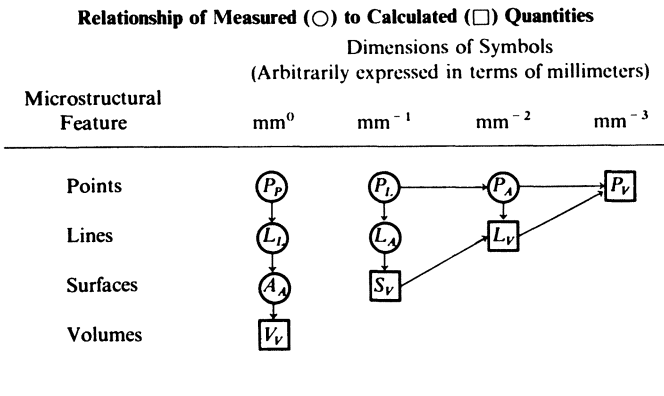
The triangular array of symbols shown in Table II are ar-
ranged systematically to show the interrelationship of the
measured to the calculated quantities (Underwood, 1967).
Note that L_A can either be measured or calculated, as can
L_L and A_A. Normally, however, L_A is calculated from P_L
measurements, and A_A is obtained from measurements of
L_L or P_P.

All symbols are interrelated except between the first
column and those on the right. By means of a rather simple,
yet powerful, choice of particle or cell diameter, this gap
can be bridged. This "diameter" is the mean intercept
length and will be discussed later.

TYPICAL DERIVATIONS

It is pertinent at this point to indicate how the basic
relationships are obtained. The methods are relatively
straightforward, and the surprising thing is that the co-
efficients are so simple.

52

The equality of volume fraction and areal ratio was first suggested by Delesse. Consider a test cube of volume $V = \ell^3$ containing irregularly-shaped volume elements (e.g., of α-phase) that are cut by a thin slice of thickness δx and area $A = \ell^2$ parallel to the (z,y) plane. The volume of α-phase in the thin slice is given by

$$\delta V_\alpha = \ell^2 \, \delta x \, (V_V)_\alpha$$

and for δx sufficiently small, by

$$\delta V_\alpha = A_\alpha (x) \cdot \delta x$$

where $A_\alpha (x)$ is the area of α-phase on the slice surface as a function of slice position x. $A_\alpha (x)$ varies irregularly with x and the average value is

$$\overline{A}_\alpha = \frac{1}{\ell} \int_0^\ell A_\alpha (x) \cdot dx$$

In the limit, the total volume of α-phase in the cube is given by

$$V_\alpha = \int_0^\ell dV_\alpha = \int_0^\ell A_\alpha (x) \cdot dx = \ell \, \overline{A}_\alpha \, .$$

Dividing both sides by V, we obtain

$$V_\alpha / V = \overline{A}_\alpha / A$$

or, in general,

$$V_V = \overline{A}_A = A_A \tag{6}$$

where the bar is omitted in order to simplify the notation. Thus, the average areal fraction, A_A, determined on planar sections through the microstructure, represents an estimate of the volume fraction V_V of the phase under consideration. Although only one coordinate was used to specify the location of the section plane, the final form of the Delesse relation is independent of any such requirement.

The relationship

$$S_V = 2 \, P_L, \quad mm^2/mm^3 \tag{7}$$

was first published by Saltykov. The importance of this equation can be appreciated from the fact that it has been rederived independently at least seven times since then. Rather than going into the complete derivation, it will suffice to indicate that a random system of surfaces is pierced with a large number of vertical test lines, then an expression is set up for the density of intersections with elementary areas having all orientations in space. The individual contributions are added to obtain the total

53

number of intersections with the total surface area.

We consider next the important equation (Saltykov; Smith and Guttman) that relates line length in a plane to an intersection count with a test line,

$$L_A = (\pi/2)\, P_L, \text{ mm/mm}^2. \tag{8}$$

The length of lines in a plane (randomly oriented or not) per unit test area, L_A is proportional to P_L, the number of (point) intersections made by unit length of a random test line. Obviously, the greater the total length of lines in the plane, the more intersections will be made with the test line. The coefficient $\pi/2$ derives from the averaging process, over all angles, of the angle of intersection of the test line with the very small, straight segments of the lines.

The quantity L_A is a basic microstructural parameter, and is also useful after further manipulations into various other forms. In corrosion studies, for example, one would want to know the length of grain-boundary traces exposed to the corrodent. The value of L_A might be required for the crack length (total or average per crack), or for the length of slip lines. If the total crack length were required, for example, then the intersections with all crack traces would be counted. Perhaps a more significant parameter than L_A would be S_V since cracks are essentially 2-dimensional in nature (Underwood, 1967-A).

If slip traces are to be measured from a tensile test specimen with circular cross-section, a plastic replica can first be made, then straightened out on a microscope slide for a P_L count. Here again, only those traces of interest need be considered (Underwood, 1961).

The equation

$$L_V = 2\, P_A, \text{ mm/mm}^3 \tag{9}$$

(Saltykov) relates the length per unit volume to the number of points of emergence per unit test area. A cube containing a random system of lines is cut by a large number of parallel test planes. By employing the principle that the probability of intersection of the planes with the elementary line segments is proportional to their projected lengths normal to the sectioning planes, it can be shown that the proportionality constant is equal simply to 2.

54

A word of caution is necessary here. Since Equation (9) is based on randomly oriented lines, it is not necessarily exact for oriented systems of lines. Depending on the angle between the oriented lines and sectioning planes, the coefficient can vary from 1 to 2. However, the coefficient 2 will always apply if adequate random sampling (of the sectioning planes) is employed.

Another important equation describes a mean free distance, λ, which may be thought of as the mean edge-to-edge distance along a straight line between particles or second phase areas. The equation may be written as

$$\lambda = (1-V_V)/N_L, \text{ mm} \qquad (10)$$

where V_V is the volume fraction of particles (or second phase), and N_L is the number of intersections with particles (or second phase regions) by the straight test line of length L (Fullman).

The equation is obtained readily. It derives from the fact that the number of particles intersected by the test line is the same as the number of matrix areas intersected (for many particles). Thus, the lineal fraction occupied by the matrix $(1-L_L)$ is λN_L, which equals the volume fraction occupied by the matrix, $(1-V_V)$. Equating the latter terms yields the above equation for λ.

This is an extremely useful quantity. It involves no assumptions as to size, shape, location, etc. of the second phase. Moreover, it is a true three-dimensional parameter even though it is obtained from the plane of polish; or, in other words, it is an average three-dimensional value obtained from many planes of polish.

In addition to the mean free distance, λ, there is another particle parameter that also possesses great value and generality. This is the mean intercept length, $\bar{L}_3$, defined in Table I as L_L/N_L. Frequently, it is used as a grain or particle "diameter". There is good reason for this choice. First, the measurement is extremely simple. For a space-filling system of grains, the grain size parameter $\bar{L}_3$ is equal simply to $1/N_L$, where N_L is the number of intersections of the grains made by the test line of total length L. For a non-space-filling system of particles of volume fraction V_V, $\bar{L}_3$ is equal to V_V/N_L, since V_V equals L_L.

Secondly, a unique value of $\bar{L}_3$ is obtained for any granular or particulate microstructure, regardless of the degree of convexity or concavity. This average length can be thought of as a lineal measure of the "size" or "diameter". No assumptions as to size or shape or reference to sphericity are required.

A third, and major advantage to the use of $\bar{L}_3$ as defined here is that it is related directly to S_V, the surface area per unit volume. From the relationships that $\bar{L}_3 = 1/N_L$ and $P_L = N_L$ for space filling grains, it is evident that

$$S_V = 2\ P_L = 2\ N_L = 2/\bar{L}_3 \ , \ mm^{-1}. \qquad (11)$$

S_V, it should be recalled, has a unique value for any system of surfaces in a volume, and so does $\bar{L}_3$.

As a final point of interest, $\bar{L}_3$ is directly related to the ASTM grain size number through S_V (Metals Handbook). An accurate, measured value of $\bar{L}_3$ permits the ASTM grain size number to be reported to as many decimal places as justified by the data.

Using the concept of mean intercept length, Fullman's expression for mean free distance can be rearranged to give

$$\lambda = \bar{L}_3 \ (1-V_V)/V_V. \qquad (12)$$

This equation geometrically links together the parameters λ, $\bar{L}_3$, and V_V, with all quantities obtained without crippling assumptions and loss in generality.

Since for separated particles $P_L = 2\ N_L$ and $\bar{L}_3 = V_V/N_L$, by simple substitution in Equation (7) we can write

$$\bar{L}_3 = 4\ V_V/S_V \ , \ mm. \qquad (13)$$

It is apparent that $\bar{L}_3$ connects the terms on the left hand side and right hand side of the symbols shown in Table II. All of the quantities in the basic equations, therefore, can be linked through the relationship of $\bar{L}_3$ to both S_V and V_V.

Tables III and IV summarize much of what has been stated previously. Applications of the results are given for two-dimensional and three-dimensional systems of grains and particles. The main difference between the two cases of contiguous and separated figures is the factor of 2 which is introduced because of edge or surface sharing in the one

56

TABLE III

PERIMETER LENGTH-TO-AREA RELATIONSHIPS FOR
TWO-DIMENSIONAL PLANAR FIGURES AND LINEAR NETWORKS

A.
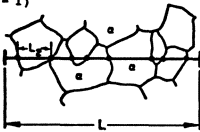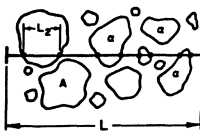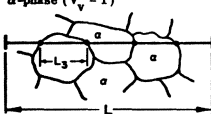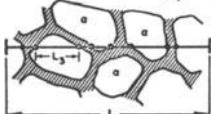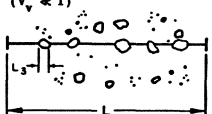
Area-filling contiguous figures of α-phase $(A_A = 1)$

One-dimensional perimeters with sharing between contiguous figures.

$$N_L = \tfrac{1}{2} + 7 + \tfrac{1}{2} = 8$$

$$P_L = 8$$

$$P_L = N_L = 1/\bar{L}_2$$

B.

Isolated figures of α-phase $\left((A_A)_\alpha < 1\right)$

One-dimensional perimeters not shared with other figures.

$$N_L = 4$$

$$P_L = 8$$

$$P_L = 2N_L = 2(A_A)_\alpha/\bar{L}_2$$

SALTYKOV

$$L_A = (\pi/2)P_L = (\pi/2)N_L \qquad\qquad L_A = (\pi/2)P_L = \pi N_L$$

TOMKEIEFF

$$\bar{L}_2 = \pi\bar{A}/2\bar{L}_p \qquad\qquad \bar{L}_2 = \pi\bar{A}/\bar{L}_p$$

CHALKLEY

$$\bar{L}_2 = \ell p/2P \qquad\qquad \bar{L}_2 = \ell p/P$$

TABLE IV

SURFACE-TO-VOLUME RELATIONSHIPS FOR SYSTEMS OF
SURFACES AND THREE-DIMENSIONAL CELLS AND PARTICLES

A.

Space-filling contiguous cells of α-phase $(V_v = 1)$

Two-dimensional cell surfaces, with sharing between contiguous cells.

$$N_L = \tfrac{1}{2} + 3 + \tfrac{1}{2} = 4$$

$$P_L = 4$$

$$P_L = N_L = 1/\bar{L}_3$$

B.

Isolated cells of α-phase $(V_v \gtrsim 1)$

Thin separating layers of finite thickness. (If considered essentially two-dimensional, treat as in Part A.)

$$N_L = \tfrac{1}{2} + 3 + \tfrac{1}{2} = 4$$

$$P_L = 8$$

$$P_L = 2N_L = 2(V_v)_\alpha/\bar{L}_3$$

C.

Dispersed particles of α-phase $(V_v \ll 1)$

Two-dimensional particle interfaces, not shared with other particles.

$$N_L = 5$$

$$P_L = 10$$

$$P_L = 2N_L = 2(V_v)_\alpha/\bar{L}_3$$

SALTYKOV

$$S_v = 2P_L = 2N_L \qquad S_v = 2P_L = 4N_L \qquad S_v = 2P_L = 4N_L$$

TOMKEIEFF

$$\bar{L}_3 = 2\bar{V}/\bar{S} \qquad \bar{L}_3 = 4\bar{V}/\bar{S} \qquad \bar{L}_3 = 4\bar{V}/\bar{S}$$

CHALKLEY

$$\bar{L}_3 = \ell p/2P \qquad \bar{L}_3 = \ell p/P \qquad \bar{L}_3 = \ell p/P$$

case and not in the other. Note also the distinction be-
tween N_L and P_L.

In Tables III and IV, $\bar{L}_p$ is the mean perimeter length;
ℓ is the length of a small test line with end-points p
that fall in the phase of interest, and P is the number of
intersections of the test line ℓ with the perimeter out-
lines. The other terms are as before.

PROJECTED IMAGES
(Underwood, 1967)

It is beyond the scope of this paper to discuss the quan-
titative measurement of structures from projected images.
The mathematics are more complicated, less exact, and de-
pend on the geometry of the foil and the amount of second
phase (Hilliard; Cahn and Nutting). Nevertheless, useful
results can be had with the simplified equations.

This subject is also discussed in another paper given later
on in the book.

PARTICLE SIZE DISTRIBUTION
(Underwood, 1967)

As in the case with projected images, methods for obtaining
particle size distributions are not as well defined as for
the basic equations discussed earlier. Whereas the latter
equations are capable of statistically exact solutions,
this is not the case for size distributions of real parti-
cles with irregular shapes (Wicksell).

This subject will also be dealt with in other papers, so
will not be discussed here (Aitchinson and Brown; Goldman,
Lewis, and Moore).

SPACINGS VERSUS DISTANCES

In systems of particles, spacings and distances should be
defined so as to remove any ambiguities in meaning. The
mean particle spacing, σ , can be defined as

$$\sigma = 1 \ / \ N_L, \ mm \qquad\qquad (14)$$

where N_L is the number of particles intersected per unit
length of a straight, random test line. The spacing σ ,
therefore, represents the mean center-to-center distance.
Thus, the mean particle diameter, or mean intercept length

$\bar{L}_3$, is given by

$$\bar{L}_3 = \sigma - \lambda . \tag{15}$$

Two other spacing parameters may be of interest in special cases. For a system of point particles in a plane, Gurland gives

$$\Delta_2 = 0.500 \ P_A^{-\frac{1}{2}} \tag{16}$$

as the average distance of separation of randomly distributed point particles, taken as nearest neighbor pairs, and

$$\Delta_3 = 0.554 \ P_V^{-1/3} \tag{17}$$

for the average separation of nearest neighbor point pairs in a volume. Note that these parameters are not the same as the ones described previously. We introduce approximations into Equations 16 and 17 when N_A and N_V are substituted for P_A and P_V, respectively.

SUMMARY

A general survey has been presented of the basic equations of stereology --, that is, the quantitative relationships that exist between quantities measured on the two-dimensional plane of polish and the magnitudes of micro-structural features that occur in three-dimensions. Other important parameters and quantities are described, including the mean free distance and the mean intercept length.

The subject of stereology is not completely new to many; however, there are still numerous experiments to be run and methods to be perfected. It is hoped that newcomers dealing with microstructures will be encouraged to apply quantitative methods in their work, and that the more experienced scientists will endeavor to advance our knowledge in this fascinating field.

REFERENCES

Aitchison, J. and Brown, J. A. C. The Lognormal Distribution, Cambridge University Press, Cambridge (1963) 176.

Cahn, J. W. and Nutting, J., Trans. AIME 215 (1959) 526.

Chalkley, H. W., Cornfield, J., and Park, H., Science 110 (Sept. 23, 1949) 295.

Delesse, A., Annales des Mines 13 (1848) Fourth Series, 379.

Fullman, R. L., Trans. AIME <u>197</u> (1953) 447; ibid., p. 1267.

Goldman, A., Lewis, H. D., and Moore, R. H., "On the Proper Use of Transformations of Log Normal Functions in Small Particle Statistics," Los Alamos Scientific Laboratory Report LA-3262, July 9, 1965.

Gurland, J., "Spatial Characteristics of Discrete Particles" in <u>Quantitative Microscopy</u>, Edited by F. N. Rhines and R. T. DeHoff, to be published by McGraw-Hill Book Co., Inc. See also: Gurland, J. and Plateau, J., Trans. ASM <u>55</u> (1962) 1046.

Hilliard, J. E., Trans. AIME <u>224</u> (1962) 906.

Metals Handbook, 2d Edition, Amer. Soc. for Metals, Cleveland, Ohio (1948) 406. See last column of Table, but note that caption is inverted.

Saltykov, S. A., <u>Stereometric Metallography</u>, 2d Edition, Metallurgizdat, Moscow (1958) 446 pp. (Available as Rough Draft Translation, ASTIA).

Smith, C. S. and Guttman, L., Trans. AIME <u>197</u> (1953) 81.

Tomkeieff, S. I., Nature <u>155</u> (Jan. 6, 1945) 24; ibid. 107.

Underwood, E. E., Metals Engineering Quarterly, ASM, Vol. 1, No. 3 (1961) 70; ibid., No. 4, p. 62.

Underwood, E. E., "A Standardized System of Notation for Stereologists", <u>Stereologia</u> Vol. 3, No. 2, Dec. 1964, p. 5.

Underwood, E. E., <u>Quantitative Stereology</u>, Addison-Wesley Series in Metallurgy and Materials, Cambridge, Mass., To be published (1967).

Underwood, E. E., "Microstructures and Properties", Chap. 16, p. 432 in <u>An Atomistic Approach to the Nature and Properties of Materials</u>, Ed. by J. A. Pask, John Wiley and Sons, Inc., New York, (1967)-A.

Wicksell, S. D., Biometrika <u>17</u> (1925) 84; ibid., <u>18</u> (1926) 151.

MEASUREMENT OF EXTRACELLULAR SPACE IN DEVELOPING RAT BRAIN FROM ELECTRON MICROGRAPHS

JOSEPH J. PYSH

Northwestern University, Medical and Dental Schools, Dept. of Anatomy
Chicago, Illinois

The neuropil of rat inferior colliculus was studied during the first two weeks of postnatal life. The extracellular space (ECS) was found to be distributed as narrow intercellular gaps about 150Å wide and intercellular lakes 0.2-3.0 µ in longest dimension (Fig. 1). Lakes were largest during the first postnatal week and decreased in size and number as development occurred. At the same time profiles of cellular elements increased in mean number and decreased in mean diameter, tending to increase with development the proportion of extracellular space distributed as intercellular gaps. Quantitation of these complex data was necessary to determine any change in the magnitude of the ECS with maturation.

Random electron micrographs, taken at a magnification of 7,500X and photographically enlarged about 5 times, were weighed on a beam balance. The ECS was then cut out with scissors along the outermost surface of plasma membranes and also weighed. From these two weights the percentage of ECS in electron micrographs was obtained at each age studied (Fig. 2). An initial trial indicated there was little variation within individual animals and a greater variation between different animals of the same age. For this reason, one measurement was obtained for each animal studied. Because the nature of the population distributions at the various ages studied is not known and the sample sizes were very small, the data were evaluated by the non-parametric Mann-Whitney U test. No significant difference was seen between the days of the first week while a significant difference was detected between

61

day 14 and days 1, 4 and 7 and between day 10 and
day 7. Thus, the measurements, which are con-
sistent with visual estimations, indicated that
the percentage of extracellular volume in the
neuropil of postnatal rat inferior colliculus is
greatest during the first week and decreases in
magnitude as development proceeds.
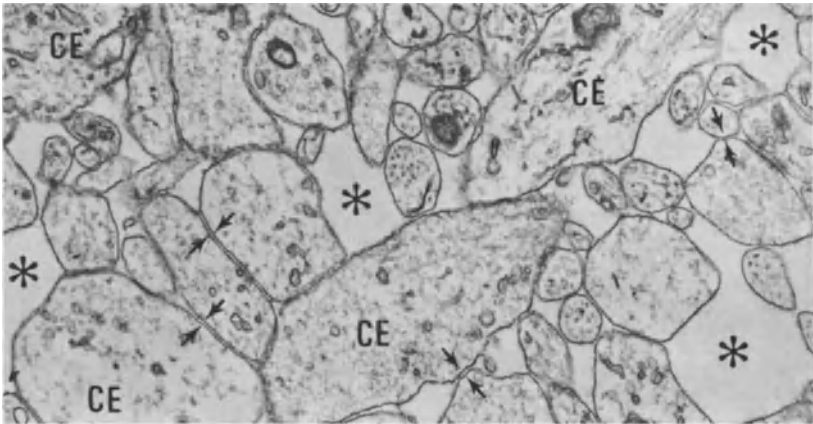
Fig. 1. Electron micrograph of 4 day old
neuropil. Note large intercellular lakes (*) and
narrow intercellular gaps (arrows). CE=cellular
elements. X27,000.

Postnatal Day	1	4	7	10	14
Percentage ECS/68μ^2 Tissue Area	17.7 17.6 15.6 11.3	23.5 20.1 19.4 18.5 15.8 11.3 11.1 10.5	17.2 15.8 14.7 14.5 13.4	16.9 13.0 11.3 11.3 10.3	13.5 12.0 11.2 8.9 8.7
Mean	15.5	16.3	15.1	12.2	10.9

Fig. 2.   Percentage of ECS per Unit Volume in
Neuropil of Rat Inferior Colliculus.

A STEREOLOGICAL METHOD FOR MEASURING THE SPECIFIC SURFACE AREA OF METALLIC POWDERS

SARKIS A. SALTIKOV

Erevan Polytechnical Institute, Armenia, U.S.S.R.

The specific surface area is an important characteristic of a metallic powder, since it determines many other properties of the powder. Up to the present, the surface area has been measured only by indirect methods, such as gas adsorption. The method to be proposed here is a direct measurement using a stereological analysis. It is also applicable to non-metallic powders.

For this analysis, it is first necessary to obtain random sections through the powder particles. This can be done by mixing the powder with one of the mediums (such as bakelite or liquid resin) used for the mounting of metallographic specimens. After the medium has solidified, a polished section is prepared by the standard metallographic techniques.

The analysis involves the simultaneous measurement of the surface area of the particles, using the random secant line method of the author (1958), and of the volume of the particles by the point-counting method of Glagolev (1941). The polished section of the mounted powder is viewed through a microscope having an eyepiece reticule on which is inscribed a square grid. A count is then made of two types of point intersections illustrated in Fig. 1: (a) The black points which are the grid corners falling within the particle profiles. The number of these points is proportional to the volume of the powder. (b) The white points which are the intersections of the grid lines with the particle outlines. The number of these points is proportional to the surface area of the particles.

If P_B and P_W are the number of black and white points counted in the analysis, N is the total number of grid corners applied and L mm the total length of grid lines, then the surface area per unit volume of the powder is given by:

$$S_V = 2(N/L)(P_W/P_B), \qquad (mm^2/mm^3).$$

It will be noted that since the surface area and volume are

measured simultaneously, it is not necessary to have a uniform dispersion of the powder throughout the mounting medium.

Glagolev's point-counting method can be replaced by Rosiwal's lineal analysis if an automatic scanning instrument is available.
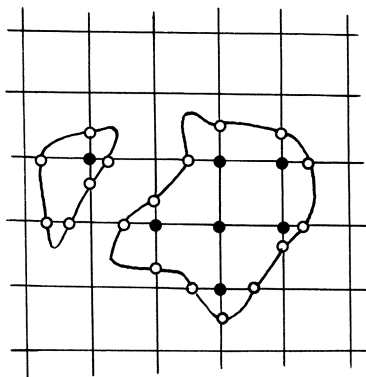
Fig. 1

REFERENCES

Glagolev, A. A., Geometrical Methods of Quantitative Microscopic Analysis, Lvov, 1941.

Saltikov, S. A., Stereometric Metallography, Moscow, 1958, Second Edition, 446 p.

ROENTGEN-STEREOMETRY AND SECTIONAL DISPLAY OF COMPUTED THREE-DIMENSIONAL DOSE DISTRIBUTIONS IN RADIO-THERAPY

ULF F. ROSENOW AND WALTER K. LEYDOLPH

University of Goettingen, Goettingen

The introduction of the computer to radiation treatment planning problems, especially to the calculations of dose distributions in irradiated patients, has led to a critical investigation of the fundamental data fed into the computer. While the physical data of the radiation are known to an accuracy of one or two percent, the data to be obtained from the patient are still subject to major inaccuracies. These mostly anatomical data are body outlines, sizes and positions of tumors in the patient, sizes and positions of tissue-inhomogenities as lung, bone, and gas in the bowel, the position of healthy organs which are sensitive to radiation and in proximity to the treatment area, and the exact position of interstitial or intracavitary sealed radioactive sources such as radium, cobalt, or caesium applicators, radio-gold or radon seeds, iridium wires, and others. In all cases a three-dimensional localization, that means a three-dimensional measurement of position and size, of certain structures at or inside the patient is necessary. A roentgen-stereoscopic method, described in the paper and in the demonstrations of Leydolph and Rosenow, was found to be best fitted to these problems of localization, because it anables a very accurate, and as well as a very fast and simple estimation of stereometric x-ray films.

Some applications of roentgen-stereophotogrammetry to radiation treatment planning problems are shown:
(1) The localization of an intrauterine radium applicator relative to the pelvic bones and lymph nodes. The latter were filled with contrast medium. (2) A tumor, indicated by lymphography, was located to place the radiation fields properly. (3) A tumor, bone and lung localization in the thorax is given in elongation, lateral view, and in some cross sections. (4) Body outline, indicated by a metal chain put on the body of the patient, and cross sections through the pelvic bones were drawn. The examples show, that roentgen-stereophotogrammetry is able to give all data of the patient, desired for radiation treatment planning. Some electronically computed isodose cross sections are shown. Besides the display of the three-dimensional results, which until now can only be done in a set of parallel planes, the method is now completely three-dimensional.

MORPHOMETRY OF THE SMALL MYELINATED FIBRES OF THE CORTEX CEREBRI*

HERBERT HAUG

Department of Anatomy, University of Hamburg, Hamburg

The small myelinated fibres in layers I to III
of the cat's visual cortex have been investiga-
ted by means of morphometric methods. The myeli-
nated fibres are the pathways for connection be-
tween the different parts of neuronal tissues.
The magnification of 9500:1 of the electron mi-
crographs was accorded with the scale of measu-
rement of the particle size analyzer (TGZ 3 of
ZEISS). In 153 micrographs 3693 myelinated fi-
bres were counted and measured.
The following results were obtained:
1) With the point-sampling method it was found
that the myelinated fibres make up 7.1 ± 1.6 V_V
of volume fraction.
2) By estimating the surface according to HEN-
NIG (1958) it was found that within a volume of
1 mm³ the myelinated fibres have a surface of
420 ± 70 mm² S_V.
3) The compound length of the myelinated fibres
within a volume of 1 mm³ is $152 \cdot 10^3$ mm L_V.
(Measurement of the length of a threedimensonal
linear tract according to HENNIG 1963).
4) The diameters of 3693 myelinated fibres were
measured with a TGZ 3 and a normal distribution
was found (see fig.). The average diameter of
myelinated fibres was found to be $0.51 \pm 0.08 \cdot 10^{-3}$ mm.
5) With values 3) and 4) a second result of vo-
lume fraction V_V of the myelinated fibres was
calculated. By this way a value of 5.2 % was
found which differs only about 25 % from the
value of 7.1 % obtained by point-sampling
(see 1).
6) With values 3) and 4) a second result of sur-
face S_V of myelinated fibres was calculated and
a surface of 390 mm² in 1 mm³ was found out. This
value differs 8 % from the result of 2) with
420 mm².

The conformity of results obtained by different ways shows for both methods and results a high degree of certainty. Further examinations in neuropil can therefore be executed with these methods. A cube of 1 mm length contains 70 000 neurons in the visual cortex of the cat. Each neuron participates in a medium length of mye- linated fibres of 2 mm.

REFERENCES:

HAUG, H., Med. Grundlagenforsch. 4, 299-344, 1962. HENNIG, A., Zeiss-Werkzeitschrift 30, 3-12, 1958. HENNIG, A., Z. wiss. Mikr. 65, 193-194, 1963.

The length of the myelinated nerve fibres in a volume of 1mm^3

Length of the fibres in m

According to HENNIG (1963) 3693 fibres were measured in an area of 48 650 μ^2. They have a compound length of 152 m

diameter of the fibres in μ
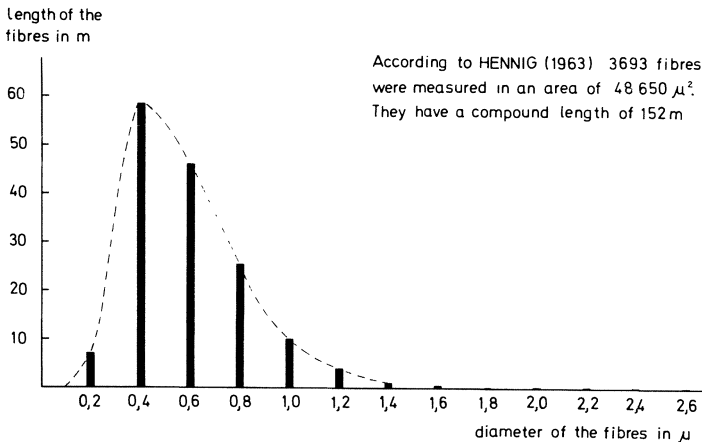
COMPARISON OF SOME QUANTITATIVE STUDIES OF TRABECULAR BONE*

M. H. BARTLEY, JR., S. TARGONSKI, S. SEAMANS AND W. S. S. JEE

Department of Anatomy, University of Utah, College of Medicine, Salt Lake City
Jarrel-Ash Co., Waltham, Massachusetts

Trabecular bone is arranged in densely packed plates through inter-connecting rods to a delicate filigree. In thin slices, trabecular bone appears as "spicules" of varying width which are constantly being re-newed (Arnold et al., 1966; Bromley et al., 1966) with progressive atrophy as a function of age. Many other factors (hormones, disease, radiation, etc.) may alter the rate of atrophy. An increase rate of atrophy may result in osteoporosis (decreased amount of bone). One of the better methods of evaluating osteoporosis is the determination of the quantity of tissue present in bone slices.

In the past, we had the point-counting and tracingpaper-cut out-weighing methods for volume determination. In the present study, these methods were compared to a newer and more rapid automated technique using the Quantimet Image Analyzing Computer Q. T. M. (Fisher, 1966; distributed by Jarrel-Ash Company).

Undecalcified lumber vertebral bodies, predominantly of spongy bone, were embedded in methacrylate, sectioned at 8 micra on a mechan-ized model K Jung microtome and stained by the Von Kossa technique (Bromley et al., 1966). Three different types of analyses were per-formed. The first, the point-counting method, used 75x projection of the bone slice on a 2 x 2 cm grid screen. Total grid intersections lying within the bone were counted as were grid intersections over-lying the mineralized bone tissue. Intersections overlying bone di-vided by total bone hits times 100 yields the percent bone. The slice was rotated six times for counting and approximately 900 intersections were counted per tissue slice. The second, tracing paper-cut out-weighing method, used a 75x tracing of the bone slice. Areas of bone and bone marrow were weighed on a Mettler-P 1200 balance. The weights of the cut out representing bone divided by the total weight of the bone and bone marrow times 100 gives the percentage of bone.

The third method utilized the Q. T. M. to determine the amount of bone and the percent bone. These readings were read directly off the meter. The determinations were performed at 15x magnification with the epidiascope and at 50x with the microscope.

Comparisons of the various methods were made using the tracing paper-cut out-weighing technique as the standard. (Table I).

If the cortex which consists of compact bone is included, there is a 20% difference between total bone and bone without cortex with the standard method. The accuracy appears similar for the three methods texted against the standard method.

The Q. T. M. method is by far the most rapid (3 min./bone slice) with the point-counting second (1-1 1/2 hours) and the tracing paper-cut-out weighing method the most tedious (8 hours). Since these methods are in close agreement in their results, the Q. T. M. would seem the most efficient way of analyzing the quantity of bone in bone slices.

TABLE I.

Percent Bone in Lumbar Vertebral Bodies Determined by Various Methods

Standard Method No. Tracing Paper Cut Out-Weigh	Point-Counting	Standard Method Tracing Paper-Cut Out-Weigh minus Cortical Bone	Epidiascope Q. T. M. minus Cortical Bone (15x)	Microscope Q. T. M. minus Cortical Bone (15x)
MEAN S.D.	MEAN S.D.	MEAN S.D.	MEAN S.D.	MEAN S.D.
37 41.10+5.47	39 67+5.63	31.95+4.74	32.19+5.25	30.40+6.18

BIBLIOGRAPHY

Arnold, J. S., M. H. Bartley, S. A. Tent and D. P. Jenkins. 1966. Skeletal changes in aging and disease, Clin. Orthop. 49:17-38

Bromley, R. G., N. L. Dockum, J. S. Arnold and W. S. S. Jee. 1966. Quantitative histological study of human lumbar vertebrae, J. of Geront. 21:537-543.

Fisher, C. 1966. The metals research image analyzing computer, Particle Size Analysis Conference, Contribution No. 9. Metals Research Ltd., Cambridge, England 1-15.

MORPHOMETRISCHE UNTERSUCHUNGEN AM LABYRINTH DER MEERSCHWEINCHENPLAZENTA

GERHARD A. MÜLLER

Anatomisches Institut, Universitaet Mainz, Germany

ECKART H. WERNICKE AND WOLFGANG M. FISCHER

Frauenklinik, Universitaet Hamburg, Germany

Tierexperimentelle Untersuchungen zum Gasaustausch in der Plazenta wurden an der Meerschw.-Plazenta durchgeführt(Fischer,1966).Da die Größe der Membranflächen für den Gasaustausch nicht bekannt war, wurde versucht, eine Bestimmung mit morphometrischen Methoden zu erzielen.

Die Diffusionskapazität der Plazenta für O_2 hängt von folgenden Faktoren ab:

$$D_{PO_2} = \frac{K \cdot F}{L} = \frac{\dot{V}O_2}{\overline{PO_2}_M - \overline{PO_2}_F} = \frac{\dot{V}O_2}{\Delta PO_2}$$

Dabei ist:

K = O_2-Diffusionsleitfähigkeit

F = Fläche, die den O_2-Transport begrenzt

L = der mittlere Diffusionsabstand für O_2 (mittlere Entfernung zwischen mütterl. u. fetalem Hb-Molekül)

$\dot{V}O_2$ = aufgenommenes O_2-Volumen in der Zeiteinh.

$\overline{P}O_2{}_M$ = mittlerer Sauerstoffpartialdruck im mütt. Blut

$\overline{P}O_2{}_F$ = mittlerer Sauerstoffpartialdr.im fet.Blut

D_{PO_2} wurde durch Perfusion und Druckmessungen mit 19,4·10^{-3} $\frac{ml \cdot O_2}{min \cdot mmHg}$ bestimmt.

Nach Messung der Fläche F und des Diff.-Abstandes L konnte D_{PO_2} auch nach $\frac{K \cdot F}{L}$ errechnet werden.

Dabei wurde K nach Thews(1963) mit

1,0·10^{-5} $\frac{ml \cdot O_2}{cm \cdot min \cdot Atm}$ angenommen.

Wurde F und L im histologischen Schnittpräparat lichtoptisch bestimmt, so ergab sich ein Wert von 18,4·10^{-3} $\frac{ml \cdot O_2}{min \cdot mmHg}$

erfolgte die Bestimmung nach elektronenmikrosk. Aufnahmen, so wurde

18,0·10^{-3} $\frac{ml \cdot O_2}{min \cdot mmHg}$ errechnet.

Bestimmung von F und L

Die Meerschw.-Plazenta hat die Form eines Rotationsellipsoids, dessen Volumen etwa 2,71 cm^3 beträgt.Sie ist in Läppchen und interlobäres Gewebe gegliedert.Mit der Punktzählmethode wurde an histologischen Schnitten 84,15% lobäres Gewebestimmt,also 2,28 cm^3.Jedes Läppchen enthält mütterliche Blutlakunen und fetale Gefäße,deren Wandfläche(Umfang) in Arealen von 100μx100μ in histologischen Schnitten gemessen wurde.Auf das lobuläre Gesamtvolumen bezogen beträgt die fetale Austauschfläche lichtoptisch gemessen 0,28 m^2,nach elektronenmikr.Aufnahmen o,30m^2. L beträgt lichtoptisch 20μ und elektronenmikr. bestimmt 12μ.

Die Größen der e-mikr. erkennbaren Strukturen,die mütterliches und fetales Blut trennen sind auf 10 000 μ^2 bezogen:

Wandlänge der

mütterl.Blutlakunen ohne Mikrovilli	808 μ
" " mit "	8080 μ
fet.Kapillaren(Basalmembran)	1321 μ
" " (inneres Lumen)	723 μ
fet.Trophoblastoberfläche mit Mikrov.	8668 μ
Mittlerer Abstand der Blutlakunen	21,3 μ
" " " Kapillaren	20,3 μ
Dicke der Trophoblastschicht	2 - 5,89 μ

Für die O_2-Diffusion spielt die Membranvergrößerung durch Mikrovilli keine Rolle, so daß für F die Fläche des inneren Lumens der Kapillaren(Innenseite der Kapillarendothelzellen) eingesetzt wurde(0,30 m^2).

Fischer,W.M.,Habil-Schrift,Hamburg,1966
Thews,G.,Ergebn.Physiol. 53,42,1963

ULTRASTRUCTURAL EQUILIBRIA IN LIVER CELL CYTOPLASM

ALDEN V. LOUD

Department of Pathology, College of Physicians and Surgeons of Columbia University, New York, N. Y.

The internal structure of cells has been shown by electron microscopy to consist of many membrane-bounded compartments, see Figures 1 and 2. Some compartments have characteristic size, shape and internal composition, such as the mitochondria (M), microbodies (m) and nucleus (N); while others have irregular shape and are characterized by their limiting membranes, such as the rough- and smooth-surfaced endoplasmic reticulum (r.e.r. and s.e.r.). These structures have been measured by applying the techniques of quantitative stereology to electron micrographs of rat liver cells (Loud et al., 1962 and 1965).

The size, shape and surface areas of cytoplasmic components are highly variable and probably reflect complex dynamic equilibria influenced by both nuclear and extracellular factors. TABLE I. shows some average measurements obtained from many cells in the central, mid-zonal and peripheral regions of normal liver lobules of the rat. Although there are known physiological and enzymatic gradients across the lobule, it was found that the surface areas of rough and smooth endoplasmic reticulum and of mitochondrial envelope maintain nearly constant ratios to each other and to the total cytoplasmic volume in all cells. The size and number of mitochondria vary markedly in different parts of the lobule, as shown in the Table and in the Figures. Their dimensions have been calculated on the basis of an assumed right circular cylindrical shape. Despite this variation, however, the internal cristae membranes of the mitochondria keep a relatively constant surface:volume ratio to the matrix substance in which they are embedded.

REFERENCES:
Loud, A.V., J. Cell Biol. 15, 481-487, 1962.
Loud, A.V., Barany, W. C. and Pack, B.A., Lab. Invest. 14, 996-1008, 1965.

TABLE I

Lobular Distribution of Liver Cell Structures

	Central	Mid-Zonal	Peripheral
u^2 Membranes/Cell			
Rough e. r.	17800	16900	16600
Smooth e. r.	14400	11300	10500
Mito. Envelope	8420	8720	7720
Mito. Cristae	15900	23700	21600
Av. Mitochondrial			
Length u	5.04	4.32	3.85
Diameter u	0.32	0.47	0.56
Volume u^3	0.41	0.75	0.95
No./Cell	1600	1300	1060
Matrix/ Cell u^3	350	550	610
$\dfrac{u^2 \text{ Cristae}}{u^3 \text{ Matrix}}$	45	43	35
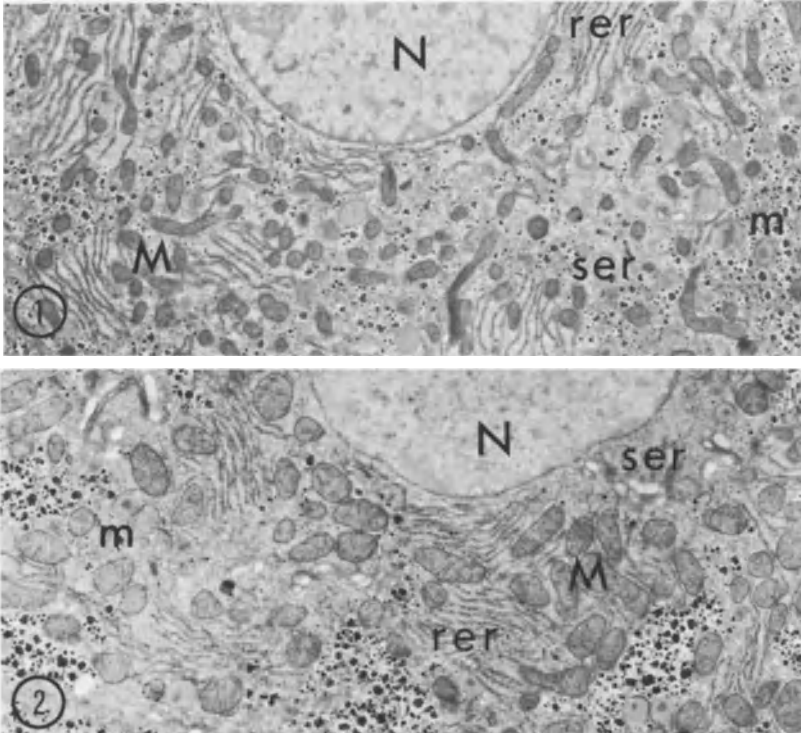
Figures 1 and 2 show portions of rat liver cells from the central and peripheral lobular zones, respectively. Magnification: 6400 X.

SERIAL SECTION ANALYSIS OF GRAIN STRUCTURES

J. H. STEELE, JR.

Department of Metallurgy, University of Florida, Gainesville, Florida

Grain structures in single phase polycrystals consist of statistical aggregates of contiguous polyhedral shaped crystals incident in boundary configurations similar to those occurring in soap froths (Smith[2]). The morphology of the grains and boundary configurations are important parameters in considering the effect of this cellular structure upon the properties. Analysis of the topological parameters is based upon a general approach for measuring the number of physically identifiable features in a sample volume from serial sections.

The theoretical basis for estimating the number of features per unit volume assumes a homogeneous structure within a sample volume V_S; where $V_S \ll V$, the total volume of the structure, and yet larger than the incremental volume between adjacent serial sections. The expected number of features within a sample volume V_S, is: $\langle N_S \rangle = \bar{N}_V V_S$ where $\bar{N}_V$ is their average density. The cumulative number of features observed with the sectioning technique after n incremental volumes $N(n)$ is given by the number observed on the initial section N_O, plus the sum over the number of new features in the n incremental volumes. Thus for n large, i.e., where the cumulative sample volume $V(n)$ is greater than V_S, the summation may be replaced by, $\bar{N}_V V(n)$, yielding:

$$N(n) = N_O + \bar{N}_V \, V(n) \tag{1}$$

The cumulative number of features should therefore increase linearly with volume sectioned, for n sufficiently large. Hence the slope of the cumulative function $N(n)$ yields the average volume density of features.

The analysis of grain boundary morphology is based upon measurement of the average volume density (number per unit volume) of grains, faces, and edges from cumulative section data. This data

74

is provided by identification of individual grains
on successive sections according to their profile
or etching characteristics. The faces and edges
are then identifiable by their incident grains. A
Jung ultramicrotome was used in a slice-electro-
lytic polish-etch-photograph cycle to obtain 72
sections from an Al-1% Mg alloy structure. The
edge configurations observed were in all identifi-

TABLE 1: Data Obtainable Using Topological
Equations With Serial Sectioning.

Parameter	Symbol	Obtained	Value
Grains/vol.	$(N_3)_v$	(Measured)	$49.5mm^{-3}$
Faces/vol.	$(N_2)_v$	(Measured)	$344mm^{-3}$
Edges/vol.	$(N_1)_v$	(Measured)	$524mm^{-3}$
Vertices/vol.	$(N_0)_v$	$=(N_1)_v-(N_2)_v+(N_3)_v$	$230mm^{-3}$
Avg. Number of:			
Vertices/face	$\bar{N}_{20}$	$=3[(N_1)_v/(N_2)_v]$	$4.57(5.1)$
Edges/vertex	$\bar{N}_{01}$	$=2[(N_1)_v/(N_0)_v]$	$4.56(4)$
Faces/vertex	$\bar{N}_{02}$	$=\bar{N}_{20}[(N_2)_v/(N_0)_v]$	$5.83(6)$
Grains/vertex	$\bar{N}_{03}$	$=2-\bar{N}_{01}+\bar{N}_{02}$	$4.27(4)$
Faces/grain	$\bar{N}_{32}$	$=2[(N_2)_v/(N_3)_v]$	$13.9(13.4)$
Edges/grain	$\bar{N}_{31}$	$=3[(N_1)_v/(N_3)_v]$	$31.8(34.2)$
Vertices/grain	$\bar{N}_{30}$	$=\bar{N}_{03}[(N_0)_v/(N_3)_v]$	$19.8(22.8)$
Avg. grain vol.	$\bar{V}$	$=1/(N_3)_v$	$0.02mm^3$
Avg. grain tangent dia.	$\bar{D}_v$	$=(N_3)_A/(N_3)_v$	$0.37mm$
Avg. face area	$\bar{S}_2$	$=S_v/(N_2)_v$	$0.024mm^2$
Avg. surface/grain	$\bar{S}_3$	$=2S_v/(N_3)_v$	$0.33mm^2$
Avg. edge length	$\bar{L}$	$=L_v/(N_1)_v$	$0.15mm$
Avg. dia. for sphere of vol. $\bar{V}$	$\bar{D}$	$=3\sqrt[3]{6\bar{V}/\pi}$	$0.34mm$
Avg. grain profile dia.	$\bar{d}$	$=4/\pi(N_3)_A$	$0.26mm$

able cases triple lines, wherein three grains and
faces impinge. The topological and geometric pa-
rameters obtained using the sectioning technique
in conjunction with ordinary 2-dimensional quanti-
tative stereological analysis are listed in tabu-
lar form with the applicable topological (Smith[2])
and sharing (Coxeter[1]) equations indicated where
used. The consistency of the data is excellent,
since the average number of vertices, triple lines

and faces per grain satisfy the Euler formula for
a simply connected polyhedron. The average vertex
configuration, indicated by $\overline{N}_{01}$, and $\overline{N}_{02}$, is sig-
nificantly different from that which would be ob-
tained if all vertices were quadruple points.

BIBLIOGRAPHY
1. Coxeter, H. S. M., Regular Polytopes, 2nd Ed.,
    Macmillan Co., New York, 1963, p. 72.
2. Smith, C. S., Metal Interfaces, Am. Soc. Met.
    Cleveland, Ohio, 1952, pp. 65-113.

SURFACE AREA AND LENGTH OF CONVOLUTIONS
OF THE CEREBRAL CORTEX

Hans Elias, Steven Kolodny and David Schwartz

Department of Anatomy, Chicago Medical School, Chicago, Illinois

The degree of convolution of the cerebral cortex and its surface area are assumed to be related to the evolutionary status of a mammal. In the past very laborious methods have been used to determine this area. Stereology has provided a reliable and efficient means of obtaining the needed information. We are presently studying brains of man, opossums, kangaroos, whales and dolphins.

The brains, after thorough hardening in 20% formalin (=approx. 7.2% formaldehyde), are cut into slices of constant thickness t. For surface area determination, a grid of parallel lines of constant distance d is layed upon each slice, and the points of intersection of the lines with the cortex-pia interphase are cummulatively counted on each slice.

The formula $S_V = 2 P_L$ (Smith and Guttman) yields the cortical surface area. The reference volume V is a parallelepiped circumscribed around a hemisphere cut parallel to the forehead. It measures 20 cm (transverse) x 20 cm (vertical) x ℓ, where ℓ is the measured length of the brain. P is the number of intersection points counted. L is the total, combined length of test lines. Since the lines are 1 cm apart and the cross section of the circumscribed parallelepiped is 20 x 20 cm^2, L = 20 x 20 x n cm, where n is the number of slices. – The other hemisphere, cut horizontally has an imaginary parallelepiped of 20 x 20 x h cm^3 circumscribed around it, where h is the measured height.

In order to obtain counts in 3 directions perpendicular to each other, the frontal sections are counted with a vertical and a transverse grid; and the horizontal ones with a grid of longitudinal lines (fig. 1). Figure 1 shows a monkey brain for simplicity's sake. The procedure is then repeated using longitudinal and transverse lines on the horizontal sections and vertical lines on the frontal sections. P in the formula will be the total number of points divided by 3. For one male human the cortical surface area was found to be 3052 cm^2, for one female brain it was 2188 cm^2.

Brains of whales are more complex than human brains. Since the average for a species and not data for one individual whale are sought, three entire brains of Globicephala macrorhyncha were sliced, frontally, horizontally and sagittally respectively. The line grid was used on every slice in three directions inclined at 60° to each other (fig. 2). Thus preferential orientation of convolutions can be equalized. At the time of writing this report only one whale brain had been measured. Its cortical surface area is estimated at 5904 cm^2.

The total length of convolutions can be obtained by Hennig's formula
$$L_V = 2 P_{\frac{A}{2}}$$
A is total test area 20 x 20 x n cm^2. P is the number of cortical convexities counted on all slices. Thus the total length of convolutions was estimated to be 2651 cm for the man, 1857 cm for the woman and 4337 cm for the whale.
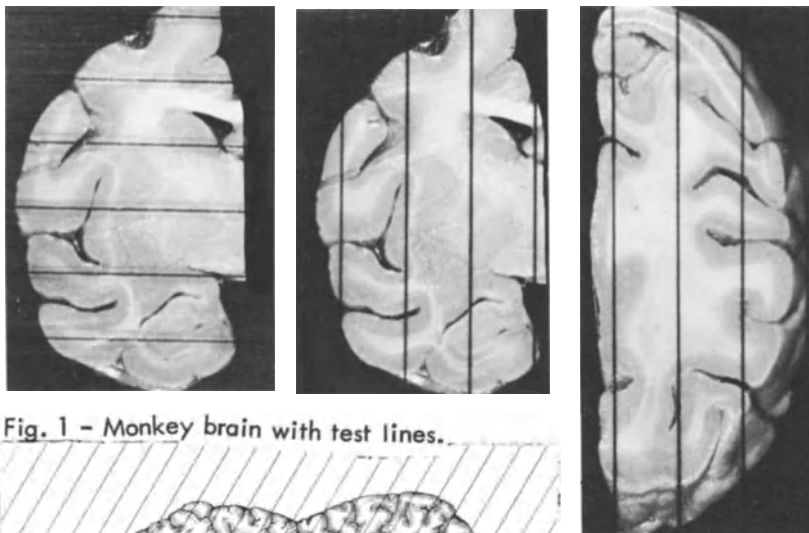
Fig. 1 - Monkey brain with test lines.
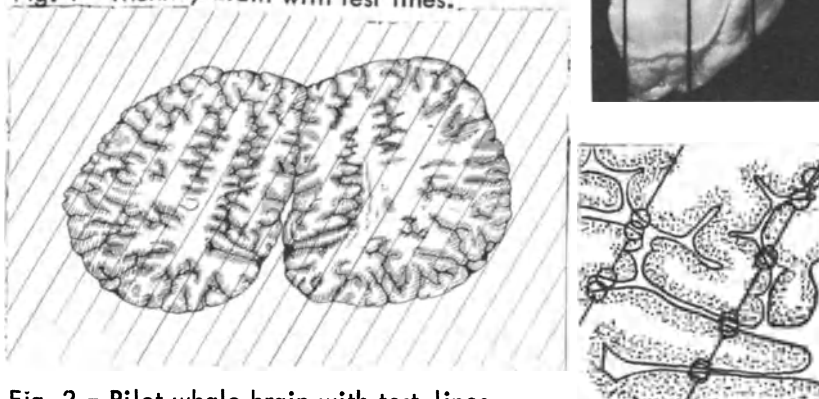
Fig. 2 - Pilot whale brain with test lines,
1 cm apart. 1/3 x

Detail from Fig. 2; 2 x

QUANTITATIVE MEASUREMENTS FROM PROJECTED IMAGES

Ervin E. Underwood

Research Laboratory, Lockheed-Georgia Company, Marietta, Georgia

Examples are given of basic terminology and the equations relating projected images to microstructural features.

PROJECTION OF FIGURES IN A PLANE ONTO A PROJECTION LINE

PROJECTION OF STRUCTURAL FEATURES IN A FOIL ONTO A PROJECTION PLANE
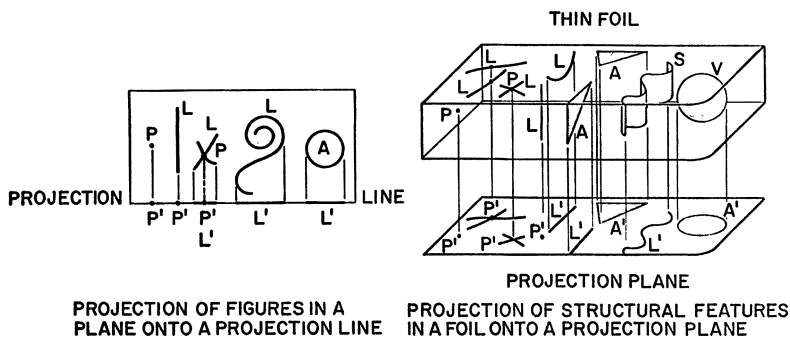
Note dimensional ambiguities on the projection line or plane.

$$\bar{A}' = \bar{L}_2 \cdot \bar{H}'$$
$$\bar{L}_2 = \pi \bar{A}' / \bar{L}_p$$
$$\bar{H}' = \bar{L}_p / \pi$$
$$N'_L = N'_A \cdot \bar{H}'$$
$$\bar{L}_2 = \bar{d}$$

$$v = \bar{A} \cdot \bar{D} = \bar{A}' \cdot \bar{L}_3$$
$$s = 4\bar{A}'$$
$$\bar{A} = \bar{L}_3 \cdot \bar{L}_2$$
$$\bar{L}_3 = 4V/S$$
$$\bar{D} = \bar{H}'$$

$$\bar{A} = \bar{L}_2 \cdot \bar{d}$$
$$\bar{L}_2 = \pi \bar{A} / \bar{L}_p$$
$$\bar{d} = \bar{L}_p / \pi$$
$$N_L = N_A \cdot \bar{d}$$
$$N_A = N_V \cdot \bar{D}$$
$$\bar{L}_2 = \bar{L}_3$$

RELATIONSHIPS AMONG CONVEX PARTICLES IN SPACE, THEIR SECTIONS, AND THEIR PROJECTIONS.
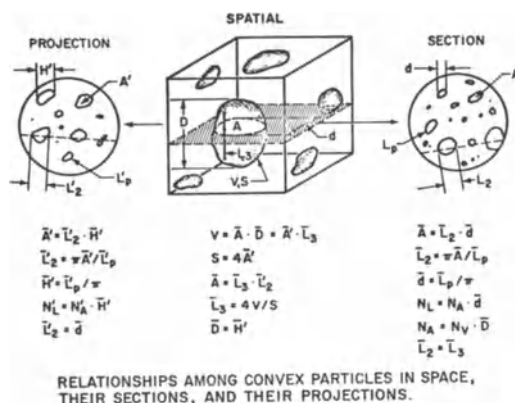
Valid in the absence of particle truncation and overlap.

79
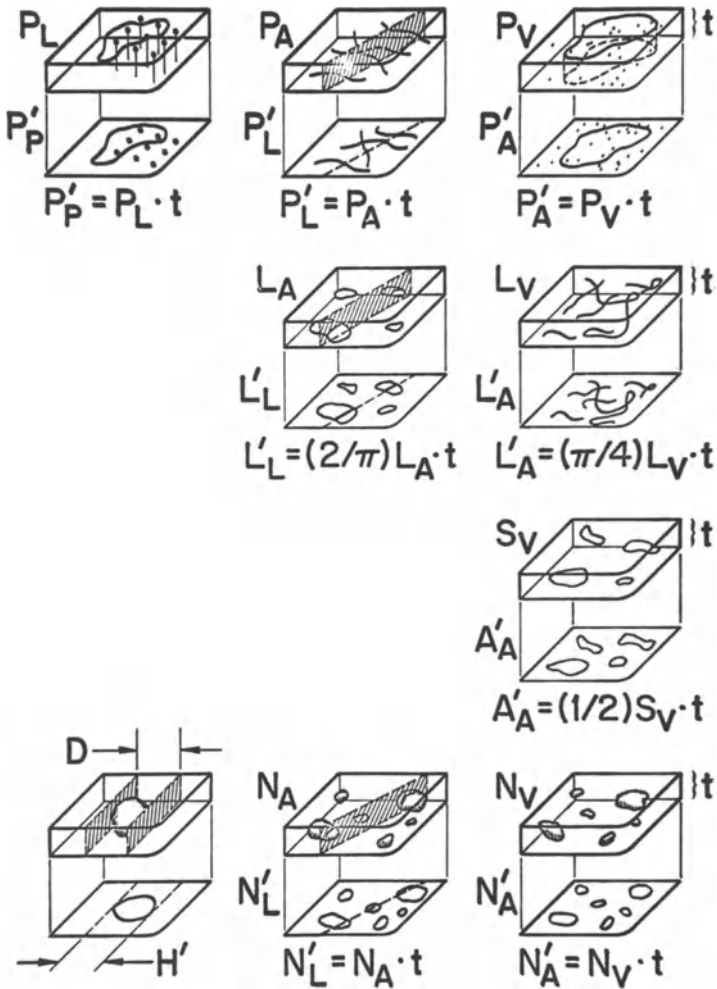
Measurements on the projected plane and their relationship to microstructural features in thin foils.

REFERENCE

E. E. Underwood, Quantitative Stereology, to be published by Addison-Wesley Publishing Co., Inc., Reading, Mass. (1967).

SHAPE   DETERMINATION

FORMBESTIMMUNG VON KÖRPERN
AUS EBENEN SCHNITTEN*

AUGUST HENNIG

Anatomisches Institut der Universität München, München

Rauminhalt und Oberfläche gehören zu den funda-
mentalen Eigenschaften der Körper. Die moderne
Technik fragt nach Trägheitsmomenten und aerody-
namischem Verhalten. Die Stereologie betritt Neu-
land mit der Frage nach der Verteilung der Figu-
ren in zufälligen Schnitten, damit Rückschlüsse
auf die Körperform möglich werden. Ihre Kenntnis
ist für numerisches Auswerten nötig.Kreiszylinder
etwa erreichen im Grenzfalle nicht mehr als die
dreifache mittlere Schnittfläche der eingeschrie-
benen Kugel, während das Volum - und Oberflächen-
verhältnis gegen ∞ strebt. Deshalb ist es nicht
möglich, eine von der Form unabhängige Beziehung
zwischen mittlerer Schnittgröße,Volumen und Ober-
fläche zu finden. Einer Formanalyse sind nur ein-
fache, mathematisch wohldefinierte Körper zugäng-
lich. Ihre Schnittflächen lassen sich eindeutig
klassifizieren und die Klassenbesetzung voraus-
bestimmen. Stünden dagegen von der Venus von Milo
auch tausende von willkürlichen Querschnitten
zur Verfügung, dann wäre der Befund auf die Ver-
mutung beschränkt: "Weiblicher Torso?, etwa le-
bensgroß". Nicht einmal ein Quadratzoll der Ober-
fläche ließe sich wiederherstellen. In solchen
Fällen geht man natürlich von parallelen und pe-
riodischen Schnitten aus. Schon wenige hundert
Serienschnitte würden hier eine fast identische
Rekonstruktion ermöglichen. Der Anatom macht vom
schichtweisen Aufbau Gebrauch, wo er präparato-
risch nicht zum Ziel gelangt. Er muß nur dafür
sorgen, daß die Zuordnung ohne Schiebung und Dre-
hung erfolgt. Sonst könnten aus einem (nicht ver-
muteten) schiefen Kegel ein gerader Kegel, aus
Schraubenkörpern gerade Zylinder abgeleitet wer-
den(Abb.1). Mit Stereologie im eigentlichen Sinn
hat aber eine derartige Synthese nichts zu tun.

---

* Herrn Professor Dr. Hans Elias zum 60.Geburts-
  tag am 28. Juni 1967 gewidmet.

83
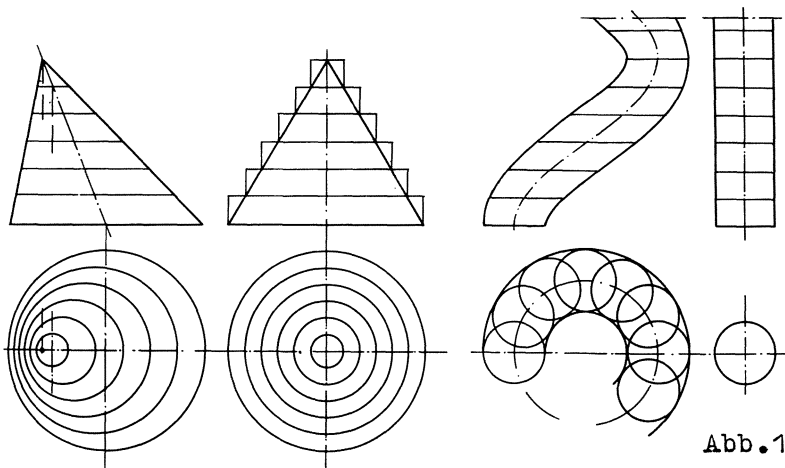
Abb.1

Die Formanalysen der Stereologie gehen vielmehr von einem Haufwerk von Körpern aus, die im Ideal- falle richtungslos gelagert sind. Diese Körper brauchen nicht gleichgroß zu sein; eine Formana- lyse ist aber nur dann sinnvoll, wenn sie einan- der möglichst ähnlich sind. Ferner müssen die Formen einer der folgenden Hauptgruppen angehö- ren: Die erste Gruppe leitet sich aus der Kugel durch stetiges Recken oder Stauchen in einer oder zwei Hauptrichtungen ab; die Deformations- faktoren können beliebig groß werden. Man erhält so das längliche und das abgeplattete Rotations- ellipsoid, das dreiachsige Ellipsoid und die Grenzfälle des allgemeinen Zylinders, des dünnen Stabes und der ebenen, gleichdicken Platte. Die andere Gruppe umfaßt die Welt der Kristalle mit regelmäßig angeordneten ebenen Flächen; sie kann nicht Gegenstand dieser Betrachtung sein.

a) DIE KUGEL

Wenn nur Kreise als Schnittfiguren vorkommen, dann ist die Kugelgestalt gesichert. Für einen Kugelhaufen ist die Größenschwankung durchaus ein Formproblem. Ihre Ableitung aus der Varia- tion der Schnittkreisdurchmesser birgt nament- lich für dicke Schnitte erhebliche Schwierigkei- ten, die von BACH [1] gemeistert wurden.

b) DER DÜNNE ZYLINDER (STAB) IN DICKEN SCHNITTEN (D $\ll$ T)

Die Form gerader Stäbe ist in den Projektionen ebenfalls sofort kenntlich. Die Frage, ob neben

84

sehr langen Stäben (durch gelegentliche sehr fla-
che Projektionen gesichert) auch kurze Stücke in
der Größenordnung der Schnittdicke T vorkommen,
kann aber nur durch einen Vergleich der wirkli-
chen Verteilung der Abschnittsprojektionen mit
der Charakteristik der Schnittbilder unendlich
langer Geraden beantwortet werden.
Ein durch die Schnittdicke T begrenzter Geraden-
abschnitt mit Neigung φ gegen die Normale er-
scheint als Strecke s = T.tg φ (Abb.2). Wie ver-
teilen sich diese Längen nach ihrer statistisch-
en Erwartung?
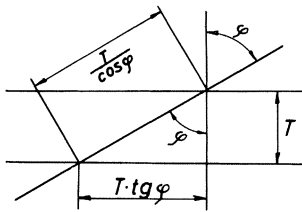
Abb.2
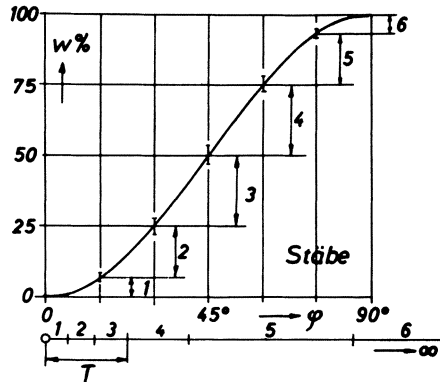
Abb.3

1. Kriterium: $w_1 \sim \sin \varphi$ (Richtung gegen Normale)

2. Kriterium: Jede Richtung im Raum (φ, ψ) muß mit
gleichem Volumanteil vertreten sein. Die Häufig-
keit w_2 muß daher umgekehrt proportional zum Ein-
zelvolumen sein. Volumen $\sim L \sim T/\cos \varphi$, also
$w_2 \sim \cos \varphi / T \sim \cos \varphi$.
$w = w_1 . w_2 \sim \sin \varphi . \cos \varphi$.

Die Summenkurve ergibt sich aus $\int_0^\varphi \sin\varphi\cos\varphi\,d\varphi \sim \sin^2\varphi$

als Sinuskurve der Abb.3. Die bekannte Schnitt-
dicke T teilt alle Projektionen in eine kürzere
und eine längere Hälfte. Einer genaueren Analyse
dient ein Maßstab mit den Projektionen T.tg φ der
Vielfachen von $\varphi = 15°$. Dank den fünf Zwischen-
punkten der experimentellen Kurve können kleine
statistische Schwankungen ausgeglichen werden.
Größere Sicherheit bietet aber erst die mittlere
wahrscheinliche Abweichung. In Abb.3 werden die
festen Ordinaten der Theorie (auch bei idealen
Bedingungen nur durch unendlich viele Versuche
einzustellen) um die Beträge $\pm r$ erweitert, die für
100 Teste zu erwarten sind [4]. Durchschnittlich
in der Hälfte der Fälle ist das Einhalten dieser

85

Schranken zu erwarten, d.h. in 2 oder 3 Ordinaten
sollte der Versuchswert sich an sie halten.
Erscheint diese Bedingung zu großzügig, dann kön-
nen, 400 Versuche vorausgesetzt, diese Grenzen
auf die Hälfte eingeengt werden.
Wollte man die vom Rand beschnittenen Projektio-
nen verwerfen, dann würden die größeren Längen
benachteiligt werden. Besser ist es, jedes zwei-
te Bruchstück mit der doppelten Länge zu werten.
Diskussion: Abweichungen der experimentellen
Kurve nach unten decken auf, daß die Bedingung
regelloser Lagerung oder Schnittführung nicht er-
füllt wurde. Unter der Voraussetzung, daß daran
kein Zweifel besteht, verrät eine Summenkurve
mit größeren Ordinaten, daß kurze Nadeln von der
Größenordnung T neben großen Längen vorkommen.

c) KREISZYLINDER UND ELLIPTISCHE ZYLINDER
IN DÜNNEN SCHNITTEN

Dieser Fall wurde in den "Contributions to the
geometry of sectioning 7" bearbeitet [6]. Das
Schaubild der Summenkurven ist in Abb.4 noch ein-
mal wiedergegeben. Nur bei Kreiszylindern können
Dickenschwankungen unmittelbar an den kleinen
Durchmessern 2b der Schnittellipsen festgestellt
werden.

Abb.4
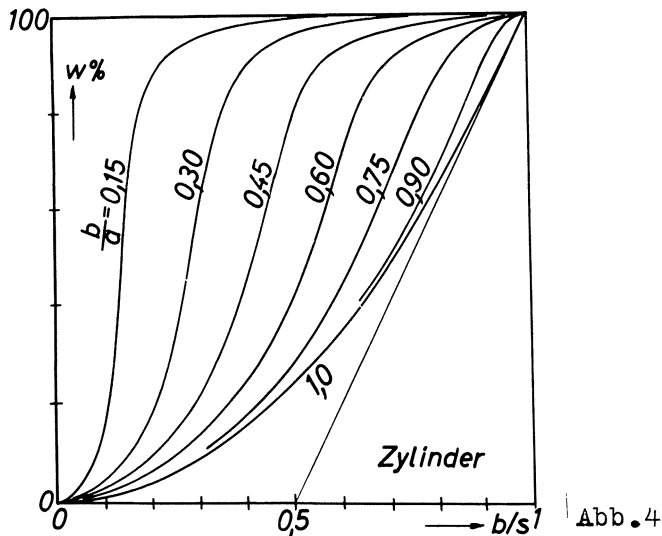
Dicke Zylinderschnitte bedürfen keiner eigenen
Betrachtung, weil die Projektionen der Mantel-
flächen geradlinig und von den elliptischen
Schnitten deutlich zu unterscheiden sind.

d) PLATTEN MIT DICKE D IN SCHNITTEN T

Auch Platten sind in Schnitten sofort zu erken-
nen: Sie liefern langgestreckte gerade Bänder in
verschiedenen Breiten. Eine vermutete konstante
Dicke D ist gleich der geringsten Schnittbreite x.
Eine Wahrscheinlichkeitsbetrachtung analog b)

ergibt (Abb.5): $\left.\begin{matrix} w_1 \sim \sin \varphi \\ w_2 \sim \sin \varphi \end{matrix}\right\}$ w $\sim \sin^2\varphi$.

Während bei Zylindern der Schnittwinkel $\varphi = 45^{\circ}$
am wahrscheinlichsten ist, sind bei der Platte
Normalschnitte vorherrschend. Der Verlauf der
Summenkurve für x folgt mit Parameter φ aus:

$$x = \frac{D}{\sin \varphi} + \frac{T}{\mathrm{tg}\,\varphi} \quad und \quad y = \int_0^{\varphi} \sin^2\varphi\,d\varphi = \frac{\varphi}{2} - \frac{\sin 2\varphi}{4}$$
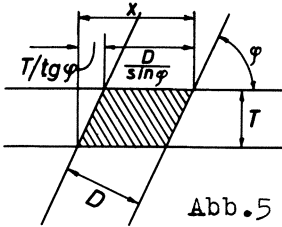
Abb.5
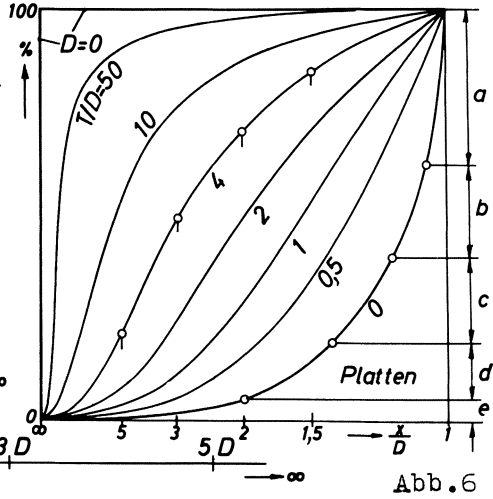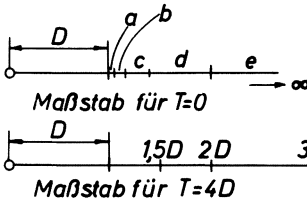
Abb.6

Für $\varphi = 0$ wird x unendlich groß. Es liegt nahe,
die Abszissenachse nach den Reziprokwerten D/x
linear zu teilen. Für ausgewählte Beträge von
T/D erhält man die Kurvenschar der Abb.6.
Diskussion: Bei sehr dünnen Blättern (D ≪ T) ist
die Größe D nicht einwandfrei anzusprechen. Für
D = T/50 z.B. haben nur 1% aller Projektionen ei-
ne Breite zwischen D und 2D. Eine Entscheidung
darüber, ob D konstant, ist daher nicht möglich.
Für stärkere Platten gilt: Nur, wenn die gering-
ste Breite nicht vereinzelt vorkommt, darf ein-
heitliche Stärke D vermutet werden. Gewißheit er-
bringt aber erst ein Vergleich der experimentel—

len mit der zugehörigen Kurve aus Abb.6. Für
Zwischenwerte von T/D muß die Summenkurve inter-
poliert oder eigens berechnet werden. Auch der
Maßstab ist von Fall zu Fall zu entwerfen,wie in
Abb.6 für T/D = 0 und T/D = 4 vorgeschlagen ist.
Ein statistisch gesichertes Abweichen nach oben
deckt das Vorkommen von Plattendicken > D auf.

e) DAS GESTRECKTE UND DAS ABGEPLATTETE
   ROTATIONSELLIPSOID IN DÜNNEN SCHNITTEN

Alle parallelen Schnitte liefern ähnliche Ellip-
sen. Wir können uns daher auf Schnitte durch den
Mittelpunkt beschränken.
Gestreckte und abgeplattete Formen lassen sich
in Schnitten von Körperhaufen durch den Augen-
schein sofort unterscheiden: Wenn die extremsten
Ellipsen zugleich durchschnittlich am größten
sind, liegen längliche Ellipsoide vor. Nähern
sich die größten Schnitte der Kreisform, dann
sind die Körper abgeplattet. Das Achsverhältnis
a/b kann aus den extremen Schnittformen abgele-
sen werden. Um auszuschließen, daß Mischungen
mit rundlicheren Formen vorliegen, bedarf es
wieder einer genaueren Analyse der Schnittformen.

a/b > 1 gilt für ge-
streckte Formen

b/a > 1 gilt für
abgeplattete Ellip-
soide (Linsen)
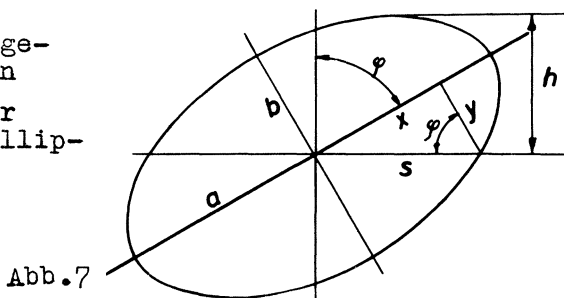
Abb.7

In Abb.7 ist ein Achsschnitt des Ellipsoides in
Stellung φ dargestellt. Die Halbachsen der
Schnittellipse sind b und s. Die Wahrscheinlich-
keit, daß diese Lage in Schnitten beobachtet wer-
den kann, hängt einerseits von der Funktiongröße
sin φ = x/s, andererseits von der Erwartung eines
Schnittes in der Lage φ ab. Deren Kriterium ist
die Erstreckung senkrecht zur Schnittrichtung,
ihr Halbwert gleich h. Daher $w \sim h.\sin\varphi$
Durch eine "Schiebung" kann aus der Ellipse a,b
eine flächengleiche Ellipse mit den Halbachsen
s und h abgeleitet werden, sodaß gilt:

$$h.s = a.b \quad \text{und} \quad h = a.b/s$$

88

Die Wahrscheinlichkeit, daß eine Schnittellipse
b,s vorkommt, ist demnach $W \sim \dfrac{a \cdot b}{s} \cdot \dfrac{x}{s} \sim \dfrac{x}{s^2}$

Aus der Ellipsengleichung folgt mit $s^2 = x^2 + y^2$:

$$x = a\sqrt{\dfrac{s^2 - b^2}{a^2 - b^2}} \left.\begin{matrix} \\ \\ \\ \end{matrix}\right\} \quad W \sim \dfrac{a}{s^2}\sqrt{\dfrac{s^2 - b^2}{a^2 - b^2}} \sim \dfrac{\sqrt{s^2 - 1}}{s^2} \quad (b = 1)$$

$$y = b\sqrt{\dfrac{a^2 - s^2}{a^2 - b^2}}$$

Für das Ellipsoid a/b = 2 wird in Abb.8 diese
Abhängigkeit von der Neigung φ dargestellt.
Man geht von runden Werten s aus, etwa von s = 1,1

Dazu
gehö-
ren
$\left\{\begin{matrix} tg\,\varphi = \dfrac{x}{y} = \dfrac{a}{b}\sqrt{\dfrac{s^2 - b^2}{a^2 - s^2}} = 2\sqrt{\dfrac{1,21 - 1}{4 - 1,21}} = 0,548; \\[2mm] W \sim \dfrac{\sqrt{1,21 - 1}}{1,21} \sim 0,379 \end{matrix}\right. \quad \varphi = 28,7°$

A = 17,1	B = 13,7	C = 20,0	D = 14,8	E = 20,1	F = 14,3
ΣF=	30,8	50,8	65,6	85,7	100
28,7°	39,8°	54,0	64,3°	79,0°	
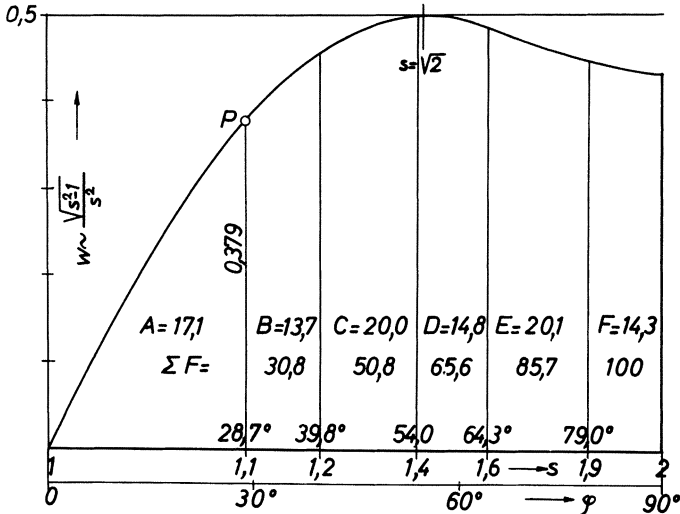
Abb.8

Über dem Abszissenwert 28,7° wird der Proportio-
nalitätsfaktor 0,379 aufgetragen (P der Abb.8).
Die Kurve hat ein Maximum, das unabhängig vom
Achsverhältnis a/b bei s/b = $\sqrt{2}$ auftritt. Das ist
schon für den Kreiszylinder gezeigt worden [3].
Wird a/b < $\sqrt{2}$, dann gehört der Größtwert zu a/b.
Setzt man die Gesamtfläche der Kurve = 100, dann
sind die von den Zwischenordinaten begrenzten
Flächen das Äquivalent der Ordinaten der Summen-
kurve in Prozent (Flächen und Punkte A bis F der
Abb. 8 und 10).
In Abb.9 sind die Abszissen dieser Kurven für
a/b = 1, 2, 3 und 4 linear nach s/b unterteilt.

89
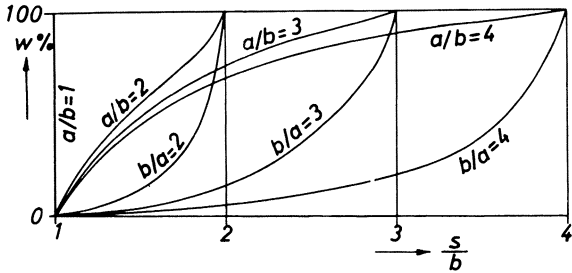
Abb.9

Bei dieser Darstellung haben nur die gestreckten
und die abgeplatteten Formen mit gleichem a/b
bzw. b/a außer dem Anfangs- auch den Endpunkt
gemeinsam. Um Überschneidungen zu vermeiden und
das geschlossene **Bild** der Zylinder- und Platten-
kurven nachzuahmen, braucht man nur die Abszis-
sen-Endpunkte a/b unter Anpassen des Maßstabes
von Fall zu Fall in einem Punkt zusammenzufassen
(Abb.10).
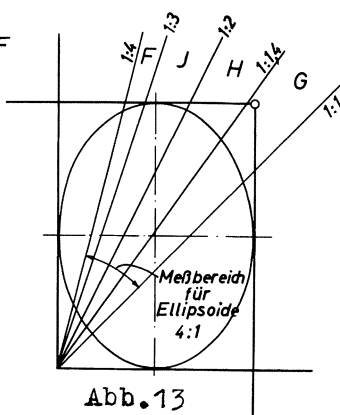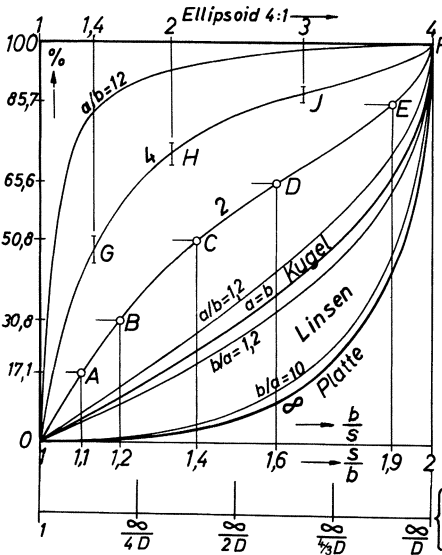
Abb.13

Abb.10

Die Scharen der Kurven für die beiden Arten von
Ellipsoiden nehmen nunmehr getrennte Bereiche
ein. So, wie die Kugel zwischen beiden Hauptfor-
men steht, muß eine Grenzlinie zwischen beiden
Bereichen existieren. Versuchstechnisch ist sie
ohne Bedeutung, weil sie samt ihrer nächsten Um-
gebung unzugänglich ist. Weil aber eine mathema-
tisch gesicherte Schranke für zeichnerisch ge-
wonnene Kurven zu begrüßen ist, soll diese Linie

durch eine Grenzbetrachtung abgeleitet werden
(Abb.11):
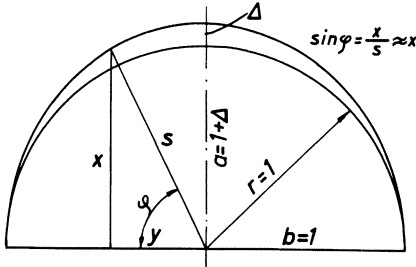
Abb.11
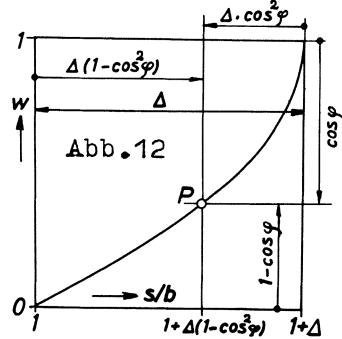
Die beiden Hauptachsen des nahezu kugel-
förmigen Ellipsoids seien a = 1+Δ und b = 1 ,
wobei Δ eine unbegrenzt abnehmende Länge sei.
Die Gleichung der Schnittellipse lautet daher:

$\frac{x^2}{(1+\Delta)^2} + \frac{y^2}{1} = 1$. Weil $\Delta^2 \lll \Delta$ und $\Delta \lll 1$, gilt:

$x^2(1-2\Delta)+y^2 \approx 1; \quad x^2+y^2 \approx 1+2x^2\Delta; \quad \sqrt{x^2+y^2} \approx 1+x^2\Delta$

Von den beiden Faktoren, die die Wahrscheinlich-
keit eines Schnittes bestimmen, hängt der erste
von $\sin\varphi$ ab, variiert also von 0 bis 1. Der an-
dere, an die Höhe gebunden, schwankt dagegen nur
von 1 bis 1+Δ , darf daher als Faktor von $\sin\varphi$
vernachlässigt werden: $\quad w \sim \sin\varphi$

$\left| w \right|_0^\varphi \approx \int_0^\varphi \sin\varphi\, d\varphi \approx 1 - \cos\varphi =$ Ordinate der Summenlinie

Das Achsverhältnis s/b der Schnittellipse für φ:

$\frac{s}{b} = \frac{\sqrt{x^2+y^2}}{1} \approx 1+x^2\Delta \approx 1+\Delta\cdot\sin^2\varphi \approx 1+\Delta(1-\cos^2\varphi)$.

s/b liefert die Abszissen der Summenlinie; ihre
Werte reichen von 1 bis 1+Δ ; Δ wird endlich
groß dargestellt.

Trägt man den Punkt P $\begin{cases} \Delta(1-\cos^2\varphi) \\ 1-\cos\varphi \end{cases}$ in das für a/b = 1+Δ

gezeichnete Feld ein (Abb.12), dann erkennt man,
daß er auf einer Parabel mit dem Scheitel in der
rechten oberen Ecke wandert. Diese Kurve zweiten
Grades trennt zwei Scharen von höherer Ordnung,
die einer einfachen mathematischen Darstellung
unzugänglich sind. Das gute Einfügen der gesich-
erten Parabel zeigt, daß die Konstruktion ohne
sichtbare Ungenauigkeit gelungen ist.
Welche Außengrenzen haben die Kurven der Abb.10?

Für Kreiszylinder und Platten springt in der ge-
wählten Abszissenteilung das Achsverhältnis der
Schnitte vom Wert 1 sofort auf ∞ ; alle endlichen
Zylinderschnitte (das sind 100%) fallen deshalb
auf die Ordinate über s/b = 1 und die Summenlinie
artet in den linken und den oberen Rand des Fel-
des aus. Um Zylinder zu analysieren, muß eine
andere Abszissenteilung gewählt werden. Im Schau-
bild für den allgemeinen Zylinder (Abb.4) wurden
die Reziprokwerte von s/b linear aufgetragen mit
dem Erfolg, daß der Grenzfall des Kreiszylinders
als Parabel erscheint.
Beim entgegengesetzten Extremfall, der Ausartung
der Linse zur ebenen Platte, gehört dagegen zur
Abszisse 1 in Abb.10 nur der singuläre Fall mit
w = 0 des Parallelschnitts; die Folge aller
Schrägschnitte erstreckt sich über die verschie-
denen Grade der Unendlichkeit der Abszissenwerte.
Die Summenkurve kann aus Abb.6 für die Platten
(Grenzkurve T = 0) wegen der reziprok überein-
stimmenden Teilung übernommen werden. Auch diese
punktweise streng definierte Kurve schließt sich
stetig an die Schar der Linsencharakteristiken
an, ein weiterer Beweis für Richtigkeit und Ge-
nauigkeit des zeichnerischen Verfahrens. Eine für
den Gebrauch geeignete Darstellung bringt [5].
Trotz dem ähnlichen Aussehen der Abb.6 und 10
besteht außer der identischen rechten Grenzkurve
kein Zusammenhang: Abb.6 gilt für eine Form und
veränderliche Schnittdicke bei festem Abszissen-
maßstab. Abb.10 setzt dagegen Schnittdicke T = 0
voraus und umfaßt alle Formen von der Platte
über die Kugel bis zum Zylinder, was nur mit Hil-
fe eines veränderlichen Maßstabes gelingt.

In der Praxis sucht man zunächst die extreme
Schnittform (vom Kreis, der auch eine Extremform
ist, kann abgesehen werden, weil er allen Ellip-
soiden gemeinsam ist). Liegt das Achsverhältnis
4:1 vor, dann verteilt man auf der zugehörigen
Kurve einige Punkte, etwa mit s/b = 1,4:1, 2:1
und 3:1 (G,H und J der Abb.10 mit den Schranken
der mittleren Abweichung bei 100 Versuchen).
Die Zuteilung zu den so festgelegten vier Form-
gruppen geschieht ohne Umweg über mühsames Messen
und Dividieren der Achslängen mit zwei beweglichen
chen Winkeln, die parallel zu den Hauptachsen an
den Schnitt angelegt werden (Abb.13 mit den Win-
kelräumen G, H, J und F; die gezeigte Ellipse ge-
hört zur Formgruppe G).

92

<u>Diskussion:</u> Überhöhung der gefundenen Summenlinie
deutet auf Beimengung von rundlicheren Formen
oder auf dreiachsige Ellipsoide hin.
<u>Übergang von Ellipsoiden zu Kreiszylindern:</u>
Während Platten und extrem flache Linsen im
Schnittbild immer zu unterscheiden sein werden,
sind die Übergänge vom langgestreckten Ellipsoid
zum unbegrenzten Zylinder fließend.
Beim Kreiszylinder sind Schnittformen mit a/b > 8
nur in 1,2% der Fälle zu gewärtigen. Sie können
daher auch in größeren Serien fehlen, besonders
wenn solch langgestreckte Flächen das Gesichts-
feld überschneiden. Überträgt man die Summenkurve
des Zylinders mit der falschen Begrenzung 8 statt
∞ in das Schaubild der Ellipsoide, dann unter-
scheiden sich die entsprechenden Kurven so wenig,
daß eine Klärung über die Natur der Körper aus-
sichtslos erscheint (Abb.14).
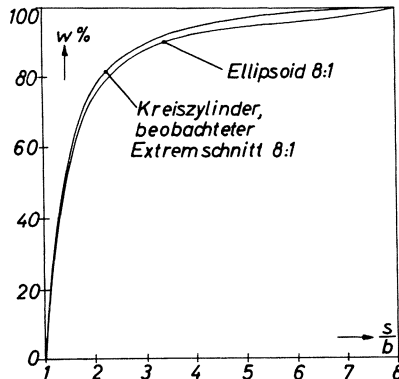
Abb.14

Hier müssen andere Kriterien helfen: Haben alle
Schnittellipsen eine gemeinsame kleine Achse,
dann liegen mit Sicherheit Schnitte von Kreiszy-
lindern konstanten Durchmessers vor. Auch eine
Verteilung der Längen der kleinen Achsen in der
Art einer Normalverteilung läßt auf Zylinder,
diesmal mit variierender Dicke, schließen.
Für Ellipsoide muß sich, genau wie für die Kugel,
eine ausgesprochen schiefe Verteilung ergeben
(die größten Schnitte treten am häufigsten auf).
Sie kann auch durch zusätzliche Größenschwankung
nicht ganz verwischt werden.

<u>Der elliptische Zylinder</u> erheischte erheblich
größere Anstrengungen [6]. Dabei ist er nur ein
Sonderfall des dreiachsigen Ellipsoids. Für die-
ses würde der graphische Lösungsweg sehr aufwen-

93

dig werden. Vielleicht gelingt mit den exakten Rechenvorschriften von BACH [2] für das Rotationsellipsoid eine Ausweitung auf den Fall dreier verschiedener Achsen.

Auch die Untersuchung der Rotationsellipsoide in dicken Schnitten steht noch aus.

Die zweite Hauptgruppe, die ebenflächig im Endlichen umgrenzten Körper, widerstehen einer Behandlung mit einfachen stereologischen Überlegungen. Hier können mathematisches Denken und die modernen Rechenverfahren Triumphe feiern. Während KNESER [7] für das allgemeine Tetraeder noch eine strenge Lösung für die Verteilung der drei- und viereckigen Schnitte (T = 0) und Projektionen (T = ∞) geben konnte, mußte Myers [8] für höhere Körper zunehmend auf exakte Befunde verzichten und auf Computerrechnung ausweichen.

LITERATUR

[1] Bach, G., Bestimmung der Häufigkeitsverteilung der Radien kugelförmiger Partikel aus den Häufigkeiten ihrer Schnittkreise in zufälligen Schnitten der Dicke δ
Z.wiss.Mikrosk., 66, 193-200, 1964
Dort weitere Literaturangaben.

[2] Bach, G., Zufallsschnitte durch ein Haufwerk von Rotationsellipsoiden mit konstantem Achsverhältnis
Z.angew. Math. Physik, 16, 224-232, 1965

[3] Hennig, A., Zur Geometrie von Schnitten
Z.wiss.Mikrosk., 63, 362-365, 1957

[4] Hennig, A., Nomogramme für den Gebrauch der Integrationsokulare von Zeiss
Zeiss-Prospekt G 40-195, 1958

[5] Hennig, A., und H.Elias, Theoretical and experimental investigations on sections of rotatory ellipsoids
Z.wiss.Mikrosk., 65, 133-145, 1963

[6] Hennig, A., and H. Elias, Elliptical cylinders. Z.wiss.Mikrosk., 66, 226-234, 1964

[7] Kneser, H., Schnitte durch Tetraeder
Berichte des Ersten Internationalen Kongresses für Stereologie, Wien, April 1963

[8] Myers, E.J., Quantitative metallography of cylinders, cubes and other polyhedrons
Berichte, Wien, April 1963

THE RELATIONSHIP BETWEEN MEAN SURFACE CURVATURE AND THE STEREOLOGIC COUNTING MEASUREMENTS

R. T. DeHoff

Department of Metallurgical and Materials Engineering, University of Florida, Gainesville, Florida

In any structural change driven by surface tension, the local geometric variable of central importance is the mean curvature of the surfaces involved. Gibbs showed[1] that the local values of both the chemical potential and of the pressure difference supported by an interface are proportional to the local mean surface curvature. A method for estimating mean surface curvature, based upon a relationship between the average of this quantity and two of the basic counting measurements of stereology, is presented in this paper.

In addition, a new counting measurement, the Rhines Tangent Count, is introduced.

The derivation of this fundamental relationship involves the following steps:

1) For two-dimensional structures:
   a) The definition of the average curvature of particle outline, $\bar{k}$;
   b) The derivation of the relationship between $\bar{k}$ and the total angle subtended by particle outline;
   c) The development of the relationship between subtended angle and the Rhines Tangent Count, T_A, or area outline count, N_A.

2) For three-dimensional structures:
   a) The definition of local mean surface curvature, H;
   b) The definition of the average of H for a structure;
   c) The derivation of the relationship between $\bar{H}$ and $\bar{k}$, when $\bar{k}$ is evaluated upon a representative section through the three-dimensional structure;
   d) The statement of the relationship between $\bar{H}$ and the counting measurements.

Curvature Relationships in
Two Dimensional Structures

Consider a two-dimensional structure consisting of at least two identifiably different kinds of areas, separated by a collection of boundaries. Focus attention upon an element of this boundary, of length, $d\lambda$. The local curvature, $k(\lambda)$, of the boundary in the region, $d\lambda$, may be defined as the reciprocal of the radius of a circle that passes through three adjacent points on the boundary[2]. The average curvature of boundary in the two-dimensional structure may be defined as

$$\overline{k} = \frac{\int_\lambda k(\lambda)d\lambda}{\int_\lambda d\lambda} \qquad (1)$$

If the "angle subtended by the arc, $d\lambda$", is the angle between normals erected at the ends of the arc, see Figure 1, it can be shown that the local curvature is the rate of change of this subtended angle with arc length, as one proceeds along the arc:[2]

$$k(\lambda) = \frac{d\theta}{d\lambda} \qquad (2)$$
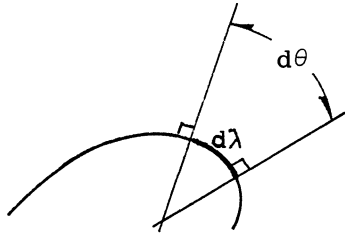
Figure 1. The local curvature of a two-dimensional arc may be visualized as the rate of change of the orientation of the normal with arc length.

96

Substitution of (2) into (1) gives

$$\overline{k} = \frac{\int_\lambda (\frac{d\theta}{d\lambda}) d\lambda}{\int_\lambda d\lambda} = \frac{\int_\lambda d\theta}{\int_\lambda d\lambda}$$

The numerator of this expression is the total angle subtended by all arc in the structure, while the denominator is the total length of that arc. More specifically, the numerator is the net subtended angle, since convex arc, which has positive curvature, subtends a positive angle, by definition, and concave arc subtends a negative angle. Thus:

$$\overline{k} = \frac{\theta_{net}}{\lambda} \qquad (3)$$

If the numerator and denominator are divided by the area of the structure observed, this relationship may be formulated in terms of normalized properties:

$$\overline{k} = \frac{\theta_{Anet}}{L_A} \qquad (4)$$

The total length of arc in unit area may be evaluated from one of the established fundamental relationships of quantitative stereology[3]:

$$L_A = \frac{\pi}{2} P_L \qquad (5)$$

The total subtended angle may be unambiguously estimated from the Rhines Area Tangent Count, obtained by sweeping a test line across a two dimensional structure, and counting the number of times the line forms a tangent with the outline of the specie of area being studied. The procedure is illustrated in Figure 2. The underlying theory will now be developed.

If the element of arc, $d\lambda$, is approached by an aggregate of sweeping test lines, those test lines whose directions of traverse lie within the angle, $d\theta$, subtended by the normals at the ends of the curved element of arc, will form tangents; those outside this range will not. If the directions of sweep are uniformly distributed over the circle of orientation, the fraction of test lines that form tangents with $d\lambda$ is the fraction of the

97

$$T_{A+} = \frac{29}{A}$$

$$T_{A-} = \frac{10}{A}$$

$$T_{Anet} = \frac{19}{A}$$
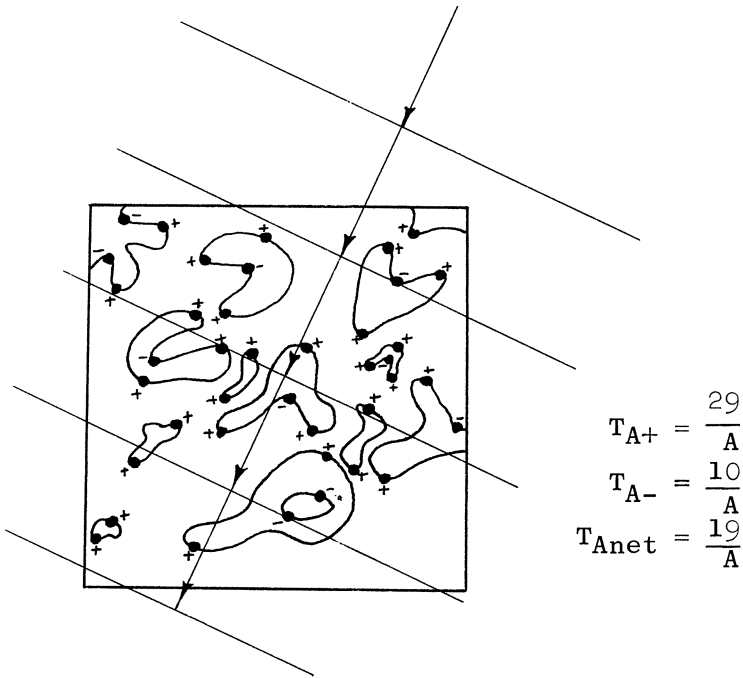
Figure 2. Illustration of the procedure for the evaluation of the Rhines Tangent Count. A is the area of structure analysed.

circle of orientation occupied by the orientation range, $d\theta$; i.e., $d\theta/\pi$. If N test lines are swept over the area, the number of tangents formed is $Nd\theta/\pi$. If the area of the structure traversed is A, the total area swept by all of the tangent lines is NA. The number of tangents formed with $d\lambda$, per unit area of structure swept, is

$$dT_A = N\frac{d\theta}{\pi}\frac{1}{NA} = \frac{1}{A}\frac{d\theta}{\pi} \qquad (6)$$

This result applies to each element of arc in the structure. The total tangent count produced by all arc contained in unit area of the structure is the sum of the counts produced by each element:

$$T_A = \int_\lambda dT_A = \int_\lambda \frac{d\theta}{A\pi} = \frac{\theta}{A\pi} = \frac{\theta A}{\pi} \qquad (7)$$

If this result is applied separately to convex

and concave elements, by separately recording the
tangents formed with each kind of arc, the net
angle subtended by particle outline in the struc-
ture may be evaluated:

$$\theta_{Anet} = \pi[T_{A(convex)} - T_{A(concave)}] \blacksquare \pi T_{Anet} \quad (8)$$

where T_{Anet} is the difference between the tangent
count for convex arc, and that for concave arc.

The substitution of equations (8) and (5)
into (4) yields a fundamental relationship of
quantitative stereology which may be used to es-
timate the average curvature of particle outline
in an arbitrary two-dimensional structure:

$$\overline{k} = 2\ \frac{T_{Anet}}{P_L} \quad (9)$$

Surface Curvature in Three-Dimensional Structures

Consider a three-dimensional structure con-
sisting of at least two identifiably different
kinds of volumes, separated by a collection of
surfaces. Focus attention upon an element of
this surface, of area, dS. The curvature of this
surface element is specified in terms of two param-
eters, called the principle normal curvatures.
These parameters are defined by the following
construction.

Consider the set of planes that intersect
this surface element, and contain the vector
which is its normal. Evaluate in the region of
dS the curvature of the curve of intersection of
each plane and the surface. It can be shown[2]
that the curvatures thus obtained vary between
some maximum and minimum value, and that the two
planes that give these extreme values of section
curvature are orthogonal. The extreme values of
section curvature obtained by this construction
are called the principle normal curvatures for
the surface, denoted K_1 and K_2.

A curvature vector may also be defined,
whose direction is normal to the curve, pointing

99

toward its local center of curvature, and whose
magnitude is the value of the local curvature.
If, for a given surface element, both principle
normal curvature vectors point into the volume
whose curvature is being measured, the surface
element is defined as convex with respect to that
volume; if both point outward, the element is
concave; and if they point in opposite directions,
the local surface is a saddle surface.

If a plane of arbitrary orientation inter-
sects the surface element, dS, the curve of in-
tersection has a curvature value in that region
which is related to the principle normal curva-
tures through the relative orientation of the
surface and the sectioning plane:(2)

$$k(\theta,\phi) = \frac{1}{\sin\phi} \ [K_1 \cos^2\theta + K_2 \sin^2\theta] \qquad (10)$$

where ϕ is the angle between the surface normal,
and the normal to the sectioning plane, and θ is
the angle between the projection of the plane
normal upon the tangent plane, and one of the
principle normal directions.

A useful parameter, of central importance in
the physics of surfaces, is the mean surface cur-
vature, H, defined as the average of the princi-
ple normal curvatures:

$$H \equiv \frac{1}{2} \ (K_1 + K_2) \qquad (11)$$

Upon an arbitrary surface, H varies from
point to point. It thus possesses a distribution
of values, and, hence, some average value. A
reasonable definition of the average value of the
mean surface curvature in a three-dimensional
structure is given by:

$$\overline{H} \equiv \frac{\iint_S H(u,v)dS(u,v)}{\iint_S dS(u,v)} \qquad (12)$$

where u and v are surface coordinates. It will
now be shown that this average mean surface cur-
vature is related to the average curvature of the
corresponding area outlines that result when a
representative collection of sectioning planes is
produced through the three-dimensional structure.

100
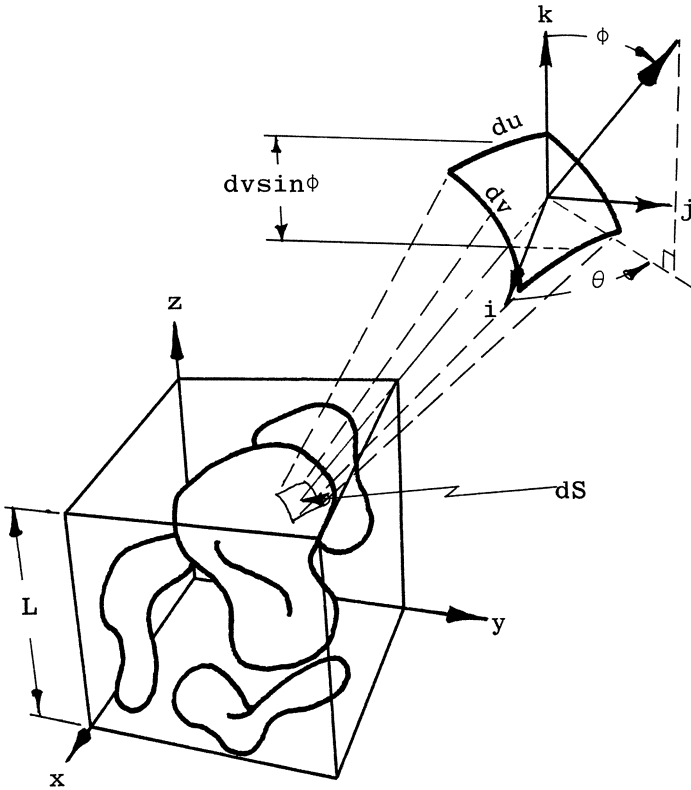
Figure 3. Illustration of the probability fac-
tors involved in averaging the curva-
ture upon a representation section
through a three-dimensional structure.

Let the dimensions of the element dS be
specified in terms of the surface coordinates, u
and v, as dudv, Figure 3. Construct a set of
test planes in the volume, all parallel to the xy
plane. In order to evaluate the average curva-
ture of a representative section through a struc-
ture, it is necessary to:

1) Calculate the fraction of all test planes
   which have orientations in an arbitrarily
   small range about some value, (θ, ϕ),
   $\frac{\sin\phi d\theta d\phi}{4\pi}$;

2) Calculate the fraction of test planes in this orientation range that are positioned so as to form an intersection with dS, $dv\sin\phi/L$;

3) Calculate the curvature that results for each of these intersections, see equation (10);

4) Multiply this value of curvature by the length of the intersection formed, du, in accordance with the definition of average curvature given in equation (1);

5) Weight this product according to the fraction of test planes that lie in the orientation range required to produce the calculated curvature, and the fraction of test planes that produce an intersection with dS, i.e., multiply the curvature-arc length product by the probability factors calculated in 1) and 2);

Averaging of this formulation over the range of orientations, and over the surface area in the structure yields the following expression for the average curvature of a representative section through a three-dimensional structure.

$$\overline{k} = \frac{\int_o^\pi \int_o^{2\pi} \int_u \int_v [K_1\cos^2\theta + K_2\sin^2\theta] \frac{1}{\sin\phi} \frac{\sin^2\phi}{4\pi} \, du\,dv\,d\theta\,d\phi}{\int_o^\pi \int_o^{2\pi} \int_u \int_v \frac{\sin^2\phi}{4\pi} \, du\,dv\,d\theta\,d\phi}$$

Integration over the range or orientation yields:

$$\overline{k} = \frac{2}{\pi} \frac{\int_u \int_v [K_1 + K_2]du\,dv}{\int_u \int_v du\,dv} = \frac{2}{\pi} \frac{\int\int_S 2H\,dS}{\int\int_S dS}$$

Since the surface coordinates have been defined so that the product, dudv, is the area of the surface element, dS, the ratio of integrals on the right hand side of this equation is precisely the average value of the mean surface curvature presented in equation (12). Thus:

$$\bar{k} = \frac{4}{\pi} \bar{H} \qquad\qquad (13)$$

Since $\bar{k}$ may be evaluated from stereologic counting measurements, as developed in equation (9), it is possible to relate the average mean surface curvature to these counting measurements:

$$\bar{H} = \frac{\pi}{2} \frac{T_{Anet}}{P_L} \qquad\qquad (14)$$

This result assumes the stature of one of the fundamental relationships of quantitative stereology, since its validity is independent of the geometry of the structure to which it is applied, and depends only upon the assumption that a representative array of sections has been uniformly sampled.

Relation Between the Number per Unit Area Count
and Mean Surface Curvature

Because both measurements sense the total angle subtended by elements of arc in a two-dimensional structure, it can be shown[4] that the T_A and N_A counts are simply related:

$$T_{Anet} = 2N_A$$

where N_A is the number of closed loops of particle outline in unit area of structure. If, in a structure, there exist loops which enclose areas of the reference phase, (convex loops), as well as loops that outline holes in that area (concave loops), the net tangent count and particle outline counts remain simply related:

$$T_{Anet} = 2N_{Anet} \qquad\qquad (15)$$

where N_{Anet} is the difference between the number of convex and concave closed outlines in unit area. It has been pointed out elsewhere[5] in this Congress that N_{Anet} is the "Eulerian Characteristic" of the representative section through the three-dimensional structure. Substitution of equation (15) into (14) yields an alternative method for estimating the average mean curvature:

$$\overline{H} = \pi \, \frac{N_{Anet}}{P_L} \qquad\qquad (15)$$

Discussion

If the elements of the structure under scrutiny are closed surfaces, then all sections will produce closed loops. Under these conditions, either equation (14) or (15) may be used to estimate the average mean surface curvature. Application of equation (14) is recommended where the number of closed loops that intersect the boundary of the area of observation is a significant fraction of the total number of closed loops in the area. This condition is most likely to be met in structures of multiple connectivity in three dimensions, in which the volume fraction of the identifiable parts are more or less equal. For small volume fractions, sections tend to produce mostly small, isolated closed loops of particle outline, and the N_A count is probably preferable.

If information is sought about interfacial features which are open, i.e., which bound only a part of an identifiable structural element, then the Rhines Tangent Count must be used.

Because it is necessary to distinguish between positive and negative curvature on a section, in order to evaluate the net loop or tangent counts, these relations may not be applied to interfaces that have no distinguishable inside or outside. For example, the grain boundary structure in a polycrystalline solid separates small contiguous crystals that are physically identical, except for their relative orientations. In this case, the interface that constitutes the grain boundary network has neither an inside, nor an outside.

It is also pertinent to point out that relationships similar to equation (15) have been developed independently and published simultaneously by J. W. Cahn (6) and Hans Giger. (5) Cahn presents procedures for applying these relationships to contiguous, or partially contiguous

structures; Giger points out the connection with
the other counting measurements in stereology
through integral geometry, and with the Eulerian
characteristic.

Conclusion

A new fundamental relationship of quantita-
tive stereology has been derived and presented.
It permits the unbiased estimation of the average
value of the mean surface curvature of identifi-
able structural elements from relatively simple
counting measurements made upon a representative
plane section through the structure. The result
may be applied with rigor to all aggregates of
closed surfaces, and to open surfaces that have
an identifiable inside and outside.

References

1. J. Willard Gibbs, The Scientific Papers of J.
    Willard Gibbs, Dover Publications, Inc., New
    York, (1961), p. 219.

2. Dirk J. Struik, Lectures on Classical Differ-
    ential Geometry, Addison Wesley Press, Inc.,
    (1950).

3. C. S. Smith and L. Guttman, Trans. AIME, 197
    (1953) 81.

4. R. T. DeHoff, Trans. Met. Soc. AIME, 239
    (1967) 617.

5. Hans Giger, Proceedings, Second International
    Congress for Stereology, Springer Verlag, In
    Press.

6. J. W. Cahn, Trans. Met. Soc. AIME, 239 (1967)
    610.

INTERPRETATION AND MISINTERPRETATIONS OF
THE MICROSCOPIC IMAGE

CLARA S. HIRES

Mistaire Laboratories, Millburn, New Jersey

Correct interpretation of a microscopic image de-
pends on accurate knowledge and understanding of
3-dimensional basic structural concepts. Gradually
these were solved by repeated checking, using many
approaches with hundreds of drawings, over 400
models and 4000 superior photomicrographs, at all
angles and focal levels. Projecting transparent
models with a simulated microscope, 2-dimensional
effects were compared with 3-D objects. Silhouette
shadow drawings of models were labelled correctly
by checking with 3-D models, separating reality
from illusion. No similar comprehensive study has
been found.

The literature is filled with 2-D descriptions.
Each science group coins its own words for the
same structure, often with contradictory meanings.
In my writing, 3-D words are used with their
common meanings, or with careful explanations.

Models were analyzed to determine whether asym-
metrical mother cell division described by others
was practical or possible. These appeared improb-
able. A relationship must exist between a spore
and the structure from which it developed.

Many spore and pollen species are derived from
spherical mother cells. Wall formation during cell
division divides this sphere into 4 similar spores.
The group of 4 is called a tetrad. We studied in
how many ways a sphere could be divided into 4
equal parts. Many possible spore models were made,
rotated and sectioned to learn the wall arrange-
ments for each structure, and later these were
organized with line drawings to be compared with
structures under the microscope, or illustrations
on a flat page, to determine the angle and focal
level examined.

The spore structure derived from a spherical mother cell, most commonly seen and misunderstood, is the "trilete" form (meaning 3 scars). This represents a 4-sided spore, the outer side curved as the surface of its tetrad. The 4 spores divide the curved tetrad surface into 4 triangular areas. The juncture of their corners produces a tri-radiating line effect on the tetrad surface.

The 60 possible wall arrangements of a single trilete spore tetrad have been misinterpreted to indicate many spore or tetrad structures, each given a different label, causing great confusion.

Each spore's 3 inner flat sides contact 3 other spores within the tetrad, resulting in a total of 12 contact sides. The edges or long corners of these sides radiate from the tetrad center, giving each spore a 3-line or triradiating effect. The central angle of each trilete spore side is 109.5°. This produces a spore structure that is a low pyramid with a curved base. An equilateral pyramid proves to be an impossible spore form.

Many use the word "equator" to describe the widest spore edge, actually 3 long corners edging the spore at the curved outer surface. These curved edges create a scalloped effect. A trilete spore can have no equator as it is a low pyramid form, although its outer curved side may appear round.

Through the microscope, 3-D walls are confused by linear perspective, shadows, diffraction, curves, angles, as well as limited focal depth. Curves appear as straight lines if turned onto one plane, obtuse angles appear acute, as illustrated by bending and turning a long plastic strip.

Fresh, living, spherical mother cells, spore tetrads and whole spores were collected at each stage of development. Many mounting methods determined how to preserve nearly normal living conditions for all species. It would have been impossible to achieve our results using only stained sectioned slides of old herbarium specimens or fossils. Most of this research was accomplished with fern spores, but representatives from other groups were included.

BIBLIOGRAPHY

Hires,C.S. - "Spores.Ferns.Microscopic Illusions
Analyzed", published by Mistaire Laboratories,
Millburn, New Jersey, U.S.A.

Hires,C.S. - "Tetrad Analysis through Sectioned
Models", Bulletin of the Torrey Botanical Club,
Vol. 83, No. 1, 72-76, 1956.

Griswold,M.M.- "Models for Spore Study", American
Fern Journal, Vol. 46, No. 1, 1-7, 1956.
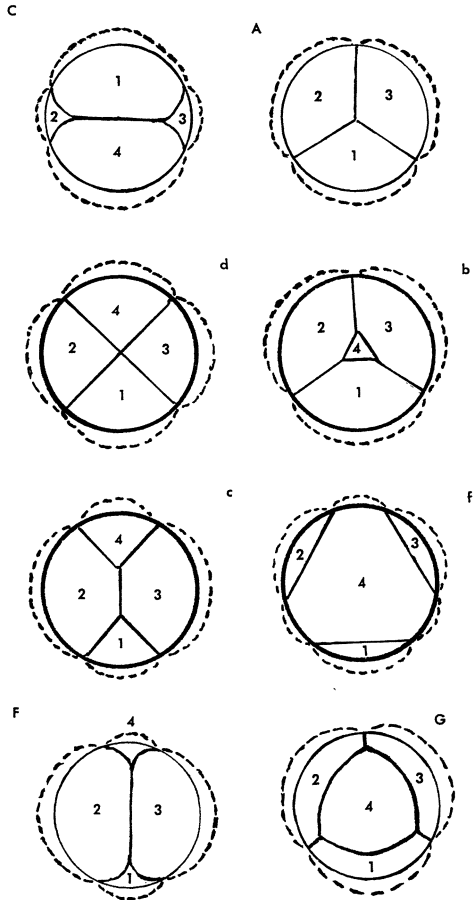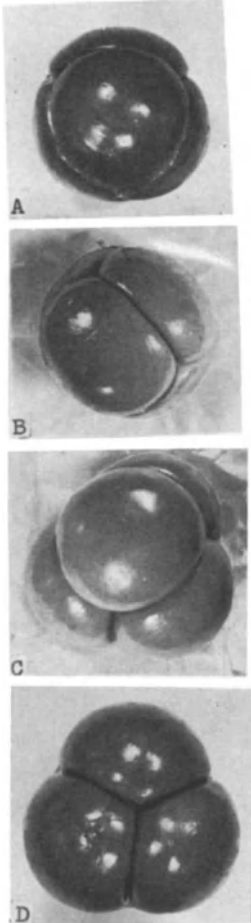
Whole spore tetrad
2 models rotated.
A-B - Spherical
C-D - Bulbous spores

Circumference I-sectioned, 2 points.
C-F - Cut between 2 spore sides.
A-G - Cut where 3 spore corners meet
Labelled as in book.

108

IID

IIC

Circumference II –
2 sections
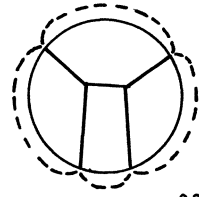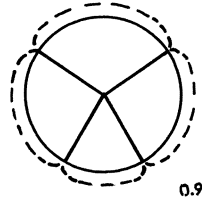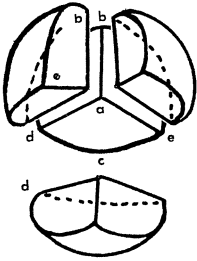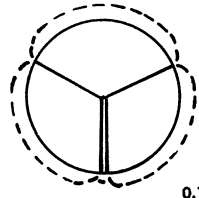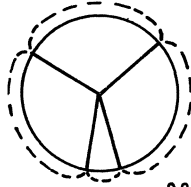
Spore tetrad separating

1a

1b
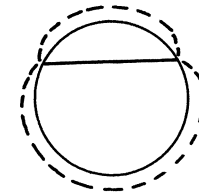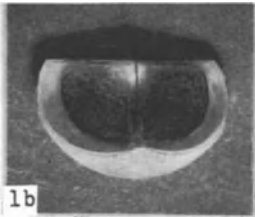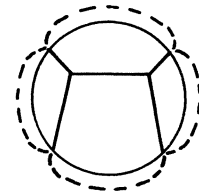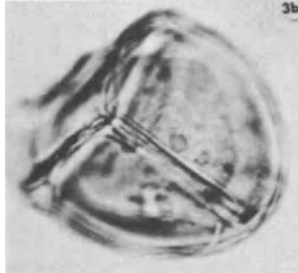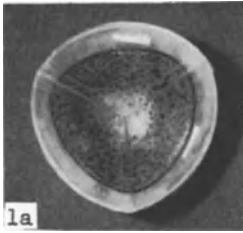
la–b – same spore
model at 2 angles

In tetrad – long spore corner:
Cut at angle.   Horizontal cut.

0.8

0.1

0.9

0.3

0.5

0.6

3b

3a

3a–b – 1 spore
2 focal levels

Labelled as in book

109

A NEW METHOD FOR MEASURING
STRAIN DISTRIBUTION

E. M. PHILOFSKY

Department of Materials Science, Northwestern University, Evanston, Illinois

J. E. FLINN

Argonne National Laboratory, Argonne, Illinois

The deformation behavior of materials consists of observing
the dimensional changes as a result of applied forces. These
dimensional changes are directly related to quantities called
strains, and the forces to quantities called stresses. This
paper describes a new method for determining the strain dis-
tribution resulting from complex stress applications. The
measurements involve the evaluation of grain boundary shape
as seen on a plane of polish before and after deformation.
In particular, the variation in grain shape across the walls
of hollow drawn metal tubes is measured to illustrate the ap-
plication of the method. The measurement of grain shape is
based on an analysis of Philofsky and Hilliard (1967) which
determines the orientation distribution for traces of grain
boundaries on a plane of polish. This analysis is described
in another paper by Hilliard (1967).

In order to determine strain, the full information provided
by the orientation distribution is not required. The change
in the ratio of minor to major axis (b/a) will be a sufficient
measure of strain, if it is assumed that the grains are ap-
proximately elliptical in shape. For this case by choosing
the reference direction parallel to the major or minor axis,
only the a_0 and a_2 coefficients need be evaluated. These are
determined from measurements of the number of intersections
that the grain boundaries make with a straight line placed
parallel to the minor axis, $P_L(1)$, and to the major axis,
$P_L(2)$. From Eq.(4) in Hilliard's paper, it can be shown that

$$a_0 = (1/2)[P_L(1) + P_L(2)],$$

$$a_2 = (3/4)[P_L(1) - P_L(2)]. \qquad (1)$$

Since the orientation distribution for the perimeter of an
ellipse is known, the quantity (a_2/a_0) can be related to (b/a)
as follows,

$$(a_2/a_0) = \left\{ \int_0^\pi \cos 2\theta \left[1-[1-(b/a)^2]\sin^2\theta \right]^{-3/2} d\theta \right\}$$

$$\div \left\{ \int_0^\pi \left[1-[1-(b/a)^2]\sin^2\theta \right]^{-3/2} d\theta \right\} . \qquad (2)$$

These integrals have been previously evaluated [Riegels, 1947]

and the results are shown in Fig. 1. The actual length of the minor axis can be evaluated from the following equation,

$$b = \left[16/\pi^2 a_0\right] \left[\int_0^\pi \left(1-[1-(b/a)^2]\sin^2\theta\right)^{-3/2} d\theta\right] . \qquad (3)$$

Thus from measurements with a straight line in two directions the first two Fourier coefficients of the orientation distribution can be evaluated and the (b/a) ratio can be graphically determined from Fig. 1. This result is combined with Eq. (3) to give the change in the dimensions of the minor and major axes, otherwise called the strain. In order to illustrate the use of this method, the analysis was applied to measuring the change in strain distribution across the walls of deformed monel (70% Ni, 30% Cu) tubes. The results are revealed in Fig. 2. This plot shows the measured radial grain dimension, $|a|$, and hoop grain dimension, $|b|$, across the tube wall for increasing reductions (deformation) from R_3 to R_{10}. It can be seen that the compressive hoop strain is the predominant strain across the tube wall, increasing from the outer to the inner diameter. There is a small compressive radial strain at the outer diameter of the wall, which diminishes at the inner diameter. This is probably due to the slight decrease in bulk wall thickness with reduction.

REFERENCES

1. E. M. Philofsky and J. E. Hilliard, (to be published).

2. J. E. Hilliard, in this volume, (1967).

3. V. F. Riegels, Archiv. d. Math., 2, 117 (1949).
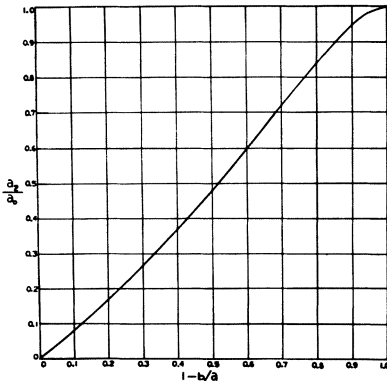
Fig. 1 Plot of (a_2/a_0) vs. (b/a) for an ellipse.
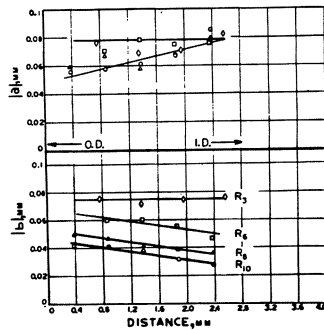
Fig. 2 Plot of radial grain diameter $|a|$ and hoop grain diameter $|b|$ vs. distance across tube wall.

THE STEREO ULTRASTRUCTURE OF THE CORNEAL SURFACES IN THE "STEREOSCAN"

SIGURD BLÜMCKE*

Institute of Pathology, 44 Münster/Westf., Westring 17, West-Germany

The "Stereoscan" is a newly - developed electron microscope to observe and photograph surface structures below light microscopic resolution. It allows to study <u>directly</u> the stereo ultrastructure of surfaces that could hitherto only be reconstructed from serial thin sections. It achieves a resolution up to 2oo $\overset{o}{A}$ at a relatively great depth of focus.

Our stereoscopic studies of the surfaces of the cornea of rabbits have led to the following results: The polygonal (mostly hexagonal) epithelial cells of the outmost layer display straight cell borders and closely arranged, partly parallelized microvilli and microplicae (see fig. 1). The endothelium is markedly different from the epithelium. Whereas it also consists of hexagonal cells, these interlock digitately on the margin towards the anterior chamber by means of very flat, long processes. This margin displays slender, solitary, widely scattered microvilli (see fig. 2).

The surface views of the cornea are compared with and verified by micrographs of cross - sectioned corneal tissue taken by the conventional electron microscope. Further ultrastructural results of the cornea surfaces are described in detail (BLÜMCKE and MORGENROTH 1966).

References
S. BLÜMCKE and K. MORGENROTH (jun.): <u>J. Ultrastruct. Res.</u> 1966 (in press)
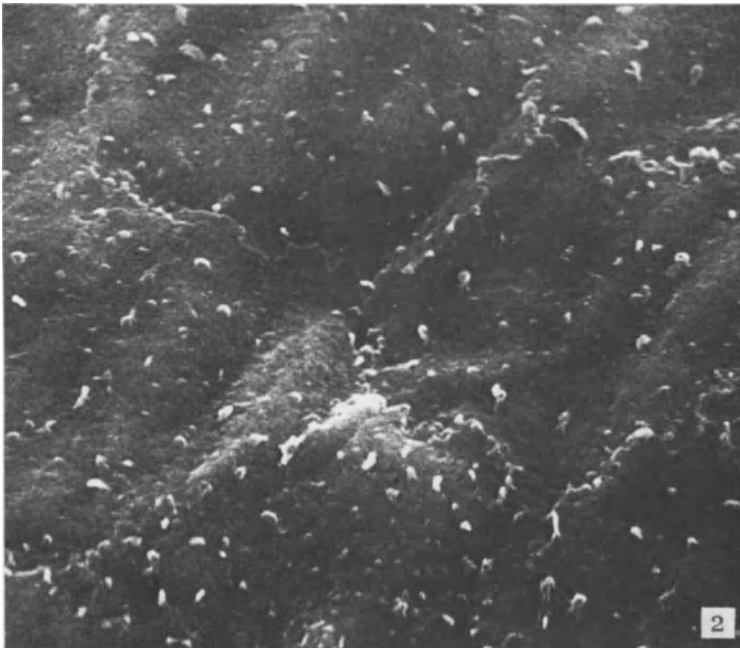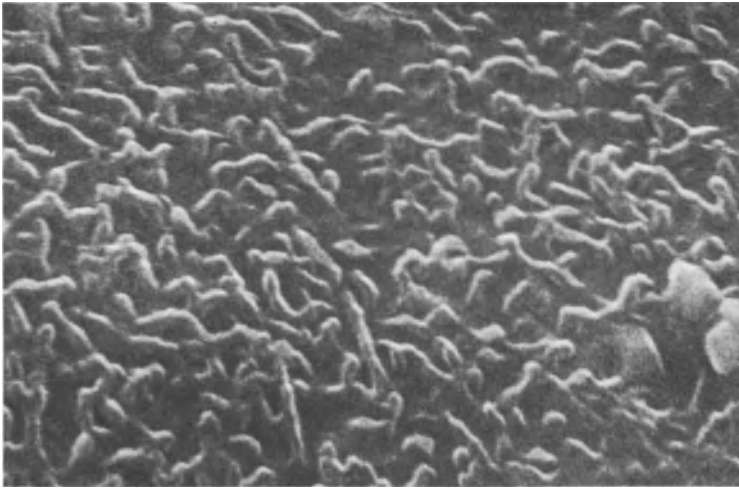
Surface views of the corneal epithelium and endothelium
taken by the "Stereoscan". Freeze-dried tissue. Coated
with evaporated carbon - gold.
Fig.1. Densely arranged microvilli and microplicae of
an epithelium cell surface. x 15.ooo.
Fig.2. Solitary slender microvilli and overlapping
cell borders of some endothelium cells. x 4,ooo.

SCANNING ELECTRON MICROSCOPY APPLICATIONS FOR MICROTOPOGRAPHY

FRANCO ROSSI

Engis Equipment Company, Morton Grove, Illinois

The basic principle of a scanning electron microscope is not unlike that of the conventional transmission microscope.The electron optical column has the electron gun at the top and the electron beam is accelerated downward by a potential of 20kV.Three magnetic lenses reduce the size of the electron source in the gun from approximately 50μ to approximately 20Au at the specimen surface.This determines the resolution of the instrument.

The electron probe is scanned across the surface of the specimen by the use of deflecting coils in the electron optical column.The scanning generator is also connected to the scanning coils of the display and photographic recording CRT.Magnification is achieved by reducing the current to the column coils and leaving the same current in the CRT coils.A small raster of fewμ is thus scanned on the specimen while the display CRT face has a raster of 10cm square.The ratio of these two rasters gives a magnification up to 200,000x.

The collection of secondary electrons emitted from the specimen is performed by a collector to which a voltage of +20kV is applied.The accelerated electrons from the specimen surface strike a scintillator and the photons thus produced reach the photomultiplier passing through a lucite guide.The signal from the photomultiplier is proportional to the secondary emission coefficient of the specimen as the beam is scanned across the surface to build up the picture line by line on the long persistence CRT recording.This signal modulates the brightness of the CRT recording display,and the micrographs show the variation of secondary electrons collected from the specimen surface.

The most important characteristic of scanning electron microscopy is the marked three-dimensional appearance shown by the micrographs.The scanning electron microscope forms its image by using mainly low energy secondary electrons which are made to follow a curved path to the collector.This curved path makes it possible to see details in deep re-entrant holes or other areas of the specimen surface that are not in the line of sight of the

collector.

Specimens suitable for scanning electron microscopy can be divided into two groups:conductive and non-conductive.The preparation of conductive specimens is very simple,requiring only clamping on the holder which is accomplished by using any suitable adhesive,and by maintaining the conductivity to earth using colloidal silver or graphite.On non-conductive specimens it is necessary to evaporate a thin film of metal in order to avoid charging of the surface under the electron beam.The thickness of the evaporation varies from few to hundreds of Au on different specimens.

For the examination of non-conductive specimens,when the evaporation of metals is not desired,the scanning electron microscope offers a wide range of accelerating potentials which can be used in order to limit the charging.

The three-dimensional appearance of the scanning electron micrographs suggests very strongly the recording of stereoscopic pairs.Various methods of stereo pairs recording and their limitations are:

1-Variation of angle of incidence of the beam with the specimen surface from 2 to 15° between successive exposures.Limitations: foreshortening of all surface distances parallel to the plane of the specimen holder.

2-Rotation of specimen through a small angle about the holder axis.Limitations:change of the position of the specimen with respect to the collector.

3-Tilting of the specimen holder on a plane normal to the beam.Experimentation utilizing this method is now in progress and shows promising results.

Another important application of scanning electron microscopy is the detection of potential variation on specimen surface,normally called conductive mode of operation.With this mode of operation the brightness of the CRT beam is modulated by the current generated by electron/hole pairs created in depletion regions of semiconductor material by the action of the primary beam.The result so produced provides unique information at high resolution on the sub-surface behavior of semiconductor devices in actual operation.
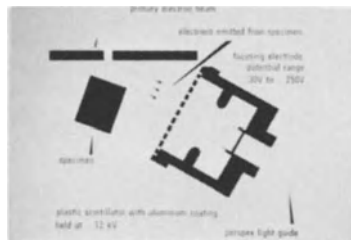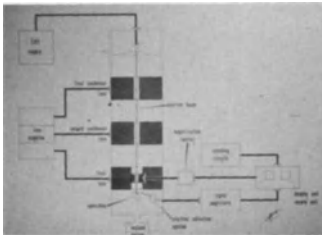
SAMPLING   AND   STATISTICAL   ANALYSIS

SAMPLING OF MATERIAL AND STATISTICAL ANALYSIS IN QUANTITATIVE STEREOLOGY

R. T. DeHoff

Dept. of Metallurgy and Materials Engineering, University of Florida, Gainesville, Florida

INTRODUCTION

All experiments in the field of quantitative stereology are essentially statistical experiments. A sample of a structure is selected for observation, and this sample is appropriately scanned. The sample and the scanning procedure may be zero, one, two, or three dimensional. Events that occur during the scan are recorded, such as the length of a lineal intercept, the intersection of a scanning line with particle outline, or the number of features observed in a two dimensional sample. These events are related, through the geometric probabilities which form the mathematical basis for the field, to the geometric properties of the structure which constitutes the population from which the sample is drawn.

In designing an analysis in quantitative stereology, the following questions must be addressed:
1) What property of the population is to be estimated?
2) What constitutes a representative sample of the population?
3) What property of the sample should be measured?
4) With what accuracy must the population property be estimated?

The answer to the first question is dictated by the nature of the phenomenon under study. The third question requires the answer to the first, coupled with a thorough knowledge of the basic relationships of the sterological field as developed elsewhere in this symposium. The second and fourth questions are fundamentally statistical, and it is to these questions that this paper is

addressed. The more practical aspect of the
fourth question, i.e., "How many measurements
must be made?", is dealt with in some detail.

HOMOGENEITY, HETEROGENEITY
AND THE REPRESENTATIVE SAMPLE

The size or extent of a sample which may be
said to be "representative" of a structure may be
expected to vary over a wide range. In general,
it will be a sensitive function of the degree of
homogeneity of the structure. Indeed, it has
been proposed that the variability of some prop-
erty from sample to sample might be used as a
measure of homogeneity. Thus, the degree to
which a sample represents the population is de-
termined by the size, or extent, of the sample,
and the distribution of inhomogeneities in the
system.

There are two basic kinds of structural in-
homogeneity:
   1) Variation of geometric properties with
         orientation, i.e., anisotropy;
   2) Variation of geometric properties with
         position, i.e., structural gradients.
In a given system, each property may possess ei-
ther or both of these kinds of variations.* Fur-
ther, the degree of inhomogeneity may be differ-
ent for each property.

The derivations of each of the fundamental
relationships of quantitative stereology assume
that the population has been sampled with an ar-
ray of "test entities", i.e., test points, lines,
or planes, which is uniformly distributed in both
position and orientation. Any test entity se-
lected at random, which would constitute an ob-
servation of the population, provides an unbiased
estimate of the geometric property of the popula-
tion being studied. However, if the population
contains long range, or large inhomogeneities,
the variability among a set of randomly selected
samples may be very large.

---

*Hilliard has pointed out that the volume frac-
tion, V_V, because it is a three dimensional prop-
erty, may not possess anisotropy.

A set of samples is <u>representative</u> of the
structure if it contains <u>a uniform sampling</u> of
all of the structural anisotropy and gradients in
the population. In a perfectly homogeneous, iso-
tropic structure, a single sample may be repre-
sentative of the population.

Isotropic Structure Containing Gradients

In an isotropic structure containing a one-
dimensional gradient, a sample is representative
if it contains the gradient. Figure 1 represents
a completely segregated two phase structure.
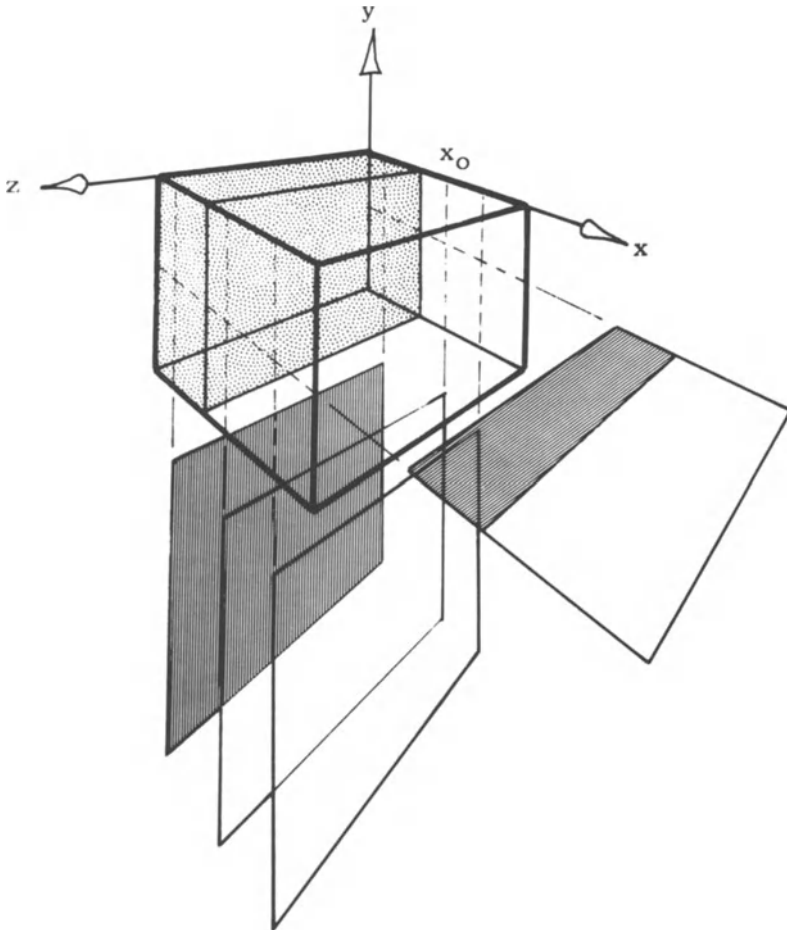
Figure 1. Illustration of a structure with
a one-dimensional gradient in volume fraction.

There is discontinuity in volume fraction at the
point x_o. Planes perpendicular to the x axis
give values of the area fraction of the dark
phase which vary from 0 to 1.00, depending upon
the position of the sectioning plane. On the oth-
er hand, planes which are parallel to the x axis,
i.e., which contain the direction of the gradient,
show an area fraction of the shaded phase which is
equal to the volume fraction of that phase. Thus,
any of the latter set of planes is a representa-
tive sample of the structure, whereas it is neces-
sary to obtain a fairly large number of planes
that are perpendicular to the x axis in order to
obtain a representative sample.

    A single plane may also be a representative
sample in a structure containing a <u>planar gradient</u>
in volume fraction, or other property. Figure 2
illustrates an extreme case of such a structure.
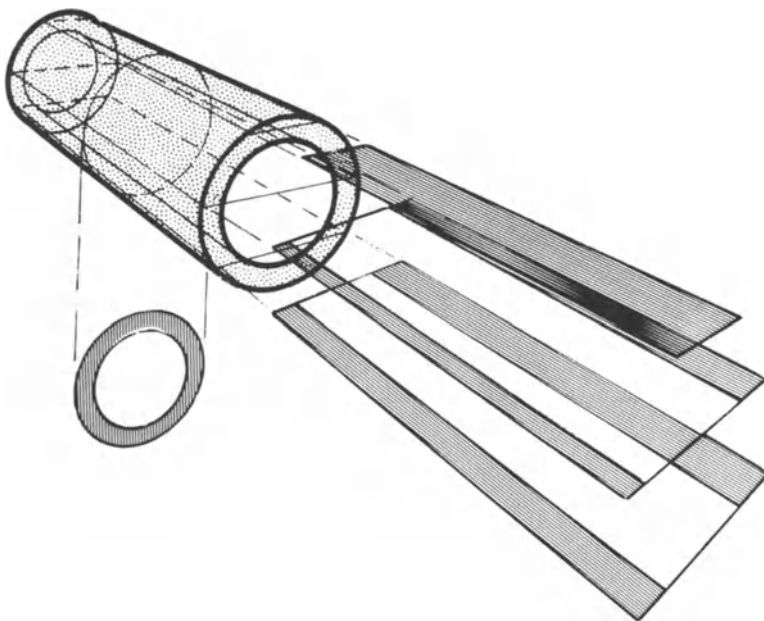
    Figure 2. Illustration of a structure with
a planar gradient in volume fraction.

In this case, one phase forms a cylindrical shell
around the other. Planes parallel to the axis of
the cylinder show an area fraction of the shaded
phases which varies from 1.00 to 0.50 as the sec-
tioning planes approach the cylinder axis. A
uniform distribution of these planes over the ra-
dius would indeed give an average value of the ar-
ea fraction which is equal to the volume fraction
of the dark phase in the structure. On the other
hand, a single sectioning plane perpendicular to
the cylinder axis has an area fraction which is
equal to the volume fraction, because it contains
the planar gradient.

It is also possible to obtain quantitative
information about the gradient in a system, e.g.,
the variation of volume fraction with position,
by taking observations perpendicular to the gra-
dient.

Structures which contain more complex gradi-
ents, e.g., a three dimensional, twisting pattern
of geometric properties, must be sampled with a
set of planes that are uniformly distributed in
position in order to obtain a representative sam-
ple.

Homogeneous Structures Possessing Anisotropy
Structures which are a result of some direc-
tional deformation are common in geology, mineral-
ogy, and the materials sciences. Such a system
may be relatively uniform in the distribution of
its geometric properties with position. Particles
or cells in such a system may be elongated or
flattened in a particular direction, or set of
directions.

Two geometric properties of three dimensional
structures exhibit this kind of inhomogeneity.
1) The interfacial area in a multiphase
structure may possess anisotropy in that
its projection on a plane may vary with
the orientation of the plane relative
to the structure. This situation is il-
lustrated for an extreme case of inter-
facial anisotropy in Figure 3. The pro-
jected area of interface in a structure
is measured by counting the number of in-

tersections a test line makes with par-
ticle outline, $N_L (\theta, \phi)$.[5,2]
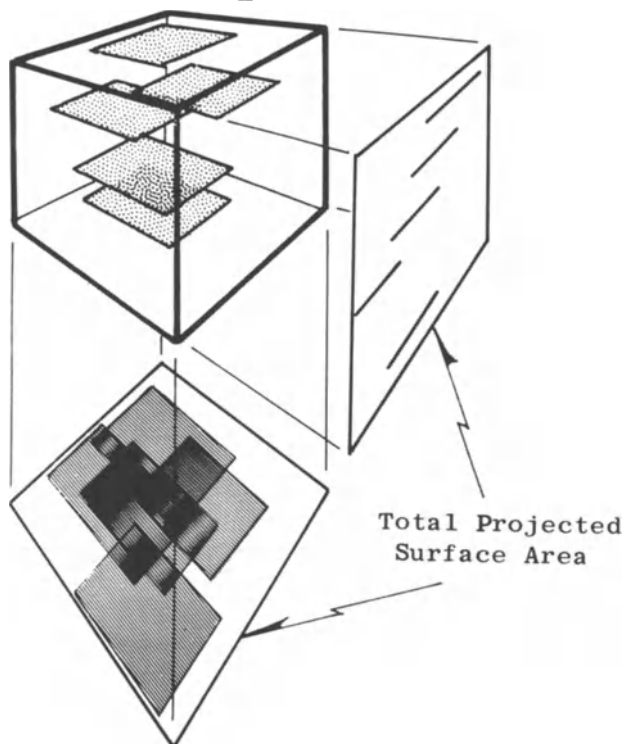
Figure 3. Illustration of anisotropy in the
total projected surface area in a structure pos-
sessing extreme anisotropy of surface area.

2) The lineal dimension of a particle
(distance between parallel tangent
planes) must vary with orientation if
the particle is not spherical. A tend-
ency for maximum or minimum particle
dimensions to be aligned will also con-
stitute a kind of structural aniso-
tropy. An extreme example of this "par-
ticle size anisotropy" is shown in Fig-
ure 4. The "total projected particle
size" in a given orientation may be
measured by counting the number of par-
ticles intersected by a test plane
whose normal has that orientation,

124

$$N_A(\theta,\phi) \cdot (5,2)$$

Total projected particle size
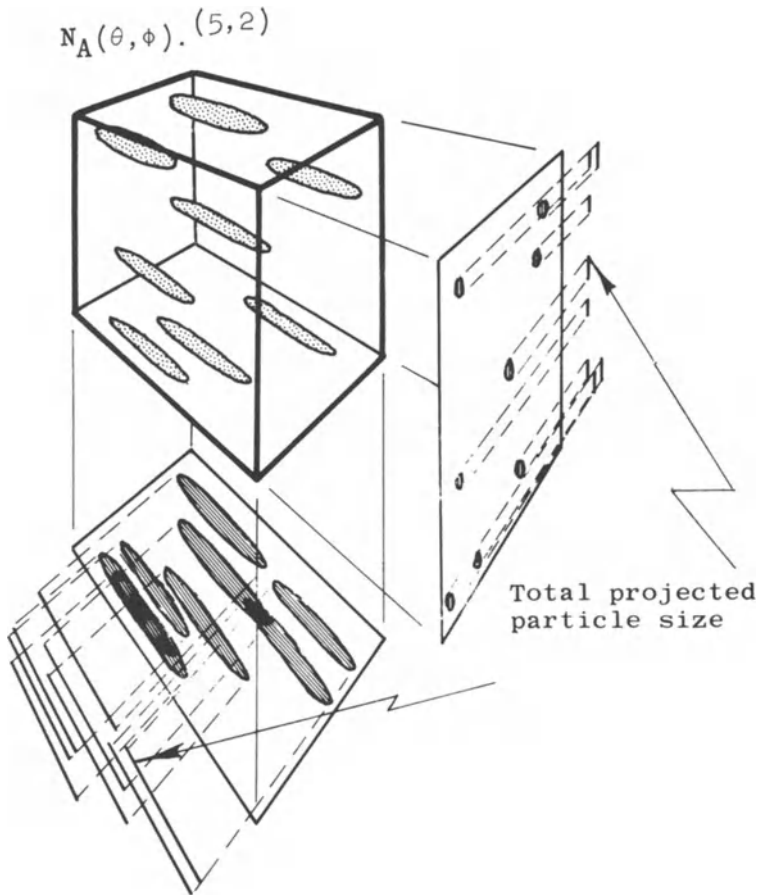
Figure 4. Illustration of anisotropy in the particle size (distance between parallel tangent planes) in an aggregate of non-spherical particles.

In the first case, a representative sample of the structure would contain an array of test lines whose directions are uniformly distributed over the orientation sphere. In the second case, it is necessary to obtain a set of sectioning planes which have orientations that are uniformly distributed in space. Neither of these require- ments are practical, however. Each new section- ing plane requires the complete repetition of the sample preparation procedure. In practice, there- fore, it is common to make observations of the

125

structure on two or three mutually perpendicular
planes. One then makes an assumption about the
distribution of the geometric property over the
orientation range. For example, it might be as-
sumed that the total projection of interface, as
determined by the oriented-line-intercept-count,
gives values which lie on a tri-axial ellipsoid
in a plot of $N_L(\theta,\Phi)$ in spherical coordinates.
In this case, a representative sample is not ob-
tained, but an hypothesis is introduced which con-
verts a sample of known relationship to the struc-
ture into a representative sample.

For a complete classification of the kinds
of anisotropy that may arise in such structures,
and the corresponding measuring techniques appro-
riate to each, see reference 2.

STATISTICAL ACCURACY
AND THE NUMBER OF MEASUREMENTS

From a practical standpoint, probably the
most important decision in the design of a stere-
ological experiment answers the question, "How
many measurements must be taken?" This question
is very closely related to the accuracy desired.
In the following discussion, it is assumed that
a set of observations have been uniformly distri-
buted over a representative sample of the struc-
ture. Deviations from population parameters due
to biased sampling or subjective errors are ne-
glected.

A single stereological observation, e.g.,
the fraction of points on a grid that lie within
a particular kind of structural feature in a sin-
gle placement of the grid, in general may produce
a range of results. A set of n single observa-
tions constitutes a "sample of size n". Individ-
ual experimental outcomes are distributed about
some average or mean value for the sample, $\bar{x}$.
The dispersion of the results about this mean is
a function of the extent of the structure which is
spanned by the observation, and the homogeneity of
the structure; it is quantitatively characterized
by a standard deviation of the observational val-
ues, (4) σ_x, given by

$$\sigma_x = \left[\frac{\sum\limits_{i=1}^{n} (x_i - \bar{x})^2}{(n-1)} \right]^{\frac{1}{2}} \tag{1}$$

where the x_i are the results of the individual observations.

If a second sample of size n were taken from the structure, it would have a mean value which is different from that of the first. Thus, in general, the sample mean values, as well as the results of individual observations, have a distribution about some mean value. The central limit theorem of statistics[4] demonstrates that this distribution is normal, with a mean value equal to the mean of the population, and a standard deviation given by

$$\sigma_{\bar{x}} = \frac{\sigma_x}{\sqrt{n}} \tag{2}$$

Thus, the sample mean values are dispersed about the mean of the population with a spread that is smaller than that of a set of single observations, and which decreases as the number of observation in the sample increases.

Because the sample mean values are normally distributed about the population mean, it is possible to assert that, if an indefinitely large number of samples are analysed, 95% of the resulting sample mean values will lie within $\pm 2\sigma_{\bar{x}}$ of the population mean. Stated somewhat differently, the probability that a particular sample containing n observations will yield a mean value which will be within $\pm 2\sigma_{\bar{x}}$ of the population mean is 0.95. For this reason, the interval in x specified by $\pm 2\sigma_{\bar{x}}$ is called the 95% confidence interval, and the ends of this interval are called the 95% confidence limits.

In a statistical analysis, the accuracy of the result is specified in terms of the 95% confidence interval. Thus, the statement that the volume fraction is 0.37 $\pm$ 0.02 implies that there is a 0.95 probability that the volume fraction of the population is between 0.35 and 0.39.

In designing a stereological analysis, the desired level of accuracy is often specified in terms of a percentage of the mean value. This

127

approach is useful because the mean value is un-
known at the outset. If an accuracy of + y per-
cent is specified, this requirement implies that
a sufficient number of measurements are to be in-
cluded in the sample so that twice the standard
deviation of the mean will equal y percent of the
mean value. Mathematically,

$$2\sigma_{\overline{x}} = (\frac{y}{100})\overline{x} = 2\frac{\sigma_x}{\sqrt{n}}$$

Solving for the number of measurements required
gives:

$$n = \left[\frac{200}{y} \quad \frac{\sigma_x}{\overline{x}}\right]^2 \tag{3}$$

where σ_x is the standard deviation of single ob-
servations, calculated from equation (1), and $\overline{x}$
is the sample mean value.

To illustrate the use of this relationship,
consider an experiment designed to estimate the
volume fraction of a particular structural fea-
ture to within + 5% of its mean value. Let it
be assumed that a representative area has been
uniformly sampled by placing upon the structure
a square grid of 25 points a total of 20 times.
Equation (1) is used to calculate σ_{V_V} for this
set of conditions, and gives a value 0.043. The
mean value of the sample is 0.173. Substitution
of these results into equation (3) shows that the
number of observations (placements of the grid)
in the sample must be increased to 99 in order to
realize the accuracy of + 5% originally specified.
In this case, the level of accuracy which will be
accepted should probably be revised. Increasing
the tolerable spread to 10%, in this case 0.017
in V_V, decreases the number of observations re-
quired to 25.

Cahn and Hilliard[3] have published a very
thorough theoretical analysis of the statistics
associated with the various methods for estimat-
ing volume fraction. They concluded that the
point count method, used as an example in the
preceding paragraph, is the most efficient of all
methods proposed. An expression for the standard
deviation of the population is derived:

$$\sigma_{V_V} = \frac{V_V}{N_1}$$

where N_1 is the number of points in the grid. This relationship makes it possible to estimate the number of readings required for a given accuracy without first measuring σ_{V_V}. However, this result is based upon a number of geometric assumptions, the most important of which is that the structural features are randomly distributed. This requirement effectively limits the analysis to small volume fractions. [1]

Similar statistical analyses for other kinds of measurements have not achieved publication. In such cases, it is necessary to rely upon the relatively standard statistical approach developed earlier. The following procedure is suggested:
1) Collect a small sample, and estimate the standard deviation, σ_x, and mean value, $\overline{x}$, of the population from it.
2) Choose the level of accuracy desired, expressed either as an absolute value, or as a percentage of the mean, y.
3) Substitute $\overline{x}$, σ_x, and y into equation (3), and calculate the number of observations required to obtain the accuracy specified.
4) In the light of this information, reassess the level of accuracy that will be tolerated.

CONCLUSION

The relationships that form the basis of quantitative stereology contain the assumption that the structure has been sampled uniformly in both position and orientation. In practice, this requirement is satisfied by selecting a representative sample, and distributing the observations uniformly upon it. The number of readings required is related to the accuracy desired, the homogeneity of the population, and the extent covered by a single observation. It is necessary to seek an optimum between the accuracy desired and the effort that may be expended in terms of the number of observations deemed practical.

REFERENCES

1. T. Gladman and J. H. Woodhead, <u>Jnl. of the Iron and Steel Inst</u>., 194, 189, 1960.

2. J. E. Hilliard, "Specification and Measurement of Microstructural Anisotropy," <u>Trans. Met. Soc. AIME</u>, 224, 1201, 1962.

3. J. E. Hilliard and J. W. Cahn, "Evaluation of Procedures in Quantitative Metallography for Volume Fraction Analysis," <u>Trans. Met. Soc. AIME</u>, 221, 344, 1961.

4. P. G. Hoel, "Introduction to Mathematical Statistics," 2nd Edition, John Wiley and Sons, New York, 1956.

5. S. A. Saltykov, "Stereometric Metallography", 2nd Edition, Metallurgizdat, Moscow, 1958.

A COMPARISON OF SAMPLING PROCEDURES IN A STRUCTURED CELL POPULATION

Sven O. E. Ebbesson and Douglas B. Tang

Laboratory of Perinatal Physiology, NINDB, San Juan, Puerto Rico
Walter Reed Army Institute of Research, Washington, D.C.

One of the most important methodological problems encountered in the quantitative study of the highly <u>organized</u> and <u>interdependent</u> cell populations which comprise the nervous system is that of sampling. This problem is an immediate consequence of the fact that any quantitative information must be obtained from the study of a sample from serial histological slices. One sampling procedure which has long been employed is to make counts or measurements in every Kth slice. Such <u>systematic sampling</u> not only provides information about the organization and structure of the particular cell population under investigation, but the resulting sample also provides estimates of various structural parameters. Systematic sampling methods can be criticized, however, because they provide, except in special situations, no internal measure of how precisely these structural parameters have been estimated. For this reason it is sometimes suggested that some form of <u>probability sampling</u> be employed, because the samples which result from such sampling procedures provide estimates of sampling variability.

In order to empirically study this problem, the superior cervical sympathetic ganglion served as a model (Figure 1) in which the efficiency of systematic sampling and three types of probability sampling could be compared. The three probability sampling methods consisted of (1) simple random sampling, (2) stratified random sampling in which one section was chosen at random within each stratum, and (3) a second form of stratified sampling in which the strata size was doubled with two sections chosen at random within each stratum, thus keeping the total number of sections that were sampled comparable. The basis of comparison of these four methods was the sampling error associated with estimating the parameter corresponding to the average number of nucleoli per 15μ section (= 510.3). The computation of these sampling errors required, for each sample size used, the enumeration of all possible samples for each method. This was accomplished with the aid of a digital computer. The results are summarized in Figure 2, which graphically shows the compari-

son of the four methods in terms of the standard error of the estimate of the average number of nucleoli per 15μ section.

The results show, as could be predicted from knowledge of the organization of the superior cervical sympathetic ganglion, that the systematic sampling of every Kth section was uniformly more efficient than the three forms of probability sampling, with simple random sampling being the least efficient.

Figure I.

Distribution of Nucleoli in a Human Superior Cervical Sympathetic Ganglion
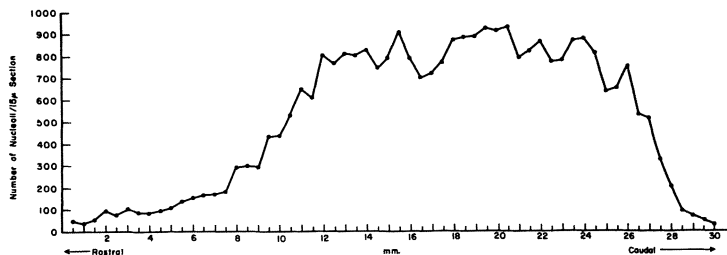
Figure 2

Comparison of the Precision of Four Sampling Procedures for Estimating the Average Number of Nucleoli Per Section
(N = 60; X̄ = 51Q3; S = 329.6)

132
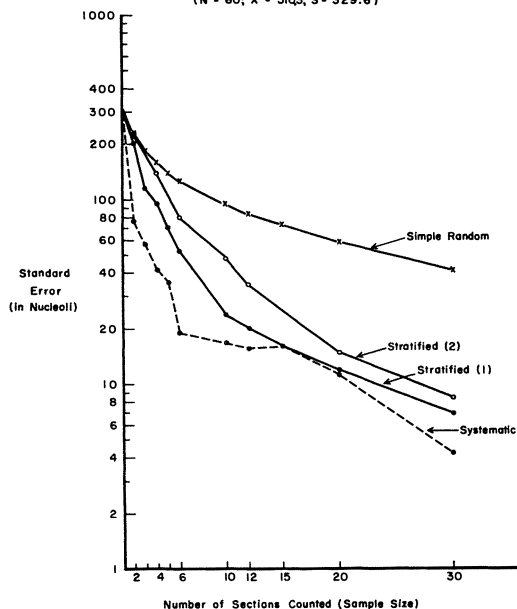
COMPUTER ANALYSIS OF PANCREATIC ISLET TISSUE

FRANKLIN W. BRIESE AND ANNA-MARY CARPENTER

*Biometry Division and Department of Anatomy, University of Minnesota,
Minneapolis, Minnesota*

We measure the absolute or relative volume of the islets
and other pancreatic tissue components using two methods
each of which requires examination of cross sections. In
the linear scan procedure, lengths of linear intercepts over
different tissue components are used to estimate correspond-
ing areas and volumes. In the point count method, points
falling on different components are used to estimate corre-
sponding areas and volumes.

Computer simulation rapidly provides information on the
sampling variation of these estimation technics. These data
would otherwise have been acquired only by years of visual
scanning and hand calculation.

For practical reasons we use only sampling plans with
parallel plane sections of tissue and parallel lines on each
selected section. In systematic sampling (with a random
start) a stack of equally spaced planes is randomly select-
ed; on each plane a grid of equally spaced lines is randomly
selected. A set of equally spaced points is randomly
selected on every line. In (restricted) random sampling,
planes, co-planar lines and co-linear points are selected
randomly at each sampling stage.

Using either systematic or random sampling plans, the
procedures give unbiased, consistent estimates of absolute
areas and volumes as well as consistent estimates of rela-
tive areas and volumes. This accuracy is independent of the
size, shape or spatial distribution of the tissue components.

For large samples, the relative efficiency of random
with respect to systematic sampling becomes less than one.
Thus, if sufficient planes and lines are sampled, the
variance of area or volume estimates is smaller for system-
atic samples than for random samples. This property is also
independent of the size, shape and spatial distribution of
the tissue components.

Unfortunately, there is no practical rule for deciding
what sample sizes are sufficiently large to guarantee the
result above. For this reason, we chose to carry out simu-
lation experiments using a digital computer. Three models
for the pancreas were simulated. In each model the
"pancreas" was a flattened ellipsoid with axes of 100, 80
and 20 units. Every islet was a sphere with radius (r)

units. The number of islets and r were chosen to give a
relative islet volume of 1%.

In the uniform pancreas model, the center of each islet
was selected uniformly from the interior of the ellipsoid.
This was done, in practice, by selecting three uniform
random numbers (one from each of the three axis lengths).
Then points were rejected (1) outside the ellipsoid, (2)
within a distance r of the ellipsoidal boundary or (3) with-
in a distance 2r of any previously defined islet center.

In the slab pancreas model, the ellipsoid was first
partitioned into slabs by equally spaced parallel planes
perpendicular to the longest axis. Within each slab, islet
centers were selected uniformly as described above. Here
all the islets were assigned to even-numbered slabs. This
model provides the worst possible situation for systematic
sampling.

In the shell pancreas model, the ellipsoid was first
partitioned by concentric ellipsoidal shells. Different
numbers of islet centers were assigned uniformly to the
between-shell spaces.

Artificial pancreases of each type were constructed by
computer subroutines. Each such pancreas was repeatedly
sectioned and analyzed for relative islet volume by both the
linear scan and point count methods using both systematic
and random sampling plans. The computer program performs
the sectioning and analyses very rapidly and prints sum-
maries for many trials on one pancreas as well as for all
trials on all pancreases used.

The most intense sampling plan used 100 planes, 40 lines
on each plane and 10 points on each line. These figures
give an expected total pancreas scan of 42000 units and an
expected total pancreas point count of 21000. The least
intense sampling plan used 20 planes, 8 lines per plane and
2 points per line. The corresponding expected values are
1700 units of total scan and 170 total points.

Under the sampling plans used, standard errors expressed
as per cent of relative islet volume ranged from 1 to 30%
for systematic linear scan, 5 to 40% for random linear scan,
1 to 90% for systematic point counting and 2 to 110% for
random point counting.

Application of the conventional random sampling variance
formula to systematically selected data generally over-
estimated the variation observed in the simulation experi-
ments. This is a conservative variance estimation procedure
but still provides a useful upper bound.

Systematic outperformed random sampling in more than
three-fourths of the cases studied. The superior precision
of systematic sampling was most pronounced for the densest
sampling grids, i.e., those with smallest traverse interval.

METHODICAL DIFFICULTIES IN MORPHOMETRY OF THE NEUROPIL OF NERVOUS TISSUE

by J.R.Wolff

Forschungsabteilung für Elektronenmikroskopie
der Freien Universität Berlin, Germany

Neuropil is a complex network of many cytoplasmic processes of different size originating from several kinds of cells. It is situated between the cells of nervous tissues. Some of these cell processes are connected to each other at specific points (synapses, glial contacts), while others seem to be distributed randomly. Some difficulties arising in electron microscopical morphometry of neuropil are: 1.) Rather high magnifications ($\geq$ 15.ooo : 1) being necessary for diagnosis of tiny cell processes limit random distribution of profiles. 2.) Total inner surface of neuropil, surface-, and volume-fractions of different elements vary not only in histological distinct layers or regions but also in even smaller units depending on the density of specific contacts. Therefore overall estimations in histological characterized regions involving heterogeneous populations are not of much use. 3.) In neuropil at least 8 different elements and 36 contact relations can be distinguished. 44 characters to be counted seperately are difficult handle during the procedure of registration and calculation. 4.) Since processes of nerve cells geometrically are comparable to cylinders with a very long axis of rotation, coefficients of configuration and the number of elements per unit of tissue volume cannot be determined. 5.) One sort of nerve cell processes (dendrites) ramifies and shows decreasing diameters. Different orders of branches possess distinct contact relations to other tissue elements. -- Possibilities to overcome some of these difficulties will be demonstrated: An arrangement for sampling at variable magnifications,random sampling, formation and comparison of sample groups characterized by a certain proportion of tissue elements, division of nerve cell processes into characters of a different diameter.

Examples for difficulty No.2 and a method to
find out factors causing not random distribution
of cell processes in nervous tissue:
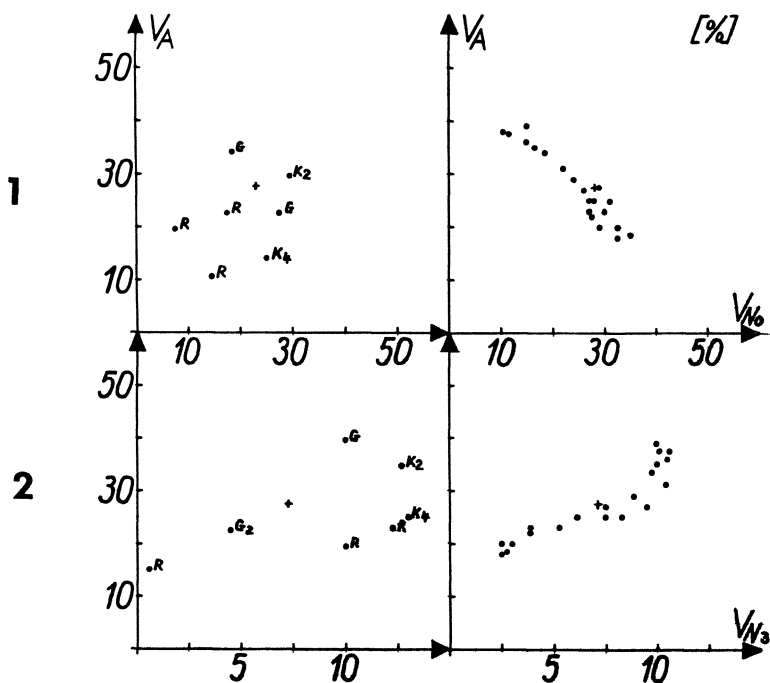
Fig.1: Correlation between the volume-fraction
of astroglia (VA) and the smallest nerve proces-
ses (VNo). a) In histologically defined regions
of the brain of rats there is no constant depen-
dence (mean values and standard deviations).
b) Samples (N=30 points) from molecular layer of
parietal cerebral cortex containing different
volume-fractions show an inverse proportion.K2
and K4 = different layers of cerebellar cortex
G2 = molecular layer of cerebral cortex, R=spi-
nal cord gray and white matter.

Fig.2: Correlation between the volume-fraction
of astroglia (VA) and the largest nerve proces-
ses (VN3=stems of dendrites). a) and b) see
fig.1. b) VA is directly proportional to VN3.

136

STEREOSCOPY, PHOTOGRAMMETRY

A METHOD OF RADIOLOGICAL STEREO-ORTHOMETRY

LUIGI MARTINO

Department of Anatomy, University of Bari, Bari

Is it possible to "know" the real size of a body which is
hidden within a thing and may be shown by radiological
examination in a double orthogonal projection?Well since
1962 I introduced a method to solve such a problem which
I described as a "Radiological Stereo-orthometry Method"
as being apt to supply a correct radiological measure-
ment of radio-opaque bodies appearing in a process radio-
logical. The method can be carried out only through a
"materialization" of the X-ray pencil which,at a given
focal distance,can be easily determined and seen by means
of a pattern on transparent plates called "pencil of rays
of incidence"(Raggiera di incidenza). The method is based
on the principle of projective geometry which states that
two pencils of rays having their axial incidence in an
orthogonal way on the centre of an object,project on two
correspondingly orthogonal screens an internal point "P"
in a given and co-ordinated modality which,in respect to
the object-centre,cannot be but one and only one. The
real distance between the "P" point and the centre can
be thus retraced by following backwards,with the support
of the two radiograms and and corresponding"pencils of
rays of incidence",the path of the two co-ordinated rays
of projection. Such a geometrical principle has been
applied in Italy(1966) in the field of cephalo-pelvi -
metry in Obstetrics besides in Neuro-surgery for inner
craniometrical examination.

Martino L. Un Metodo di Stereo-ortometria radiologica .
"Acts of Accademia Pugliese delle Scienze";
Vol. XX - pp.983-1015 ,Bari 1962 .

Settlement of the Radiograms and of the "Pencil of rays of incidence" (Radial-pencil) in the ri-dimensional process of distances of the point "p".
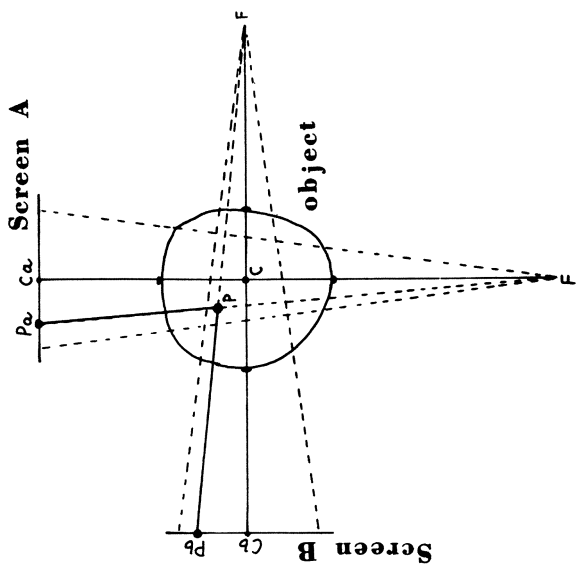
Projective coordination of the shades of an opaque point "p" in a double orthogonal projection.

STEREOLOGY AND BIOPHOTOGRAMMETRY

WALTER LEYDOLPH AND ULF ROSENOW

Universität Göttingen, Göttingen

Stereology and Biophotogrammetry examine three-
dimensional objects for the purpose of using the
results in scientific research.
What stereology means is well known here.
Biophotogrammetry has been defined by the Ameri-
can Society of Photogrammetry as "The science or
art of obtaining reliable measurements by means
of photography."
Most scientists in both fields aim at three-
dimensional quantitative information about their
objects. This includes the identification of an
object, the real length in each direction,
straight on or bent (arteries of the heart), the
surface area of irregular objects, the volume
e.g. of an artery in the heart, etc.
In biophotogrammetry we often have different ob-
jects as well as different scientific questions
than those that are met with in stereology.

How is biophotogrammetry done in practice?
All our objects must be photographed with the
help of normal light or with X-rays.
For this purpose we created special stereo-mea-
suring cameras that produce the stereogramm, con-
sisting of two pictures. With stereo-measuring-
pictures we have the opportunity to see the ob-
ject three-dimensionally, and this object is ac-
curatly interpretable and reproducible. When
used in an evaluation apparatus the object model
is exactly measurable and all points, lines etc.
can be drawn in whatever scale is suitable.
For evaluation purposes there are apparatuses
which have a wide range of applications.
The procedure applied here is the reversal of
that of taking the stereogramm.
In the stereogramm (Fig. 2 in (1)) one can see
a human heart post mortem, taken with X-rays
photogrammetrically measured and evaluated in

elongation, lateral and basic view.
The evaluation apparatus in combination with an
electronic computer enables us to evaluate the
volume of the arteries.

In (1), fig. 1 a stereogramm of a bull and
evaluations of it in iso-altitude lines and
cross sections of back and loin for purposes of
race breeding and selections are shown.

These measuring lines can also be called sec-
tions or profiles. Thus it is clear that from
all profiles we have the exact position, we see
the measured shape, of each measured line or
profile, we have the exact length, and from all
these data we can easily calculate the circum-
ference, surface or volume.

The carcass of an animal slaughtered for meat
production can also be evaluated. We can distin-
guish here between the main tissues namely
muscle, fat and bone.

Another example shows the development of the
third layer of subcutaneous fat in pigs. The de-
velopment of this layer was easily observed with
the aid of the interpretation of our stereo-
gramm. In this case other scientists, working
with histological slices and the microscope,
failed to reveal the structure of this layer.
Also slices of about 100 microns thickness,
which had undergone a special extraction proce-
dure, gave this result and demonstrated the mi-
croscopical sphere of photogrammetry.
Lastly it is nescessary to mention the X-ray
photogrammetry which will be referred to and
discussed by Mr. Rosenow. The interpretation of
X-ray stereogramms gives increased information
compared to the viewing of only one X-ray film.
The accuracy of the measurements usually lies
within the limit of about one half of a milli-
meter.

REFERENCES:
(1) Leydolph, Rosenow, Janke: "Biophotogrammet-
ry" Demonstration to the papers of L. and R. on
this congress.
(2) Heyden, Leydolph, Smidt in "Archiv für
Gynäkologie" 200, 47-59 (1964)

THE STEREO ULTRASTRUCTURE OF NATURAL AND ARTIFICIAL SURFACES OF BIOLOGICAL MATERIALS

KONRAD M. MORGENROTH

Institut für Medizinische Physik der Universität Münster, Westfalen

Observations with the"Stereoscan"yielded new re-
sults concerning the stereoultrastructure of var-
ious biological materials.The following specimens
prepared according to a variety of methods, were
studied:

Surfaces of plant leaves with their various wax
coatings (Fig. 1) and stomata (Fig. 2).
Isolated chromosomes of human and animal cells.
Surface of freeze-dried fractured kidney (Fig. 3
and 4), lung, and liver tissue.
Endothelial surface of the aorta.
Mesothelial surface of the peritoneum taken from
the liver surface.
Surface of the mucous membrane of the uterus,epi-
thelial surface with gland duct and the fractured
freeze-dried tissue.

These surfaces views give an immediate impression
of the submicroscopic stereostructure without the
necessity of reconstructing the surface by serial
sections. The methods of preparing the tissue are
published (Blümcke, S. and K. M. Morgenroth 1966,
Amelunxen, F. et al. 1966) in detail.

REFERENCES:
Blümcke, S., and K. M. Morgenroth, Ultrastructure
Res., 1966, (in press)
Amelunxen, F., K. Morgenroth jr., and T. Picksak,
Z. f. Pflanzenphysiol., 1966, (in press)
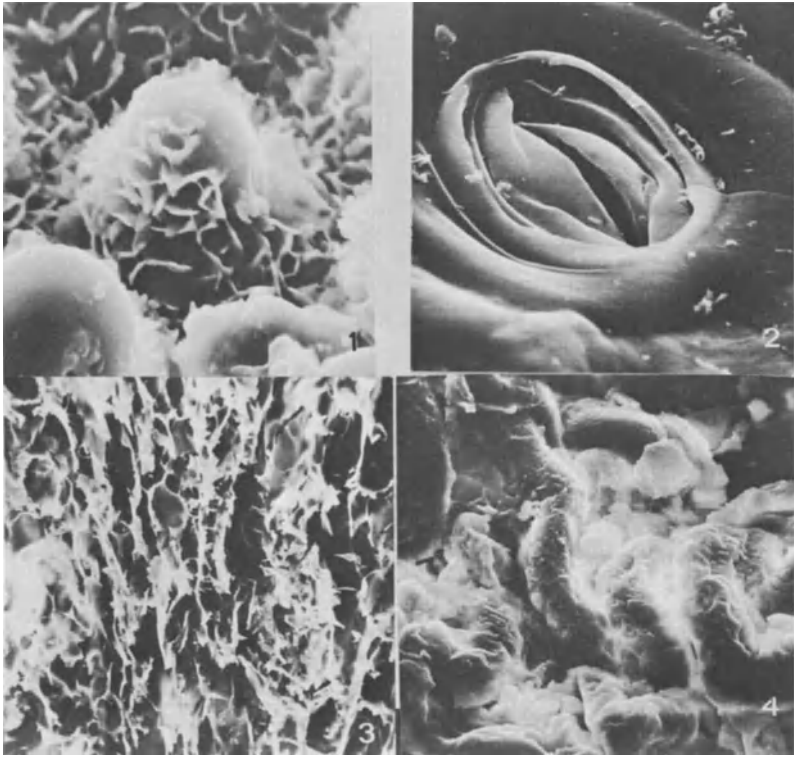
Fig. 1. Surface view of a leaf of Euphorbia
myrsinites with papilla and wax coating.
Magnification: 1 9oo : 1

Fig. 2. Surface view of poppy-head with stomata.
Magnification: 3 7oo : 1

Fig. 3. View on the artifical surface of freeze-
dried fractured kidney, renal cortex with renal
tubules. Magnification: 3oo : 1

Fig. 4. View on the artifical surface of kidney,
capillary vessels of glomerulus of Malpighi, for-
malin fixation, dehydration with alcohol.
Magnification: 1 ooo : 1

CRANIOENCEPHALIC STEREO-TOPOMETRY

Luigi Martino

Department of Anatomy, University of Bari, Bari

Skull-encephalic topometry can be realized only when cen-
tesimal measuring-systems can be referred to the outer
surface of the skull,so as to be proportional to the
skull itself and show the space co-ordinates of all its
points. In 1947 already at the IX Congress of "Società
Italiana di Anatomia" and later in 1950 and the years
that followed,I proposed to use as the only size-basis
the distance between the Glabella and Inion points.Such
a size-basis (conventionally at 100 the value of skull
longitudinal-measurement)easy to detect in all skulls,
enables the establishment of comparison among human
skulls and mammalian ones. Taking the Glabello-iniac dis-
tence as a proportinal measuring system in itself,I pro-
posed the institution of centesimal glabello-iniac"curved"
exocranial scales (sagittal-median,right transverse basic-
cranial,left transverse basic-cranial,bi-temporal) which
in all form a cranial metric cap defined as "hecatimeric"
(centesimal). In practice I have been using the "elastic"
hecatimeric cap which provides the surface of any human
"cranium" with 393 given reference-points distributed
orderly on numbered scales set at the three planes of
space. By means of the "radiological" hecatimeric elastic
cap it is possible to locate and single out the endo-
cranial points likely to be shown by X-ray examination.
By using glabello-iniac centesimal straight scales (to be
brought at the three planes of space on tha Glabella
point)every point of human as well as mammalian skulls is
enclosed as though in a spacial cube and gets a stereo-
topo-metrical determination in co-ordinate connection
whith its own term of data.

Fig. 1. "Elastic hecatimeric head-cap" with "metric curve scales" which offers 393 fixed superficial points of reference.
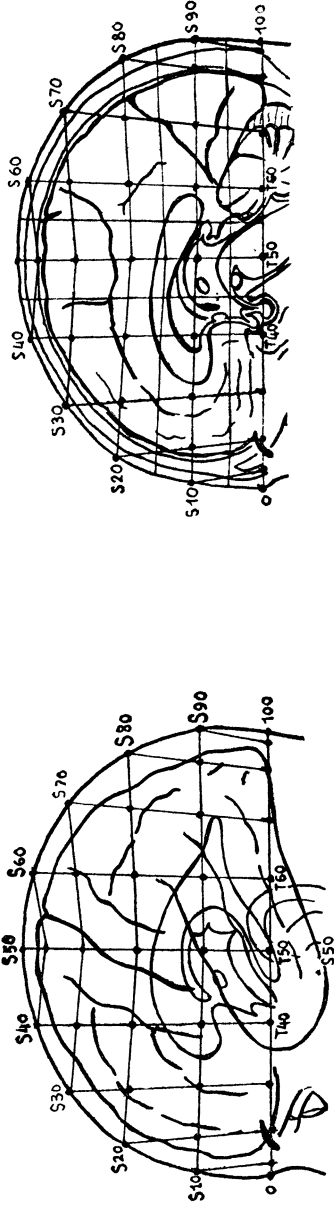
Fig. 2. "Superficial cranic fields" (30 on the right and 30 on the left side) with the corresponding cranio-encephalic medium-normal projections.

AFTER DINNER TALK

Structure and Rotation of
BARRED AND SPIRAL GALAXIES
Interpreted by Methods of Hyperstereology
(i.e. Extrapolation from n – to (n + 1) – Dimensional Space)

HANS ELIAS

Department of Anatomy, Chicago Medical School, Chicago, Illinois
(Presidential Address)

"How bombastic!" will some of you have exclaimed when reading the word Hyperstereology. The prefix "Hyper" when used in mathematics, however, has a specific meaning. It designates an amplitude of at least one dimension more than an analogous structure would have in our own, three-dimensional space. A hypersurface, for example, is a manifold of n-dimensions suspended in (n + 1) dimensional space if $n \geq 3$. Although known only to a minority of mathematicians, hypergeometry exists since 1843 (Cayley) and thus antedates by five years the first publications in stereology (Delesse).

n-dimensional geometry is closely akin to stereology which we sometimes call "extrapolation from two to three dimensional space." For n-dimensional geometry is extrapolation from three to four dimensional geometry. In fact, this is the way I hit upon it.

In the 12th grade (Oberprima) of the high school (Realgymnasium) in Darmstadt, after completion of a course in two dimensional analytical geometry, we had just been introduced to the equation for the sphere. While hiking through the woods with my classmate Ludwig Borngässer, (now professor of mathematics at the Darmstadt Institute of Technology, and general director of the Prussian State Library) we talked about the possibility of writing the same formula, but adding one more variable:

$$r^2 = x^2 + y^2 + z^2 + w^2 \ .$$

We recognized at once, that this equation must represent a space of constant positive curvature in which spherical trigonometry would reign. But it followed that such a curved space must float in a more extensive space.

There appears to be a special mentality common to many stereologists which leads them to the study of n-dimensional geometry.

Two years ago when some of us met in Dr. Rhine's home in
Gainesville in order to begin work for this meeting, I mentioned
that someone ought to speak about n-dimensional geometry. I
expected to be met by astonishment. But lo and behold, all my
colleagues: Dr. Rhines, Dr. DeHoff and Dr. Underwood knew the
field well, in fact much better than I; for they all are mathema-
ticians, while I have abandoned the queen of the sciences many
years ago. Therefore, I can only speak as an amateur about hy-
perstereology.

Many mathematicians regard hypergeometry simply as an abstract
way of manipulating equations of four or more variables. They
consider it at best a convenient operational method; some go as
far as to compare hypergeometry with spiritism. On the other
hand, some of us think that hyperspaces might be realities; but
that our senses are too limited to perceive them.

It is perhaps like with classical music or mathematics: A special
mentality is needed for an appreciation of hypergeometry.

Let me try, for those of you to whom this is a new field, to use
a very elementary approach:

Our world has three dimensions: length, height, and width. These
can be measured with rods; and directions are reversible. We
often hear of time as a fourth dimension. And indeed it is. In
our Thursday morning session, devoted to serial section cinemato-
graphy, we shall see films in which a transformation of co-ordi-
nates has been achieved: Length has been transformed into time.
Two dimensional levels originally behind each other will be seen
one after the other. Also in motion pictures, time is transformed
into the length of the film. As such it can be rolled on a spool;
and it can be re-transformed into time when the film is projected.
But time is a dimension fundamentally different from length. It is
irreversible and it can not be measured with rods.

The fourth dimension with which this presentation deals is not
time. It in no way differs from length, width or height. It can
be measured with rods. It only "points" in a direction perpendic-
ular to each of the latter.

Any line perpendicular to all straight lines in our own universe
has the direction of a fourth dimension.

Let us consider an upper corner of a room (fig. 1) as the origin of a Cartesian co-ordinate system. If we could visualize a line which passes through that origin and which is perpendicular to the three edges which meet there, then we would have a perfect conception of a four dimensional system of co-ordinates where the position of each point is defined by four numbers. While Cartesian co-ordinates in three-space S_3 are the perpendicular distances of a

FIGURE 1.

point from the xy plane, the xz plane and the yz plane, in a four-space S_4 the Cartesian co-ordinates of a point are its distances from the xyz-space, the xyw-space, the yzw-space and the xzw-space.

No person experienced in hypergeometry can really visualize it. But we can do two things which help conceptually. We can mentally discard one of our familiar co-ordinates say the x axis, and then roam about, mentally of course, in the yzw space which intersects our own xyz space, in the yz plane which it has in common with it. Another method is to construct projections of hyperobjects upon the xyz space, just as we can gain a conception of portions of our S_3 by projecting them on a plane. In S_3, this technique of dimensional reduction by projection is known as perspective. Hyperperspective can, analogously, produce three-dimensional images of four dimensional objects. And these three dimensional images can, in turn, be reduced to two-dimensional pictures by further projection. Some of the textbooks of n-dimensional geometry are using this technique.

The subject of n-dimensional geometry has been covered by a number of textbooks and in a few novels. It has been treated by an elementary, Euclidean approach, analytically, as projective geometry and topologically. In short, every approach used in plane and three dimensional geometry has been applied to n-dimensional geometry. I have no time tonight to familiarize you with the many fascinating and often perplexing findings of hypergeometry.

What I want to discuss is the question of the reality of a space or of spaces of more than three dimensions.

At this stage of human and scientific evolution there is no <u>direct</u> evidence of the existence of hyperspace. If hyperspace exists, our inability to perceive it must be due to the limitations of sensory perception imposed upon us by the physical body which nature has given us as an observatory. But our lack of ability to notice hyperspace is no proof of its non-existence, just as our inability to see ultra-violet, Roentgen, infrared and radio waves does not prove that electron-magnetic waves shorter than 4000 A or longer than 7700 A can not exist.

But let us look for indirect evidence. At first, however, let us imagine a world of one dimension, a line. In this world live two creatures Adamino and Evita. Each is a line segment of finite length. They have neither thickness nor width. But they can move about in their linear world at will. They can move North or South. They can not pass one another. Adamino remains always North of Evita. And when they touch, Evita's North end must always touch Adamino's South end. Both have traveled together widely; and they found their world to be a world of infinite extension. For they never could find an end. One day, however, they decided to explore the universe more efficiently, each taking off in opposite directions. After a long and arduous trip, Adamino noticed to the far North of him a creature. He had never seen, before, any creature except Evita. But what he saw now (and it was less than half the distance of their previous trips from home) was the South end of a person. Cautiously, he proceeded. The stranger was standing still and obviously trembling with fear. As Adamino approached he heard a scream. It was Evita's voice; and she called "Oh Adamino, come help me. There is a stranger due South." For a long time Adamino and Evita could not understand how it had been possible that they had encountered one another far from home, and they saw each other from a side from which they had never beheld one another. Finally, they drew the following conclusion: "Our world can not be infinite. It must be finite and closed. In order to be closed, it must be curved". Since the concept of curvature implies a radius of curvature perpendicular to the curved object, Adamino and Evita had to conclude that their world was but a line infinitesimally thin, located on a two dimensional surface.

A. R. Forsyth, at the conclusion of his book "Geometry of Four Dimensions" (Cambridge 1930) says that if at any time in the future it should be found that our own universe were curved we would have to draw the necessary conclusion of the existence of a more extensive space.

It was only six years after this prophetic statement was made that Hubble (Astrophy. J. 1936) concluded from his observations concerning the distribution of masses in our universe that the universe must be curved. If this assumption of curvature were true (and it happens to be subscribed to by many astronomers), it would follow that a four dimensional space is a reality, and that the universe is a hypersphere suspended in it. The radius of curvature is so great, however, that it is unnoticeable on the terrestrial scale and even on the galactic scale. In the universe, the sum of angles in a triangle formed, perhaps, by the centers of three galaxies located at huge distances from each other, should be greater than 180°. But we can measure only one of the three angles. Direct goniometrical confirmation is not possible.

Let us now turn to the method of stereology and let us, tentatively, assume that the universe is, indeed, a hypersphere floating in four-dimensional space. It is, if you wish, a hypersphere, capable of dividing hyperspace into an internal and an external portion. Solids in the universe, S_3 may be entirely contained in it, such as a figure drawn on a sheet of paper is entirely contained in its surface. However, as a figure on a screen can be the projection of a three-dimensional object created because a complex beam of light has been intercepted by the screen, as a figure on a plane of polish through an alloy or a rock, or a figure in a histological slice is just a section through a three-dimensional solid, so may certain objects in the universe be sections which S_3, a hypersurface, cuts out of hyper-solids pertaining to S_4.

If the behavior of some of the objects in S_3 defies explanation on the basis of physics, one may try extrapolation to S_4, or hyperstere-ology. If hyperstereology leads to an intellectually satisfying explanation of the physically unintelligible phenomenon, the probability of S_4 being a reality is increased.

Let us take an example from cosmology. As you know, I am not a professional astronomer. I know about cosmology only through reading and through my occasional attending the sessions of the astronomy section of the AAAS. I am a human anatomist. But to me, the object of my investigation, man, is only one of the myriads of inhabitants of the universe. Therefore, galaxies have always held great fascination for me. Pictures of spiral nebulae give the impression of mighty whirlpools spinning with high velocity and loosely held together by the gravitational attraction of the stars and interstellar matter which compose them. It is reasonable to assume that the stars or star clusters in a spiral nebula should obey, in their orbit around the centers of the nebulae, the laws of Kepler. It was with great surprise when I read a paper by Mayall and Aller (Astrophys. J.,1942)

in which it was reported that in the main disk of "nearby" spiral nebulae the third law of Kepler did not hold. The inner portions of the disks of these galaxies behave like rigid bodies: The angular velocity of far-out star clusters and supernovae is as great as of those near the center. This rigidity is obvious even to the eye when viewing photographs of barred nebulae. Barred galaxies have a large inner portion of the shape of a straight rod. Not only is the rigidity of nebulae unexplained, but even their structure. Kovalevski, (Sciences, 1966) says: "The spiral structure of this disk has not yet been explained".

Could stereology provide an interpretation of this astonishing observation? To answer this question, I proceeded (Experientia, 1956) in strict compliance with stereological procedures, although at the time (eleven years ago) the word stereology was not known.

Assuming that S_3 is a hypersphere, i.e. analogous to a surface in S_3, it can intersect a hypersolid, i. e. a portion of S_4, bounded by three-dimensional spaces. A nebula as it appears to us in S_3 is a solid (with hazy boundaries). It may be a section of some hypersolid. It is assumed, because of the "red-shift" (Doppler effect) exhibited by distant nebulae that the universe is expanding. Thus, each region of the universe moves perpendiculary to itself through S_4. As it moves outward it intersects the same hypersolids at succesive levels; and if these hypersolids are not strictly shaped like straight hypercylinders, with their axis oriented as a radius of S_3, the size, shape or orientation in S_3 of the solids which are their sections must change.

The question arose: Is there a class of hypersolids which, when sectioned by an S_3 yield solids shaped like spiral nebulae; and will the successive sections appear as phases of a rigid rotation of the same object? There is, indeed such a class of figures. Their core has the following configuration:

$$w = f(d) + k$$

$$x = \pm\, d \cos \varphi$$

$$y = \pm\, d \sin \varphi \tag{1}$$

$$z = z$$

154

It is the locus of straight lines parallel to the rotational axis of a nebula which pass through all points of a double helicoid, the axis of which (w) is perpendicular to S_3.

To account for the width of the arms of a galaxy we must endow this three-dimensional, twisted space with thickness perpendicular to the spiral arms, in the direction indicated by a double-pointed arrow in figure 2 and thus make a hypersolid out of it. But this hypersolid would extend to infinity in the z direction where it not also bounded by the ellipsoidal hypercylinder

$$z = b^2 - \frac{b^2}{r^2} (x^2 + y^2) \qquad (2)$$

$$w = w$$

This would account for the observed flatness of the nebulae. If

$$f(d) = 0, \qquad (3)$$

the shape of the main portion of a barred nebula would result. When $F(d) = md^2$, the generators of the basic helicoid are parabolae and the structure and rotatory behavior of a spiral nebula results.
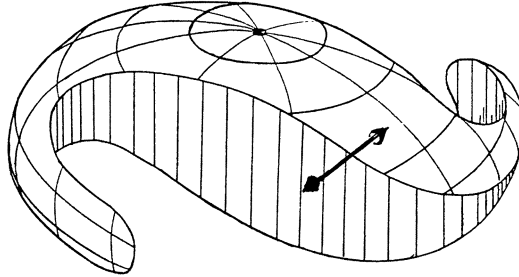
FIGURE 2.

Figure 2 shows the solid cut out of (1) and (2) by S_3, if (1) is endowed with thickness. Forgetting now the thickness of (1) we will reconstruct its section with S_3 at the present moment, i. e. when $w = 0$ (w being parallel to the radius of curvature of S_3, i. e. normal to S_3). If we make m = 1 and k = 1 in (1), the unit of measurement would be the elongation of the radius of curvature of the universe while the nebula rotates by 1° of angle. At this time (w = 0), we substitute 0 for w in (1) and (3). We obtain $0 = d^2 + \varphi$ and therefore $\varphi = (-d^2)$.

We can now plot the section which S_3 produces at w = 0, neglecting z whose value does not matter since we are looking down on the section along the z axis, increasing d by increments of 1.

155

This curve is shown in figure 3 in the form of black dots.
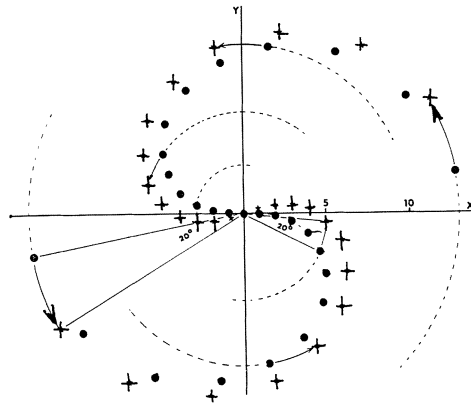
FIGURE 3.

When w = 20 the section is given by plus signs in figure 3. All points have rotated clockwise by 20°. In other words, the angular velocity is constant and is independent of the distance from the center; and the arms are trailing.

Fortunately, I found an object in our universe which resembles that hypothetical hypersolid, except that it lacks the dimension z. It is a noodle called spirella or rotino (fig. 4). Such a spirella was cooked to soften it, embedded in paraffin and mounted in a sliding microtome with a motion picture camera placed above it.

This noodle was cut into serial sections and the surface of the block was photographed after each cut on a single frame of film. To achieve contrast, the exposed surface was painted with potassium iodide solution every time darkening the starch of which the noodle chiefly consists. The negative film shows the picture of a rotating spiral nebula. Figure 5 shows a few frames from the film. In the films which will be shown Thursday morning by Dr. Hegre and Dr. Postlethwait you will notice a homologous effect: Viewing successive serial planes of a rigid three-dimensional object, one gains the impression of motion which in reality does not exist.

We can also account for the evolution of spiral nebulae according to Hubble's hypothesis, namely that they evolve from spherical, over lenticular forms to open spirals if we assume for small values of w, m and b to be relatively large, and to become smaller with growing w, while r increases in value. Figure 6 shows the core surface of this particular hypersolid. The circular arches represent the universe at

156

FIGURE 4 A.
Extruded noodles shaped like double helicoids.
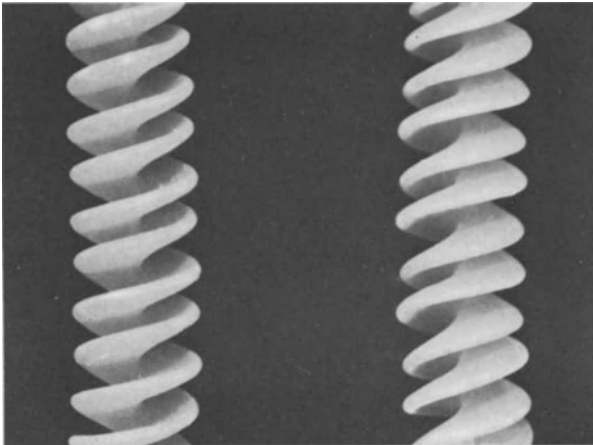
FIGURE 4 B.
Double helicoidal noodles with parabolic generators.

FIGURE 5.
Five serial sections through a double helicoidal noodle, cinematographically recorded.

different "times" or with different lengths of w. In this model one could substitute time for the length of w, assuming that the universe continously expands.
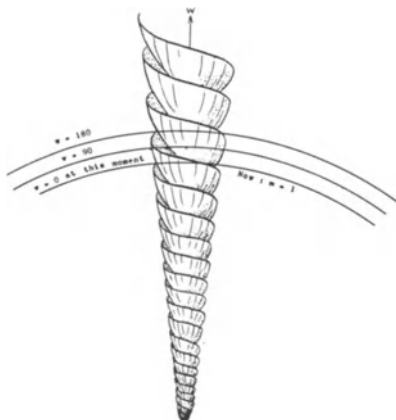
FIGURE 6.

Even if w = t, w would nevertheless not be identical with t, because time is not of the same kind as length. Also a tree only grows and never shrinks so that its height may be proportional to its age. In spite of this potential proportionality we measure its height in meters or yards, but its age in years.

The rigid rotation of galaxies and their barred or spiral structure is just one phenomenon not explicable on the ground of physics. It is not impossible that with time other things which defy an explanation based on three-dimensional physics might be understood on the basis of hypergeometry.

It is up to us stereologists to keep our eyes and ears open to reports on inexplicable phenomena. Maybe we shall be able to help our collegues in other disciplines through our training in extrapolation.

BIBLIOGRAPHY

Cayley, 1843, quoted by D. M. Y. Sommerville, An introduction
    to the geometry of N dimensions, 1929, reprinted in 1958 by
    Dover Publ. N. Y.

Elias, H., 1956, Vierdimensionale Geometrie und ihre praktische
    Anwendung zur Erklärung kosmologischer Probleme, Experientia
    12: 362 – 364.

Forsyth, A. R., 1930, Geometry of four dimensions, Cambridge.

Hubble, J., 1936, Astrophys. J. 84 : 517 – 531.

Kovalevsky, J., 1966, La galaxie, Sciences, rev. franc. 46: 28 – 43.

Mayall, N. V., 1950, Publ. Obs. Michigan 10 : 19 – 28.

Mayall, N. V. and L. H. Aller, 1950, Astrophys. J. 95: 5 – 19.

SIZE DETERMINATION

THE DETERMINATION OF THE SIZE DISTRIBUTION OF PARTICLES IN AN OPAQUE MATERIAL FROM A MEASUREMENT OF THE SIZE DISTRIBUTION OF THEIR SECTIONS

SARKIS A. SALTIKOV

Erevan Polytechnical Institute, Armenia, U.S.S.R.

ABSTRACT

A new method is proposed for determining the particle-size distribution based on the principle that the distribution of random cross-sectional areas of any body depends only on its shape. The method is applicable to both spherical and non-spherical particles, whereas all existing methods are applicable only to spherical particles. The proposed method is also very simple and less elaborate than most existing procedures.

INTRODUCTION

One of the most difficult problems of stereology is the determination of the number of particles per unit volume and their size distribution. The methods so far used have been applicable only to spherical particles. These methods are based on the measurement of the distribution of section diameters (E. Scheil. H. Schwartz S. Saltikov), section areas (W. Johnson, S. Saltikov) or chord lengths (A. Spector et al). All these procedures are fairly elaborate. The investigation of H. Aaron, R. Smith and E. Underwood[1] shows that these procedures are approximately equal in precision and are in good agreement with one another. It has been our objective to devise a method which is suitable both for non-spherical as well as for spherical particles and to simplify the computational procedure.

PARTICLE DISPERSION

In our analysis the following assumptions will be made about the particle dispersion:

a. The particles may be mono- or poly-dispersed, that is all the particles may be of the same or different sizes.

b. All the particles must have the same shape and differ from one another only in size.

c. The shape of the particles must be such that a random

plane can intersect a particle only once. The distribution of particles in space should be statistically uniform, so that the number of particles per unit volume, N_V, has a statistically constant value.

d. The particles are randomly oriented in space.

The shape of the particles may be that of a cube or some other regular polyhedron, nonregular polyhedron, ellipsoid or cylinder but must be the same for all particles in the dispersion.

Since the shape of all the particles is the same, only one linear parameter is necessary to specify the size. A convenient parameter for this purpose is $\bar{H}$, the mean caliper diameter of the particle which is equal to the distance between tangent planes averaged over all orientations of the particle. For a sphere $\bar{H}$ is equal to its diameter. For a cube H varies from a to a $\sqrt{3}$, where a is the edge length of the cube. (Fig. 1)

In many cases the value of $\bar{H}$ may be calculated analytically or by using the known stereological correlation. For example, the latter method yields for a cube

$$\bar{H} = (3/2)\ a\ .$$

If it is difficult to estimate the value of $\bar{H}$ analytically, it may be determined experimentally from a model of the particle having the same shape.
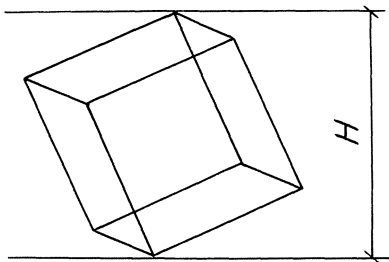
Fig. 1

As has been previously shown by the author[3], the number of particle intersections, N_A, per unit area of the sectioning plane is given by:

$$N_A = N_V \bar{H} \tag{1}$$

or, for spherical particles:

$$N_A = N_V D . \tag{2}$$

The parameter $\bar{H}$ is thus of great significance.

It is obvious that there will usually be a continuous distribution of sizes of particles in a material. However,

for the purposes of computation we must assume that the
sizes vary discretely. In other words, we must divide the
continuous distribution into a finite number of class
intervals containing particles of the same size. By in-
creasing the number of class intervals, it is possible to
approximate as closely as required the true distribution.

Experience has shown that the diameters of spherical
particles usually follow a log-normal distribution. It is
therefore desirable to use a logarithmic scale for the
class intervals. We have used such a scale with the factor
$10^{-0.1}(=0.7943)$. The first ten class intervals are listed
in Table 1 for the case where the maximum linear particle
dimension is unity.

TABLE 1

Linear sizes of particles by groups

1.	1.0000	5.	0.3981	9.	0.1581
2.	0.7943	6.	0.3162	10.	0.1259
3.	0.6310	7.	0.2512	11.	0.1000
4.	0.5012	8.	0.1995		etc.

PARTICLE SECTIONS

If the particles are not spherical then it is no longer
possible to specify the size of the section by its diameter.
In this case the size distribution of sections must be
characterized either by the distribution of section areas
or the distribution of chord lengths. In the present work
we use the first variable--the distribution of section
areas--as a basis for determining the size distribution of
the particles.

For all possible sections
through a solid of given
shape, there will be at least
one having a maximum area.
In the case of a sphere, for
example, the section having
the maximum area is the one
passing through its center.
For a cube the sections having
the maximum area are those
passing through any two oppo-
site edges of the cube, as
shown in Fig. 2. These
sections are rectangular with sides a and $a\sqrt{2}$.

Fig. 2

165
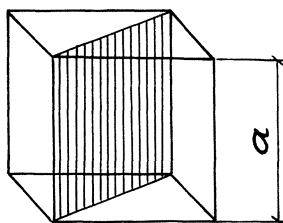
In order to specify the size of a section of a particle it is convenient to use the ratio A/A_{max} instead of the absolute area. The maximum sectional area is thus unity.

The correct choice of the maximum sectional area of an observed article is very important. It should be kept in mind that an infinite number of planes can pass through the center of a sphere, whereas for a cube there are only six planes which yield the maximum sectional area.

It is therefore necessary when analyzing non-spherical particles to examine a large number of sections to find a section which not only has the greatest area but also has the shape of the maximum section through the given body, e.g. for a cube this is a rectangle with side lengths in the ratio of 1:1.41.

Once the maximum sectional area of the largest particle in the system has been established we can immediately determine the linear size of the largest particle including the mean caliper diameter $\bar{H}$. For the particles of different sizes we find the value of $\bar{H}$ from the data in Table 1.

In specifying the linear size of particles we used a class interval based on a logarithmic scale with the factor $10^{-0.1}(=0.7943)$. Consequently, for the sectional areas we must use a logarithmic scale with the factor $(10^{-0.1})^2 = 10^{-0.2}(=0.6310)$. The class intervals for the relative sectional areas are listed in Table 2.

TABLE 2

The relative sectional areas A/A_{max} by groups

1.	1.0000 – 0.6310	6.	0.1000 – 0.0631
2.	0.6310 – 0.3981	7.	0.0631 – 0.0398
3.	0.3981 – 0.2512	8.	0.0398 – 0.0251
4.	0.2512 – 0.1585		etc.
5.	0.1585 – 0.1000		

Let us assume that a given body is intersected by a large number of random planes. By grouping the resulting sectional areas into the class intervals given in Table 2, and expressing the number in each class interval as a percentage we obtain the distribution of sectional areas which is characteristic of that body. The same distribution will be obtained if one random plane intersects a large number of equal-size, randomly oriented particles having the same shape and distributed statistically uniformly in space.

The distribution N_A vs A/A_{max} is uniquely and completely determined by the shape of the body and it is this distribution that forms the basis of the present method for determining the size distribution of particles having the same shape.

For spherical particles the distribution N_A vs A/A_{max} can be easily calculated. It is shown in Fig. 3 and the numerical values are given in Table 3.
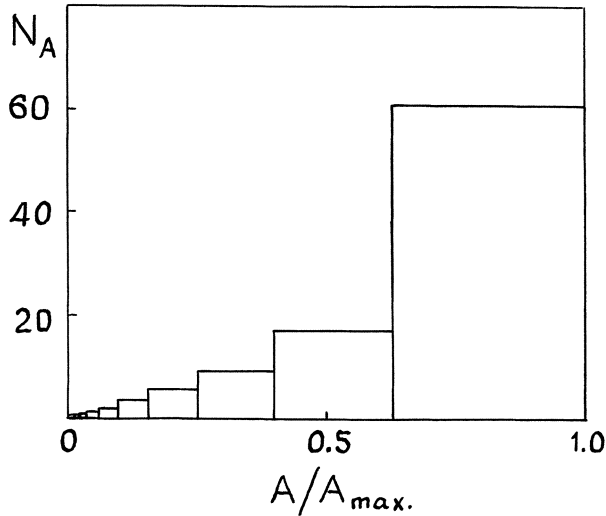
Fig. 3

However, for particles of other shapes the calculation of N_A vs A/A_{max} is very difficult or almost impossible. In this case the distribution may be found experimentally by using the method described by F. Hull and W. Houk[2]. The distribution experimentally found for a cube is shown in Fig. 4. It will be noted that this distribution differs greatly from that for spherical particles. The largest sections of a sphere also have the greatest frequency, whereas for a cube they have a low frequency. Conversely, for a sphere small sections occur rarely; but they are frequently seen in cubes because of intersections close to the vertices or edges of the cube. For the present, we can only use the distribution N_A vs A/A_{max} for spherical particles, since the class intervals in A/A_{max} used by F. Hull and W. Houk differ from those given in Table 2.

TABLE 3

Dependence A/A_{max} vs N_A for spherical particles

Group No.	Limits of section Areas A/A_{max}	Percent of sections of given group N_A
1	1.0000 - 0.6310	60.749
2	0.6310 - 0.2512	16.833
3	0.3981 - 0.2512	8.952
4	0.2512 - 0.1585	5.200
5	0.1585 - 0.1000	3.134
6	0.1000 - 0.0631	1.926
7	0.0631 - 0.0398	1.195
8	0.0398 - 0.0251	0.747
9	0.0251 - 0.0158	0.469
10	0.0158 - 0.0100	0.294
11	0.0100 - 0.0063	0.185
12	0.0063 - 0.0040	0.117
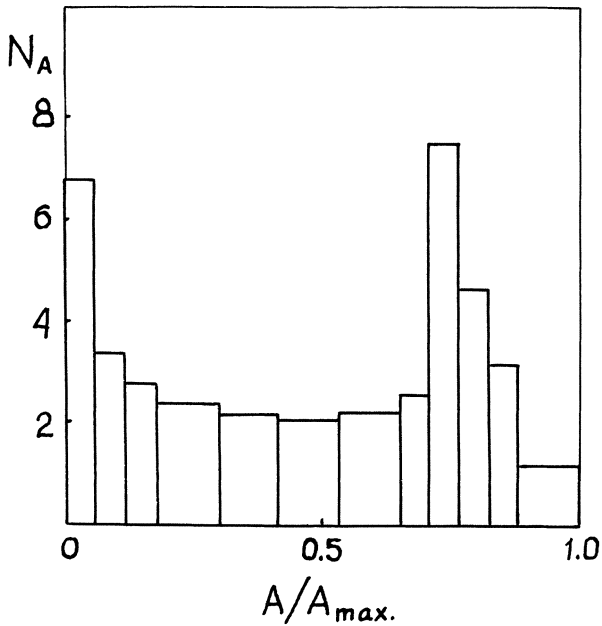
Fig. 4

COMPUTATIONAL PROCEDURE

The continuous distribution of particle sizes can be considered as a finite number of class intervals in each of which the particles are all of the same size. The dependence N_A vs A/A_{max} for each of these intervals is the same as that shown in Fig. 3. The total dependence N_A vs A/A_{max} for the whole distribution can be expressed as a sum of the dependences in each class interval. This total dependence is what is measured experimentally and is what is used for determining the particle-size distribution.

Let us consider a group of spherical particles having the following distribution of diameters:

Diameter of Particle	Number of Particles
D_1	N_{V1}
D_2	N_{V2}
D_3	N_{V3}
...	...

The largest particles have the diameter D_1, while the particles in the next interval $D_2 = 0.7943\ D_1$, then $D_3 = 0.6310\ D_1$, etc. (see Table 1.) Let the sectional areas formed by the intersection of a random plane with this group of particles be represented as follows:

Section Area	Number of Sections
$A_1 - A_2$	N_{A1}
$A_2 - A_3$	N_{A2}
$A_3 - A_4$	N_{A3}
....	....

The section $A_1 = A_{max}$ is the largest section of the largest particle, $A_2 = 0.631\ A_1$, $A_3 = 0.398\ A_1$, (see Table 2.) It is obvious that particles of diameter D_1 will contribute sections of all class intervals from $A_1 - A_2$ and downwards. Particles of diameter D_2 will contribute sections to class interval $A_2 - A_3$ and below, etc. We will denote by N_A (1)

the total number of sections from particles of diameter D_1 contained in all the intervals of sections. Similarly, the total number of sections from particles of diameter D_2 will be denoted by N_A (2); etc.

It is clear that sections in the interval $A_1 - A_2$ can come only from particles of diameter D_1, and also that the number of sections in this interval, i.e. N_{A1}, is 60.749% of all the sections from particles of diameter D_1 (see Table 3). Consequently the total number of sections from particles of diameter D_1 is given by:

$$N_A(1) = \frac{N_{A1}}{0.60749} = 1.6461\ N_{A1}. \tag{3}$$

From the data given in Table 3 we can calculate the number of sections from particles of diameter D_1 in all the remaining section class intervals. For example, for the interval $A_2 - A_3$ the number of sections from particles of diameter D_1 is:

$$0.16833 \times 1.6461\ N_{A1} = 0.2771\ N_{A1}.$$

The sections in the interval $A_2 - A_3$ can only be produced by particles of diameter D_1 and D_2. Since the total number of sections in this group is N_{A2}, and the particles of diameter D_1 produce $0.2771\ N_{A1}$ sections in this interval, it is clear that the number of sections produced by particles of diameter D_2 is equal to:

$$N_{A2} - 0.2771\ N_{A1}.$$

This number of sections is 60.749% of the total number of sections from particles of diameter D_2. It therefore follows that the total number of sections from particles of diameter D_2 is given by:

$$N_A(2) = (N_{A2} - 0.2771\ N_{A1})\ /\ 0.60749$$

$$= 1.6461\ N_{A2} - 0.4561\ N_{A1}. \tag{4}$$

In the same way we can successively determine the total number of intersections produced separately by the particles in each class interval; i.e. $N_A(1)$, $N_A(2)$, $N_A(3)$, etc.

It follows from Equation 2 that for particles in any particular class interval

$$N_A(K) = N_K\ D_K,$$

where K is the class interval number. For $N_A(K)$ we substitute the observed values of $N_A(1)$, $N_A(2)$, $N_A(3)$ etc., and for D_K we substitute D_1, D_2, D_3, etc.; we thus obtain the number of particles per unit volume in each class interval, i.e. N_{V1}, N_{V2}, N_{V3} etc. From these values it is possible to construct a size-distribution curve and determine the parameters of the distribution (the mean diameter and standard deviation).

The calculation described above is fairly long and time-consuming, and becomes increasingly difficult as the number of class intervals is increased. However, a much simpler procedure is available. We have derived a general formula which gives directly the number of particles in any particular class interval. This formula is valid for spherical particles where the number of class intervals is 12 or less. The number of particles in the Kth class interval is given by:

$$N_{VK} = \frac{1}{DK} \left[1.6461 \, N_{AK} - 0.4561 \, N_{A(K-1)} - \right.$$

$$- 0.1162 \, N_{A(K-2)} - 0.0415 \, N_{A(K-3)} -$$

$$- 0.0173 \, N_{A(K-4)} - 0.0079 \, N_{A(K-5)} -$$

$$- 0.0038 \, N_{A(K-6)} - 0.0018 \, N_{A(K-7)} -$$

$$- 0.0010 \, N_{A(K-8)} - 0.0003 \, N_{A(K-9)} -$$

$$\left. - 0.0002 \, N_{A(K-10)} - 0.0002 \, N_{A(K-11)} \right] \qquad (5)$$

In using Equation 5 the calculation for a given class interval of particles is continued until the index N_A reduces to zero. For example, for the fifth class interval (N_{V5}) the first five terms in the brackets are used. Only for the 12th class interval (N_{V12}) are all the terms used.

The amount of computation involved in the present method is much less than that of W. Johnson--S. Saltikov's method. Instead of the bulky tables of coefficients which are used in the methods of E. Scheil, H. Schwartz, H. Schwartz--S. Saltikov, and W. Johnson--S. Saltikov, we have one simple general formula (Equation 5). This formula can be used for any number of class intervals up to 12. In practice, it is usually unnecessary to have more than 12 class intervals.

The coefficients of Equation 5 are determined for the dis-

tribution of section areas N_A vs A/A_{max} for spherical particles, as shown in Fig. 3 and listed in Table 3. Consequently, Equation 5 cannot be used for non-spherical particles. But the same method can be used to derive similar formulae for particles of other shapes. For this it is necessary to know the distribution of section areas N_A vs A/A_{max} for the particular particle's shape. In this case D_K is replaced in Equation 5 by the mean caliper diameter of the particle in a given class interval, $\bar{H}_K$.

THE CALCULATION OF THE SIZE DISTRIBUTION OF PARTICLES

In applying this method it is necessary to determine the distribution of sectional areas of the plane of polish. For this purpose it is possible to use a special scale of areas corresponding to the class intervals listed in Table 2, or to use other methods.

TABLE 4

The two-dimensional distribution of ferrite grain areas

Group No.	Diameter D, microns	Grain Area A/A_{max}	Number of Grain N_A, mm^{-2}
1	63.10–50.12	1.0000–0.7943	104
2	50.12–39.81	0.7943–0.6310	161
3	39.81–31.62	0.6310–0.3981	253
4	31.62–25.12	0.3981–0.2512	230
5	25.12–19.95	0.2512–0.1585	138
6	19.95–15.85	0.1585–0.1000	69
		Total	955

TABLE 5

The distribution of ferrite grain sizes (diameters)

Group No.	Diameter D, microns	Number of Grains N_V, mm^{-3}
1	63.10	2713
2	50.12	4341
3	39.81	8313
4	31.62	7596
5	25.12	3359
6	19.95	491
	Total	26813

Figure 5 shows a simple area scale that can be used for sections of spherical particles; if necessary, the scale can be extended in either direction. The circle having the largest diameter corresponds to the largest particle section seen in the specimen and is therefore D_1, and the succeeding circles correspond to D_2, D_3, etc. The particle sections lying between D_1 and D_2 form the first class interval of sections (N_{A1}), those sections lying between D_2 and D_3 constitute the second class interval (N_{A2}) etc.

We have analyzed the structure of an iron specimen consisting of ferrite grains. The distribution of grain areas measured on the plane of polish is listed in Table 4. Using Equation 5 we calculated the number of grains per unit volume for each of the class intervals. The results are listed in Table 5 which gives the three-dimensional distribution of ferrite grain diameters.

×200　　　　　　　　D, μ

100

79

63

50

40

32

25

20
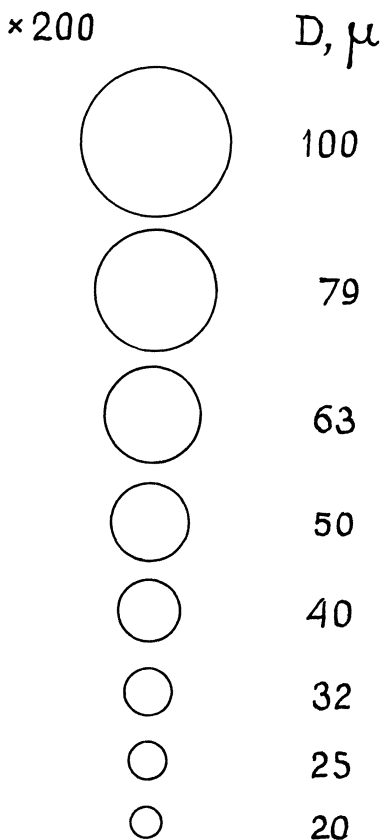
Fig. 5

CONCLUSION

A simple method for determining the size distribution of particles in an opaque material has been proposed. This method is based on the distribution of areas produced by the random sectioning of a solid with the same shape as the particles. The same principle of calculation can be used to determine the size distribution from a measurement of the distribution of random chord lengths.

REFERENCES

1. Aaron, H.B., Smith, R.D., and Underwood, E.E., First International Congress for Stereology, Proceedings, Vienna, 1963.

2. Hull, F.C., and Houk, W.J., Trans. AIME., 197, 565 (1953).

3. Saltikov, S.A., Stereometric Metallography, Moscow, 1958, Second Edition, 446 p.

SIZE DISTRIBUTION OF PARTICLES DERIVED FROM THE SIZE DISTRIBUTION OF THEIR SECTIONS

G. Bach

Technische Hochschule, Braunschweig

1. METHODS USING MEAN VALUES

1-1. THE GENERAL FORMULAE

Let us consider opaque and convex particles distributed at random in space and which are included in a transparent structure. The determination of the size distribution of these particles from the size distribution of their sections with a body B of known shape (for example a plate, a plane, a cylinder, a line) belongs to the main problems of stereology. To-day the chief resource appropriated to such problems consists in an ingenious combination of methods belonging to three branches of mathematics. These are INTEGRAL GEOMETRY, GEOMETRICAL PROBABILITY and STATISTICS. If a convex body B moves in the space occupied by the particles (presupposing a mutual penetration of the body and the structure and the particles) or if the body is detached from the structure at random, which is the same thing from a statistical point of view, a combination of methods of INTEGRAL GEOMETRY and STATISTICS yields certain relations between the hits of the body B with the particles and mean values concerning the particles itselves. As a hit we define that part of a particle, which lies within the body B.

174

Let us introduce some notations:

TABLE 1

		of the hits av- of the body B eraged over all movements of B	averaged over all particles of the struc- ture
Volume	V	V_B	$\overline{V}$
Surface area	S	S_B	$\overline{S}$
Mean diameter	D	D_B	$\overline{D}$
Number		N_B	N_V (per

unit volume of
the structure)

A straightforward application of the methods above mentioned leads to the following formulae:

$$N_V = \frac{N_B}{V} - \frac{SD_B}{2V^2} + \left(\frac{\pi}{32}S^2 - VD\right)\frac{S_B}{2V^3} + \left(VSD - V^2 - \frac{\pi}{64}S^3\right)\frac{V_B}{V^4} \ ,$$

$$(1) \quad \overline{V} = \frac{V_B}{VN_V} \ , \qquad \overline{S} = \frac{VS_B - SV_B}{N_V V^2} \ ,$$

$$\overline{D} = \frac{D_B V^2 - \frac{\pi}{32}S_B SV + \left(\frac{\pi}{32}S^2 - DV\right)V_B}{N_V V^3}$$

It's obvious that these formulae allow an immediate estimation of the "particle-quantities" $N_V, \overline{V}, \overline{S}, \overline{D}$ from the "hit-quantities" N_B, V_B, S_B, D_B using the known "body-quantities" V, S, D.
Let us consider now some special cases.

1-2. THE CASE OF CONGRUENT PARTICLES

The knowledge of the particle-quantities plainly makes it possible to define the particles, provided that all particles are congruent and described exactly by three parameters at most (for example three axial ellipsoids, right prisms).

1-3. THE CASE OF RANDOM PARTICLE SIZE

Let us assume the particles are described exactly

by one quantity x which is a random variable with density function $G(x,p_1,p_2,\ldots)$. The p_i-s are parameters of the distribution (say the cumulants for example).

Let $N_V = \int_0^\infty G(x,p_1,p_2,\ldots)dx$ be the total number of particles per unit volume. Then we have the following relations

$$N_V\overline{V} = \int_0^\infty V(x)G(x,p_1,p_2,\ldots)dx$$

$$(2) \quad N_V\overline{S} = \int_0^\infty S(x)G(x,p_1,p_2,\ldots)dx$$

$$N_V\overline{D} = \int_0^\infty D(x)G(x,p_1,p_2,\ldots)dx \quad .$$

Therefore we can estimate at most three cumulants of the distribution function using the known quantities $N_V,\overline{V},\overline{S},\overline{D}$. Of course this is important, if we only want to determine certain parameters of a known density function, because there are many distributions completely described by three parameters. But the method is relative unimportant if the type of the distribution is unknown.
In the foregoing we have asssumed that we were able to estimate, at the best, the "hit-quantities N_B,V_B,S_B,D_B observing the body B. But what can we really do?

1-4. THE BODY B IS A PLATE OF THICKNESS T

Usually the body B is a plate P consisting of two parallel planes in distance T, T may also be zero. If N_A,V_A,S_A,D_A are the number, the volume, the surface area and the diameter of the hits per unit area of the plate, we get from (1)

$$(3) \quad N_A = N_V(T+\overline{D}), \quad V_A = N_V\overline{V}T, \quad S_A = N_V(T\overline{S}+2\overline{V}),$$
$$D_A = N_V(T\overline{D} + \frac{\pi}{16}\overline{S}) \quad .$$

Plainly we can determine the quantities $N_V,\overline{V},\overline{S},\overline{D}$ from these equations, but the question is how to obtain the quantities V_A,S_A,D_A.

Of course one can derive the values of N_V and $\bar{D}$
by using measurements of N_A in at least two plates
of different thickness. If the particles are con-
gruent and exactly described by one parameter
only, the two quantities N_V and $\bar{D}$ allow a complete
analysis of the particles. In all other cases we
plainly need an information about one of the other
quantities at least. But as we only can observe
the projections of the hits on one of the faces
of the plate, we have to go in search of relations
between the hits and their projections on the
faces of the plate.

1-4.1   THE CASE OF CONGRUENT SOLIDS OF REVOLUTION

Let us now assume that all particles are congruent
solids of revolution which are formed by rotation
about the greatest diameter of the solid. In what-
ever manner we cut such a solid in slices of
thickness T, the projection of a piece on the
slice faces possesses one axis of symmetry at
least. Therefore we can measure the length of the
greatest axis of symmetry of the projection, say
L, and the length of the diameter perpendicular
to this axis, say Q. The mean values of the quan-
tities L and Q in dependence on the thickness of
the slice can be determined for a great number of
solids of revolution.
Assuming ellipsoids for example, we get the fol-
lowing relations:

$$(4) \qquad L = \frac{\pi c \left(\frac{a}{2}\right)^2 + J_1 T}{J_2 + T} \quad , \quad Q = a\, \frac{\frac{\pi}{4} J_2 + T}{J_2 + T} \quad .$$

Here the ellipsoid is formed by rotation of the
ellipse with axes a and ca about the axis ca. The
values of the quantities J_1 and J_2 are

$$J_1 = \frac{a}{2}\left\{1 + \frac{c^2 \arccos \frac{1}{c}}{\sqrt{c^2 - 1}}\right\}$$

$$(5) \quad 1 \le c < \infty$$

$$J_2 = \frac{a}{2}\left\{c + \frac{\log(c + \sqrt{c^2 - 1})}{\sqrt{c^2 - 1}}\right\} \quad ,$$

$$J_1 = \frac{a}{2}\left\{1+ \frac{c^2}{\sqrt{1-c^2}}\log\frac{1+\sqrt{1-c^2}}{c}\right\}$$

(6) $0 < c \leq 1$

$$J_2 = \frac{a}{2}\left\{c+ \frac{\arccos c}{\sqrt{1-c^2}}\right\} \quad .$$

Making use of these relations we plainly can esti-
mate the wanted values of a and c from the known
quantities L and Q. Using the relation $N_A = N_V(T+\bar{D})$,
observing the fact that $\bar{D} = J_2$, we further can de-
termine N_V.

Of course one can represent the above equations by
means of nomograms, which allow an immediate esti-
mation of a and c from L and Q (compare Fig. 1).

Passing to the limit c = O we get the values of L
and Q for a disk of diameter a

(7) $$L_{disk} = \frac{T\frac{a}{2}}{T + \frac{a\cdot\pi}{4}} \quad , \quad Q_{disk} = a\,\frac{T + \frac{a\cdot\pi^2}{16}}{T + \frac{a\cdot\pi}{4}} \quad .$$

For $c \to \infty$ and simultaneously $a \to 0$, provided that
ac remains constant = b, we get the value of L for
a needle of length b

(8) $$L_{needle} = \frac{\pi}{2}\,\frac{T\frac{b}{2}}{T + \frac{b}{2}} \quad .$$

Of course our results include the wellknown re-
sults for spheres of diameter a:

(9) $$L_{sphere} = Q_{sphere} = a\,\frac{T + \frac{a\cdot\pi}{4}}{T + a} \quad .$$

Let us now return again to more general particles.

1-5. THE BODY B IS A PLANE

If the plate degenerates into a plane, we get from
(3) with T=0:

(10) $N_A = N_V\bar{D}$, $V_A = 0$, $S_A = 2N_V\bar{V}$, $D_A = \frac{\pi}{16}N_V\bar{S}$.
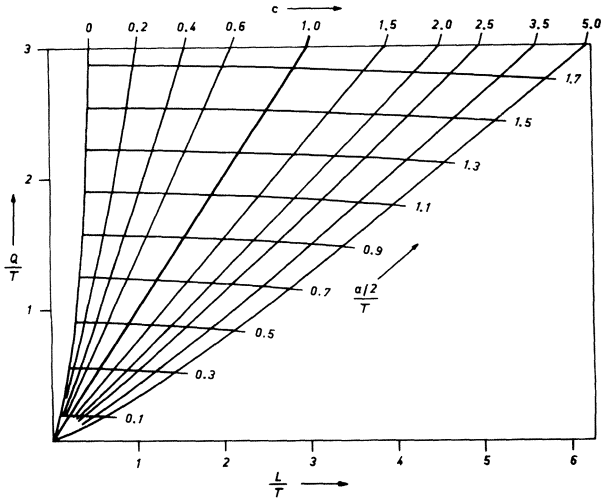
Fig. 1.

Nomogram for reading off the values of $\frac{a/2}{T}$ and c from the quantities $\frac{L}{T}$ and $\frac{Q}{T}$.

For details compare chapter 1-4.1.
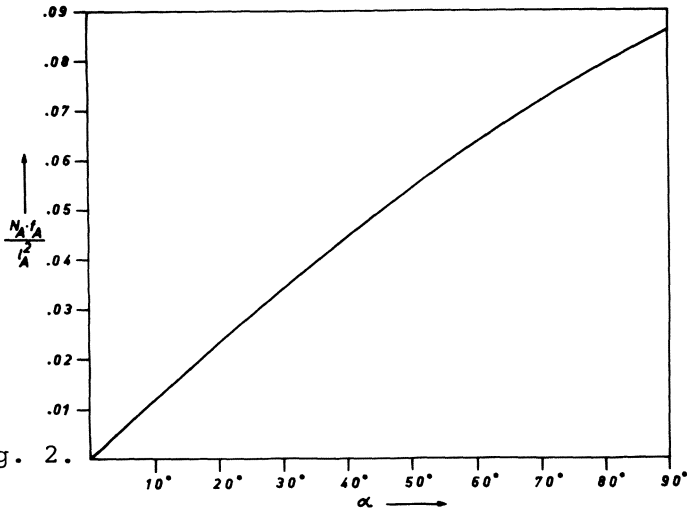
Fig. 2.

Nomogram for reading off the value of α (angle of elevation of the cone) from the quotient $N_A f_A / l_A^2$. Details compare chapter 1-5.1.

The three quantities N_A, S_A, D_A do not allow a determination of the four values $N_V, \overline{V}, \overline{D}, \overline{S}$ without further assumptions about the particles. Note that in this case $S_A = 2f_A$, $D_A = l_A/4$. Here f_A denotes the area of the hits per unit area of the plane, l_A the perimeter of the hits per unit area.

Let us quote some of those assumptions:

1-5.1 THE CASE OF CONGRUENT PARTICLES

First it may be assumed that the particles are congruent and that we know the specimen of them (for example spheres, ellipsoids, cubes and so on) Further let the particle under consideration be exactly described by at most two parameters x and y. In this case the volume, the surface area and the mean diameter are known functions of x and y. Then the four quantities $N_V, \overline{V}, \overline{S}, \overline{D}$ reduce to three

unknown values N_V, x and y, which can be determined

in general from the three known quantities $N_A, f_A,$

l_A.

If the particles are right prisms with quadratic basis x^2 and height y, we get the following relations

(11)

$$x = \frac{3\pi f_A}{2l_A \pm \sqrt{4l_A^2 - 6\pi^2 N_A f_A}} \quad , \quad N_V = \frac{N_A}{x + \frac{y}{2}}$$

$$y = \frac{3\pi f_A}{2l_A \mp \sqrt{4l_A^2 - 6\pi^2 N_A f_A}} \quad .$$

The upper signs are valid in the case $y \geq x$, the lower in the case $y \leq x$.

If the particles are circular cones with basis πR^2 and height $H = R \cdot \tan\alpha$, we have the relations

(12)

$$\frac{8}{3\pi^3} \cdot \frac{\sin\alpha \cdot (\sin\alpha + (\pi - \alpha)\cos\alpha)}{(\cos\alpha + 1)^2} = \frac{N_A f_A}{l_A^2} \quad ,$$

$$(12) \quad R = \frac{l_A}{N_A} \cdot \frac{2}{\pi^2} \frac{(\pi-\alpha)\cos\alpha + \sin\alpha}{\cos\alpha +1}, \quad N_V = \frac{2N_A}{R(\pi-\alpha +\tan\alpha)}$$

From the first equation we get the value of α and
then from the second the value of R. Now we know
the height H and the last equation allows the de-
termination of N_V. Of course in solving the tran-
scendental equation for α **one** will use a nomogram,
which allows an immediate determination of α (com-
pare Fig. 2).

Besides direct determination of l_A and f_A by using
template-methods of course one may use for an es-
timation of l_A the wellknown relations between the
number of intercepts which an unit lenght of ran-
dom test line makes with the particle outline and
for an estimation of f_A the fraction of points in
a random placed grid of test points which lie in
the section areas.

1-5.2   THE PARTICLE SIZE IS A RANDOM VARIABLE

For the next let us assume that the particles are
exactly described by one parameter x. Then we may
allow that x is a random variable with a two par-
ametric density function $G(x,p_1,p_2)$. Using the
formulae (2) and (10) we plainly can estimate the
two parameters in addition to N_V.

Note that the efficiency of this method of deter-
mining the particle size distribution depends es-
sentially on the choice of $G(x)$.

1-6. SUMMARY OF THE FOREGOING CHAPTERS

Previously we have dealt with methods of a very
general nature. They used the relations between
the mean values of the hits and the particles
themselves and were founded on certain theorems
from Integral Geometry.
The main difficulties lie in the measurement of
the quantities V_B, S_B, D_B. Nevertheless we were able
to figure out approximately the size distribution
of the particles by using a suitable distribution
function, which was fitted by means of the method
of moments.
Plainly the determination of the size distribution

of particles is always possible, if we know the
relations between the frequency distributions of
the particle sizes in space and the frequency dis-
tributions of the sizes of their hits within the
body B. But up to this day this problem has been
solved in an applicable manner for spheres only.

2. SPHERES

2-1. THE INTEGRAL EQUATION AND ITS SOLUTION

In the case of spheres let us denote the density-
function of their radii with $s(r)$ (normed in such
a manner that

$$N_V = \int_0^\infty s(r)\,dr \ ).$$

Let the related density function of the radii of
projected circles, observed per unit area of the
plate (with thickness T), be $c(r)$ (that means

$$N_A = \int_0^\infty c(r)\,dr \ ).$$

Then the two density functions are connected by
the following integral equation

$$(13) \qquad c(r) = 2r \int_r^\infty \frac{s(t)\,dt}{\sqrt{t^2-r^2}} \ + Ts(r) \ .$$

The solution of this equation is given by

$$(14) \qquad s(r) = \frac{\sqrt{2}}{\sqrt{\pi}}\cdot\frac{r}{T}\int_\infty^r f\{\frac{\sqrt{2\pi}}{T}\sqrt{t^2-r^2}\}\frac{d}{dt}\ \{\frac{c(t)}{t}\}dt \ .$$

The function $f(x)$ is expressed by means of the
ERROR-FUNCTION:

$$(15) \quad f(x) = \sqrt{2\pi}\cdot e^{x^2/2}\{1-\Phi(x)\}, \quad \Phi(x) = \frac{1}{\sqrt{2\pi}}\int_{-\infty}^x e^{-\frac{t^2}{2}}\,dt.$$

2-2. THE METHOD OF MOMENTS

From the solution (14) we get at once an expres-
sion of the quantity N_V:

$$(16) \qquad N_V = \frac{\sqrt{2}}{\sqrt{\pi}} \cdot \frac{1}{T} \int_0^\infty c(r) f\left\{\frac{\sqrt{2\pi}}{T}r\right\} dr \ .$$

If we multiply the equation (13) with r^k and integrate over r from 0 to ∞, we have

$$(17) \qquad c_k = \frac{\Gamma(\frac{1}{2}) \Gamma(1+\frac{k}{2})}{\Gamma(1+\frac{k+1}{2})} s_{k+1} + Ts_k \ .$$

Here c_k and s_k denote the k-th moment about zero of the density function c(r) and s(r) respectively $\Gamma(x)$ denotes the wellknown GAMMA-function. Having calculated $N_V = s_0$ from (16), we plainly can determine the s_k-s for all values of k by using the c_k-s, which can be estimated from the observed distribution of the radii of the projected circles. Using these values of the s_k-s it is obvious how to construct the distribution function s(r) by means of polynomial approximations. Polynomials in r^2 with the weighting function

$$(18) \qquad 2\cdot\frac{N_A}{c_2}\cdot r\cdot e^{-N_A r^2/c_2}$$

turned out to be easy to manage.

2-3. THE CALCULATION OF THE CLASS FREQUENCIES OF
       SPHERES FROM THOSE OF CIRCLES

Using the same classification of the radii of spheres and circles with class intervals of width h, an approximative integration of the equation (13) leads to a formula, which allows the calculation of the class frequencies of spheres from those of circles and inversely:

$$(19) \qquad S_i = \frac{C_i - 2h \sum_{j=i+1}^n S_j \cdot \alpha_{j,i}}{T + 2h\alpha_{i,i}} \ , \quad i=n,n-1,\ldots$$

183

The coefficients $\alpha_{j,i}$ must only be calculated once. S_i and C_i denote the frequencies of spheres respectively of circles with radii between ih and (i+1)h.

2-4. RELATED DISTRIBUTION FUNCTIONS

On the other hand the integral equation gives us the possibility of determining the distribution functions of circles related to certain definite distributions of spheres. For a two parametric distribution function of spheres which can be used for approximating a great number of distributions, let us quote the PEARSON distribution of type III (compare Fig. 3):

$$(20) \qquad s(r) = \frac{1}{n!}\{\frac{n+1}{\mu}\}^{n+1} \cdot r^n \cdot e^{-(n+1)r/\mu} \ .$$

The two parameters n (which is a positive integer) and μ (the arithmetic mean of the radii of spheres) can be estimated by using the mean value $\bar{r}$ of the observed radii of circles and their variance σ_r^2 .

With the abbreviations

$$(21) \quad \frac{\bar{r}}{T} = u, \quad \frac{\sigma_r^2+\bar{r}^2}{T^2} = v, \quad \frac{T}{\mu} = x, \quad \frac{n+2}{n+1} = y$$

we have

$$(22) \quad 32u^2x^3+\{128u^2-(64-6\pi)u-3\pi^2v\}x^2+\{128u^2-$$
$$-(128-4\pi)u+32-6\pi -6\pi^2v\}x +8\pi -16\pi u = 0,$$

$$(23) \quad y = \frac{2}{\pi}\cdot x\{(2+x)u-1\} \ .$$

Having solved the equation (22) for x, we get from the equation (23) the value of y and then with (21) the values of μ and n.
The related distribution of circles in a plate of thickness T is given by

$$(24) \quad c(r)= \frac{\{\frac{n+1}{\mu}\}^{n+1}}{(2\mu +T)n!}r^n\{(-1)^n2r \ \frac{d^nK_o(\frac{(n+1)r}{\mu})}{d(\frac{(n+1)r}{\mu})^n} \ + x\}.$$

Here χ is used as abbreviation for $Te^{-(n+1)r/\mu}$.
K_o denotes the modified HANKEL-function of order
zero:

(25) $$K_o(x) = \int_0^\infty e^{-x \cdot \cosh\tau} d\tau$$

3. SUMMARY

We have tried to solve stereological problems with
methods combining theorems from INTEGRAL GEOMETRY,
GEOMETRICAL PROBABILITY and STATISTICS. The essen-
tial results are assertions about mean values of
the convex particles under consideration. Under
certain assumptions we can obtain the particle
size distribution by solely using these mean val-
ues. The special case of spherical particles with
arbitrary distribution function has been solved
completely.

4. REFERENCES

Bach, G.,   Kugelgrößenverteilung und Verteilung
            der Schnittkreise; ihre wechselseitigen
            Beziehungen und Verfahren zur Bestim-
            mung der einen aus der anderen.
            Symposium über quantitative Methoden in
            der Morphologie, Wiesbaden 1965
            To appear in the next time by Springer-
            Verlag

Bach, G.,   Zufallsschnitte durch Haufwerke von
            Körpern, Braunschweig 1966

Bateman Manuscript Project (Erdelyi, Magnus, Ober-
hettinger u. Tricomi),
            Higher transcendental functions I-III
            McGraw Hill, New York 1953

Hadwiger, H., Altes und Neues über konvexe Körper,
            Birkhäuser Verlag 1955

Further references may be found in the references
cited above.
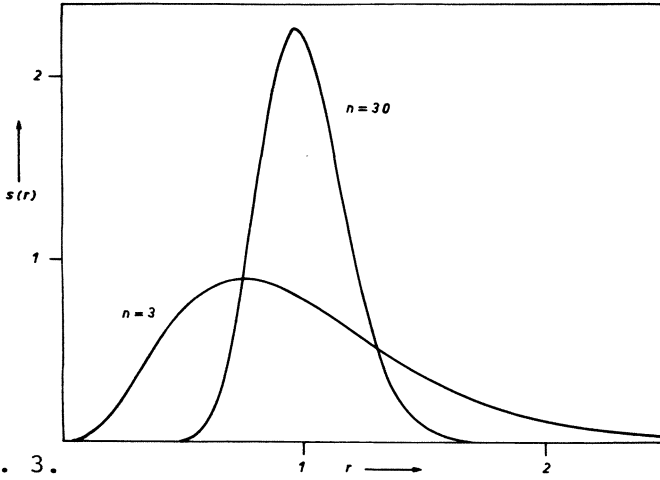
Fig. 3.

Two examples for density functions of PEARSON
type III (parameters $\mu=1$, n=3 and $\mu=1$, n=30).
For details compare chapter 2-4.

SIZE DISTRIBUTION OF CUBIC PARTICLES

Edward J. Myers

Mechanics Department, Air Force Institute of Technology,
Wright-Patterson Air Force Base, Ohio

For a distribution of particles embedded in an opaque solid, the number of particle profiles observed on a unit test area is related to the number per unit volume by the equation

$$N_A = N_V \cdot \overline{D} \qquad \text{(DeHoff and Rhines, 1961)} \qquad (1)$$

$\overline{D}$ is the average distance between tangent planes on all particles in the structure. Where the particles are cubes of uniform size but randomly oriented, Eq (1) becomes

$$N_A = N_V \cdot 1\ 1/2\ a \qquad \text{(Myers, 1963)} \qquad (2)$$

"a" is the cube edge. The profile sections observed have 3, 4, 5, or 6 sides, with 4-sides predominant, comprising, on the average, 48.7% of the total (Myers, 1963). Since some sections will be nearly square, "a" can be estimated closely and Eq (2) used to determine N_V.

Such a dispersion of cubic particles may also be analyzed by lineal traverses, and from the relation that the average projected area of any convex body equals one fourth its surface area we have

$$N_L = N_V \cdot 1\ 1/2\ a^2 \qquad (3)$$

Combining Eqs (2) and (3) gives Eqs (4) and (5)

$$N_V = 2\ N_A^2\ /\ 3\ N_L \qquad (4)$$

$$a = N_L\ /\ N_A \qquad (5)$$

N_V and "a" are computed directly as N_A and N_L are both measurable. The volume fraction is also obtained from

$$V_V = 2\ N_L^2\ /\ 3\ N_A \qquad (6)$$

The above methods are complementary and should make straightforward a complete analysis of uniformly-sized, randomly-oriented cubic particles dispersed in an opaque solid.

When the size of cubic particles varies, Eqs (4), (5), and (6) cannot be used with accuracy. Eqs (2) and (3) will be correct within each size class, but Eq (2) is more convenient to use; however, an estimate of "a" for cubes in different size classes must be made from the profile sections observed. Of the different types of planar sections cubes have, the 4, 5, and 6-sided sections are good indicators of the true size of the particle. For convenience, because of their greater frequency, if only 4-sided sections are counted and if each is assigned to a size class, then for each size the appropriate modification of Eq (2) is

$$N_V \text{ (total)} = \frac{N_A \text{ (4-sided)}}{(1.5a)(0.487)} \tag{7}$$

The 4-sided sections fall into two groups, trapezoids (68.2%) and parallelograms (31.2%), with rectangles and squares as special cases of each. The parameter of the section which gives the closest estimate to the cube size is the altitude, which is the perpendicular distance between the nearest (or only) parallel sides. The altitude function (call it q) over the required spherical coordinate range, $0 \le \theta \le 45°$, $0 \le \phi \le \text{arccot} (\cos \theta)$, is

$$q = a \sqrt{\frac{1 + \tan^2\phi}{1 + \tan^2\phi \cos^2\theta}} \tag{8}$$

For parallelograms the range in q is from 1.0a to 1.095a, with 1.0a most likely and 1.095a least. The average value of q can, in principle, be computed, but is estimated to be not over 1.03a. For trapezoids q varies from 1.0a to 1.224a, with 1.0a most likely and 1.224a least. The average value of q for this case appears to be under 1.05a. Thus if q of any 4-sided section is taken as the estimate for "a", the error in N_V will be at most 5%. This should be acceptable for most work in view of the statistical nature of all such results and the possibility of imperfect orientation randomness. If more careful classification of sizes is justified, this may be done by considering the acute angles of the profile sections as indicators of their orientation.

REFERENCES

DeHoff, R. T., and F. N. Rhines, Trans. Met. Soc. AIME, 221, 1961, p. 975.

Myers, E. J., First International Congress for Stereology, Congressprint, Vienna, 1963, p. 15/1.

DETERMINATION OF THE BETA GRANULE MASS IN PANCREATIC ISLETS USING LINEAR SCANNING METHODS

A. M. CARPENTER AND A. LAZAROW

Department of Anatomy, University of Minnesota, Minneapolis, Minnesota

Linear scanning technics were used to quantitate islets of normal, alloxan subdiabetic and alloxan diabetic animals. At low magnification (light microscope), the islet volume was determined on aldehyde-fuchsin stained sections. With oil immersion objectives, the volumes of the cellular components of the islets were obtained. In addition, by scanning electron micrographs, the volume of beta granules quantitated was expressed as per cent of beta cell cytoplasm. Using the successive values, beta granule "mass" (% beta granules x % beta cells x % islet volume) are expressed as per cent of pancreatic volume. These data are correlated with estimates of insulin expressed as units per gram of pancreas.

	N	SD	D
Age, mos.	12	11	11
Duration, mos.		9	9
No. animals	10	13	5
FBS, mgm %	110	121	450
Urine sugar, gms %	0.0	0.02	4.0
Plasma insulin, μU/ml[1]	56	36	15
Diabetic index	1	4	>10
Islet volume, % total pancreas	1.3	0.6	0.4
Identified beta cells, Volume % islet	71	60	32
Identified beta cells, Volume % total pancreas	0.94	0.37	0.12
Beta granules, volume % beta cell	3.7	2.1	1.2
Beta granules, volume % total pancreas	0.0340	0.0080	0.0015
Beta granule protein, μgm/gm pancreas*	75	13.96	0.35
Maximum insulin content in units/gm pancreas[#]	1.9	0.35	0.09

1 Assay by Dr. Carl Morgan
* Estimated assuming that 25% of the granule is protein
# Maximal amount of insulin that could be contained in all
   the beta granules in a gram of pancreas.

UNFOLDING PARTICLE SIZE DISTRIBUTIONS

W. L. NICHOLSON AND K. R. MERCKX

Battelle Memorial Institute, Pacific Northwest Laboratory, Richland, Washington

General treatment for unfolding particle size distributions
in a 3-dimensional specimen is possible if the particles'
spacial distribution, the sampling method, and the observa-
tional method are described by probabilistic models. Par-
ticles within "k" discrete groups are sized with a single
characteristic dimension (e.g., diameters for spheres). The
spacial distribution of particle centers is assumed uniform.
The sample consists of all particles intersected by a probe.
AF_i/τ is the intersection probability for an ith size par-
ticle, with A the characteristic dimension of the probe and
τ the specimen volume. The observations of sampled parti-
cles are sized into c cells. P_{ji} is the conditional probabil-
ity that an ith size particle is in the jth cell. The
number of observations in the jth cell is m_j. The expected
values and the covariances of the m_j's are linear functions
of the specimen population densities ρ_i. Population
density estimates $\hat{\rho}_i$, and their covariances follow from the
Gauss-Markov Theorem. For k = c these are

$$\hat{\rho}_i = (1/A) \sum_{j=1}^{c} Q_{ij}^{-1} m_j$$

$$Cov(\hat{\rho}_s, \hat{\rho}_t) = (1/A)^2 \sum_{j=1}^{c} Q_{sj}^{-1} m_j Q_{jt}^{-1} - (1/\tau) \hat{\rho}_s \delta_{st}$$

where Q_{ji}^{-1} is an element from the inverse of the Q matrix
with coefficients $Q_{ji} = P_{ji} F_i$.
The details of this development and its extension to the
case c > k have been given by Nicholson and Merckx. The
case c = k and the covariance estimation are new contribu-
tions.

For most types of particles where a geometrical character-
istic (e.g.-length of an intersection of a linear probe,
area of a planar section, etc.) is observed, a correspon-
dence between particle sizes and cell boundaries can be es-
tablished such that P_{ji} vanishes for j > i. The resultant
Q matrix is triangular. Unfolding, inversion of Q matrix,
can be done by successively solving for the density

estimates, starting at the largest observed size. This
method for unfolding spherical particle distributions cut
by planar sections has been described by Scheil. For cases
with fewer than k cells, a single unfolding matrix based on
k cells can be used for either uniform or exponentially in-
creasing cell boundaries. A scale factor adjusts the unfold-
ing matrix to the absolute cell length. Schwartz, Saltykov,
and Johnson have noted these relationships and have devel-
oped tables for spherical particles sampled by planar
sections. A computer program estimating the densities and
covariances for any triangular Q matrix has been described
by Nicholson and Merckx.

A portion of the information from the sampled particles may
be lost or distorted during the observational process.
Realistic modeling of this process, coupled with the
general development, accounts for such distortions.
Shadowed replicas of spherical voids in a specimen are a
case in point. Information is lost when replicas break
during stripping or fail to cast shadows. Truncation of
the P_{ji} matrix accounts for these effects. Distortion
during replication and stripping alter the remaining terms
in the P_{ji} matrix. Data from irradiated uranium specimens
containing voids were unfolded by using the replicated
surface model and the standard planar probe model. The im-
proved modeling resulted in smaller variances; hence, in
better density estimates.

Johnson, W., Metal Progress, vol. 49, no. 1, 1946.
Nicholson, W. L., and Merckx, K. R., BNWL-210. To be
published.
Saltykov, S. A., Stereometric Metallurgy, Moscow, 1958.
Scheil, E., Zeitschrift für Metallkunda, vol. 27, no. 9,
1935.
Schwartz, S. A., Metalls and Alloys, vol. 5, no. 6, 1934.

A SIMPLE FORMULA FOR THE CALCULATION OF SPATIAL SIZE DISTRIBUTIONS FROM DATA FOUND BY LINEAL ANALYSIS

G. BOCKSTIEGEL

Höganäs, Sweden

Simple formulae permitting the calculation of the true spatial size distribution of spherical bodies are derived, based on the distribution of chord-lengths as found with Rosiwal's lineal analysis, thus avoiding the use of laborious recursion methods.

Be $N(D)dD$ the number per unit volume of spheres, randomly distributed in space, and having diameters between D and $D-dD$,

$n(l)d$ the number of chords per unit length, produced by a Rosiwal-traverse through this space, and having lengthes between l and $l-dl$,

D_{max} the diameter of the largest spheres present.

From geometrical and statistical principles the following (mathematically strict) relationship between $n(l)$ and $N(D)$ can be derived[1]

$$n(l)\,dl = \frac{\pi}{2} l\,dl \int_{l}^{D_{max}} N(D)\,dD \qquad (1)$$

Integration over one size class, i.e. between l_{i-1} and l_i, yields

$$\int_{l_{i-1}}^{l_i} n(l)\,dl = \frac{\pi}{2} \int_{l_{i-1}}^{l_i} l \int_{l}^{D_{max}} N(D)\,dD\,dl \qquad (2)$$

With the abbreviation $n_i \equiv \int_{l_{i-1}}^{l_i} n(l)\,dl =$ number per unit length of all chords with lengthes between l_{i-1} and l_i, and applying the mean-value roule of integral calculus, (2) converts to

$$n_i = \frac{\pi}{2} \int_{l_{i-1}}^{l_i} l\,dl \cdot \int_{l_i-\varepsilon}^{D_{max}} N(D)\,dD = \frac{\pi}{4} (l_i^2 - l_{i-1}^2) \int_{l_i-\varepsilon}^{D_{max}} N(D)\,dD \qquad (3)$$

with $l_{i-1} < l_{i-\varepsilon} < l_i$. Correspondingly it is found

$$n_{i+1} = \frac{\pi}{4} (l_{i+1}^2 - l_i^2) \int_{l_i+\varepsilon'}^{D_{max}} N(D)\,dD \qquad (4)$$

with $l_i < l_{i+\varepsilon'} < l_{i+1}$. From (3) and (4) follows

$$\int_{l_i-\varepsilon}^{l_i+\varepsilon'} N(D)\,dD = \frac{4}{\pi} \left(\frac{n_i}{l_i^2 - l_{i-1}^2} - \frac{n_{i+1}}{l_{i+1}^2 - l_i^2} \right) \qquad (5)$$

193

For practical applications, the integration limits $l_{i-\varepsilon}$ and $l_{i+\varepsilon'}$ can be sufficiently well approximated by the class centers $l_{i-1/2}$ and $l_{i+1/2}$. With the abbreviation

$$N_{i+1/2} \equiv \int_{l_{i-1/2}}^{l_{i+1/2}} N(D)\,\mathrm{d}D =$$ number per unit volume of spheres having diameters between $l_{i-1/2}$ and $l_{i+1/2}$ it follows:

$$N_{i+1/2} = \frac{4}{\pi}\left(\frac{n_i}{l_i^2 - l_{i-1}^2} - \frac{n_{i+1}}{l_{i+1}^2 - l_i^2} \right) \tag{6}$$

This conversion formula between N and n is valid for any kind of size class divisions. It should be noted that, in graphical representation, n_i and n_{i+1} are to be plotted over the upper class limits l_i and l_{i+1} respectively, while $N_{i+\frac{1}{2}}$ is to be plotted over the class center between l_i and l_{i+1}.
In many cases it is advantageous to use a logarithmic size class division with the modulus $\sqrt{2}$, which can be defined by the recursion formula $l_i^2 = 2\,l_{i-1}^2$. Applying this recursion formula to (6) we obtain

$$N_{i+1/2} = C\,\frac{2\,n_i - n_{i+1}}{2^i} \tag{7}$$

where $C = 4/\pi\,l_0^2$, and l_0 = upper limit of the lowest size class. Since C is independent of the size class number i, it is of only secondary importance and disappears anyway when turning from the absolute numbers $N_{i+\frac{1}{2}}$ to the relative numbers $N_{i+\frac{1}{2}}/\sum N_{i+\frac{1}{2}}$.
From modern image analysing computers one often obtains direct readings of the cumulative number, a_i, of chords longer than l_i. Because of the definition $a_i \equiv \sum_{j=i+1}^{\infty} n_j$

(7) in this case converts to

$$N_{i+1/2} = C\big[(2a_{i-1} - a_i) - (2a_i - a_{i+1})\big]/2^i \tag{8}$$

Although formulae (6), (7), (8) are derived for spherical bodies, it is meaningful to apply them also to non-spherical bodies, when regarding the calculated distribution N as an equivalent distribution of sphere sizes yielding the same chord-length distribution n as the non-spherical bodies. It has been shown[1] that this equivalent distribution of sphere sizes and the true distribution of non-spherical bodies have the following properties in common: 1) the same volume proportion of the space containing them, 2) the same mean diameter and 3) the same specific surface area.

Reference:
1) Bockstiegel, G, Zeitschr. f. Metallkunde 57(1966)8 pp 647-652

THE DIRECT DETERMINATION OF THE NUMBER OF CONVEX PARTICLES PER UNIT VOLUME AND THE MOMENTS OF THEIR SIZE DISTRIBUTION BY AN INTERCEPT ANALYSIS ON A SECTION

J. E. HILLIARD

Department of Materials Science, Technological Institute, Northwestern University, Evanston, Illinois

Several analyses are available for determining the size distribution of particles in an opaque material from measurements on a section. The analyses differ from one another in the property measured on the section and the procedures used for the numerical solution of the integral equation relating the property to the particle-size distribution. However, all the analyses have the serious disadvantage that it is extremely difficult to determine how the statistical sampling error is propagated into the observed particle-size distribution curve. The stereologist thus has no means of knowing the reliability of his result and, what is equally important, he is unable to determine how many measurements he should make in order to get a result of the required accuracy.

An examination of the applications of particle-size analyses reveals that all the information provided by a distribution is but rarely required or utilized. In most cases it would suffice to know the number of particles per unit volume, N_V, and the first few moments of the distribution as defined by:

$$\mu_n'(D) = \int_0^{D_M} D^n f(D)dD,$$

where n is the order of the moment and f(D) the frequency function of particle size. The first moment gives the average size, the second moment is a measure of the deviation from the average, and the third moment will indicate the degree of asymmetry (or skewness) in the distribution. The advantage of using moments is that they can be determined directly from measurements on a section and it is feasible to relate the standard deviation in their estimation to the number of measurements made.

DeHoff has shown how N_V and the first two moments of the size distribution can be determined from three simple

types of measurements if it is assumed that the distribution follows a two parameter function. More recently, Hilliard has devised a procedure for determining moments of any order without any assumption about the form of the distribution. The only requirement is that the particles be convex and all of the same shape.

The measurement required for this analysis is the distribution $N_L(L)$ of lengths intercepted by a straight test line with particle profiles on a section. This distribution can be determined by a scanning instrument or manually by traversing the specimen under the cross hairs of a microscope and recording the traverse lengths, L_i, in the individual particles. The only computation required is the determination of the moments:

$$\mu_n'(L) = (1/N)\sum L_i^n ,$$

(where N is the total number of intercepts) and the limiting value of the slope of the $N_L(L)$ versus L distribution as $L \to 0$. From these two quantities, N_V and $\mu_n'(D)$ can be found directly by use of the following two expressions:

$$N_V = (2\alpha_0/\pi)[dN_L(L)/dL]_{L=0},$$

and

$$\mu_n'(D) = (2n\alpha_n N_L/\pi N_V)\mu_{n-2}'(L), \qquad (n \geq 1) ;$$

where D is the size of particle as defined by the maximum intercept length (equal to the diameter for a sphere), N_L is the total number of intercepts per unit length, and the α's are constants depending on the shape of the particle and are unity for spherical particles.

REFERENCES

DeHoff, R. T., Trans. Met. Soc. AIME, 233, 25 (1965).

Hilliard, J. E., (to be published.)

ACKNOWLEDGEMENTS

NUMBER   OF   PARTICLES   IN   UNIT   VOLUME

NUMBER OF PARTICLES PER UNIT VOLUME*

HERBERT HAUG

Department of Anatomy, University of Hamburg, Hamburg

Introduction

The mathematical basis of morphometry - inclu-
ding counting of particles - in translucent sli-
ces does not depend on the magnification. Never-
theless a difference exists in accomplishment
between the morphometry in light and electron
microscopy. This difference depends on the re-
lation between the size of structure and the
thickness of slice (furtherdown abbreviated with
T). In light microscopy this relation (e.g.cells
nuclei etc.) lies in general in the same class
of size and we can recognize a classification
of size of a structure without difficulties. In
electron micrographs T is very small, and struc-
tures to be measured (e.g.organelles of cells,
such as mitochondria etc.) are several times
larger than T. In this case it is impossible to
distinguish such a classification of structures.
This is easy to explain because a larger body
is cut into many profiles of different sizes.
All profiles noticed in a slice smaller than
this body can, but must not, originate from a
body of the same size. This problem is well
known to our colleagues from the metallurgical
discipline. In mitochondria - one of the most
important structures of biology - the size is
ranging from one to twenty times T in electron
micrographs. For those who are not familiar with
biology it is essential to know that in a cell
mitochondria are a sort of power station. Their
frequency, size and distribution are of great
interest for the interpretation of the metabo-
lism and the function of a cell or a tissue.
I have counted mitochondria in the neuropil of

the cerebral cortex. The neuropil is the tissue
between the cell bodies. It consists of many
processes of cells, and here are the contacts
between the neurones.

Material

The investigation was carried out in the neuro-
pil of the cat's visual cortex. The slices have
a thickness of about 400 Å. The electron micro-
graphs were made randomly, but all micrographs
with a pericaryon were omitted and in this way
only mitochondria of the neuropil measured. The
final magnification of micrographs is 30 000 : 1.

Goal of investigation

The actual number and actual size distribution
of the mitochondria of neuropil in the unit vo-
lume are calculated from measurements of the
number and size distribution of their profiles
in a known area.

Problems of investigation

An exact solution of our problem is only pos-
sible for shapes like spheres.

The second problem concerning the ways
of measuring will be discussed later. The in-
fluence of the small T on the results obtained
from electron micrographs is the third and an
important problem.

Methods

1) The first method is to pass through a se-
quence of calculations from the measured values
to the final values.
2) With mathematical rules of distribution we

can compute various theoretical distributions.

Methods of measuring

1) I have counted 2449 mitochondria with a par-
ticle size analyser (TGZ 3 of ZEISS) in 80 elec-
tron micrographs in an area of 2353 μ^2. 6 mito-
chondria were measured by hand.
            The illuminated circle of measuring
was chosen in such a manner that the overlapping
menisci had the same area as these parts inside
the circle without parts of a mitochondrium
(HENNIG 1957).
2) The volume fraction of the mitochondria was
determined with the point sampling method.
3) The surface of mitochondria in a volume was
ascertained according to HENNIG (1958).

From the values given in 1) the actual numbers
of the size distribution may be computed. If
this correction is exact we can calculate the
volume fraction and the surface per unit volume
from the values of 1) and compare them with the
results given in 2) and 3). Of the four results
estimated in these different manners two should
be similar.

The TGZ 3 distinguishes in counting between 48
classes of size from 1.5 to 27.7 mm diameter.
In order to be able to correct the data I have
reclassified 16 classes. As to the correction
1 class includes 3 classes of counted values.

Estimation of actual number per unit volume

1) Calculation of the actual number with the aid
of classes of correction: this problem is solved
for plane sections by metallurgists (SCHEIL 1931,
SCHWARTZ 1934, SALTIKOV 1958, UNDERWOOD – in
press –, EXNER 1966). They have presented va-
rious tabulations for 10 to 15 classes of cor-
rection. The new and main problem of the present
paper concerns the influence of T on the results.
For solving this problem I had to go my own way.
It was necessary to divide the tabulation into
two steps. I think that the basis of tabulations
of the metallurgists is the result of similar
steps.

The first step is the calculation of the size of structures to which the profiles belong. In the second step one computes the actual number of the structures per unit volume. In both steps T must be observed. It can be expected that by decreasing the diameters of particles towards T the influence of T increases.

It is necessary to introduce some symbols:

d = diameter of profile

D = diameter of structure

n_A = counted number of profiles in an area A

N_A = number of structures in an area A

N_V = actual number of structures in a volume V

T = thickness of a slice

f_{ij} = factor of correction to evaluate N_A from n_A (the first letter i explains that the factor is to be used for correction of class i; the second letter j marks the class j to which the profiles of d are given for correction)

k = factor belongs to a correction for such small parts of structures that thus can not be perceived and therefore can not be measured.

A dash on the head of symbol means the average value.

The first step of correction is similar to the method of tabulation used by SCHEIL. It is necessary to compute gradually the value N_A from the largest class of correction to the smallest one. This lengthy way can not be avoided, because I do not see any other possibility at the moment to include T in the correction. I have calculated tables to correct 3 sizes of T. These are the thicknesses 0 (equal to a plane section), 0.04 and 0.08 μ. 0.04 μ corresponds to the adjustment of thickness in cutting. The formula of correction is the following:

$$N_{A10} = f_{10-10} \cdot (n_{A10} - N_{A11} \cdot f_{10/11} - N_{A12} \cdot f_{10/12} \cdots - N_{Ai} \cdot f_{10/i}) \quad (1)$$

For each size as well as for T I had to calculate a single table. Table 1 shows an example

of the factors of correction for class 5. The smaller the class of size the greater is the difference of correcting data for various T's.

Table 1: Example of correction for class 5

Class	Diameter in μ	$\emptyset$	Factor f for T in μ 0.04	0.08
5	0.289	x 1.704	x 1.630	x 1.569
4	0.234	− 0.343	− 0.306	− 0.277
3	0.178	− 0.181	− 0.162	− 0.146
2	0.123	− 0.133	− 0.119	− 0.107
1	0.068	− 0.048	− 0.043	− 0.039

The result of this correction gives the number of cut structures of different sizes per area of slice. The definite correction will be made with the formula of HENNIG (1958).

$$N_V = N_A \ \frac{V}{A \cdot (D + T - 2k)} \tag{2}$$

After the last correction we have the number N_V per unit volume. In fig. 1 the influence of the two steps of correction for a T of 0.04 μ is seen. In order to compare the measured values with the intermediate and final results—every one is obtained with various methods of analy-sing—I have converted the values to similar scales. The first step of correction shifts the maximum to the right and the second and definite one to the left. The latter maximum is situated more to the left than in counted values. Fig. 2 compares the results for different T's. Struc-tures with a size which is more than ten times T do not show a noteworthy difference in numbers per volume. The smaller the diameters of struc-tures are related to T – the more remarkable is the influence of this relation on the results. We must conclude that T is to be observed in structures which are smaller than ten times T. This fact is a pity because we biologists can not make use of the work of metallurgists as to the correction of size distribution data. Our main structures in electron microscope are most-ly in a size which is less than ten times lar-ger than T.

For controlling my own results I have calculated
some of my own values of counted profiles with
the tabulation of SCHWARTZ to compare them with
the values when T equals 0. The difference be-
tween the number per volume calculated according
to SCHWARTZ and according to tabulation of my-
self is very small and does not exceed five per-
cent. Both methods of correction are based on
the same principle. Furthermore the total number
of structures were calculated with the aid of
the table of SALTIKOV (1958).

Comparision of this procedure of correction and
the other forms of correction with the estimated
values of volume fraction and surface per unit
volume will be given later.

2) Calculation with a theoretical distribution:
BACH* has determined the mathematical moments of
the above mentioned counted distribution. With
the aid of these moments he has computed a theo-
retical distribution which corresponds with a
distribution of PEARSON and it has the formula:

$$G(R) = c \cdot R^n \cdot e^{-(n+1)\frac{R}{Rm}} \qquad (3)$$

BACH has calculated the distribution of profiles
within a T of 0.04 μ. Fig. 3 compares the ascer-
tained distribution of profiles with BACH's
theoretical distribution. In fig. 4 the final
distribution of the structures per unit volume
shown by BACH and by myself are compared. The
main course of both distributions is similar.
But it can be noticed that a number of irregu-
larities do not exist with BACH. The maximum of
BACH's distribution is situated about 0.05 μ
more to the right than my results. I think that
the irregularities of the declining part of dis-
tribution are due to the existence of actual
classes of size of mitochondria. (See later)

3) Calculation from the average value of profi-
les: BACH (1965) has also developed a relative-
ly simple method for correction of numbers of
spheres in various T's. This method assumes

---

* I wish to express my thanks to Dr. BACH for
  working on my results and for his permission
  to publish his calculations.

spheres of about the same size. The measured distribution of profiles probably does not represent a normal distribution. Nevertheless final values could be calculated with this procedure. In the following section I am going to compare alle the results obtained with the various methods.

Comparison of the results

Table 2: Results of different corrections and their comparison (T = thickness in μ, N_V = number per 1 μ^3, D = average diameter in μ, S_V = surface in μ^2 per 1 μ^3, V_V = volume fraction in %)

	T	N_V	D	S_V	V_V
directly evaluated	0.04	–	0.294	1.33 ±0.22	8.9 ±1.4
own correction	$\emptyset$	4.0	0.277	1.22	8.7
	0.04	3.4	0.283	1.07	8.7
	0.08	3.0	0.287	0.96	7.1
SALTIKOV	$\emptyset$	4.0	–	–	–
BACH (1965)	0.04	2.7	0.361	1.39	12.5
BACH (new values)	0.04	3.3	0.283	1.05	7.4

In table 2 the average values of all results of correction are collected and compared.

1) Number per unit volume N_V

The numbers found in 1 μ^3 were between 2.7 mitochondria according to BACH (1965) and 4.0 according to SALTIKOV (1958) The number of 4.0 assumes that T equals O. The result of my own correction is the same as that of SALTIKOV. It justifies the statement that the basis of both methods is the same. The N_V of mitochondria calculated for T = 0.04 μ according to BACH's new correction and to my own is 3.4. The difference between the values calculated for T = 0.04 and T = 0 is about 20 %. This difference of 20 % is caused by the smaller classes of structures.

2) Average diameter D

The average diameter of the counted profiles is
0.294 μ. According to BACH's new correction and
my own correction all D's are smaller. The rea-
son for this is that the maximum of the final
distribution lies to the left of the average va-
lue of the profiles. According to BACH (1965) a
D of structure was found to be 0.361 μ. This
enlargement of D is due to the assumption of
structures of similar size.

3) Comparison of volume fraction V_V and sur- face S_V

V_V and S_V in 1 μ was calculated for all results
of correction except SALTIKOV's. The results
differ more or less from the values obtained by
point sampling and by the method of HENNIG (1958).
As to my own results for different T's all va-
lues are below the experimental data. The values
for T = 0.04 lie near the limit of confidential
scope. The difference does not exceed 20 %.
BACH's new correction is very similar to my own
correction, and it can be assumed that both me-
thods of correction are well suited for further
investigations. In BACH's new method we must
accept that we can not detect actual size clas-
ses.

Discussion
Interpretation of the results

The calculation of the volume fraction for mito-
chondria of different sizes is shown in fig. 5.
We notice several maxima. The peak of each maxi-
mum is about twice the volume of the preceding
one. Such a doubling of the volumes from one
class to another is often found in biology, but
it has not yet been reported on mitochondria.
However, I do not consider the doubling of vo-
lume as finally proved. But in the future such
a possibility must be taken into consideration.

Interpretation of methods

The problem of numbers and size distribution in
a plane section well known by the metallurgists
is new for biologists. Unfortunately it is im-
possible to transfer the methods of metallogra-
phy immediately to biological problems because

in biology one always works with translucent
slices of given thickness. It is therefore ne-
cessary to evolve new methods.

In this paper a method is presented which is ba-
sed on the same principle as the methods of
SCHEIL, SCHWARTZ and SALTIKOV. However, it ob-
serves T and is therefore divided into two steps.
It is impossible for a biologist to reduce the
calculation to a single step, because there are
no norms for T, for magnification of the electron
micrograph, and for size of the investigated
structures.

I think it would be desirable, if by common ef-
forts a program for computers could be evolved,
that will solve that problems of numbers and
size distribution for every case, with or with-
out T. With such a program for computers all
scientests could calculate optimally and uni-
formly the distribution of structures which can
be handled like spheres. The program should in-
clude the calculation of volume fraction and
surface per unit volume. It would be possible to
control and compare the results with those ob-
tained by other methods.

BACH has evolved a second method. He searches
for a distribution which is similar to the va-
lues obtained by measuring profiles. But he
needs likewise a computer with programs. Wor-
king with my values he came to the same average
results. However, his results differ slightly
from my own because my results show a small but
defined classification, that can not be seen
with BACH's. Therefore, further investigations
on mitochondria must be carried out in order
to clarify this problem and to find out whether
BACH's variation of PEARSON's distribution can
be generally applied in biology.

One important limitation must be recognized:
No exact results of size distribution in elec-
tron microscopy of biological material are pos-
sible without the aid of highly developed in-
struments for measuring and computing results.
Without such means the time required for inves-
tigations would be far too long.

REFERENCES:

BACH, G., Z. wiss. Mikr. 64, 265-270, 1959.
BACH, G. Metrika 9, 228-233, 1965. BACH, G.,
Habilitationsschrift Braunschweig 1966. EXNER,
H.E., Z. Metallkunde 57, 755-763, 1966. HAUG,
H., Proceedings 1. Intern. Kongr. f. Stereologie
Wien 1963, Nr. 17. HAUG, H., in: E. WEIBEL (ed.)
Quantitative Methoden in der Morphologie, Ber-
lin-Heidelberg-New York: Springer 1967, S. 58-
78. HENNIG, A., Mikroskopie 12, 174-202, 1957.
HENNIG, A., Zeiss-Werkzeitschrift 30, 3-12, 1958.
SALTIKOV, S.A., Metallurgizdat, 2nd Edit. Mos-
kau, 1958. SCHWARTZ, H.A. Metals and Alloys 5,139,
1934. SCHEIL, E., Z. anorg. allgem. Chem. 27,
201, 1931. UNDERWOOD, E.E., in: F.N. RHINES and
R.T. DeHOFF (ed.) Quantitative Metallography,
Chapter VII, McGraw-Hill Book Company, Inc.-

Addendum: In the last years BACH has evolved a
formula which could be the basis to a common
program for computers. He has calculated the
distribution of my values with this formula. The
results and a comparision with my own results
is seen in fig. 6.

number
20

FIG 1

Counted numbers of mitochondria in a slice
of 0.04 μ thickness and steps of correction
the values for a volume of tissue

n_A = counted number per 100 μ^2 area

N_A = first correction calculation of
numbers of diameters of the
structures per 100 μ^2 area

N_V = second correction calculation
of the actual numbers in
27 μ^3 volumen

0.1 0.2 0.3 0.4 0.5 0.6 0.7 0.8 0.9 1.0 diameter in μ

number

FIG. 2

Correction of counted numbers of mitochondria
for different thickness of slice.
Values calculated for 27 μ^3

.... for a slice with 0.08 μ thickness

————— for a slice with 0.04 μ thickness

- - - - - - for a section without thickness

20

15

10

5

0.1 0.2 0.3 0.4 0.5 0.6 0.7 0.8 0.9 1.0 diameter in μ

number

18

16

14

12

10

8

6

4

2

FIG 3

Comparison of counted numbers n_A in an area
of 100 μ^2 and calculated numbers of profiles
of a Pearson distribution after Bach

- - - - - n_A = counted numbers

————— = distribution of Pearson
after equation

$$G(R) = c \cdot R^n e^{-(n+1)\frac{R}{Rm}}$$

$n = 3, Rm = 0.142, T = 0.04$

0.1 0.2 0.3 0.4 0.5 0.6 0.7 0.8 0.9 1.0 diameter in μ

number

18

16

14

12

10

8

6

4

2

FIG. 4

Comparison of different methods of correction
for 0.04 μ thickness of slice

- - - - - - N_V = Own correction, values for 27 μ^3

————— N_V = distribution of spheres after
equation of Pearson

$$G(R) = c \cdot R^n e^{-(n+1)\frac{R}{Rm}}$$

$n = 3, Rm = 0.142, T = 0.04$

0.1 0.2 0.3 0.4 0.5 0.6 0.7 0.8 0.9 1.0 diameter in μ

number
20
15
10
5

C 1
0.0031 μ³

C 8
0.025 μ³

C 16
0.05 μ³

C 40
0.125 μ³

C 64
0.2 μ³

C 128
0.4 μ³

0.1 0.2 0.3 0.4 0.5 0.6 0.7 0.8 0.9 1.0 diameter in μ

Volume fraction
10 ‰
9 ‰
8 ‰
7 ‰
6 ‰
5 ‰
4 ‰
3 ‰
2 ‰
1 ‰

FIG 5

Comparison between the actual
number N_V of mitochondria and
their volume fraction in percent

------ N_V = number per 27 μ³

——— V_V = volume in percent

Arrows indicate
possible classes
of volume of
mitochondria

number
18
16
14
12
10
8
6
4
2

FIG. 6

Comparison of own correction with BACH's new
correction. All values for 0.04 μ thickness of slice

------ N_V = own values

——— N_V = BACH's values

0.1 0.2 0.3 0.4 0.5 0.6 0.7 0.8 0.9 1.0 diameter in μ

210

THE CALCULATION OF THE MEAN CALIPER DIAMETER OF A BODY FOR USE IN THE ANALYSIS OF THE NUMBER OF PARTICLES PER UNIT VOLUME*

J. E. HILLIARD

Department of Materials Science, Technological Institute, Northwestern University, Evanston, Illinois

INTRODUCTION

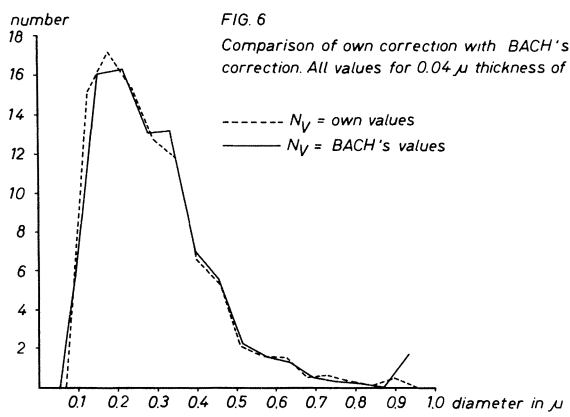It is easily shown that the expected number of particle profiles $\bar{N}_A$ per unit area of a plane section of orientation (ϕ, θ) is given by:

$$\bar{N}_A(\phi, \theta) = N_V \bar{D}(\phi, \theta),\tag{1}$$

in which N_V is the number of particles per unit volume and $\bar{D}(\phi, \theta)$ is the average projected height of the particles on a line of orientation (ϕ, θ). If the particles are randomly oriented, then Eq. (1) can be written as

$$\bar{N}_A = N_V \bar{D},\tag{2}$$

in which D is the projected height averaged over all orientations of a particle; i.e.,

$$D = (1/4\pi) \int_0^{2\pi} \int_0^{\pi} D(\phi, \theta) \sin\phi \, d\phi \, d\theta.\tag{3}$$

This average is variously referred to as: "the average altitude", "the mean distance between tangent planes" or "the mean caliper diameter".

It is apparent from Eq. (2) that the density of particle profiles seen on a section depends not only on N_V, but also on $\bar{D}$ and therefore on the size distribution and shape of the particles. With but few exceptions, N_V cannot be determined from measurements on random sections unless all the particles have the same shape and, even if this condition is satisfied, it is necessary to measure the size distribution of some property observed on the section. (One exception is when all the particles are of the same size as well as shape; in this case it is necessary only to measure N_A.) In analyses based on the measurement of the distribution of profile areas (see, for example, the contribution by S. A. Saltikov in this volume) a necessary first step is the calculation of D for the particular shape of particle

*Written by special invitation, not presented at Congress.

present in the specimen. It is this aspect of the analysis that we will be concerned with here.

<div align="center">CALCULATION OF D</div>

The calculation of D from Eq. (3) is tedious unless the particle shape is very simple. Fortunately, there are more general expressions available which are much easier to use. It has been shown by Minkowski (1903)* that for convex particles free from singularities:

$$D = (1/4\pi)\iint(\rho_1^{-1} + \rho_2^{-1})dS, \text{ (convex particles)} \qquad (4)$$

in which ρ_1 and ρ_2 are the principal radii of curvature and the integration is over the whole surface, S, of the particle. We will now show how Eq. (4) can be generalized to cover the case of particles (such as cylinders) having a discontinuity or edge in the surface.

For simplicity we will limit ourselves to straight edges formed by the intersection of two plane surfaces of the particle. (The reader can easily extend the argument to the case of curved surfaces and edges.) Consider a particular edge in the particle of length ℓ_i and let α_i be the dihedral angle ($<\pi$) between the surfaces meeting at this edge. In order to permit the use of Eq. (4) we will replace this sharp edge by a smooth surface of small radius r. This surface will be cylindrical with its axis parallel to the edge and will meet the adjoining surfaces tangentially. It is easily shown that the cylindrical surface subtends an angle $(\pi - \alpha_i)$; its area is thus $(\pi - \alpha_i)r\ell_i$. The radii of curvature over the cylindrical surface are constant: $\rho_1 = r$ and $\rho_2 = \infty$. It thus follows from Eq. (4) that the contribution of this cylindrical edge to D is: $(1/4\pi)(\pi - \alpha_2)r\ell_i/r = (1/4\pi)(\pi - \alpha_i)\ell_i$ which, it will be noted, is independent of value selected for r. Allowing for all edges we obtain:

$$D = (1/4\pi)\left\{ \iint(\rho_1^{-1} + \rho_2^{-1})dS + \sum(\pi - \alpha_i)\ell_i\right\}, \qquad (5)$$

in which the integration is over the smooth surfaces of the particle and the summation is over the edges. In the case of a convex polyhedral particle, $\rho_1 = \rho_2 = \infty$ because all the surfaces are flat. The integral is thus zero and Eq. (5) reduces to:

---

* A derivation of Eq. (4) is also given in the more accessible publication of Kendall and Moran (1963).

$$D = (1/4\pi) \sum (\pi - \alpha_i)\ell_i, \text{ (convex polyhedra);} \qquad (6)$$

a result first derived by Santaló (1936). For regular polyhedra, Eq. (6) yields:

$$D = a(E/2\pi)\arccos[\cos(\pi/f)/\sin(\pi/n)], \qquad (7)$$

$$\text{(regular polyhedra);}$$

where a is the edge length, E the number of edges, f the number of faces at a vertex and n the number of sides to each face.

By the use of Eqs. (4)-(7) the mean caliper diameter can be computed for any particle, in some cases virtually by inspection. Results for some of the more common shapes are listed in the Table. In order to make the table more comprehensive, the surface area (s) and volume (v) are also listed since these parameters frequently occur in stereological formulae. For example, the average intercept length, $\bar{L}$, in a particle is given by:

$$\bar{L} = 4v/s. \qquad (8)$$

Also, as has been pointed out by DeHoff (1964), various dimensionless ratios formed from D, v, and s can be used to characterize the shape of particles. For example, Ds/4v ($= D/\bar{L}$) has a minimum value of 3/2 (achieved in a sphere). For regular polyhedra this limiting value is approached approximately as $15/F^{3/2}$, where F is the number of faces.

<div align="center">TABLE</div>

Mean-Caliper Diameter (D), Surface Area (s) and Volume (v) for Particles of Various Shapes.

Sphere of radius r:

$$D = 2r$$
$$s = 4\pi r^2 = 12.56637r^2$$
$$v = (4/3)\pi r^3 = 4.18879r^3$$

Hemisphere of radius r:

$$D = [1+(\pi/4)]r = 1.78540r$$
$$s = 3\pi r^2 = 9.42478r^2$$
$$v = (2/3)\pi r^3 = 2.09440r^3$$

*Cylinder of length ℓ and radius r:

$D = (1/2)[\ell + \pi r]$

$s = 2\pi r[\ell + r]$

$v = \pi \ell r^2$

Thin Rod of length ℓ:

$D = \ell/2$

Thin Disc of radius r:

$D = (\pi/2)r = 1.57080r$

$s = 2\pi r^2 = 6.28319r^2$

†Oblate Spheroid, axes $2a \geq 2b$, $\epsilon = [1-(b/a)^2]^{1/2}$:

$D = b+(a/\epsilon)\arcsin\epsilon$

$s = 2\pi a^2 + \pi (b^2/\epsilon)\ell n[(1+\epsilon)/(1-\epsilon)]$

$v = (4/3)\pi a^2 b$

†Prolate Spheroid, axes $2a \geq 2b$, $\epsilon = [(a/b)^2-1]^{1/2}$:

$D = a+b(1/\epsilon)\text{arcsinh}\epsilon$

$s = 2\pi b^2 + 2\pi(a^2/\epsilon)\arcsin(b\epsilon/a)$

$v = (4/3)\pi ab^2$

Parallelepiped of edge lengths a, b and c:

$D = (1/2)(a+b+c)$

$s = 2(ab+bc+ca)$

$v = abc$

Tetrahedron of edge length a:

$D = a(3/\pi)\arccos(1/3)^{1/2} = 0.91226a$

$s = a^2\sqrt{3} = 1.73205a^2$

$v = (a^3/12)\sqrt{2} = 0.11785a^3$

---

* DeHoff (1964) has made plots from which D, v and s can be read off for cylinders and spheroids for any ratio of the two parameters.

† Values of D taken from Mack (1956).

Cube of edge length a:

$D = (3/2)a$

$s = 6a^2$

$v = a^3$

Octahedron of edge length a:

$D = a(6/\pi)\arccos(2/3)^{1/2} = 1.17548a$

$s = a^2 2\sqrt{3} = 3.46410a^2$

$v = a^3(2/9)^{1/2} = 0.47140a^3$

Dodecahedron of edge length a:

$D = a(15/\pi)\arccos[(1/2)+(1/10)\sqrt{5}]^{1/2} = 2.64312a$

$s = a^2 3[5(5+2\sqrt{5})]^{1/2} = 20.64573a^2$

$v = (a^3/4)[15+7\sqrt{5}] = 7.66312a^3$

Icosahedron of edge length a:

$D = a(15/\pi)\arccos\left[[1+(2/5)\sqrt{5}]/[(3/2)+(3/10)\sqrt{5}]\right]^{1/2}$

$\quad = 1.74210a$

$s = a^2 5\sqrt{3} = 8.66025a^2$

$v = a^3(5/12)(3+\sqrt{5}) = 2.18169a^3$

Tetrakaidecahedron of edge length a:

$D = 3a$

$s = 6(1+2\sqrt{3})a^2 = 26.78461a^2$

$v = (8\sqrt{2})a^3 = 11.31371a^3$

REFERENCES

DeHoff, R. T., Trans. Met. Soc. AIME., 230, 764 (1964).

Kendall, M. G., and Moran, P. A. P., Geometrical Probability, Charles Griffin and Co., London (1963). (p. 81).

Mack, C., Proc. Camb. Phil. Soc., 52, 246 (1956).

Minkowski, H., Math. Ann., 57, 447 (1903).

Santaló, L.A., Integralgeometrie 5, Actualités Scientifiques et Industrielles, No. 357, Hermann et Cie., Paris (1936).

215

ANISOTROPY, ORIENTATION IN SPACE

DETERMINATION OF STRUCTURAL ANISOTROPY

J. E. HILLIARD

*Department of Materials Science, Technological Institute, Northwestern University,
Evanston, Illinois*

ABSTRACT

Methods are described for specifying and measuring the
degree of anisotropy in (a) lineal arrays in two-dimensional
space and (b) lineal and areal arrays in three-dimensional
space. From a measurement of the anisotropy in these fea-
tures, it is possible to determine the average shape of
grains, cells, or particles provided that there is a common
axis of alignment.

INTRODUCTION

For the purpose of characterizing a structure, or of
correlating it with some other property, it is often neces-
sary to have means of specifying the degree and type of
anisotropy present. It is apparent that the anisotropy can
be described in terms of the preferred orientation of one-
or two-dimensional features in the structure. Furthermore,
the average shape of grains, cells, or particles can be re-
lated to those preferred orientations if the latter features
have a common axis of alignment.

Several means of specifying anisotropy have been advo-
cated in the past. For example, for a two-dimensional array
of lineal features, Saltikov (1958) has suggested a polar
plot (which he termed"roses-of-the-number-of-intersections")
of the density of intersections, $P_L(\theta)$, on a test line
applied to the lineal features at an angle θ with respect
to a reference direction. The disadvantage of this param-
eter (which is also shared by most of the others that have
been proposed) is that it is a derived rather than a funda-
mental property of the structure, and for this reason it is
not easily correlated with other orientation dependent prop-
erties. In order to avoid this difficulty, Hilliard (1962)
suggested the use of distribution functions that define ex-
plicitly the fraction of line length or boundary area lying
in a given direction. In this chapter methods will be de-
scribed for determining these distribution functions from
measurements on sections through the structure. Quite apart
from the specification of anisotropy, these functions are
important in establishing the optimum procedures for the

analysis of total line length or boundary area in aniso-
tropic structures. This application has recently been
developed in detail by Hilliard (1968).

We will first consider the analysis of two-dimensional
lineal arrays, and then treat the more difficult case of
lineal and areal arrays in three dimensions.

TWO-DIMENSIONAL LINEAL ARRAYS

Specification of Orientation Distribution

The orientation distribution of a lineal array will be
defined by $L_A(\theta)$ where $L_A(\theta)d\theta$ is the total line length per
unit area to which tangents have angles in the range
$\theta \pm (d\theta/2)$ with respect to a given reference direction. The
line length over a finite range of θ is given by the inte-
gral of $L_A(\theta)$ over that range. It is assumed that the sense
of a line is indeterminate so that $L_A(\theta)$ has a periodicity
of π. Thus the total line length per unit area is given by:

$$L_A = \int_0^\pi L_A(\theta)d\theta. \tag{1}$$

An isotropic array will be defined as one for which $L_A(\theta)$
is independent of θ. (i.e., all orientations are equally
probable). For this case we have from Eq. (1):

$$L_A(\theta) = (1/\pi)L . \qquad \text{(isotropic array)}. \tag{2}$$

In the case of an anisotropic array, $L_A(\theta)$ will be greater
than the value given by Eq. (2) for those directions in
which the line density exceeds the average.

Measurement of $L_A(\theta)$

The analysis consists of superimposing a second or
test array of lines having a known orientation distribution
$L_A'(\omega)$. This test array is applied randomly with respect to
translation but with a fixed orientation μ between the ref-
erence directions of the two arrays. A count is then made
of the number of intersections, $P_A(\mu)$, per unit area that
the test array makes with the other array as a function of
μ. It has been shown by Hilliard (1962) that the expected
number of intersections is related to the orientation dis-
tributions by:

$$\bar{P}_A(\mu) = \int_0^\pi \int_0^\pi L_A(\theta)L_A'(\omega)|\sin(\mu+\theta-\omega)|\,d\theta\,d\omega.$$

Philofsky and Hilliard (1967) have given a general solution

to this equation. The known function $L'(\omega)$ and the meas-
ured function, $P_A(\mu)$, are expanded in a Fourier series. If
$t_{2k}(\omega)$ and $t_{2k}(\mu)$ are the complex coefficients as defined
by:

$$t_{2k}(\omega) = (1/\pi)\int_0^\pi L'_A(\omega)\exp(-2ik\omega)d\omega, \tag{3}$$

then the coefficients, $t_{2k}(\theta)$ of the distribution function
of the array being analyzed are given by:

$$t_{2k}(\theta) = [(1-4k^2)/2\pi] [t_{2k}(\mu)/t_{-2k}(\omega)]. \tag{4}$$

Philofsky and Hilliard (1967) have given expressions
which permit the construction of test figures having any re-
quired orientation distribution, $L'_A(\omega)$. It is possible to
devise test figures (having positive and negative segments)
for which the net number of intersections is directly pro-
portional to a given Fourier coefficient of the lineal
array being analyzed. The simplest case is for the zeroth
coefficient for which the corresponding test figure is a
circle. Once the coefficients have been determined, either
by the use of these special test figures or with test
arrays of another form, the function $L_A(\theta)$ can be obtained
by Fourier inversion.

It is also possible to reduce the results to a single,
"anisotropy" parameter. One such parameter that correlates
well with the visual impressions of anisotropy is:

$$\psi = t_2(\theta)t_{-2}(\theta)/t_0^2(\theta). \tag{5}$$

For an isotropic array, $t_{2k}=0$ for $|k|>0$, thus $\psi=0$. For a
lineal array having the highest possible anisotropy (corre-
sponding to all the line elements being parallel with one
another) the Fourier coefficients are all equal, thus $\psi=1$.
Hence, ψ takes values between 0 and 1 depending on the
degree of anisotropy. This parameter also has the desirable
property of being invariant with respect to the choice of
reference direction.

Expected Number of Intersections for Random Orientation
of Arrays

It follows from Eqs. (1) and (4) that the zeroth
coefficients are related to the total line lengths in the
arrays by:

$$L_A = \pi t_0(\theta),$$

and

$$L'_A = \pi t_0(\omega). \tag{6}$$

Similarly, the expected number of intersections when the two arrays are superimposed randomly with respect to both translation and orientation is given by:

$$\bar{P}_A = (1/\pi)\int_0^\pi P_A(\mu)d\mu = t_0(\mu).$$ (7)

Substituting from Eqs. (6) and (7) into Eq. (4), we obtain:

$$\bar{P}_A = (2/\pi)L_A L_A'.$$ (8)

Dividing through by the line length of the test array we recover the well-known expression:

$$\bar{P}_L = (2/\pi)L_A.$$ (9)

The foregoing derivation has the advantage of emphasizing that Eq. (9) is independent of the form of the test line-- it can be straight, curved, continuous or discontinuous--and of demonstrating (through Eq. [8]) the underlying symmetry of the relationship.

THREE-DIMENSIONAL LINEAL AND AREAL ARRAYS

Specification of Orientation Distribution

The orientation of a line element in three dimensions will be defined by ϕ and θ, the co-latitude and longitude of its tangent. The sense of the line element will be assumed indeterminate, so that $(0 \le \phi \le \pi/2)$ and $(0 \le \theta \le 2\pi)$. The orientation distribution will be specified by the function $L_V(\phi,\theta)$ where $L_V(\phi,\theta)\sin\phi d\phi d\theta$ is the line length per unit volume with orientations in the range $\phi \pm (d\phi/2)$ and $\theta \pm (d\theta/2)$. The total line length per unit volume is therefore:

$$L_V = \int_0^\pi \int_0^{\pi/2} L_V(\phi,\theta)\sin\phi d\phi d\theta.$$ (10)

An isotropic array is one for which

$$L_V(\phi,\theta) = L_V/2\pi.$$ (11)

The orientation of an areal element will be defined by the angles ψ and ω of its normal, and the orientation distribution of an areal array by the function $S_V(\psi,\omega)$. Corresponding to Eq. (11) we have for the total boundary area per unit volume:

$$S_V = \int_0^{2\pi} \int_0^{\pi/2} S_V(\psi, \omega) \sin\psi \, d\psi \, d\omega, \qquad (12)$$

and for an isotropic array:

$$S_V(\psi, \omega) = S_V/2\pi. \qquad (13)$$

Measurement of $L_V(\phi, \theta)$ and $S_V(\psi, \omega)$.

As in the two-dimensional case, the experimental esti-
mation of the orientation distribution $S_V(\psi, \omega)$ is based on
the interaction of a test array with the areal array. It
has been shown by Hilliard (1962) that the expected number
of point intersections generated when a lineal test array is
"superimposed" on an areal array randomly with respect to
translation, but with their axes coincident, is given by:

$$\bar{P}_V = \int \cdots \int L_V(\phi, \theta) S_V(\psi, \omega) \sin\phi \sin\psi \, |\cos\gamma| \, d\phi \, d\theta \, d\psi \, d\omega, \qquad (14)$$

in which the integration is over the allowable range of the
angles and where:

$$\cos\gamma = \sin\phi \sin\psi \cos(\theta - \omega) + \cos\phi \sin\psi \qquad (15)$$

As shown by Philofsky and Hilliard (1967), a solution to
Eq. (14) can be obtained by expanding the functions in
spherical harmonies, thus:

$$\bar{P}_V = \sum \left\{ \alpha_{2n}''' [2n/(4n+1)]^2 \left[\alpha_{2n}'' \alpha_{2n}' + (1/2) \sum_{h=1}^{h=2n} [(2n+h)!/(2n-h)!] \right. \right.$$

$$\left. \left. \times \left[\alpha_{h,2n}'' \alpha_{h,2n}' + \beta_{h,2n}'' \beta_{h,2n}' \right] \right] \right\} \qquad (16)$$

in which the coefficients are defined in terms of Lengdre
polynomials, P_{2n}, and associated Lengendre polynomials, P_{2n}^h,
by:

$$\alpha_{2n}''' = (4n+1) \int_0^1 \cos\gamma P_{2n}(\cos\gamma) d(\cos\gamma), \qquad (17)$$

and

$$\alpha_{2n}'' = [(4n+1)/2\pi] \int_0^{2\pi} d\theta \int_0^1 L_V(\phi, \theta) P_{2n}(\cos\phi); \qquad (18)$$

223

$$\alpha''_{h,2n} = [(4n+1)(2n-h)!/2\pi(2n+h)!]$$

$$X \int_0^{2\pi} d\theta \int_0^1 L_V(\phi,\theta)\cosh\theta P_{2n}^h(\cos\phi)d(\cos\phi); \qquad (19)$$

$$\beta''_{h,2n} = [(4n+1)(2n-h)!/2\pi(2n+h)!]$$

$$X \int_0^{2\pi} d\theta \int_0^1 L_V(\phi,\theta)\sinh\theta P_{2n}^h(\cos\phi)d(\cos\phi). \qquad (20)$$

The single primed coefficients are similarly defined with respect to the function $S_V(\psi,\omega)$.

Equation (16) permits the determination of the orientation distribution of either lines or boundaries in three-dimensional space. In the former case test planes are applied to the structure, in the latter case an array of test lines is used. The coefficients α_{2n}, $\alpha_{h,2n}$ and $\beta_{h,2n}$ are first computed for a series of test arrays. These arrays are then superimposed on the structure and the number, P_V, of intersections counted for each array. These values are substituted in Eq. (16) yielding a set of simultaneous equations which can be solved for the unknown coefficients. The orientation distribution function is then constructed from these coefficients. The resolution obtainable depends on the number of coefficients estimated and this, in turn, is determined by the number of test arrays used. It will be apparent that a considerable amount of counting and computational effort may be required. Fortunately, in most cases of anisotropy that occur in practice, some degree of symmetry will be present and this can greatly simplify the analysis. We will now consider one of these special cases.

Measurement of $S_V(\psi,\omega)$ When an Axis of Symmetry is Present.

An anisotropic structure with an axis of symmetry is commonly found in materials that have been fabricated by wire-drawing or extrusion. Such symmetry will also be present in many naturally occurring organisms. If the ψ axis is chosen so that it is parallel to the symmetry axis, then the function $S_V(\psi,\omega)$ will be independent of ω. Thus,

$$S_V(\psi,\omega) = S_V(\psi)/2\pi. \qquad (21)$$

Because of the non-dependence on ω, the associated Legendre polynomials in the expansion of $S_V(\psi,\omega)$ vanish and Eq. (16)

reduces to:

$$\bar{P}_V = \sum [2\pi/(4n+1)]^2 \alpha'_{2n} \alpha''_{2n} \alpha'''_{2n}. \tag{22}$$

It has been shown by Philofsky and Hilliard (1967) that the coefficients for $S_V(\psi)$ can be determined from an intercept analysis on a single plane of polish parallel to the axis of symmetry. Therefore, for this case, the determination of the orientation distribution of the boundaries requires no more effort than the analysis of a two-dimensional lineal array.
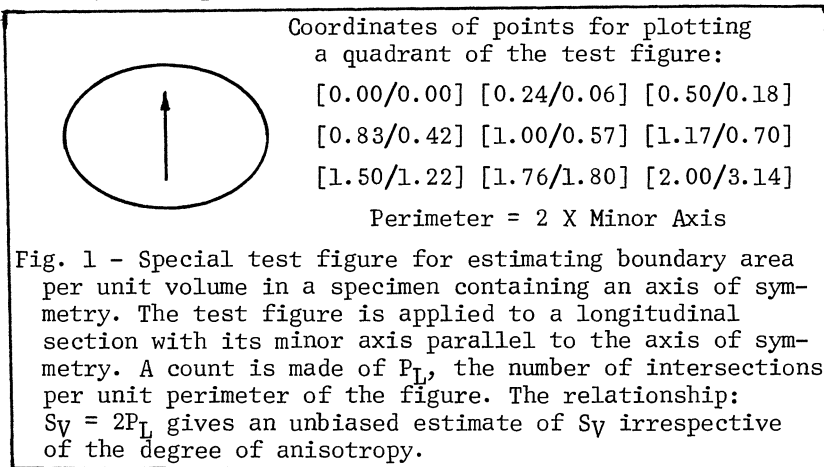
Estimation of S_V When an Axis of Symmetry is Present.

In general, when anisotropy is present, it is necessary to make measurements on several sections of different orientations in order to obtain a reliable estimate of S_V, the total boundary area per unit volume. We will now show that for the special case in which an axis of symmetry is present, it is possible to obtain an unbiased estimate of S_V from measurements on a single section, irrespective of the degree of anisotropy.

As in the case of an anisotropy analysis, the section is chosen parallel to the axis of symmetry, so that Eq. (22) is applicable. We first note that, according to Eqs. (12) and (18), the boundary area per unit volume is related to α'_0 by:

$$S_V = 2\pi\alpha'_0. \tag{23}$$

Now, it is possible to construct a test figure (shown in Fig. 1) whose perimeter has an orientation distribution

Coordinates of points for plotting a quadrant of the test figure:

[0.00/0.00] [0.24/0.06] [0.50/0.18]

[0.83/0.42] [1.00/0.57] [1.17/0.70]

[1.50/1.22] [1.76/1.80] [2.00/3.14]

Perimeter = 2 X Minor Axis

Fig. 1 - Special test figure for estimating boundary area per unit volume in a specimen containing an axis of symmetry. The test figure is applied to a longitudinal section with its minor axis parallel to the axis of symmetry. A count is made of P_L, the number of intersections per unit perimeter of the figure. The relationship: $S_V = 2P_L$ gives an unbiased estimate of S_V irrespective of the degree of anisotropy.

satisfying the condition $\alpha_{2n}''=0$ for $n\geq 1$. For such a test figure, it follows from Eqs. (22) and (23):

$$\bar{P}_V = 2\pi\alpha_0''\alpha_0'''S_V.$$

It can be shown that $\alpha_0''=(1/2\pi)L_V$ where L_V is the perimeter of the test figure per unit volume of structure; also, by Eq. (17), $\alpha_0'''=1/2$. Hence:

$$\bar{P}_V = (1/2)L_VS_V.$$

Dividing through by the perimeter of the test figure, we obtain:

$$S_V = 2\bar{P}_L, \tag{24}$$

where P_L is the number of intersections per unit length of test figure perimeter. Equation (24) is, of course, a familiar one; however, it is important to recognize that in this particular case it applies only for a test figure of the form shown in Fig. 1. Any other test figure (for example, a straight line) applied to a section parallel to an axis of cylindrical symmetry will yield a biased estimate of S_V.

Expected Number of Intersections for a Random Super-
    imposition of an Areal and Lineal Array

We have so far assumed that the areal and lineal arrays are superimposed such that their reference axes are parallel. We will now obtain an expression for the expected number of point intersections created when the two arrays are superimposed randomly with respect to both translation and orientation.

It follows from Eq. (16) that the expected number of intersections for a random orientation of the arrays is obtained by considering only the zeroth-order harmonics. As already shown: $\alpha_0'''=1/2$, $\alpha_0''=(1/2\pi)S_V$ and $\alpha_0'''=(1/2\pi)L_V$. Thus:

$$\bar{P}_V = (1/2)L_VS_V. \tag{25}$$

If we are estimating S_V, then the line array is the test element. Dividing through by its total length we obtain:

$$\bar{P}_L = (1/2)S_V. \tag{26}$$

Alternatively, if L_V is being estimated, then the test

element is an areal array, and Eq. (25) gives:

$$\bar{P}_A = (1/2)L_V. \tag{27}$$

It will thus be seen that the two well-known relationships, [Eqs. (26) and (27)] are, in fact, special cases of the more general and symmetric relationship expressed by Eq. (25).

SUMMARY

It has been shown that the anisotropy in the spatial distribution of lineal and areal features can be specified by distribution functions. Methods are given for determining these distribution functions from measurements on sections through the structure. The analysis of anisotropy in three-dimensions will be very tedious in the general case unless it is feasible to use an automatic scanning instrument. However, the analysis may be greatly simplified if some symmetry is present. For the case of a cylindrical axis of symmetry it was shown that the orientation distribution of areal features can be determined from measurements on a single section. In this case, it is also possible (by the use of a special test figure) to obtain an unbiased estimate of the total boundary area per unit volume.

An example of anisotropy analysis and its applications to a practical problem has recently been given by Philofsky and Flinn (1967).

REFERENCES

Hilliard, J. E., Trans. Met. Soc. AIME, 224, 1202 (1962).

Hilliard, J. E., Contribution to: Ceramic Microstructures-- Their Analysis, Significance and Production, Third International Materials Symposium, Berkeley, California, 1966 (to be published).

Hilliard, J. E., and Philofsky, E. M., (1967)(to be published).

Philofsky, E. M., and Flinn, J. E., (this volume).

Saltikov, S. A., Stereometric Metallography, 2nd Ed., Metallurgizdat, Moscow, (1958).

ACKNOWLEDGEMENTS

A REVISED TABLE FOR THE RAPID DETERMINATION
OF THE ORIENTATION OF FACE-CENTERED CUBIC
METALS FROM OCTAHEDRAL TRACES

RALPH H. ATKINSON

Guest Scientist, Stevens Institute of Technology
Hoboken, New Jersey

The first table for the determination of
orientation from octahedral traces was published
by Belaiew[1] in connection with his work on the
Widmanstaetten structure of steel. It was a
table for about one hundred orientations and the
corresponding sets of trace angles. The tedious
calculations, which were performed by an astrono-
mer friend of Belaiew's and must have taken at
least fifty working days, reached a high standard
of accuracy.

Belaiew used the octant ZXB (see Figure 1)
as his triangle of reference, apparently failing
to realize that this octant consisted of three
equivalent triangles ZAC, AXC and CXB any one of
which, in conjunction with its mirror image would
suffice for all possible orientations.

The author in his revision of Belaiew's
table has used the triangle ZAC and its mirror
image triangle ZAC' as triangles of reference.
Belaiew's co-ordinates ϕ and ω have been retained,
the co-ordinates of a pole P being as follows:

ϕ:- the angle between the projection of
the normal in the XY plane and the
X axis.

ω:- the angle of tilt of the 001 axis of
the crystal.

The computer program for the first revised
table was published by DeLuca[2]. Subsequently

the table was expanded to give trace angles for
more than 700 different orientations[3].

DISCUSSION

Experience has shown that with the table
it takes about one minute to ascertain the orien-
tation corresponding to a set of four octahedral
traces, once the trace angles have been measured.
Even speedier operation could be achieved by
making a chart similar to the one published by
Takeuchi, Honma and Ikeda[4], but retaining the
present ϕ and ω co-ordinates for expressing the
orientation instead of their geographical co-
ordinates based on meridians of latitude and
longitude.

The monumental tables of Drazin and Otte[5],
which are primarily designed for determining
cubic crystal orientations when only three traces
are available, can also be used with four traces
but the procedure is comparatively complicated
and time-consuming, compared with the revised
Belaiew table.

ACKNOWLEDGMENT

The author wishes to thank Dr. Jess H. Davis,
President of Stevens Institute of Technology, for
his courtesy in according him guest privileges in
the use of research facilities; also Dr. Alfred
Bornemann, head of the Department of Metallurgy,
for suggesting the project and giving helpful
suggestions and encouragement.

REFERENCES

1. N.T. Belaiew, J. Inst. Metals, 1923, vol. 29,
   pp. 379-406.
2. R. DeLuca: "Trace Angle Determination".
   Technical Report No. 17-5, American Society
   for Metals, Metals Park, Ohio, 1963.

3. R.H. Atkinson and R. DeLuca, "Trace Angles Corresponding to Different Orientations of Face-Centered Cubic Crystals". Table is not yet published but Xerox copies are available on request.
4. S. Takeuchi, T. Honma and S. Ikeda: Sci. Rep. Research Inst. Tohoku Univ., Series A, 1959, vol. 11, pp 81-93.
5. M.P. Drazin and H.M. Otte. "Table for Determining Cubic Crystal Orientations From Surface Traces of Octahedral Planes". Paul M. Harrod Co., Baltimore, Maryland. 1964
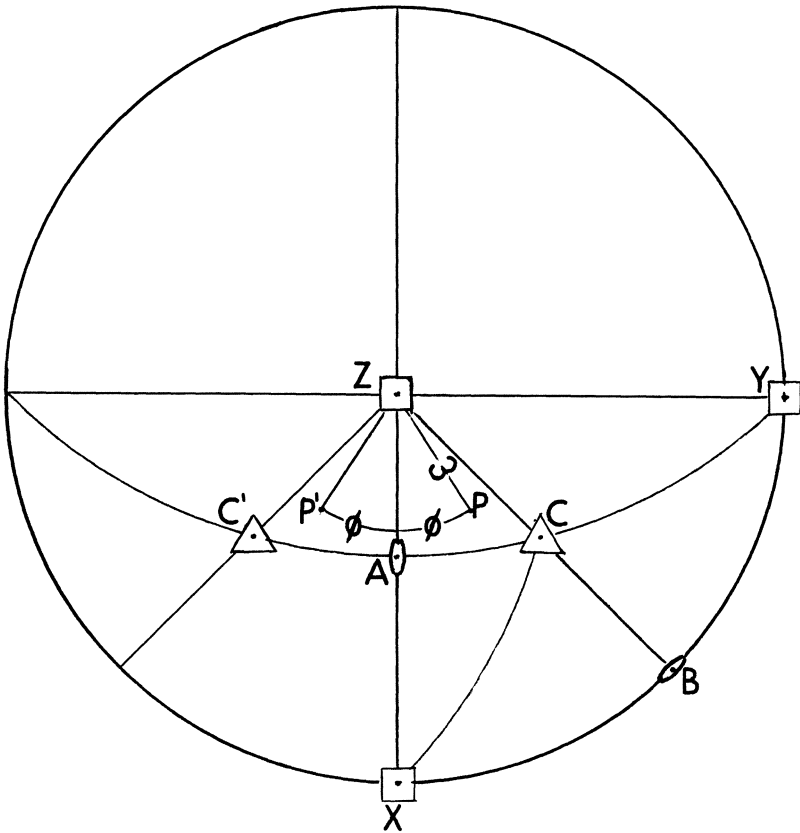
Fig. 1 Stereogram depicting reference triangle and co-ordinates for expressing crystal orientation.

SEQUENCE-ANALYSIS, A NEW METHOD FOR THE QUANTITATIVE DETERMINATION OF THE ARRANGEMENT OF PHASES IN OPAQUE SAMPLES

GERHARD DÖRFLER

Analytisches Institut der Universität Wien, Vienna

The existing methods of lineal analysis permit a nearly complete characterisation of two-phase samples. However, a quantitative description of multiphase samples remains unsatisfactory because there is no evidence about the spatial distribution of the phases present, which is a very important parameter for the calculation of diffusion problems and solid-state reactions.

The proposed method, called "sequence-analysis", is based on lineal analysis, whereby the sequence of the different phases along the test line is registered. The principle is shown in Fig.1 From the data gained by lineal analysis and sequence analysis, the following stereometric parameters can be calculated: V_V, the volume fractions of all components, S_V, their surface area, which will be better called here "interface area per unit volume"

Fig. 1

and all other parameters obtainable from lineal analysis. S_V is therefore divided into several fractions, which express how much of the total surface area of component A is in contact with the surface areas of B,C or D respectively. These values can be obtained, as mentioned, by registering the frequency of the sequences A/B, B/C etc. 'Similar measurements on two-phase structures have been made by GURLAND.
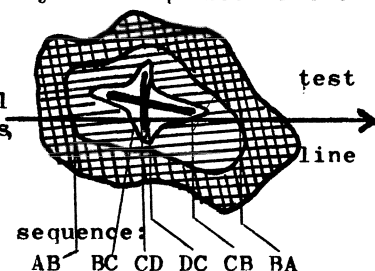
The new parameter, the "proximity"parameter, can be determined with the aid of the equation given below. This parameter gives the relative amounts of all interfacial areas in contact with the S_V of the selected phase.

$$P_{A/B} = \frac{S_{A/B}}{S_{V_A}}$$

$P_{A/B}$ = proximity of phase A against B

$S_{A/B}$ = interface area between phases A and B

231

TABLE 1

Sequence	Total counts	S_V	Proximity (%)
A/B	130	18,0	59,3
A/C	0	0	0
A/D	90	12,4	40,7
A total		30,4	100,0
B/A	130	6,6	11,6
B/C	620	31,2	54,6
B/D	380	19,2	33,6
B total		57,0	99,8
C/A	0	0	0
C/B	620	37,8	100,0
C/D	0	0	0
C total		37,8	100,0
D/A	90	41,8	19,1
D/B	380	176,8	80,9
D/C	0	0	0
D total		218,6	100,0

Table 1 gives an example for the analysis of a four-phase alloy. The proximity values permit the following very interesting conclusions to be drawn: A has a proportionally large contact area with B and D, but no interface area with phase C. On the other hand, C is always surrounded by B. It can be concluded from these facts, that any transport of material from A to C is strongly influenced by B, therefore the diffusion co-efficients of the encountered elements in B form the most important factor for the solid state reaction between A and C. It seems to be apparent, that the proximity-values permit a more accurate calculation of re-action-kinetics in multi-phase systems.

A fully automatic device for sequence-analysis is described by DÖRFLER

References:

Dörfler, G., : Radex Rundschau in press

Gurland, J., : Trans. Met. Soc. AIME 215 (1959) 601

TOPOLOGY   AS   RELATED   TO   STEREOLOGY

MEASUREMENT OF TOPOLOGICAL PARAMETERS

F. N. RHINES

*Chairman, Department of Metallurgical and Materials Engineering, University of
Florida, Gainesville, Florida*

The most rudimentary aspects of geometric
form are those which are expressed by the topolo-
gical parameters. Two of these will be discussed
in the present paper, namely: (1) number of sepa-
rate parts of the geometric entity, and (2) its
connectivity, called genus. Topological parame-
ters are typically independent of physical dimen-
sions, such as length, area, volume, mean curva-
ture and are unchanged by any deformation that
may be performed upon the geometric entity, so
long as the deformation does not involve cutting,
or joining.

These parameters can be used as a means for
classifying geometric types. For example, all
sets composed of three separate parts, such as
three spheres, a group composed of a sphere, a
cube and a tetrahedron, a three-link chain, or a
door hinge composed of two straps and a pin, be-
long to a single class, insofar as number is con-
cerned. Similarly, a torus, a teacup with loop
handle, or a garden hose, all belong to the class
of shapes having a genus of one, because each is
penetrated by a single hole.

The topological parameters of such simple
forms are readily evaluated by inspection and need
not be of concern to the stereologist. It is
where their numerical values become large, while
the structure represented is in the range of the
microscopic, that applications of stereological
interest arise. Thus, since the hardness of a
metal increases as its grain size diminishes, it
becomes useful to be able to evaluate the number
of grains in unit volume of the metal; the behav-
ior of a filter medium must be responsive to the
number of its channels and the frequency of their
interconnection, wherein genus is an appropriate
index.

Intuitively, it might appear that both num-
ber and genus should be subject to evaluation

235

through the two-dimensional structure of a statis-
tically representative cross section. Surprising
though it may seem, such is never the case. It is
always necessary to obtain three-dimensional infor-
mation in order to determine number, or connectiv-
ity. Occasionally, this is easy to do, as for ex-
ample, when it is known (three-dimensionally) that
all of the bodies to be counted are spheres, or
are ellipsoids of known axial ratio, or otherwise
fall within one of the classes of special shapes
for which special counting procedures have been
developed$(3,5,7,10)$. Unfortunately, most real
cases involve bodies of non-uniform shape, so that
an "on the spot" three-dimensional measurement
must be made to evaluate number. The same is gen-
erally true in the measurement of genus.

     Real bodies, which it may be desired to count,
are observable by virtue of their having bounding
surfaces. Each separate body must have a closed
surface. Such surfaces are said to be orientable,
which is to say, they have a distinguishable "in-
side" and "outside." It is necessary, of course,
to assume a consistent convention with respect to
whether the "inside" is toward the solid phase
and the "outside" toward the atmosphere, or what-
ever may be appropriate. Every separate body must
have at least one closed surface, but it may have
more, if, for example, it has a completely con-
tained (closed) void. The void, itself, would
have a closed surface, which would be inside out,
with respect to the enclosing surface of the body
(i.e., concave closure). In counting closed sur-
faces, therefore, it may be important to distin-
guish "inside" (concave closure) from "outside"
(convex closure). The count of particles, irre-
spective of porosity, is the sum of the convexly
closed surfaces and the experimental method of
measurement should be able to make this distinc-
tion.

     Genus, as applied to closed orientable sur-
face is measurable, in principle, by counting the
number of connections that would have to be cut
in order to open the body out into one single
string of connected parts with no remaining holes.
Stated in another way, genus is the largest number
of cuts that can be made without severing the

body into separate parts.

Any multiply connected body may be viewed as
a network composed of "branches" that connect
with one another at "nodes." This is readily seen
(with slight sacrifice of mathematical rigor), be-
cause the connectivity of a body is not changed
when the volume contained by its enclosing surface
is shrunk without reducing the space occupied by
the body; compare Fig. 1a with 1b. Having per-
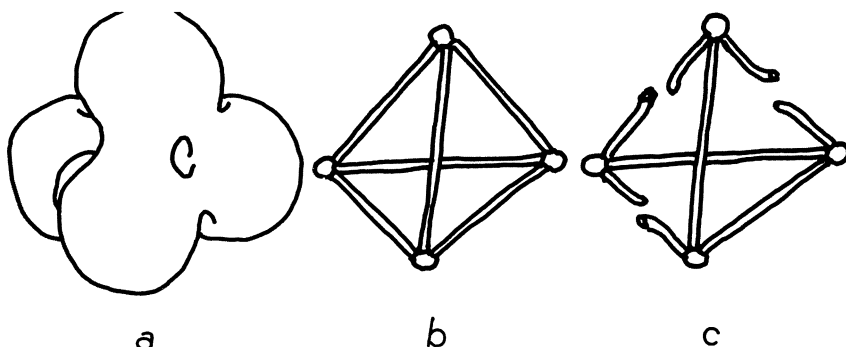formed this deformation it becomes easy to picture

Fig.1. A multiply connected body (a), shrunk to
       lineal branches and nodes (b), three of
       which may be cut (c) without cutting the
       body in two. The genus is, therefore,
       three.

the cutting of branches to count genus, see Fig.
1c. It is an important law of topology that the
numerical value of the genus "G is associated
with the number of branches "b" and the number of
nodes "n" by the relationship:

$$G = b - n + 1. \qquad (1)$$

The evaluation of genus thus becomes a matter of
identifying and counting the branches and nodes.
In doing so it sometimes appears that a degree of
capriciousness enters into the identification of
nodes and branches. In Fig. 2a, for example,
there may be ambiguity with respect to whether
there are two nodes and six branches (Fig. 2b) or
one node with five branches (Fig. 2c). It does
not matter which view is adopted, however, insofar

237

as the evaluation of genus is concerned, because
both yield the same value of the genus (Eq. 1).

<div align="center">
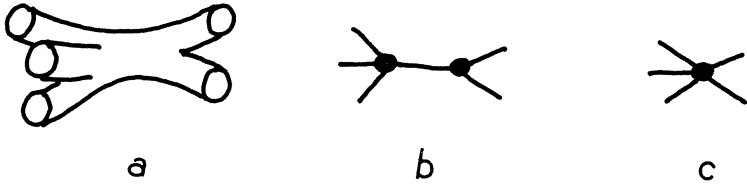
a   b   c

</div>

Fig.2.   Configuration (a) might be interpreted as
two nodes and six branches (b), or, equiv-
alently, one node and five branches (c).

In applying the parameters of topology in the
description of the structure of a material which
may be considered to consist of a pattern that re-
peats indefinitely in space, it is necessary to
introduce a concept of "per unit volume," i.e.,
number per unit volume (N_V) and genus per unit
volume (G_V). This concept is foreign to formal
topology and is replusive to the mathematician,
because it leads to such unnatural occurrences as
a fraction of a geometric body, or a fraction of
genus, at the boundary of the "unit volume."
Topological parameters are necessarily expressed
in whole numbers. Provided, however, that a suf-
ficiently large sample is used, the fractional
numbers of branches and nodes may either be ig-
nored or taken into account by a corrective pro-
cedure, with satisfactory preservation of preci-
sion in the measurement. Thus, for large values of
of the parameters:
$$G_V = b_V - n_V \tag{2}$$
where the subscript (V) represents "per unit
volume."

Experimental Determination of Number and Genus

Two kinds of experimental methods, that dif-
fer in principle, have been employed in the meas-
urement of N_V and G_V. One is based upon the di-
rect observation of the three-dimensional form of
the body and is applicable when it is possible to
look into, or through, the body to see all of its
surface. The other consists in a system of iden-
tification of continuity and discontinuity of
surface by the use of a set of serial sections

<div align="center">238</div>

cut consecutively through the body.[1] Thus far,
the second method, though laborious, has been
found the more manageable and its use will be con-
sidered primarily in the following.

The method of serial sectioning: requires first
that a sequence of sections through the material
be made at intervals that are smaller than the
smallest particle, or the shortest branch of the
structure. Attention is now directed to the sur-
faces (interfaces) of the structure that appear as
lineal traces in each two-dimensional serial sec-
tion. If the structure is two-phased and the sec-
tion is of sufficient extent, each such line will
be found to form a closed loop enclosing one of
the two phases of the structure. It becomes a
matter of personal judgement to determine whether
each surface, that is represented by a loop in
one section, extends through the section and is
represented by a loop in the next section, or ter-
minates between sections, or splits into two, or
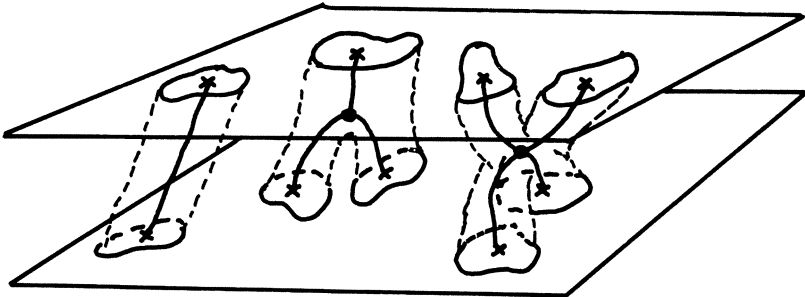more loops in the next section; see Fig. 3. The

Fig.3. Illustrating the problem of identifying
        lineal features in one serial section
        with those in the next section.

uncertainty of such decisions diminishes as thin-
ner sections are used, but there is always a prac-
tical limit to the precision that can be so a-
chieved.

     An analysis of the result requires first
that N_V be determined. This is conveniently ac-
complished by the method of DeHoff and Aigel-
tinger[4], if photographs of the sections are a-
vailable. Color coding, or some equivalent sym-
bol, is used to identify connected loops from

section to section. Starting with one loop in
any section, the enclosed area is colored (red,
for example). Then connected areas in the next
section are similarly colored, proceeding both
forward and backward through the serial sections,
until no more connected areas can be identified.
In this way a single body is identified. By re-
peating the process with different colors, or sym-
bols, until all loops have been accounted for, the
separate parts of the system will have been iden-
tified.

It remains to count the separate, parts. Each
totally contained part counts one. If the number
of contained parts is large as compared with those
that intersect boundaries of the sample, it is
satisfactory to count as one-half each body that
intersects the bounding surface, as one-quarter
each body that intersects bounding edge and as
one-eighth each body that intersects bounding cor-
ner. If there is only one body of the counted
phase, contained within the sample, then: N = 1,
despite the fact that this body intersects the
sample boundary repeatedly. Where there is more
than one body indicated, but the number of con-
tained bodies is not large, it is advisable to re-
peat the measurement, using a larger sample.
With reasonable care the error from all sources
should not be much more than about 2 percent of
the total.

The evaluation of G_V depends upon counting
the nodes and branches in unit volume of sample
(Eq. 2). This may be accomplished by using the
serial sections to construct a branch-node chart;
Fig. 4.

Considering only one of the phases at a time,
each closed loop in a section represents a point
upon a branch. If, in passing from one section
to the next, two or more branches become associ-
ated into one, or vice versa, the passage of a
node is indicated. This is shown on the chart by
bringing the branches together; Fig. 4. When all
of the branches in unit volume of sample have
been thus traced and plotted as a branch-node
chart, it is a simple matter to count the nodes
and branches and to compute G_V. Where a branch

intersects the boundary of the sample it is count-
ed as a half. A sample of suitable size should
display but few branches that do not terminate in
a node at at least one end. Again, the error in
the evaluation of genus should reasonably be held
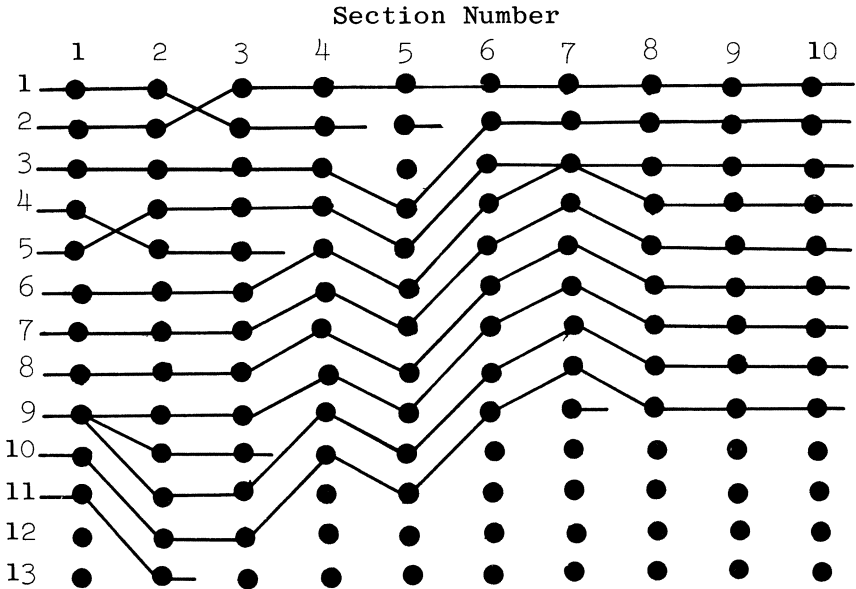to about 2 percent of the total count.

Section Number

Fig.4.   A branch-node chart for a grain boundary
         network of triple lines and quadruple
         points. Quadruple points exist where
         four branches join either at or between
         sections. (Craig[8])

     The microtome, which has long been used in
making microsections of botanical and biological
subjects, is now available for the sectioning of
such inorganic materials as can be cut with a
steel, or diamond, blade. An essential feature of
any microtome that is to be used in topological
measurement is that it should provide means for
measuring the thickness of each section cut.

     Metals do not generally yield a usable micro-
tome slice, but rather a crumpled, or rolled frag-
ment of metal. For this reason it is necessary to
photograph the newly planed surface between cuts.

241

A microtome arranged for this operation is shown
in Fig. 5. Not shown in this photograph is a de-
vice consisting of a glass tube and rubber sleeve
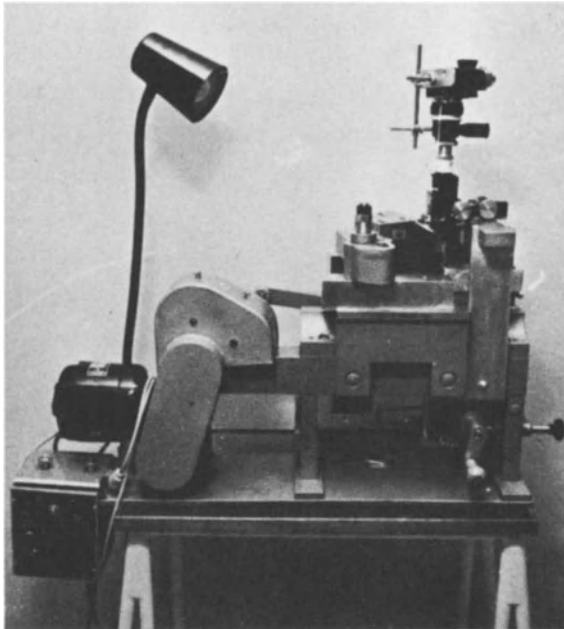

Fig.5.   Diamond microtome used for the serial
         sectioning of metals. The microscope has
         been added to permit the rapid photography
         of sections.

which can be fitted to the specimen after a cut.
An etching solution is introduced into the tube,
followed by washing and drying agents. In this
way an etched microsection can be developed in a
few seconds. A photomicrograph is then taken and
the process is repeated after the next cut. Each
photograph must be identified with the depth of
cut and must be oriented by some identifying mark
in the specimen; a small drilled hole will serve
the latter purpose.

The method of direct observation: requires a
three-dimensional view of all of the surface of
the subject. If the system is separated into

distinct translucent parts, little more is needed
than a traveling reference line in the eyepiece of
the microscope to be able to count them in a not
too thick sample. Where particles have intricate
shapes and are intertwined, or when the body is
multiply connected, a more elaborate procedure is
required.

A method devised by the present author and
perfected by DeHoff[6] depends upon counting the
occurrence of tangency between a sweeping refer-
ence plane and the surface of the structure. This
operation measures the integral curvature of the
surface, each occurrence of tangency representing
2π steradians of integral curvature. Any convex
body will thus produce two convex tangencies, de-
noting 4π steradians of curvature, which is neces-
sary for closure; Fig. 6a. If the convex body is

a
$+2\pi$ —————— convex
$+2\pi$ —————— convex

b
$+2\pi$ —————— convex
$+2\pi$ —————— concave
$+2\pi$ —————— concave
$+2\pi$ —————— convex

c
$+2\pi$ —————— convex
-2π —————— saddle
$+2\pi$ —————— concave
$+2\pi$ —————— convex
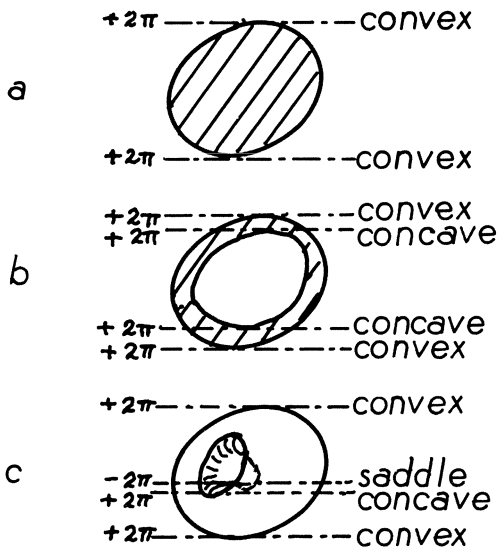
Fig.6. Manner of occurrence of space tangents
        between a plane and curved surface.

hollow, an additional two tangencies will occur
where the reference plane touches the concave sur-
face of the internal cavity, Fig. 6b; this repre-
sents an additional 4π steradians of curvature,
denoting closure of the surface of the internal
cavity. The total tangency reading in this case

would be 4 (i.e., 8π steradians) and denoting 2
closed surfaces. Such tangencies are thus seen to
be additive.

Now suppose that the solid convex body is
dented upon one side and again swept with the ref-
erence plane; Fig. 6c. As before, there must be
two points of tangency with convex surface. In
addition, there may occur tangency with concave
surface of the dent and also tangency with saddle
surface in the region where convex surface is
joined with the concave surface of the dent. If
concave tangency occurs, it is geometrically nec-
essary that the saddle tangent should also occur.
Since the net curvature of the body must be 4π
steradians, it can be seen that the saddle curva-
ture must be negative, so that:

4π(convex)$+2\pi$(concave)-2π(saddle) $= 4\pi$(closure).

Where a hole passes all the way through a
body, -4π steradians of integral curvature exists.
Thus, each unit of <u>genus</u> is associated with -4π
steradians, just as each unit of <u>number</u> is asso-
ciated with $+4\pi$ steradians.

If the tangencies recorded in unit volume of
sample are designated plus and minus, i.e., T_{V+}
and T_{V-}, according to whether they refer to sim-
ply curved or saddle surface, then:

$$N_V - G_V = \frac{1}{2} (T_{V+} - T_{V-}). \qquad (3)$$

This relationship is useful in the determination
of number when the genus is zero, or for determin-
ing genus when the number of separate parts is
unity. Where both N_V and G_V have values above the
minimum, a separation of N_V and G_V is possible
only if N_V can be otherwise evaluated.

The reading of the tangent count requires
three-dimensional perception. It must be possible
to move either the eye, or the sample, in order to
see the shape of the surface well enough to dis-
tinguish positive and negative tangency with the
superimposed image of the reference plane. For
this reason single-tube optical microscopy and
microradiography have proved unsatisfactory. The
use of stereoscopic methods is also difficult at
best. It is believed that holography may provide

a practical solution. Optical holography, using
ultraviolet light to achieve image magnification,
is within immediate reach for the examination of
translucent materials. X-ray holography may e-
ventually bring opaque objects within reach of
the tangent count.

An Example of the Use of Topological Measurement

An example of the use of topological evalua-
tion is to be found in a study of grain growth in
Al + 1% Mg, by K. R. Craig.[2] The fundamental
nature of the grain structure had been summarized
by C. S. Smith.[8] Each grain is a single crys-
tal differing in the spatial orientation of its
lattice from all of its immediate neighbors. The
grain boundary is, thus, an interface between a
pair of differently oriented crystals. Such
boundary has a surface energy and a surface ten-
sion in its plane. Boundaries, meeting along a
common edge (triple line) in sets of three, ad-
just toward three intersecting angles of 120° each,
in order to minimize surface energy. Four grains
meet at a point, which is also the point of inter-
section of four triple lines. These lines tend
to be separated by six mutual angles of 109° 28'
each, again to minimize surface energy. Thus, the
grain structure may be described in terms of a
network consisting of quadruple points (nodes n)
mutually connected by triple lines (branches b).
This is a topological network and because every
quadruple point (n) is associated with four half
branches ($\frac{1}{2}$ b):

$$b = 2\,n \tag{4}$$

wherefore, from Eq. 2:

$$G = n(+\ 1). \tag{5}$$

Smith has also shown that there is no single
space-filling polyhedron which can be stacked so
that the angular requirements of the triple lines
(edges) and of the quadruple points (corners) are
met. It follows that the topological network com-
posed of triple lines and quadruple points must
always contain strain in the form of bending,
which tends to be relieved as the grains become
larger and the quadruple points farther apart.

Accordingly, a process of readjustment tending to-
ward the elimination of quadruple points (and
hence grains) occurs whenever the molecular activ-
ity is sufficient to provide mobility. This proc-
ess is called grain growth. It has been postu-
lated that grain growth is accompanied by a trend
toward a constant ratio of quadruple points to
grains wherein the average grain has 13.394 faces,
34.195 edges and 22.789 corners (9); i.e.:

$$G_V/N_V = \text{constant.}$$

To test these hypotheses, Craig evaluated the
topological parameters of the grain structure in
an aluminum alloy which was annealed at $500^{\circ}C$ for
increasing time intervals to promote grain growth.
In order to count grains (N_V) he lettered each
grain with the same symbol in successive microtome
sections; see Figs. 7a and b. The lines of inter-
section of grain boundary with the section were
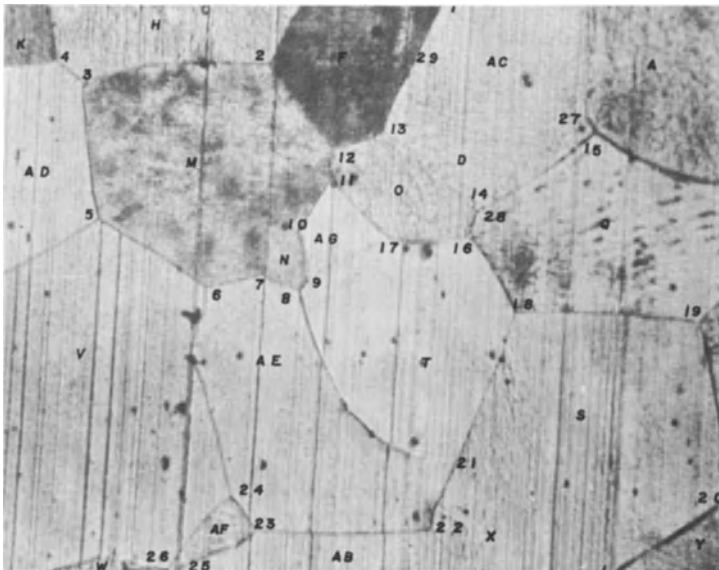
Fig. 7.   Two serial sections through an Al-1% Mg
          alloy showing grain boundaries (Craig[2]);
          Fig. 7a this page.

246
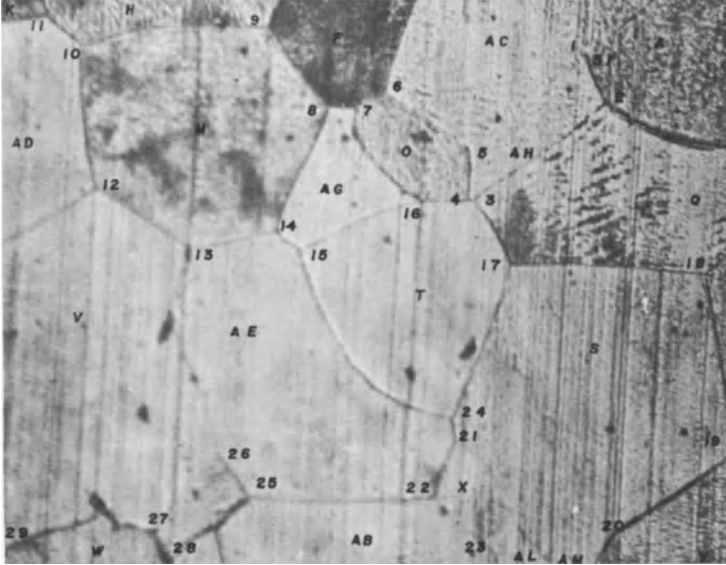
Fig.7b. See caption previous page.

numbered and quadruple points were identified by
observing the changes of grain boundary trace con-
figuration represented in Fig. 8a and b. An ex-
ample of the first kind of quadruple point can be
seen by comparing the configuration between the
number 14 and 16 in Fig. 7a with that between the
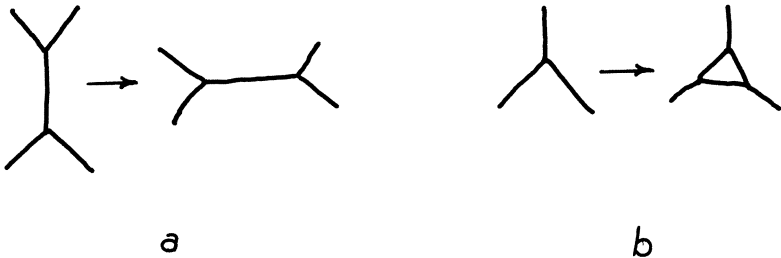numbers 3 and 4 in Fig. 7b. The results for three

a   b

Fig.8.   Successive grain boundary traces that
         indicate the passage of a quadruple
         point; type (a) and type (b).

samples of different grain size are given in the
following table.

Annealing time, minutes at 500°C;	G_V quad pts/in^3	N_V grains/in^3	G_V/N_V	Average grain intercept, inches
2.5	8.7×10^6	2.8×10^6	3.11	7.11×10^{-3}
5	6.5×10^6	1.6×10^6	4.06	8.5×10^{-3}
15	2.2×10^5	4.8×10^4	4.60	27.6×10^{-3}

Owing to the time consuming nature of the measure-
ments, the range of grain sizes covered is small;
yet it is apparent that, as the grains grow: (1)
the number of quadruple points diminishes without
seeming to approach any limit, while (2) the ratio
of quadruple points to grains tends toward a
steady value, close to that which has been antici-
pated (i.e., 5.7).

Acknowledgement

The author wishes to thank Mr. K. R. Craig
for permission to use his data in this paper.
Special thanks are also due Dr. R. T. DeHoff for
reviewing this manuscript.

Bibliography

1 Buteau, L. J., J. Kronsbein, and R. T. DeHoff,
   Trans. AIME, 233, 1961-1969, 1965.

2 Craig, K. R., Masters Thesis, University of
   Florida, Gainesville, Florida, December 1965.

3 DeHoff, R. T., Trans. AIME , 230, 764-769, 1964.

4 DeHoff, R. T., and E. H. Aigeltinger, unpub-
   lished continuing research at the University
   of Florida, Gainesville, Florida.

5 DeHoff, R. T., and F. N. Rhines, Trans. AIME,
   221, 975-981, 1961.

6 DeHoff, and F. N. Rhines, "Chapter X, Quantita-

tive Metallography." In process of publication, McGraw-Hill Company.

7   Fulman, R. L., _Trans. AIME_, 197, 1267-1268, 1953.

8   Smith, C. S., _Trans. AIME_, 175, 15-51, 1948.

9   Smith, C. S., _Metals Review_, 9, No. 33, 1964.

10 Smith, C. S., and L. Gutman, _Trans. AIME_, 197, 81-87, 1953.

A STUDY OF CONTACT AND CONTIGUITY OF DISPERSIONS IN OPAQUE SAMPLES

J. GURLAND

Division of Engineering, Brown University, Providence, Rhode Island

This study is concerned with the estimate of the degree of continuity of a particulate phase dispersed in an opaque matrix.

1) <u>Measurement of Contiguity</u>. The fraction of the total internal surface of a phase α shared with particles of that same phase in a two-phase mixture of α and β is indicated by the contiguity ratio (Gurland, 1958):

$$C_\alpha = \frac{2S_{\alpha\alpha}}{2S_{\alpha\alpha} + S_{\alpha\beta}} = \frac{2P_{\alpha\alpha}}{2P_{\alpha\alpha} + P_{\alpha\beta}} \qquad [1]$$

where $S_{\alpha\alpha}$ is the area of the interface between α particles, and $S_{\alpha\beta}$ is the area of the interface between α particles and matrix β, per unit volume of mixture. The interfacial areas may be obtained from simple intercept measurements on a random plane, after Smith and Guttmann (1953). $P_{\alpha\alpha}$ and $P_{\alpha\beta}$ are the numbers of intercepts between a random line of unit length on a plane of polish and the interparticle and interphase interfaces, respectively. The equations are valid for any distribution of particle sizes and shapes.

2) <u>Relation Between Contiguity, Mean Free Path, and Mean Intercept Length</u>. Combining the preceding equation with the definition of the mean free path through the α phase ($\lambda_\alpha = 2f_\alpha/P_{\alpha\beta}$) and with the number of intercepted particles ($f_\alpha/\bar{L}_\alpha$), one obtains (Fischmeister and Exner, 1966, Gurland, 1963):

$$\lambda_\alpha = \frac{\bar{L}_\alpha}{1 - C_\alpha} \qquad [2]$$

where $\bar{L}_\alpha$ is the mean intercept length of the individual particles [i.e., $\bar{L}_\alpha = 2f_\alpha/(2P_{\alpha\alpha} + P_{\alpha\beta})$] and f_α is the vol-

ume fraction of the α phase. This relation, also, is valid for any distribution of particle sizes and shapes.

3) **Contiguity of a Random Mixture.** Consider a dense aggregate of α and β particles in which the juxtaposition of α and β surfaces occurs in a random manner. In this case, after Cremens (1963) and Gurland (1966), the expected contiguity of the α phase in the random mixture is:

$$C_\alpha^R = \frac{f_\alpha \bar{L}_\beta}{f_\beta \bar{L}_\alpha + f_\alpha \bar{L}_\beta} \qquad [3]$$

and, if $\bar{L}_\alpha = \bar{L}_\beta$, in a random mixture: $C_\alpha^R = f_\alpha$.

4) **Measurement of Number of Contacts.** In general, the number of contacts cannot be obtained without detailed knowledge of the size or shape distribution of the contact areas. (Cahn and Hilliard, 1959). For an idealized structure of uniform particles, Gurland (1958) assumed flat, circular areas of contact of equal radii, and, under these conditions, the average number of contacts ($\bar{m}_{\alpha\alpha}$) of a particle of α phase with contiguous particles of the same phase is given by:

$$\bar{m}_{\alpha\alpha} = \frac{8}{\pi^2} (\frac{M_{\alpha\alpha}}{N_\alpha})^2 \frac{P_{\alpha\beta} + 2P_{\alpha\alpha}}{P_{\alpha\alpha}} \qquad [4]$$

where $M_{\alpha\alpha}$ is the number of contacts and N_α is the number of particles intercepted, per unit area of a random plane.

5) **Contact in Random Mixtures.** In the special case of a random two-phase mixture of particles of one size with equal grain boundary and interfacial energies:

$$\frac{\bar{m}_{\alpha\alpha}}{\bar{m}_{\alpha\alpha} + \bar{m}_{\alpha\beta}} = f_\alpha \qquad [5]$$

THE TOPOLOGICAL PROPERTIES OF
STRUCTURAL COMPONENTS

J. KRONSBEIN AND J. H. STEELE, JR.

Dept. of Metallurgy, University of Florida, Gainesville, Florida

Topological properties are those geometric properties which do not change under continuous deformation. Those aspects of interest for structural components are <u>global</u> properties related to the connectivity, and measurable by serial sectioning. These include the <u>number of separate parts</u>, and the connectivity, <u>defined as the number of linearly independent closed paths which cannot be shrunk to a point entirely within a component.</u> This property will be discussed for connected components which are finitely embedded in E^3(Euclidean 3-space). These restrictions allow the application of the Euler equations wherein the characteristic of polyhedral coverings is related to the connectivity. The Euler equations depend explicitly upon the dimensionality, $n \leq 3$. Thus the <u>dimensionality</u> of any structural component under <u>consideration</u> must be defined. As an example, an interface which is the transition region between physically identifiable 3-dimensional regions may be assumed to be 2-dimensional.

Consider first the 1-dimensional case where a structural component is represented by a connected linear graph G formed by N_1 branches which intersect in a set of N_0 vertices. The connectivity P_1^G of G is related to the characteristic, $(N_0 - N_1)$, through the following equation:

$$N_0 - N_1 = P_0^G - P_1^G \tag{1}$$

where $P_0^G = 1$ for a connected graph. Geometrically P_1^G is the maximum number of branches which can be removed from G without separating it into more than P_0^G parts. If $P_1^G = 0$, then G is simply connected and forms a tree, as only one path exists between any two vertices. Where $P_1^G > 0$ multiple paths exist in the graph and it is said to be multiply connected.

A 2-dimensional component may be considered as a closed, orientable surface S in E^3, since it is usually formed as a bounding interface of a physically identifiable 3-dimensional component. The genus of such a connected surface S represents

geometrically the number of simple closed curves which can be cut on S without dissecting it. It is related to the characteristic, $(N_0-N_1+N_2)$, of a polygonal covering of S by a finite number N_2 of polygonal regions or faces formed by the N_1 branches and N_0 vertices of a connected linear graph placed upon it. The covering of S yields the Euler equation:

$$N_0 - N_1 + N_2 = 2 - P_1^S = 2 - 2p \qquad (2)$$

A 3-dimensional component may be represented as a finite connected region M in E^3, which is bounded by a set of closed, orientable surfaces, $S=(S_i:i=1,2,..,P_0^S)$. These surfaces must completely enclose M as a physically identifiable interior region. The region M together with its bounding surfaces S forms a closed bounded 3-dimensional region $\overline{M}$ in E^3, which can be subdivided into a finite set of contiguous, simply connected polyhedral regions. An Euler equation based upon such a covering of $\overline{M}$ relates the characteristic $(N_0-N_1+N_2-N_3)$ to the number and genus of its separate bounding surfaces S. The equation which can be proven by induction for finite coverings is given by:

$$N_0 - N_1 + N_2 - N_3 = P_0^S - p \qquad (3)$$

where N_0, N_1, N_2 and N_3, refer respectively, to the number of vertices, branches, faces, and polyhedral cells in the covering. P_0^S and p are the number and genus of the bounding surfaces of M. The connectivity of $\overline{M}$ is equal to the genus of the bounding surfaces, since only closed paths around multiply connected bounding surfaces cannot be snrunk to a point entirely within $\overline{M}$. One of the surfaces of the set S encloses the remainder. Also the "exterior" region is subdivided into P_0^S disjoint parts by the bounding surfaces S of $\overline{M}$.

These concepts provide a method for experimentally measuring the genus of the bounding surfaces and thus the connectivity of 3-dimensional structural components.[1] They also allow the connectivity to be used as a basis for defining network models of multiply connected structural components.[2]

BIBLIOGRAPHY

1.Kronsbein, J., L. J. Buteau, and R. T. DeHoff, Trans. Met. Soc. AIME, 233 (1965), p. 1961.

2.Rhines, F. N., Plansee Proc., 3rd Seminar, Reutle/Tyrol, 1958, p. 38.

METHODS   IN   GENERAL

A SYSTEM OF BASIC STEREOLOGIC FORMULAE

HANS GIGER

Department of Anatomy, University of Bern, Bern

1. The basic stereologic formulae of Delesse,Tom-
   keieff-Hennig and DeHoff can be condensed in the
   following system of formulae,which is valid for
   a class of very general structures in three-di-
   mensional space.A generalization for k-dimensi-
   onal space is possible.
2. Let us consider in three-dimensional space a
   point set{A}with the following properties I,II,
   III. K may be a sphere with radius R and volume
   V(K),which has its centre in the origin of the
   system of coordinates.Then

I. A={A}∩K,the intersection of{A} and K,shall be a
   normal body for each R.The class of normal bo-
   dies was introduced to Integral Geometry by Had-
   wiger.This class of bodies seems to contain all
   point sets and figures in space,which may be
   considered normal within the ordinary meaning
   of the term.In three-dimensional space volume
   V(A),surface S(A),integral of mean curvature
   M(A) of normal bodies can be uniformly defined
   by Crofton Integrals existing in the sense of
   Riemann. A clear idea of the integral of mean
   curvature M(A) can be given for a convex body.
   Here M=2πB,where B is the mean thickness of the
   body.

II. The intersection A∩D of A with a plane closed
   region D with area a and circumference b shall
   be a normal point set for each position of D.
   This assumption does not follow from the fact,
   that the intersection A∩E of A with a plane E
   is normal.   c(A∩D),b(A∩D),a(A∩D) denote the
   Eulerian characteristic,the length of the boun-
   deries and the area of the intersection A∩D.
   The Eulerian characteristic of a two-dimensional
   point set can be interpreted as the difference
   of the numbers of its outer and inner bounda-
   ries.The Eulerian characteristic of a one-di-

mensional point set equals the number of the li-
near elements which belong to the point set.
III. The following limits are assumed to exist:
$V_V = \lim_{R \to \infty} V(A)/V(K), S_V = \lim_{R \to \infty} S(A)/(K), M_V = \lim_{R \to \infty} M(A)/V(K).$

V_V, S_V, M_V are the densities of volume, surface and
integral of mean curvature of the point set $\{A\}$
respectively.

3. Let $D_2 = (b,a)$ be a simply connected plane region
with circumference b and area $a, D_1 = (\ell)$ a plane
curve of length ℓ, D_0 a point; then the follo-
wing system of formulae is valid:

$D = D_2$: $V_V = a_a$

$S_V = (4/\pi) b_a - (4b/\pi a) a_a$

$M_V = 2\pi c_a - (b/a) b_a + ((b^2 - 2\pi a)/a^2) a_a$

$D = D_1$: $V_V = \ell_\ell$

$S_V = 4 c_\ell - (4/\ell) \ell_\ell$

$D = D_0$: $V_V = c_p$

a_a, b_a, c_a are the mean densities of area, length
of boundaries and Eulerian characteristic of
the intersection $\{A\} \cap D_2$. These densities are de-
fined by the quotients of these functionals and
the area a of D_2.

ℓ_ℓ, c_ℓ are the densities of length of the linear
segments and the Eulerian characteristic in $\{A\} \cap D_1$.
c_p can be interpreted as the probability that
the point D_0 lies within the structure $\{A\}$.
The system contains the formulae of Delesse, Tom-
keieff-Hennig and DeHoff, which are obtained for
an infinitely large circle $D = D_2$ or straight seg-
ment $D = D_1$.

4. To demonstrate the validity of the system, the
definitions of $V(A), S(A), M(A)$ given by Hadwiger
must be combined with the cinematic integrals
of two-dimensional Integral Geometry given by
Blaschke and Santalo.

Hadwiger, H. "Normale Körper im euklidischen Raum
und ihre topologischen und metrischen Eigenschaf-
ten", Math. Zeitschr., 71, 124-140, (1959).
Blaschke, W. "Vorlesungen über Integralgeometrie",
Verlag der Wissenschaft. Berlin, p.54, 3. Aufl.,
(1955).

GRAPHISCHE METHODEN IN DER STEREOLOGIE

AUGUST HENNIG

*Anatomisches Institut der Universität München, München*

Als einfaches Beispiel graphischen Vorgehens haben Sie
das Ellipsoidproblem kennen gelernt. Für jedes Rota-
tionsellipsoid existiert eine Summenkurve für die Ver-
teilung der Achsverhältnisse der Schnitte. Ob diese
Kurven exakt abgeleitet werden können, hängt von der
Integrierbarkeit der Kurven nach Abb.8 ab. Die Ordina-
ten der gewiß sehr verwickelten Funktion könnten dann
mit der Gruppenbesetzung des Versuches verglichen wer-
den.
Wieviel anschaulicher ist aber der Vergleich zweier
Kurven! In diesem einfachen Falle beschränkt sich das
graphische Verfahren darauf, eine punktweise errechnete
Kurve mit dem Planimeter zu integrieren. In komplizier-
ten Problemen wächst der Umfang des graphischen Anteils
am Lösungsgang. Bei den dreiachsigen Körpern, etwa dem
elliptischen Zylinder, treten im Laufe der Konstruktion
Kurvenfelder auf (Abb.1), die mathematisch kaum mehr
darstellbar sind, von ihrer Integration zu schweigen.
Die Fehler einer mathematischen Näherung sind schwer zu
überschauen, die Zeichenfehler einer unanfechtbaren
Konstruktion können klein gehalten werden.
Probleme dieser Art sind theoretischer Natur, denn sie
suchen Eigenschaften von Körpern, wie es auch Volumen
und Oberfläche sind.
Hingegen liegt der Ableitung der Größenverteilung von
Kugeln aus der Charakteristik der Schnittkreise eine
experimentelle Aussage zugrunde (Abb.2). Die Schnitt-
kreisverteilung kann durch einen mühevoll kombinierten
integrierbaren Ansatz nur angenähert dargestellt werden.
Ist dieser Weg mit vernünftigem Aufwand nicht gangbar,
dann müssen die Gruppenbesetzungen des Versuchs schritt-
weise herangezogen werden, wobei innerhalb jeder Gruppe
die Kugeldurchmesser konstant gesetzt werden müssen.
Die mathematische Betrachtung liefert eine allgemeine
Rechenvorschrift, die in Tabellenform mechanisch an-
wendbar ist.
Der graphische Weg muß von Fall zu Fall neu beschritten
werden, erfordert daher einen etwas höheren Zeitaufwand
und einen geschulten Zeichner. Dem stehen entscheidende
Vorteile gegenüber: Erstens können die statistischen

Abb.1
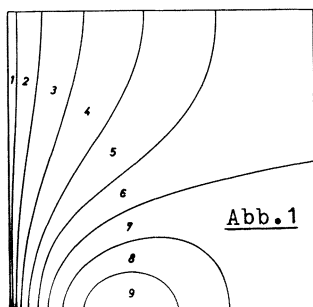
Nach Hennig-Elias:
Elliptical cylinders

Obere Kurve: Verteilung der
    Schnittkreisdurchmesser
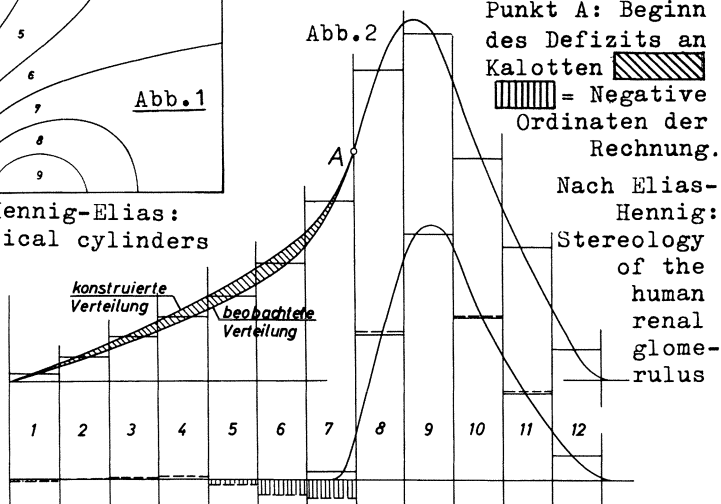Untere Kurve: Verteilung
    der Kugeldurchmesser
    Punkt A: Beginn
    des Defizits an
    Kalotten
    = Negative
    Ordinaten der
    Rechnung.

Nach Elias-
    Hennig:
    Stereology
    of the
    human
    renal
    glome-
    rulus

Abb.2

A

konstruierte
Verteilung

beobachtete
Verteilung

1 2 3 4 5 6 7 8 9 10 11 12

Schwankungen der Gruppenbesetzung mit Hilfe einer Sum-
menkurve, sei es im Wahrscheinlichkeitsnetz, sei es in
gewöhnlichen Koordinaten, soweit ausgeglichen werden,
daß die Kugelverteilung nicht noch unsteter ausfällt.
Zweitens ist jede Umgruppierung möglich.
Der Zwang zu unsteter Kugelverteilung verfälscht die
Lösung, umso mehr, je gröber die Gruppenbildung ausfiel.
Das rechnerische Verfahren ist aber daran gebunden.
Sind etwa nur acht Gruppen vorhanden (was auf nur 3 - 4
Kugelklassen hinausläuft), dann können die 15 Spalten
der Tabelle von Saltykov nicht ausgenützt werden.
Liegen dagegen mehr als 15 Gruppen vor, dann ist man
zum Zusammenlegen von je zwei Gruppen, also zu einer
unerwünschten Vergröberung gezwungen.
Zeichnerisch läßt sich jede Stufenfolge durch eine zü-
gige Verteilung ersetzen (planimetrische Kontrolle für
jeden Abschnitt!) und aus ihr umgekehrt jede beliebige
neue Unterteilung finden.
Weil man beim Konstruieren stets am Problem bleibt,
werden Regelwidrigkeiten sogleich richtig gedeutet:
Wenn etwa im Punkt A keine Restordinaten für kleinere
Kugeln bleiben, sondern im Gegenteil die konstruierte
Kurve die gegebene zu überhöhen beginnt, dann deutet
dies auf flache Kalotten hin, die wegen schwacher Fär-
bung nicht beobachtet wurden oder aus dem Schnitt her-
ausgefallen sind.
Das Rechenschema führt hier zu unmöglichen negativen
Klassenbesetzungen.

AUTOMATIC   MEASURING   AND   COUNTING   DEVICES

# AUTOMATIC MEASURING AND SCANNING DEVICES IN STEREOLOGY

HELLMUT F. FISCHMEISTER

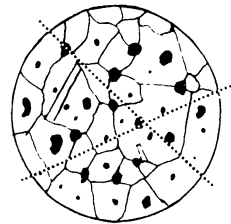*Chalmers Technical University, Gothenburg*

1. SCANNING STRATEGY

The object of a scanning operation is to collect the information need-
ed to reconstruct a structure in space from plane sections through it.
Thus, scanning is essentially a sampling process. Three principal solu-
tions present themselves: line scanning, point scanning and feature-
to-feature scanning (fig. 1). The last of these is mainly suited to the
visual measurement of the number and size of unconnected objects
(such as blood corpuscles or powder particles) whose arrangement in
the specimen plane is without interest.
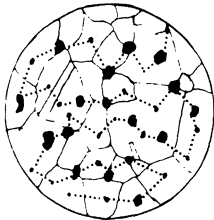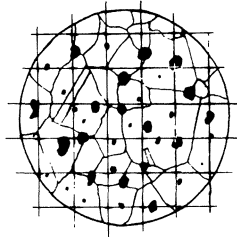
a) feature-to-feature scanning   b) step scanning   c) line scanning

The information collected must be sufficient with regard to the
level of accuracy desired in the reconstruction of the spatial struc-
ture, and it must be collected economically, without picking up re-
dundant data.

Normally, the structural detail to be resolved requires a magnification
at which each field covers only a small fraction of the specimen area,
and we must then complement our strategy for scanning the individual
fields with one for the selection of fields to be scanned. The two can
be combined into the rule that the total amount of data required for
the desired accuracy - and no more - should be taken from locations
distributed as evenly as possible over the whole specimen area. The
larger the specimen, the fewer lines or points should be evaluted per
field of view. It is therefore desirable that a scanner should allow

wide choice in the density of sampling points, or lines, and that transition from one field to the next should be fast, preferably automatic.

The amount of independent information gained per scanning line or point decreases as their density is increased – expecially when the spacing between the points or lines becomes smaller than the size of the elements (sections of tissue cells or crystal grains) which make up the image (HENNIG 1958, HILLIARD 1961, 1966). With a very fast scanner, e. g., a television camera, the time required to scan all image points is inessentially smaller than that for selective sampling. However, the redundant information amassed by a total scan may be a psychological danger. The accuracy with which each field is measured has little bearing on the accuracy with which the structure of the specimen as a whole is being assessed.

If these aspects of sampling strategy are considered, the slower mechanical scanners are often not so inferior to the electronic ones as the ratio of their speeds would indicate, because they do their sampling more efficiently. Also, their lower speed makes possible continuous supervision and adjustments to the local character of the specimen. With some kinds of specimen material – and not so infrequently the ones most interesting for research – contrast and perfection simply cannot be brought to the high standard required for completely automatic scanning. Therefore, we shall devote part of this presentation to manual or semi-automatic scanners.

2. MECHANICAL SCANNERS

21. Point Counters.

Fig. 2 shows a simple type of instrument for the stepwise scanning of specimens, in which the translation of an ordinary microscope stage is arrested at equal intervals by "click" springs. First described by CHAYES (1949), such a stage is now marketed by LEITZ (W. Germany).
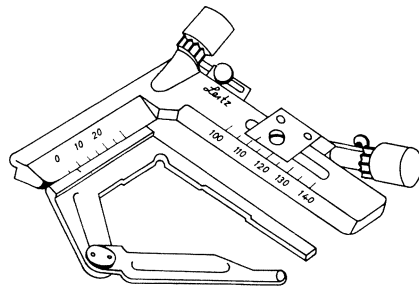

Fig. 2 Point counting stage

In more sophisticated instruments made by SWIFT (England) and
RATHENOWER OPTISCHE WERKE (E. Germany), the step motion
along one coordinate is controlled by an electrically actuated ratchet
mechanism. The specimen is automatically advanced one step as the
operator presses the button which records the identity of the constit-
uent last analysed in a bank of electrical registers.

For most point counting operations, these instruments can be replaced
without loss of time by much cheaper equipment, a point counting
eye-pice (HENNIG 1958, HILLIARD 1961, 1966). However, stepping
stages are now used with electronic scanners for automatic transition
from one field to the next, as suggested by the author in 1961.

22. Line scanners.

In most line scanners, the scanning line is traced out by the cross
hair center of the eyepiece as the specimen is being moved across
the microscope stage. For quantitative evaluation, the lengths of
line traversed within linear features (traces of sectioned surfaces)
must be counted.

Earlier, purely mechanical equipment comprises many ingeneous de-
signs. SHAND (1916) combined two parallel, micrometerdriven
carriages so that the specimen could be moved by either one of the
two micrometer screws, their motion being additive. This allowed
the analysis of structures with two constituents. SCHEUMANN (1931)
devised the classical "integrating stage", later marketed by Leitz, in
which the movements of six micrometer-driven wedges were additively
transferred to the specimen, allowing six constituents to be analysed
simultaneously.

While these early instruments relied on various ways of mechanically
adding displacements due to several drives, later systems used one
single drive mechanism, operating continuously, and coupled to this
electrical or mechanical revolution counters for the periods during
which each of the constituents were traversed. The best known in-
strument of this type is the HURLBUT-counter (1939). The continuous
drive principle greatly increased the working speed of these instru-
ments. - A detailed review of these earlier developments has been
published elsewhere (FISCHMEISTER 1961, 1966).

Electronic pulse counting techniques suggested a versatile way of
measuring the individual intercepts of the scanning line (FISCH-
MEISTER 1959, SMITH 1960) and of sorting them into size groups for
the analysis of size distributions. An instrument of this type is shown
in fig. 3. (FISCHMEISTER 1961, 1963). As shown, the instrument can

analyse the volume fraction and size distribution of two constituents; extension to more than two constituents is simply a matter of adding further recording units.

Fig. 3
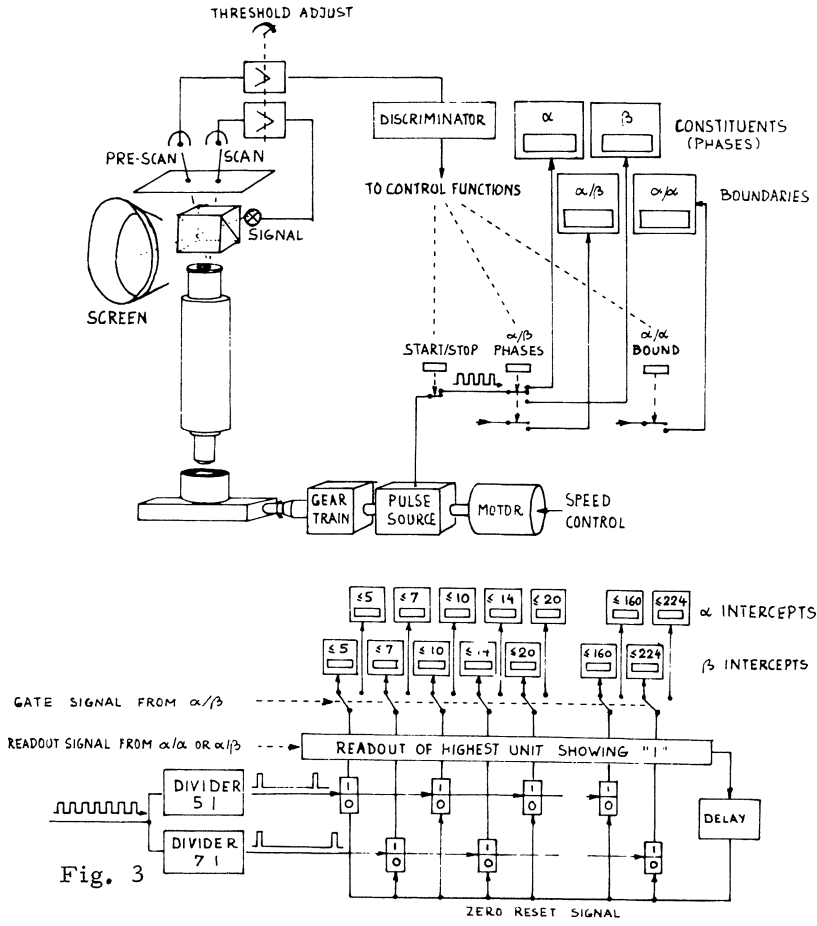
A pulse source coupled to the stage translation generates a fixed number of pulses per unit length of traverse, independent of traversing speed. Pulse rates from 0.2 - 5 pulses per μm can be selected, according to the fineness of the detail to be analysed. Each constituent is assigned one volume fraction register and a series of counters to record the size distribution of its intercepts. The traveling specimen is observed either by a human operator or by a pinhole-and-photocell detector. When passing from a region of α-constituent to one of β, the αβ-tangent is depressed (or a corresponding switching function operated by the photocell), whereupon the pulses are directed into the β-counter for as long as β is being traversed. On

266

leaving the β region, the contact is opened and the pulses go into the α-counter for the length of the α-intercept which follows. Thus the sums of the α- and β-intercepts are recorded in the counters marked α and β, and the volume fraction of any constitutent can be calculated from the numbers recorded there:

$$V_{V\alpha} = L_{L\alpha} = \frac{\Sigma L_\alpha}{\Sigma L_\alpha + \Sigma L_\beta + \ldots \Sigma L_\kappa}$$

Each transition β/α or α/β is also registered in a separate counter(α/β). From the number $P\alpha\beta$ of intersections of α/β-boundaries with the scanning line, the specific boundary area $S_{\alpha\beta}$ can be calculated:

$$S_{\alpha\beta} = 2 \, P_{\alpha\beta}/L_t$$

as well as the contiguity of any of the constituents (GURLAND 1958)

$$K_\alpha = \frac{S_{\alpha\alpha}}{S_{\alpha\alpha} + S_{\alpha\beta}}$$

Internal boundaries (αα,ββ)are recorded by the contact "αα". This and the αβ-contact operate on the intercept size analyser. This distribution analyser consists of two chains of binary counting elements (flip-flop circuits), which record the number of pulses received between two signals from the αα- and ββ-keys. Each chain can record numbers on a binary scale, 1, 2, 4, 8 . . . A frequency divider transmits each fifth pulse to the first chain and each seventh to the second chain. Thus the two chains together classify the pulses belonging to one intercept in terms of the scale 0.5, 0.7, 1.0, 1.4, 2.0, 2.8, 4.0 . . . which resembles very closely the geometrical progression $\sqrt{2}^1$ commonly used for logarithmic size distributions. An interlocking network blocks readout from all elements in the chain save the highest one to have received a pulse at any given momemt. Thus when readout is effected by the operation of the αα- or αβ-tangent on leaving the entity being traversed, only one of the output registers is actuated. Which of the two sets of counters receives the readout pulse is determined by the position of the α/β contact during the intercept just traversed.

For specimens of high perfection and contrast the operation of all switching functions can be left to the photocell detector. The operator can still supervise the correct function of the apparatus on a projection screen attached to the microscope, and he can continuously adjust the switching threshold of the detector so that all boundaries are correctly recorded. For this purpose, a pre-scanning cell watches a mock scanning point somewhat in advance of the real scanning point. A light flash appears on the screen at the position of the pre-scanning point whenever an entity passing under it gives a sufficient signal to

trigger the counting circuits.

The proper domain of such instruments comprises difficult specimens, measurements with high accuracy, and situations where the volume of work does not justify the expense of a fully automatic scanner.

The principle can be applied to other image forming systems than microscopes. Electron micrographs can be analyzed by attaching the circuitry described above to a slide projector equipped with a motor driven stage and pulse generator. (FISCHMEISTER 1963). THEISEN (1964), MELFORD & WHIDDINGTON (1964) and DOERFLER (1966) have applied the same principle to a mechanically scanning micro-probe. In metallography and mineralogy, the ability of the micro-probe to discern structural entities directly by chemical composition rather than by shape, transmittance or reflectance offers considerable advantages. Especially interesting is DOERFLER's development (1967) of circuitry for the automatic recording of phase sequences, which makes possible a characterization of the topological relationships bet-ween phases on the basis of GURLAND's (1958) concept of contiguity. – Finally, the same circuitry could be used to analyze the output signal of a scanning electron microscope (COSSLETT & DUNCUMB 1956), of which commercial versions are now available (e.g. the "stereoscan" of Cambridge Instruments, England) or of a scanning laser microprobe.

3. AUTOMATIC SCANNERS

31. Scanning principles.

The motion of the scanning point through the image can be accomplished in three ways (fig. 4): by physical translation of the specimen stage past a stationary microscope and detector; by letting a small sampling spot travel over the image plane; and by illuminating the specimen with a fine light spot that moves in the focal plane of the illuminator system.

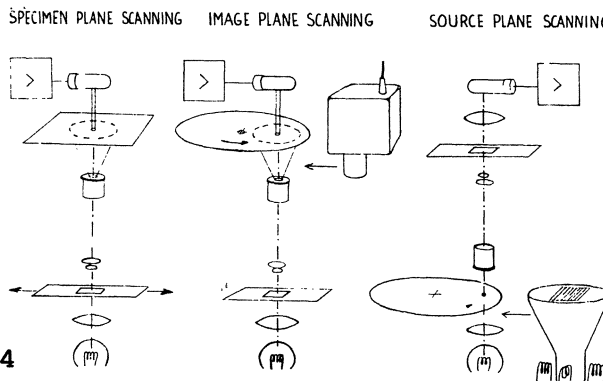SPECIMEN PLANE SCANNING   IMAGE PLANE SCANNING   SOURCE PLANE SCANNING

Fig. 4

The first of these methods severely limits the scanning speed, although fair speeds have been attained by the oscillatory motion of spring suspended specimen stages (HAWKSLEY et al. 1954). The highest speeds are reached with electron beams sweeping out a line pattern such as in a cathoderay or vidicon (television camera) tube.

All three principles have been used in commercial apparatus. HAWKSLEY's oscillating stage forms part of the Automatic Particle Counter and Sizer made by Casella Electronics Ltd. (England); a vidicon tube performs image plane scanning in the Quantimet Image Analyzing Computer of Metals Research Ltd. (England); source plane scanning was used in the Flying Spot Microscope developed by YOUNG & ROBERTS (1951, also ROBERTS & YOUNG 1952) and later marketed by Rank Cintel Corp. (England). – As a point of historic interest, the first wholly automatic scanner described in the literature seems to have been a blood cell counter by LAGERCRANTZ (1948) that used a specimen plane scanning method. FLORY & PYKE (1953) described the first application of the vidicon principle to the scanning of biological materials. A period of intense development during the fifties brought the solution of most of the basic problems of automatic scanning; the simultaneous improvement of electronic component standards and the transition to solid state circuitry facilitated the development of reliable commercial instruments in a price class that allowed their use as routine instruments in metallurgical quality control or in medical screening work. Detailed reviews of this development are available (WALTON 1954, GILLINGS 1955, FISCHMEISTER 1961).
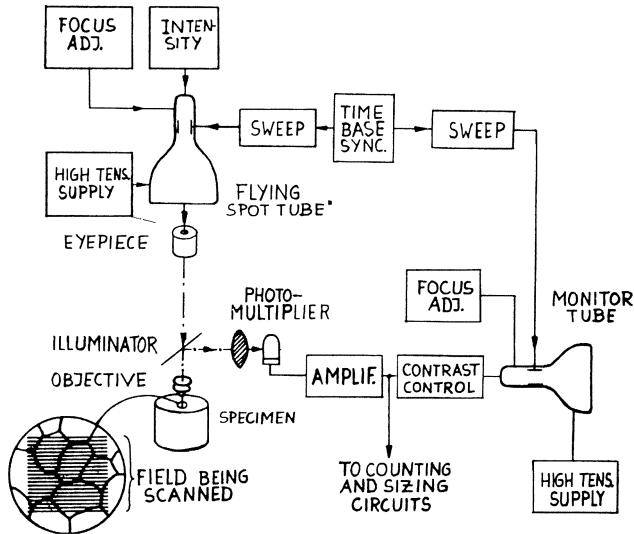
Fig. 5 The flying spot microscope.

32. The flying spot principle.

Fig. 5 shows the basic circuitry of an electronic scanner. The flying spot microscope is chosen as an example because several other important instruments (scanning electron microscopes and microprobes) are based on the same principle, and because the descriptions of the Quantimet given in other papers at this conference will exemplify image plane scanning. The basic functions are, of course, the same for both types of scanners.

A light spot sweeping over the screen of a high-intensity cathode ray tube is projected "backwards" through a microscope onto the specimen. A photocell looks at the specimen through the microscope condensor (fig. 5 shows an arrangement based on reflected light optics). As the demagnified spot sweeps across the specimen, the output of the photocell varies as shown in fig. 6. Sharp signals – as in the center fields of fig. 6 – require an ideally small scanning spot and sharp transitions from dark to light specimen areas. For real specimens and scanning conditions, filtering, contrast enhancement and pulse shaping circuits are needed to make the signal approach the ideal shape. – The modified signal is displayed on a monitor screen whose sweep is synchronized with that of the flying spot tube, and is also passed on to the counting and logic circuits which perform the actual measurements on the image. In all automatic scanners of this type, some kind of marker, e. g., a light blob, appears on the monitor at the spot where the counting operation is triggered. Thus the operator can ad-
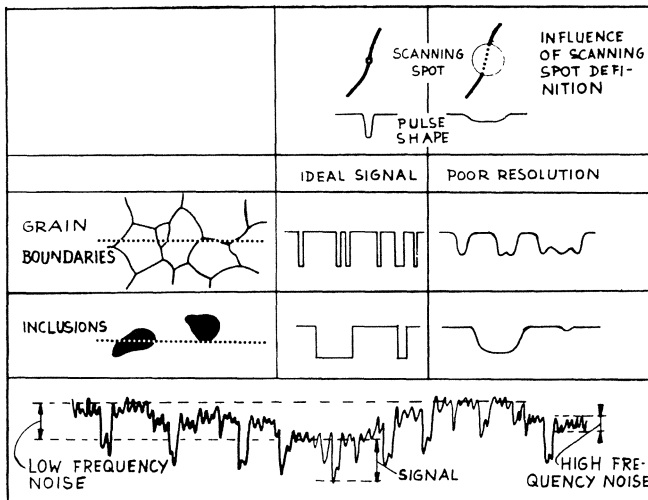

Fig. 6 – Factors influencing signal shape.

270

just the contrast and the discrimination level of counting until all en-
tities are correctly recorded. For instance when measuring the area
fraction of all dark image elements, the points recorded as belonging
to the dark phase can be shown up extra bright. In practice, it is
often impossible to "fill in" exactly all dark area and no more; as in
a television receiver, extreme contrast enhancement leads to distor-
tion of the image. The best that can be accomplished normally is a
cancelling out of the areas erroneously incorporated in either phase
over the whole field of view. This rectifies the volume fraction, but
gives incorrect size distributions.

The geometrical resolution of the instrument depends on the spot dia-
meter of the source tube and on the optical demagnification. Spot
diameters down to 0.1 μ have been claimed for the Rank Cintel Fly-
ing Spot Analyzer. However, as the spot travels, it is lengthened
somewhat by the afterglow of the screen phosphor. Resolution in the
scanning direction therefore is a function of scanning speed. (This
disadvantage is avoided with mechanical scanners). - The resolution
of scanning tubes is usually expressed in lines per field diameter.
This is of importance only for the visual quality of the monitor image,
since from the point of view of sampling efficiency, lines that are to
form a viewable image are far too close at any rate.

With respect to grey tones, resolution is also a function of scanning
speed. Noise due to fluctuations of source intensity, photocell sensi-
tivity, amplification and to thermal processes in components becomes
more difficult to distinguish from the image signals the less time there
is for it to average out (cf., bottom row of fig. 6). Low speed mech-
anical scanners working with photomultiplier cells have an advantage
here over flying spot or vidicon scanners. Partly for this reason and
partly to bring down the expense of logical and counting circuitry,
existing electronic scanners are normally equipped to analyze no
more than two phases. However, two newly developed instruments
described at this conference, the I-SCAN (vidicon type) and the
AMEDA (mechanical specimen plane scanner with photomultiplier
detector) handle up to sixteen different grey shades. - For a very
thorough discussion of the optimization of resolution and information
retrieval in automatic scanning devices, the reader is referred to
MOORE (1966).

33. Recognition of features.

It has been remarked before that a scanner which is to present a view-
able monitor image has to put many scanning lines through most im-
age features. Chords of one given feature therefore occur in the sig-
nal trains from several successive lines, interspersed with signals from

neighbouring features. For operations like the determination of vol-
ume fractions or of intercept size distributions this presents no prob-
lem, but in counting the number of features per unit area, some logi-
cal function must be provided to avoid repeated recording of every
feature. The various solutions of this problem are all based on com-
parison of the next-to-last scan line with the present one, either by
means of memory storage or by means of duplicate, multiple or slit-
shaped scanning spots (reviewed by FISCHMEISTER, 1961). The
principle is shown in fig. 7. A coincidence circuit prevents counts
from being registered as long as equal signals are being delivered by
both scan lines within a certain acceptance interval in the scanning
direction, the width of which can be adjusted. The system counts
correctly features of all shapes except those with reentrant contours
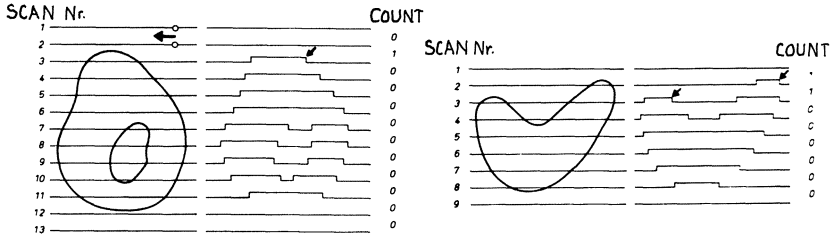cutting through the scanning direction (fig. 7). This problem has yet
to be solved.

Fig. 7 - Particle counting by the double spot method.

By means of a delay circuit that blocks the counting function describ-
ed above for a certain length of traverse (fig. 8b) it is possible to
count only intercepts longer than a selected value. Repeated scanning
with varying delay lengths gives the distribution of all chords in the
field. With similar techniques, the longest chord of each feature can
be identified and recorded (fig. 8c). Another measurement to which
electronic scanners easily lend themselves is the caliper diameter per-
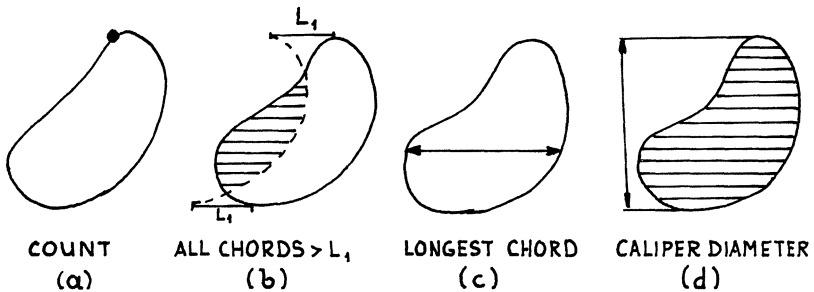pendicular to the scanning direction (fig. 8d).

COUNT	ALL CHORDS > L₁	LONGEST CHORD	CALIPER DIAMETER
(a)	(b)	(c)	(d)

Fig. 8 - Quantities that can be identified by a scanner.

272

4. CONCLUDING REMARKS

Most stereological parameters can be determined by simple counting operations requiring no more equipment than a point counting eye-piece or template, incorporating text lines of known length.

Size distribution measurements are the proper domain of line scanners. Both measurement and conversion to spatial data are much easier for line intercepts than for profile areas; also the determination of pro-file areas cannot be automated but has to be performed by visual matching against templates or circles with variable diameter as in the Zeiss Particle Size Determinator. Area sizing techniques have been evaluated by FISCHMEISTER (1961, 1966).- The strength of semi-automatic single line scanners, as compared to template methods, lies in the ease with which all stereological data are collected in one single run; and in relation to fully automatic scanners, they are eas-ier to apply to "difficult" specimens.

Fully automatic scanners require specimens of a perfection rarely reached without costly development of specialized preparation tech-niques. Inclusion counting in metals and the counting and sizing of dispersed cells in biological smear specimens are examples of speci-man categories that do not present great difficulties.

Few specimens are so uniform that conclusions can be based on one single field of view. Therefore, scanners should normally be used in conjunction with stepping stages which allow the fields presented to the scanner to be uniformly distributed over the whole specimen area. - In favorable cases, where human control of the scanning operation is not necessary, the output from each field can be automatically printed and the next field can be brought into view automatically, as in the Quantimet automatic data handling system.

REFERENCES

CHAYES, F. (1949): Am. Mineralogist 34, 1, 600.
CHAYES, F. (1955): Am. Mineralogist 40, 126.
COSSLETT, V. E. and DUNCUMB, P. (1956) Nature 177, 1172.
DÖRFLER, G. (1966), Z. analyt. Chem. 221, 357.
DÖRFLER, G. (1967), Radex Rundschau "Fortschr. d. Metallographie"
FISCHMEISTER, H. and M. MÜLLER (1959) Z. Metallkde. 50, 478.
FISCHMEISTER, H. (1961) in "Quantitative Metallography" symposium
    at Gainesville, Florida. Ed. R. DE HOFF and F. RHINES, McGraw-
    Hill Co. (in print). Also published in Acta Polytech. Scandinavica,
    Chem. Met. Ser. C 56, 1966.

FISCHMEISTER, H. (1963) Proc. 1st Internat. Congr. Stereology and Z. prakt. Metallographie 2 (1965) 251.

FISCHMEISTER, H. (1966) in "Quantitative Methoden der Morphometrie", ed. E. WEIBEL, Springer Verlag Heidelberg, 1967.

FLORY, L. E. and W. S. PYKE (1953) RCA Review 14, 546.

GILLINGS, D. W. (1955) Instrument Practice 9, 763, 886.

GURLAND, J. (1958) Trans. AIME 212, 452.

HAWKSLEY, P. G. W., J. H. BLACKETT, E. W. MEYER and A. E. FITZSIMMONS (1954) Brit. J. Appl. Physics Suppl. 3, 165.

HENNIG, A. (1958) Zeiss Werkzeitschr. 6 78.

HENNIG, A. (1966) in "Quantitative Methoden der Morphometrie", ed. E. WEIBEL, Springer Verlag Heidelberg 1967.

HILLIARD, J. E. and J. W. CAHN (1961) Trans. AIME 221, 344.

HILLIARD, J. E. (1966) in "Recrystallization, Grain Growth and Textures", ASM Metals Park, Ohio 1966, p. 267.

HURLBUT, C. (1939) Am. J. Science 237, 253.

LAGERCRANTZ, C. (1948) Nature 161 25; Acta Physiol. Scand. 26, (1952) Suppl. 93,1.

MELFORD, D. A. and R. WHIDDINGTON (1964) Metallurgia 70 49.

MOORE, G. (1964) Photogr. Sci. Eng. 8 152.

MOORE, G. (1966) Proceed. 3d Intern. Materials Symp. Berkeley, Calif. June 13, 1966; Natl. Bureau of Standards Rept. 9428, U. S. Dept. Comm. Oct. 1, 1966.

ROBERTS, F. and J. Z. YOUNG (1952) Proc. IEE 99 747.

SCHEUMANN, K. H. (1931) Mineral. Petr. Mitteil. 41 180.

SHAND, S. J. (1916) J. Geol. 24 394.

SMITH, C. S. (1960) Trans. AIME 218 58.

THEISEN, R. (1964) Z. Metallkde. 55 128.

WALTON, W. H. (1954) Brit. J. Appl. Physics Suppl. 3 121.

YOUNG, J. Z. and F. ROBERTS, (1951) Nature 167 231

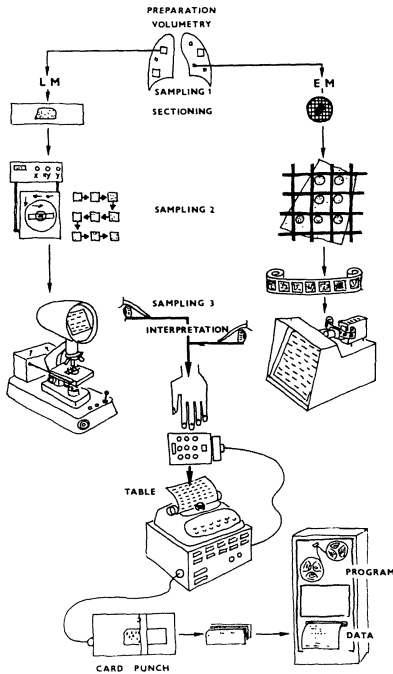# A SEMI-AUTOMATIC SYSTEM FOR STEREOLOGIC WORK IN LIGHT AND ELECTRON MICROSCOPY

Ewald R. Weibel

Department of Anatomy, University of Bern, Bern

In biologic work interpretation of structures on
sections cannot be automated without unduly com-
plex computer programs. Since our present know-
ledge does not allow us to consider every detail
represented in our preparations, simplifications
of often high degree must be introduced in order
to arrive at meaningful information. Furthermore,
unavoidable and uncontrollable artifacts would
seriously affect automated analysis, while an
experienced investigator will immediately reco-
gnize and "over-look"them.

It has therefore been our aims (a) to introduce
automation in all those steps which do not re-
quire special skill but which can be considered
"routine operations", and (b) to design a consi-
stent system applicable or adaptable to a large
number of different problems.

Fig. 1 presents a survey of the general procedu-
res necessary to arrive from a specimen to mor-
phometric data through stereologic studies in
light and electron microscope. Sampling I yields
sections; the blocks are selected by random sam-
pling, preferably with stratification (1).
Sampling II yields "micrographs"; systematic di-
stribution of fields gives best section coverage.
In electron microscopy the micrographs are re-
corded on film by placing the screen tangentially
into a specified corner of the supporting grid
meshes (2). In light microscopy fields can be
sampled with the automatic sampling stage micros-
cope manufactured by WILD HEERBRUGG INC. (3, 4).
Sampling III yields point-samples of structures
for easy enumeration. A number of test systems
have been devised for adaptation to various pro-
blems (2). In light microscopy they are either

PREPARATION
VOLUMETRY

L M

SAMPLING 1
SECTIONING

E M

SAMPLING 2

SAMPLING 3

INTERPRETATION

TABLE

PROGRAM

DATA

CARD PUNCH

Fig. 1:
Diagram of system

introduced as eyepiece graticules or as projection screens. For electron micrographs a compact projector unit with exchangeable screens has been constructed.

Interpretation is left to the investigator who classifies the "point events" into a data recorder. After evaluation of each sample a push-button triggers automatic printing of the data on a table and, optionally, into punch cards for direct computer evaluation (3). An adaptable computer program yields morphometric and statistical data.

References:

(1) E.R.Weibel: Morphometry of the Human Lung.
    Heidelberg:Springer (1963)
(2) E.R.Weibel, G.S.Kistler and W.F.Scherle:
    J. of Cell Biology 30, 1, pp. 23-38 (1966)
(3) E.R.Weibel: Automatic sampling stage micros-
    cope and data print-out unit (Demonstration,
    this volume)
(4) R.H.Gander: A Morphometric Microscope with
    Automatic Sampling Stage (this volume).

A SYSTEM FOR STEREOMETRIC ANALYSIS USING THE ELECTRON MICROPROBE

GERHARD DÖRFLER

Analytisches Institut der Universität Wien, Vienna

The electron microprobe is an extremely valuable
tool for the quantitative determination of the chemical
composition of microvolumes. By the well-known scanning-
technique, concentration-diagramms and pictures of the
distribution of selected elements can be made.

This scanning technique allows a lineal analysis
of a material to be made, by using the chemical compo-
sition of the phases present for means of their identi-
fication. Two instruments have been constructed pre-
viously for phase-analysis (THEISEN;   MELFORD et al.),
but neither employs the lineal analysis technique.

The working-principle
of the "phase-integrator" is
shown in Fig. 1 . Setting the
X-ray-spectrometers of the
microprobe for the appropri-
ate element, the line-scan
across two different phases
in a matrix (Fig.1a) yields
a concentration-diagram as
given in Fig.1b. The rate-
meter-voltage can be easily
discriminated by electronic
means, which results in the
selection of one phase (Fig.1c).
This discriminated voltage,
which corresponds to a cer-
tain concentration-range of
a characteristic element,
opens a switching circuit
trough which pulses of uni-
form frequency can pass to
a counting unit. The passage of these pulses is stopped,
when the voltage at the exit of the switching circuit
becomes zero (Fig 1d). The pulse groups coming to the
counting unit, represent the intercepts of the phase
encountered. The basic arrangement of the "phase-inte-
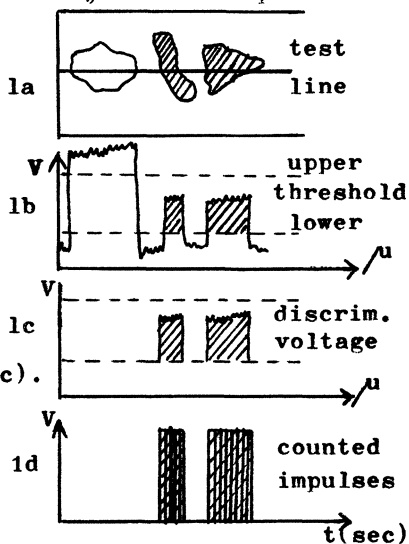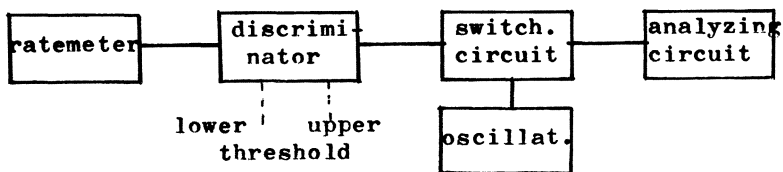grator" (PI) is given in Fig 2.

Fig. 1

```
┌──────────┐    ┌──────────┐    ┌──────────┐    ┌──────────┐
│ratemeter │────│ discrimi-│────│ switch.  │────│analyzing │
│          │    │  nator   │    │ circuit  │    │ circuit  │
└──────────┘    └──────────┘    └──────────┘    └──────────┘
                   ╎     ╎                          │
                lower ╎  upper              ┌──────────┐
                threshold                   │oscillat. │
                                            └──────────┘
```

Fig. 2

It is apparent, that the pulse-groups, representing N_L , can be used to calculate all known parameters of stereo- logy; i.e. V_V, S_V, D etc. Moreover, several units such as depicted in Fig. 2 can be operated simultanously to measure all phases present, as well as to define one phase by the presence of two elements. A more complete discussion of the results and limitations of the PI is given by DÖRFLER (1)

Recently the PI has been used in conjunction with the "sequence-analyzer" (DÖRFLER (2)). With this combi- nation, the"proximity-values" can be measured automati- cally. The sequence-analyzer consists of several logic devices, flip-flops and and-gates ,to register sequences such as A/B, B/C etc.

Perhaps the most interesting development has been the recording of the pulses leaving the PI's switching circuit onto magnetic tape and subsequently analyzing them by a digital computer. This requires only a very simple sorting-program and permits a very efficient data-reduction. With this method one obtains the calcu- lated values for V_V, S_V, grain-sizedistribution, proximi- ty etc. This also allows the analysis of a greater number of samples than present techniques in the same time and thus facilitates the search for correlations between the properties of a material and its structure. Furthermore the use of a microprobe in lieu of a normal microscope to make a lineal analysis, has the great advantage, that the phases present can be determined from their chemical composition, which is intuitively a better means for discrimination than the reflectivity or the transparency of these phases for normal light.

References:

Dörfler, G. (1) : Z. Analyt. Chemie 221 (1966)p357

Dörfler, G. (2) : Radex Rundschau in press

Melford, D.A. and R. Whiddington: Metallurgia 70(1964)
                                                    p 49
Theisen, R. :   Z.f. Metallkunde 55 (1966) p128

A COMPUTER-LINKED, SCANNING, MICROSPECTRO-PHOTOMETER USING THE TWO-WAVELENGTH METHOD

D. E. ABRAHAMSON AND A. LAZAROW

Department of Anatomy, University of Minnesota, Minneapolis, Minnesota

A significant problem in the application of absorption spectrophotometry to tissue sections is that the chromophores are often not uniformly distributed; thus, the Beer-Lambert law cannot be used to relate transmittance to the quantity of absorber. There are three methods to compensate for the resulting distributional error: (i) The conventional method, which is suited for large objects, requires measurements be made only over homogeneous regions. (ii) The scanning method (1) integrates the results of many measurements each of which is made over an area sufficiently small so that the absorber distribution can be assumed to be homogeneous. (iii) The two-wavelength method requires measurement of the transmittance at two wavelengths for each field; the mass of absorber in the field is then calculated using the two-wavelength equations (2,3). It has been shown that the scanning and two-wavelength methods are equally accurate (4).

The two-wavelength method requires that the absorption spectrum be known, over a region of the specimen in which the chromophore is uniformly distributed. This spectrum is used to select the two wavelengths at which the transmittance can be accurately measured over the non-homogeneous regions, and at which the ratio of the extinction coefficient is equal to two.

Our instrument (see Figure) includes light sources for the ultraviolet and visible spectral ranges, a light source monochromator equipped with a servo control, a microspectrophotometer equipped with apertures and optical components which satisfy all requirements of microspectrophotometry, and photomultiplier readout circuits (5). The output signals are digitalized and recorded on punched paper tape for input into a digital computer.

During measurements of absorption spectra, the wavelength is scanned, and the intensities of the incident and transmitted light beams are recorded. Computer programs are available to calculate the absorption spectra, taking into account systematic errors in the readout apparatus.

In cases where the signal to noise ratio is not high, mul-
tiple spectral scans are made, and an average absorption
spectrum is calculated.

   Two options are available for two-wavelength measure-
ments. In the first, the light source monochromator is
programmed to switch between the two-wavelengths, and the
transmittances are recorded. In the second, white light is
passed through the specimen; the beam then passes through
a beam splitter, sending half of the beam into each of two
monochromators, one set to isolate each of the two wave-
lengths. The intensities of these two components of the
beam are sensed with photomultipliers and recorded on
punched paper tape. In either case a computer program is
available to calculate the mass of absorber, using the two-
wavelength equations.

   The use of two monochromators and a beam splitter per-
mits specimen scanning because the transmittances at both
wavelengths are measured simultaneously. For specimen
scanning, the stage is driven by a servo motor, and the
stage position (in one axis) is recorded.
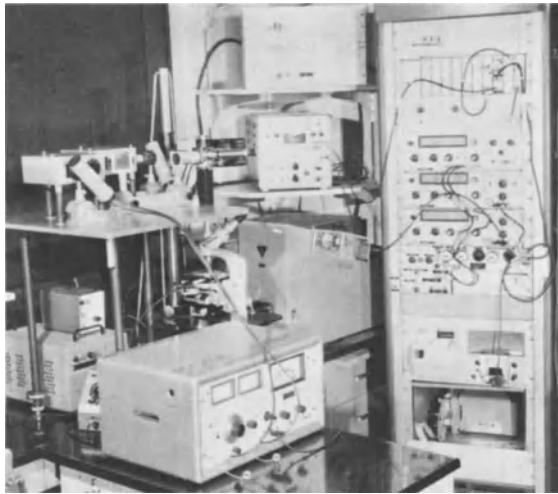
(1) Caspersson, T. & G. Lomakka, Ann. N. Y. Acad. Sci., 97,
    449-463, 1962.
(2) Patau, K., Chromosoma, 5, 341-362, 1952.
(3) Ornstein, L., Lab. Invest., 1, 129-132, 1952.
(4) Mendelsohn, M. & B. Richards, J. Biophys. Biochem.
    Cytol., 4, 707-709, 1958.
(5) Abrahamson, D. E. & A. Lazarow, in preparation.

APPLICATION OF COMPUTERS TO
QUANTITATIVE ANALYSIS OF MICROSTRUCTURES

(Paper from platform and Demonstration D-9)

GEORGE A. MOORE

Metallurgy Division, Institute for Materials Research, National Bureau of Standards,
Washington, D.C.

1: GENERAL REQUIREMENTS

Evaluation of particle size and shape, a necessity for any stereological projection beyond volume fraction, requires continuity of observations over the section. Observations must be made on a dense raster at a resolution approximating that of the microscope, yielding up to one million observations per field. Such masses of data are obtainable only from automatic scanning equipment, and require computer processing of the image. (Figure 1)

Dense rasters are admittedly inefficient in determining area and volume fractions. Binomial statistics apply to area fraction, provided the effective number of independent observations is reduced to four times the number of intercepts. Precision of volume fraction is worse, following Poisson statistics applied to the number of observed particles, but with the standard deviation multiplied by a factor (0.44 to 1.41) varying with structure and concentration. *

Statistical errors must be combined with an error in edge observations proportional to the number of intercepts and to the video signal error. Correct phase discrimination can be established to $0.5 \, N_i$ by visual matching, and to $0.1 \, N_i$ by edge differentiation with present equipment. The two errors combine to yield best precision at an intermediate apparent particle size to be attained by choice of magnification. This size, and the overall error in either area or volume fraction, decreases with increased raster resolution and scanner precision, and with better resolution, contrast, and photographic uniformity in the micrograph. (Figure 2)

2: SCANNER TYPES

Presently feasible scanner equipment falls into two basic classes: Direct image scanners based on a television camera (Vidicon) can yield 200^2 observations per field with a signal accuracy of ½ stop (25 to 30%), using common commercial components. Best present Vidicon technology can yield 200^2 observations with a 4 to 5% signal error, or 400^2 observations at ½ stop accuracy. Non-uniform response over the field, and distortion of the raster are troublesome. Commercial systems may thus be expected to determine an area fraction near 50% with a precision near 1% under best conditions, thus at least to equal any feasible manual determination. This type should be adequate for normal diagnostic and quality inspection purposes, and for survey work requiring many fields for valid sampling. The unit should, however, be restandardized for each field.

Mechanical-optical systems, either facsimile picture scanners or moving stage microscopes, can provide constant illumination and photo-sensitivity as well as a geometrically precise raster. A circuit precision of 0,2% is attainable, but non-uniformity of specimen or photograph will limit the overall signal precision to about 1%. The present drum scanner provides up to 960^2 observations per micrograph. Moving stage units can scan a larger field at the same resolution, giving several million observations. All systems except the slower moving stage are now electronically limited at 40K to 80K bits per second, and provide information at roughly equal rates. For evaluation of standard micrographs, referee measurements, and critical research problems, the higher precision of a mechanical-optical system appears necessary. The facsimile form provides flexibility to treat many subjects, opportunity for photographic improvement of images, and adequate operating speed; with an area precision in the range of 0.25%. This is an order of magnitude better than is attained by hand methods.

3: COMPUTER IMAGE PROCESSING

Three levels of computer processing of a digitalized image from a scanner should be recognized and distinguished from processing of data derived from an image.

(a) An elementary computer or counter system incorporated in the scanner unit can tally points-in-phase and intercepts, providing area fraction and mean intercept width for particles of a selected tone range. The correct tone range can not be pre-determined, hence scans at several tone levels are normally required to objectively select the correct tone value.

For any more elegant analysis, each observation must be represented by a digitalized tone value and the entire record submitted to a general purpose computer; usually by way of a digital magnetic tape record. Digital classes spaced at about six standard deviations of the signal, thus about 16 tone characters, are generally adequate.

(b) A small business type computer; treating one image line at a time, can tally the apparent area for several tone ranges to determine the correct range. Successive observations may be compared for more precise edge determination. A histogram table of intercept lengths can be accumulated and used to compute a statistical estimate of the number and size distribution of particles in a section or volume.

(c) A large and competent scientific computer makes it feasible to logically transform binary phase images in many useful ways. These include substitutes for photographic steps and erasing classes of objects which should not be measured. Serial sections or time lapse pictures can be logically compared to show either differences or connectivity and stereological relationships. Morphological models may be derived by the machine to explain complex shapes. Logical dissection of an image permits each particle to be measured in at least 17 ways, yielding parameters which, when classified into histograms, give a comprehensive description of the area and probable volume structure. (Figures 3 & 4)

---

* References and a detailed discussion are available from the author in a report under the same title.
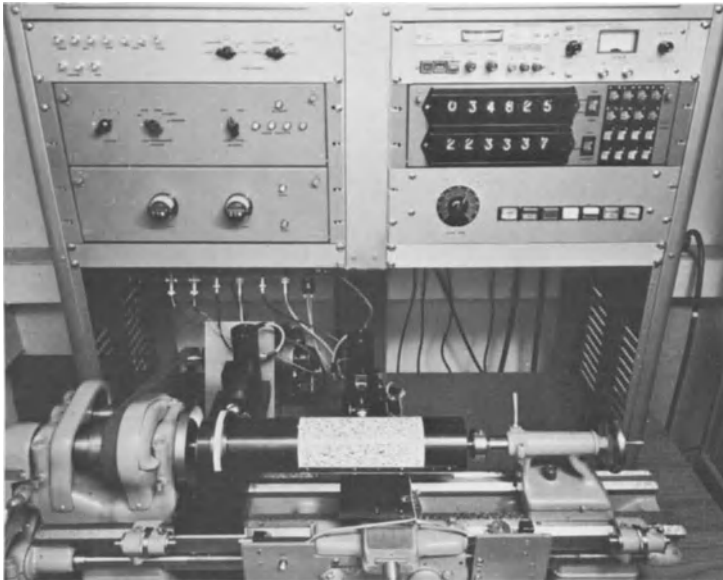
Figure 1: Precision Scanning Analog - Digital Input Equipment.
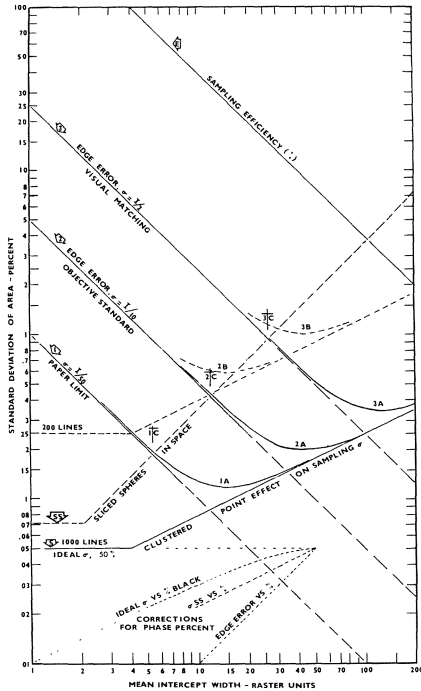(Model 3) Used for Analysis of Micrographic Prints up to 24 x 24 cm.

Figure 2:

Curves for Estimating Expected Precision of Area Measurement for Various Micrographs and Scanning Conditions. (For 50% Black)

2B to 3B: Expected Range for Vidicon Systems.

2A to 3A: Performance Range of Scanner Shown in Figure 1.

2C and 3C: Best Expected Precision of Volume Fraction for Spheres Occupying 50% of Volume, Using 1000 Line Raster.

Corrections: Curves Shown May Be Shifted Downward by Indicated Amount when Area Is Not 50% Black.

283
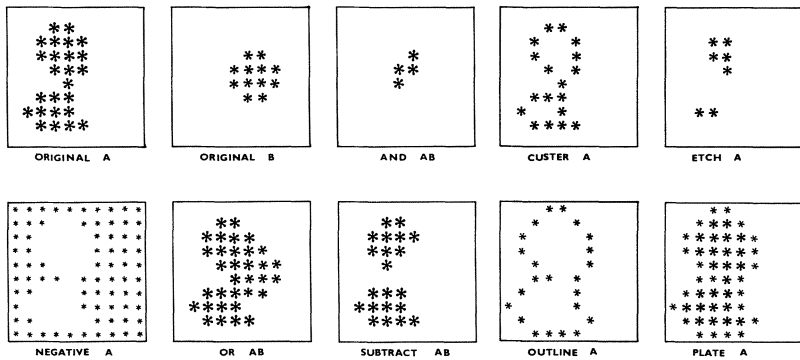
Figure 3: Logical Transformation of Matching Sections of 2 Binary Images. Patterns Shown Are Produced by Computer Following Indicated Commands.
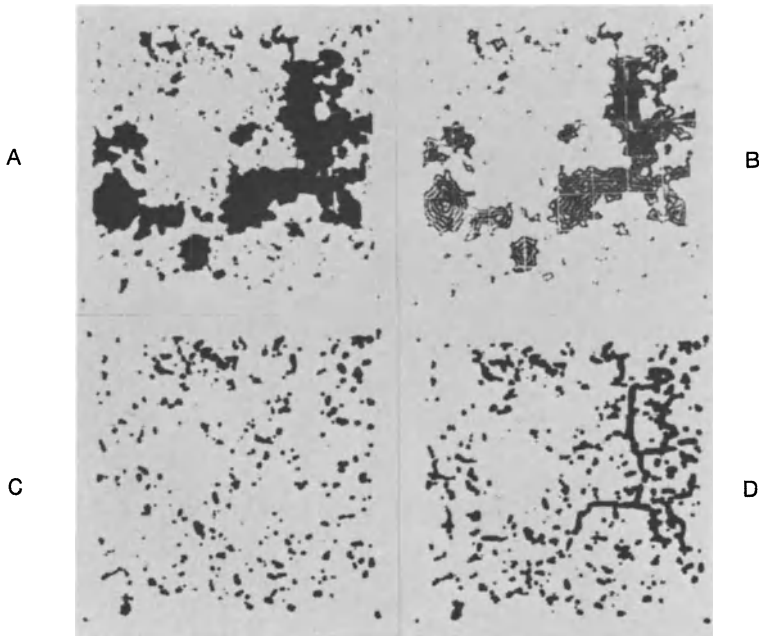
Figure 4: Computer Model of Nucleation and Growth of Complex Void Structure in Niobium-Tin Powder Alloy.

A: Computer Display of Original Binary Image.
B: Shell Custer Generates Growth Ring Pattern.
C: Nuclei of Smallest Voids Only; Presumed Last Formed.
D: Sum of All Void Nuclei for 11 Size Classes or Generations. Note the Crack Pattern.

284

THE METALS RESEARCH IMAGE
ANALYSING COMPUTER

Colin Fisher

Metals Research Limited, Cambridge, England

The Quantimet is the first internationally accepted image analysis in-
strument and makes all the measurements necessary for stereological
problems including Surface area, Intersect counts, Chord size distribu-
tion, form factors etc. The complete self contained system makes 30
measurements on each field of view resolving 100,000 picture points
at a speed of 1 field of view per second. All measurements can be
pre-programmed to be printed, displayed electronically or recorded
on punced paper tape. The selection of fields of view over the speci-
men is also pre-programmed for anything up to 1/2 a million fields
over a very wide renge of patterns up to 1" x 2". Successful appli-
cations include research and production assessment of non-metallic
inclusions in metals, grain size deteminations, carbide segregation
assessment, grain size and porosity of ceramics, bricks and sintered
materials, soil sample assessment, particle size analyses, biological
and medical cell population studies, bacteria colong counts, particle
track photograph analysis, autoradiograph investigation and many X-
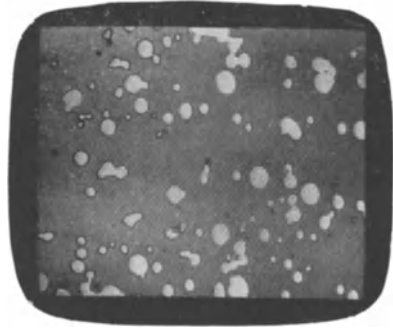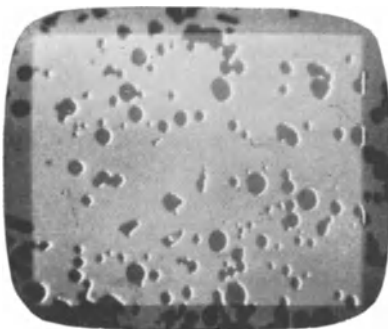ray and electron microscope photography applications.
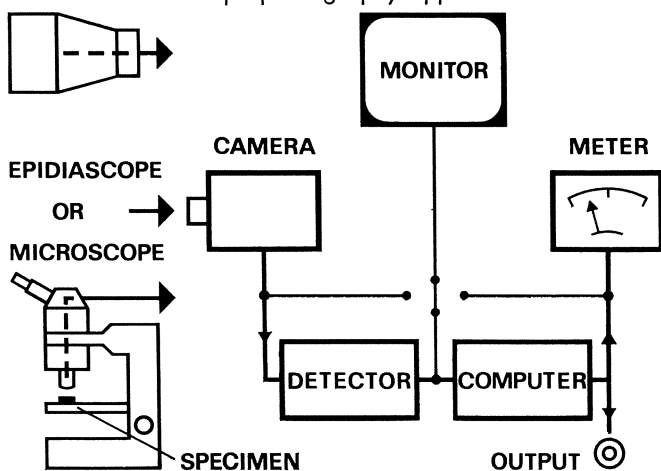
The Simplified Block Design

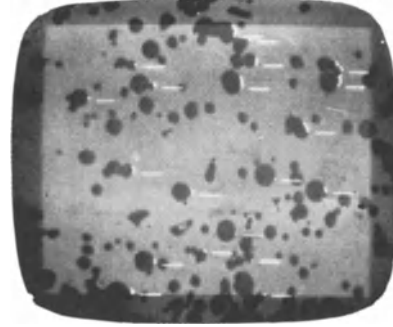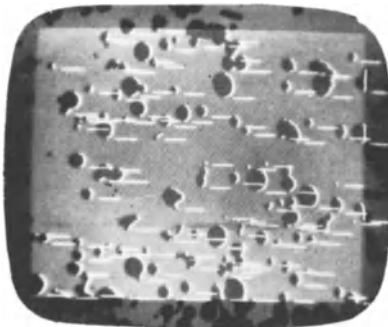## The Quantimet Image Analysing Computer

Typical Operating Displays (powder measurements)

Total Feret diameter = 2.43mm   Total Projected Area = .037mm^2

Number of Particles = 135   Number greater than 30µ = 20

RATIONALIZATION IN DIRECT MICROSCOPICAL MEASUREMENT

Dietrich Eichner

Department of Anatomy, University of Muenster, Muenster

Compared to indirect measurements in projected
pictures or in photographs direct microscopical
measurements have the advantage of estimating the
histological structures much more accurate,but
using the well known methods with special oculars
they turn out to be a cumbersome and time consu-
ming work.On the other hand there is no doubt that
for example cell nuclei measurements are of great
value for histologists in forming an opinion
about cell activity;this has been confirmed by
the combination of quantitative cytochemical in-
vestigations with cell nuclei measurements.This
paper deals with a new way to carry out direct
microscopical measurements quickly,without fatigue
and with the necessary precision.
Since a couple of years a new drawing tube is
available,manufactured by WILD OPTICAL COMPANY,
HEERBRUGG/SWITZERLAND,which can be used on a bin-
ocular microscope.This apparatus also can be em-
ployed in the inverse way reflecting scales,pat-
terns or figures of known dimensions into the mi-
croscopical picture(Fig.1).It is of great advan-
tage to use white marks an a dark black back-
ground to avoid irradiations and to get a perfect
histological picture(Fig.2).The plate with the
marks is moved by hand below the eyepiece of the
drawing tube until it fits the histological struc-
ture to be measured.A simple blood cell counter,
manufactured by BOSKAMP KG,HERSEL/BONN,GERMANY,is
linked to the micro-screw of the microscope,so the
thumb of the hand operating the keyboard easily
corrects the microscopical picture.The classifica-
tion as well as the microscopical magnification
both depend on the object to be measured.

For the measurement of larger areas-as glomerula-
the use of a point-net according to the suggesti-
ons of ATTARDI is recommended.
Bibliography:
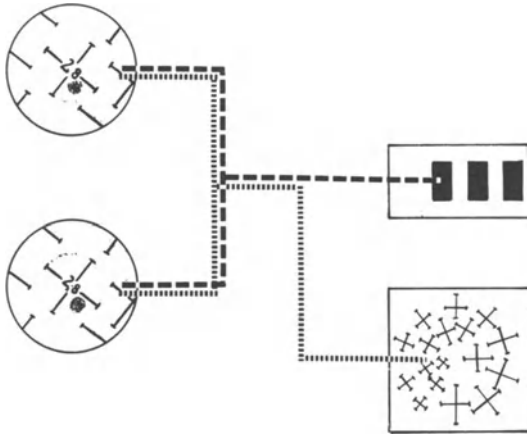Eichner,D.,Z.mikr.anat.Forsch.29,381-387,1963

Fig.1.Principle of direct microscopical measure-
ment.Right:scale with crosses and the microscopi-
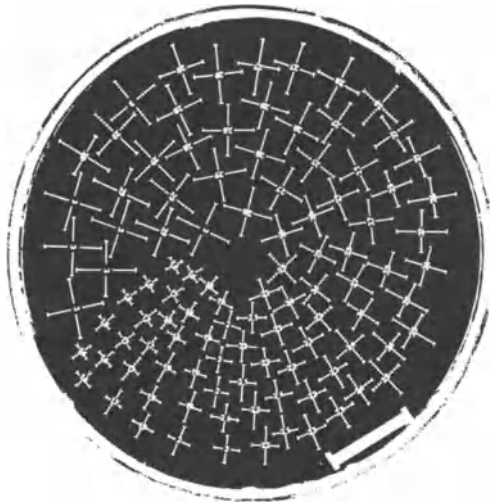cal preparation.Left:the microscopical picture

Fig.2.Scale for cell nuclei measurement.Size re-
duced.

MORPHOMETRIC MICROSCOPE WITH
AUTOMATIC SAMPLING STAGE

R. H. Gander

Wild-Heerbrugg, Heerbrugg

In order to facilitate the process of obtaining stereological data from microscopic specimens, a microscope was modified and various additional equipment developed, as described below.

The starting point was based on the well-proven Wild M20 research microscope, in which the coarse adjustment actuates the limb and the fine adjustment moves the stage.

Naturally, we could have adapted the existing mechanical stage by simply adding two drive units. It was felt, however, that this might not be suitable for the necessary continuous operation required – and an instrument should, of course, be designed for intensive use and not be left lying idle on the bench. The existing stage, suitably modified, could not be guaranteed for a long life, free from breakdowns, for there is a big difference between moving the stage frequently by hand and moving it by remote control, easily and efficiently, at much higher speeds and over larger distances, by means of a drive motor. A suitable new stage, with ball bearing tracks, specially treated spindles and a movement of 50x25 mm (2x1 in.).

The slide holder is mounted on a rotating plate, let into the stage, so that the specimen can be orientated as required. The drive housing, behind the microscope, contains two motors, each with two gears and a central idling position, selected by a short gear lever. In the neutral position the stage may be moved by hand in the normal way. In the other two positions the coordinate spindles are each driven by an efficient motor and gear system. The gearing is arranged to give each spindle two speeds, of around 500 μ per second and 2,000 μ per second respectively. In this way it is also possible to move the stage continuously, either forwards, backwards, to the right or to the left, by means of a four position joystick control. The stage simply follows the movement of the joystick, at the preselected speeds, allowing specimens to be quickly scanned over the 5 x 2.5 mm (2x1 in.) range. At the end of the range the stage stops automatically.

The scanning of the specimen helps to determine the optimum spacing of the fields to be counted. The field spacing can then be set on an electronic, preselecting counter, at distances from approximately 50 μ to 20,000 μ. Operation of a push-button switch will then move the stage (and the specimen) over the set distance in the selected abscissa or ordinate direction. If the step movement of the stage reaches the end of its range, it switches automatically to the opposite direction. A further setting permits the step movements of the stage to occur automatically after a time interval of 1/10 to 15s. Lastly, the stage may also be set to move automatically, line after line; that is, in a continuous meander-type backwards and forwards movement, with the line spacing being predetermined by the preselector counter, as already described. This allows a systematic scanning of the specimen, in contrast to the arbitrary or freely-controlled scanning with the joystick control mentioned earlier. A reset step counter indicates the total number of movements made in any step series. The right eyepiece tube contains an eyepiece with a Weibel or crosshair graticule. This allows binocular observation and presents an image in which the graticule pattern is superimposed on the specimen. The base of the instrument contains a powerful quartz-iodine lamp, permitting the binocular tube to be replaced by a projection head with a built-in graticule slide and Fresnel lens. With these facilities the automatic sampling stage both lightens and simplifies the work involved in morphometric counting operations, allowing the observer to concentrate on the specimen and the correct data to be fed into a counter unit.
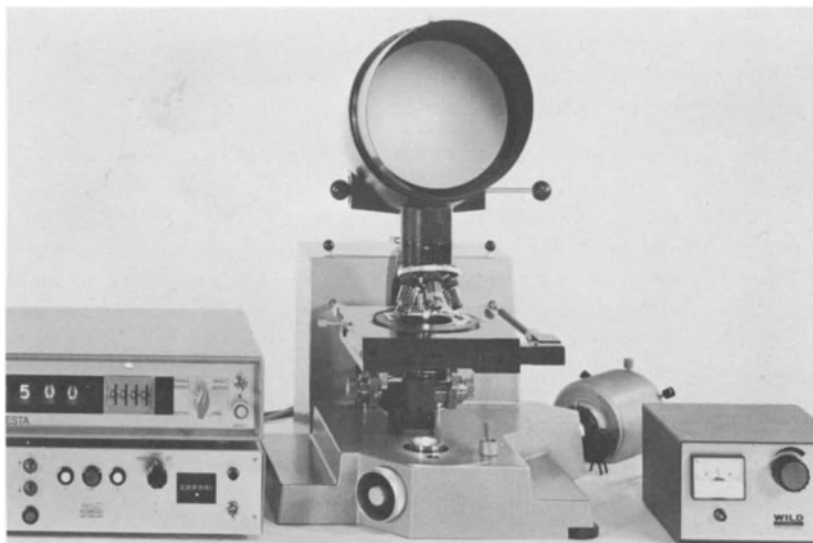
Morphometric Microscope with automatic sampling stage.

290

RECONSTRUCTION FROM SERIAL SECTIONS

RECONSTRUCTION FROM SERIAL SECTIONS

WENDELL J. S. KRIEG

Department of Anatomy, Northwestern University Medical School, Chicago, Illinois

When we study microscopic sections we are usual-
ly dealing either with a recurring pattern or
with a shape or group of shapes of objects whose
outlines modulate through the series. Methods
for visualization differ with the two cases. In
the first case we use random or systemically
spaced samples, in the latter we must build up
a picture, mental or actual, of the three-dimen-
sional configuration. Only the latter will be
dealt with in this communication.

There are two ways of reconstructing space re-
lations of objects within a block of tissue:
plastic and graphic. The Born wax plate method
of reconstruction is classic and need not be
dwelt on here. Suffice it to say, for those in
other fields than anatomy, that if we trace the
successive outlines of a structure as they pro-
ject, from a series of sections, on a wax plate
made as many times thicker than the section as
the number of units of magnification of the
image, we have when we stack the plates, a mag-
nified simulacrum of the object in the original
tissue block, after the stepped outline is
smoothed off by local heating.

This method was much used in the nineteenth cen-
tury when the details of embryology were being
worked out. It can be carried to any elaboration
—simultaneously reconstructing several systems,
holding detached or weak parts together with
wire or wax bridges, differentially coloring the
parts, or making a dissectible model. The pro-
cedure is rapid and is pleasant to work with.
The artistic tyro sees himself a sculptor, the
model is impressive and is permanent, and the
hot beeswax smells good. I always wonder that
my anatomical confreres do not use it more.

However, to the seeker for complete expression
the method has its disadvantages. The model oc-
cupies space, it can only be viewed by a few in
the original, though of course it can be photo-
graphed or drawn for publication. Also being
rigid, opaque and solid it does not show what is
inside any shape, and outside structures mask
deeper ones. When it is desired to demonstrate
anything complex the burden of reconstruction
imposes a limitation on its practicality. For
embryology, where one is usually dealing with a
limited number of forms and with distinct out-
lines the method is at its best. But the limit-
ations show up in neuroanatomy, for there are
many cell masses and many fiber systems in a
single section, each being a unit we desire to
portray.

For several decades I have used a simple graph-
ic method of reconstruction which has now been
applied to almost everything I can think of in
the brains of rat, monkey and man. Its proced-
ure is very simple. One merely projects on a
sheet of paper the outline of any structure in
a series of sections and draws its shifting
trace in proper relation, so that one obtains
a contour map of the object. A number of objects
present in the sections can be simultaneously
mapped in contour on this sheet of paper, using
perhaps different colored pencils for the dif-
ferent units, or for the different sections,
preferably in spectral order.

It is easy to transform a contour map into a
shaded topographical map by visualizing the
light as coming from the upper left and shading
wherever the contours indicate a slope away
from the light. Quickly the structures take
three-dimensional form subjectively for the ob-
server, and refinements can be added as the pic-
ture automatically develops. For the final ren-
dering, for publication, I generally use pen
drawn lines, as the line cut method is cheaper
than the halftone, and direction of shading
lines can be utilized to intensify the illusion
of third dimension.

As shown in the examples (figs. 1,2) accurate
depictions of great complexity can be built up,
and one can work one's will on rendering shapes

294

transparent in order to show deeper structures,
cutting windows, suppressing, intensifying,
schematizing. One great advantage is that nucle-
ar masses can be represented as hollow shells,
so that the fiber bundles inside them can be
rendered simultaneously.

By use of the slice method of reconstruction one
can make a fresh start whenever too much would
get hidden and the reference to the data source
is kept by the relations on the front surface
of each slice. Thus one's reconstruction becomes
like a picture of a series of slabs of a partic-
ular atmospheric Swiss cheese.

The slice reconstruction method is at its best
when used as an atlas division of a textbook of
neuroanatomy, since the course of all tracts and
the shape of all nuclei can be represented in
one series that runs from one end of the brain
to another, and specific references can be made
to this series as each item is discussed.

The slice reconstruction method is also a re-
search method. Nuclei and cortical areas some-
times have indistinct limits or questionable
identity. By projecting the seeming outline from
a series one can average out irregularities or
fill in uncertainties, and any real unit should
reconstruct into a closed space. Fiber trails in
experimentally degenerated material (Marchi
method) sometimes grow faint or cross other sys-
tems or seem interrupted. Scale reconstructions
direct search to the right points and enable
extrapolations. As a graphic record on a uniform
series of outlines in an 18-year project recon-
structing fiber tracts after 200 assorted les-
ions in the monkey brain, the method was inval-
uable as a full 3-D record of observations and
for exact cross comparisons.

To trace a single tract the length of the brain
through a series of full face slice reconstruc-
tions is somewhat wasteful of journal or book
space,and moreover, if running directly for and
aft, does not permit a very impressive visual-
ization.

If the slices could be viewed on the oblique
they would occupy less space, and a set of them

could be stood up, slightly separated, a tract could be followed through the whole brain on a single page size illustration, or two.

But for each slice we now have not a full face stack of sections to imagine, with one outer edge for all; rather each enlarged section has a separate set of edges, like an oblique view of a stack of glass panes. Moreover, each section is foreshortened and distorted obliquely. For the first condition we must graphically lay down a keel ticked off to show the position where each section sits vertically on it. For the second condition we construct an oblique grill which corresponds to a rectilinear grill over the section outline and redraw the outline square, thus producing a properly distorted section for any position.

This is a lot of trouble, but it only had to be done once for the whole monkey brain project. As long as this much trouble is taken, we might as well make the rendering more realistic by constructing our grills in true perspective, with vanishing points and foreshortening. So we applied the established principles of making a perspective drawing from a plan and an elevation, (the procedure is well explained in the Encyclopedia Britannica article "Perspective"), and set up a standard set of properly perspectively distorted grills for the nine slabs into which we regularly group the sections of the monkey brain (fig.3). This set can be copied directly by anyone who wants to make a perspective reconstruction.

Armed now with a set of distorted standard section outlines and a longitudinal scale ("keel") for positioning them one by one while reconstructing, we key in a sheet of matte acetate as an overlay and wherever the tract falls in the distorted section, or whatever the distorted oblique trace of a nuclear cell group may be, we trace it on the overlay sheet. In the end we have a trace which represents the 3-D course of the tract or the shape of the nucleus of the brain slices. We do not have to draw the obliquely reconstructed brain slices each time, that would be abhorrent; instead we trace our final outline onto a photograph of the reconstructed brain

represented as a transparent object. The structure in question is then realistically shaded, with a proper regard to how many layers of brain shell it is behind, making it dimmer accordingly (fig.4).

An example of the use of the method is shown. Clearly it is a useful and valuable one, but when many lesions are to be reported it is somewhat too much trouble. The full face slice reconstructions remain the standard procedure for ordinary recording and the one used for hundreds of published illustrations on the brain from our hand. It is a pity that it has not been more generally adopted. Some descriptive neuroanatomical papers might be more easy to take.

BIBLIOGRAPHY

Encyclopedia Britannica, "Perspective."
    1955 ed.

Krieg, W.J.S., "Connections of the Cerebral
    Cortex. II. The Macaque. B. Materials
    and Methods." J. Comp. Neur. 91:39-66,
    1949.
Krieg, W.J.S., Functional Neuroanatomy (Book),
    874 pp. Brain Books, Evanston, Illinois,
    1966.
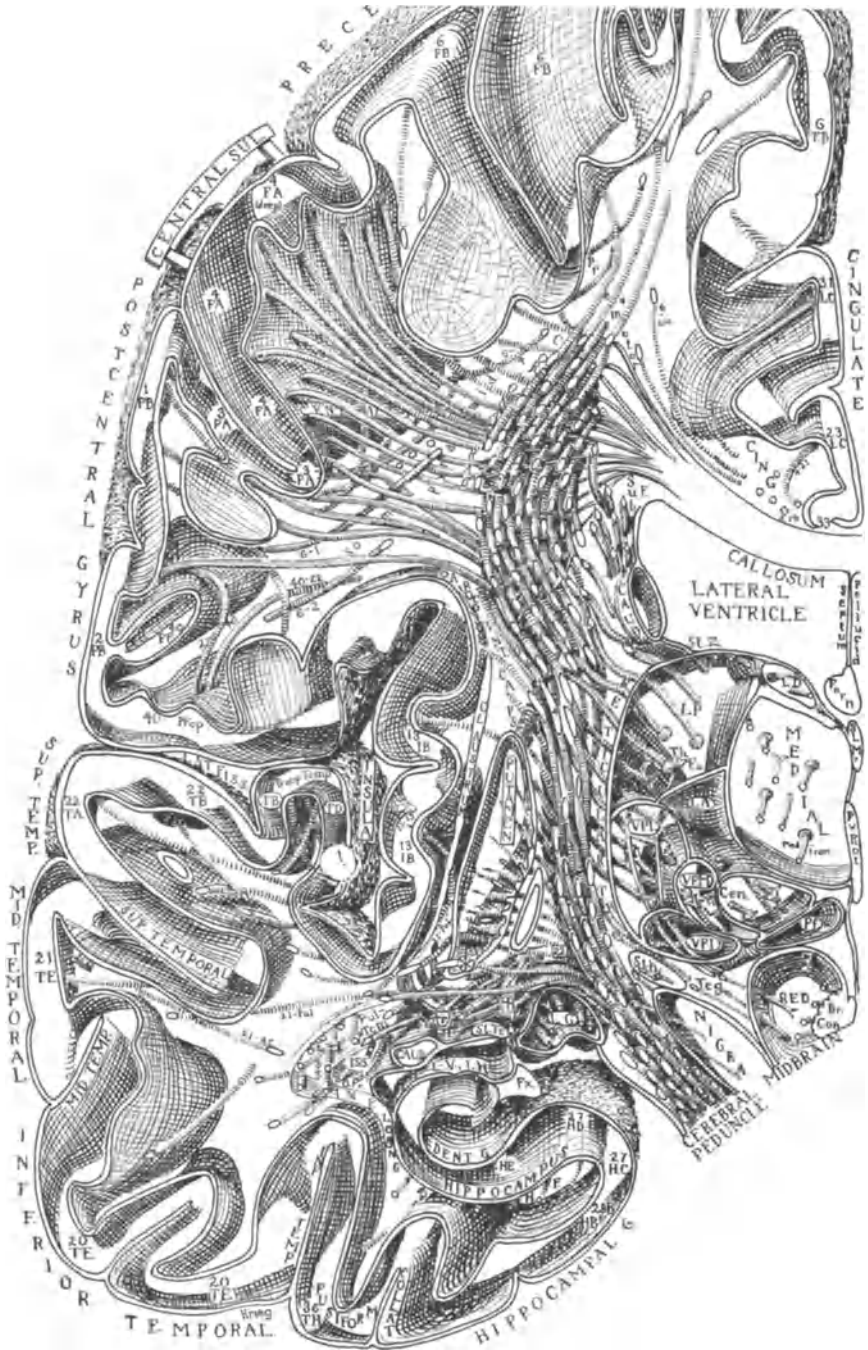
FIGURE 1. Reconstruction of diencephalic nuclei.
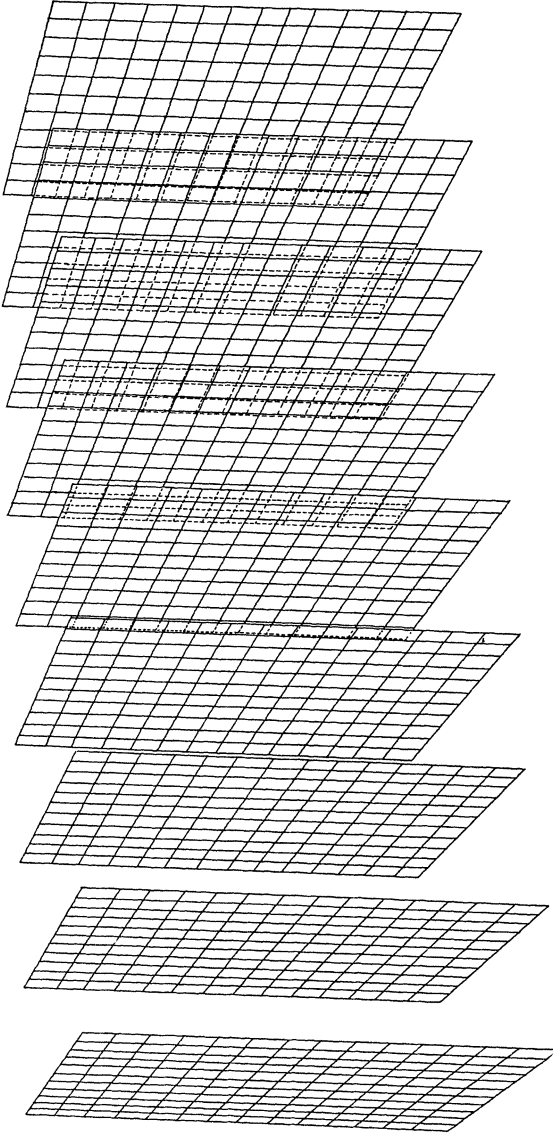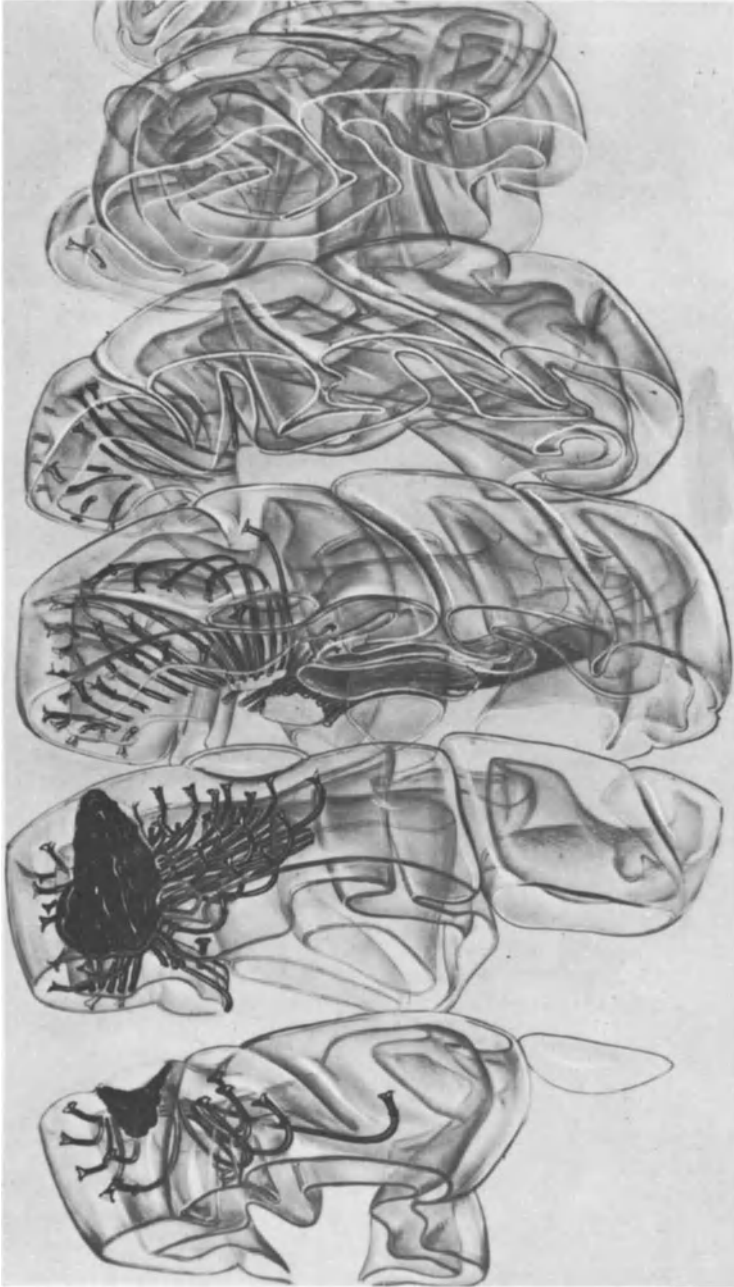
298

FIGURE 2. Slice reconstruction of human cerebrum.

FIGURE 3. Perspectively distorted grills for each slab in proper relations for reconstruction.

FIGURE 4. Transparent slice reconstruction of cerebrum of monkey visualizing course of fibers emanating from experimental lesions.

GLASS PLATE RECONSTRUCTION FROM SERIAL SECTIONS USED IN THE STUDY OF NEONATAL BILIARY ATRESIA

YOSHIKUNI OHTA

Department of Anatomy, Osaka Dental College, Osaka

EDWARD W. MILLHOUSE, JR.

Department of Anatomy, Chicago Medical School, Chicago, Illinois

Liver specimens for this study were obtained at Children's Memorial Hospital (Chicago) from biopsies of 9 infants ranging in age from six weeks to six months, suffering with congenital extrahepatic biliary atresia. The specimens were fixed with either 10% neutral formalin or Bouin's solution, embedded in paraffin, and 200 to 300 serial sections at 8μ were cut. The sections were stained by either hematoxylin-eosin, or van Gieson, or Mason's trichrome methods. Employing the glass plate method of Hans Elias, selected areas were reconstructed with the bile ducts drawn in green ink, the hepatic artery in white, and the portal vein in blue. The painted glass plates from each of the serial sections are piled up in their specific numerical order, thus presenting a reconstructed glass block model. The morphological structures observed in the histological sections can be examined in an effective manner by the three dimensional models in various directions with the naked eye.

Motion pictures of the reconstructed models using Kodachrome film and a 16 mm Bolex comera were made. From a glass model, containing 100 to 150 slides, the slides either singularly or in pairs were placed on a viewing box containing 100 or 150 watt light bulbs. Additional illumination was supplied by #2 photoflood lamps placed above and to the side of the viewing box and at least three feet away to eliminate any reflection. As single or paired glass slides were placed on top of each other 16 frames were taken and this repeated as additional slides were added to the reconstructed model on the viewing box. This method of cinematography is extrememly useful in viewing a reconstructed area and permits stopping at a particular point or reversing the movie and restudying

a special area many times. Therefore the en-
tire reconstructed glass model may be examined by
both motion pictures and visually at the same
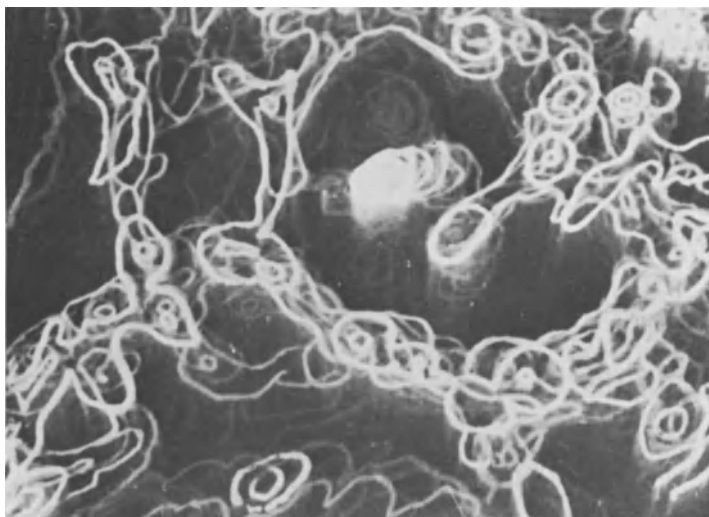time.

FIGURE 1. Surface view of glass model showing pro-
           liferation of ductules.

By this approach the bile duct proliferation and
the formation of the tubular structures of the
liver cells in congenital extrahepatic biliary
atresia have been studied. Degenerative and re-
generative changes in the portal area following
the progressive degree of the fibrosis in the in-
terlobular areas have been observed and demon-
strated by the methods described above. Figure 1
illustrates a portion of a glass model demonst-
rating the cylindrical network in a portal area
from the third stage of the proliferation.

By viewing the movie and glass models, it is
possible to observe the following: (1) the pro-
cess of the bile duct and ductule proliferation,
(2) the process of the tubularized transformation
of liver cells, and (3) the communication between
(a) the preexisting ducts and the proliferated
ducts and (b) the liver cells and the prolifer-
ated bile ducts.

THE TECHNIQUE OF POLYPLANETIC MICROSCOPY

HENRI COUDERC AND ROBERT GORENFLOT

*Laboratoire de Biologie Végétale Bt 490, Faculté des Sciences d'ORSAY,
ORSAY (Essonne)*

The practical abscence of depth of field in micropho-
tography leads to bidimensional images.

Several microphotographic transparencies superimpo-
sed with spacings proportional to the corresponding planes
of the object form a stereosolid (or photosterosynthesis).

We have developped this long standing technique in
several directions :

– For the very quick realization of such stereosolids,
a special stand enables us to use Polaroïd type transparen-
cy emulsions.

– The use of three-layered subtractive color emul-
sions gave us the microphotographic recording of three dif-
ferent planes of the object on a same photograph. The se-
lection of each plane is obtained by means of coloured fil-
ters.

But these techniques are not available for living and
thick objects of wich it was up to now impossible to obtain
an accurate microphotograph. We have solved the problem
by designing a " Polyplanetic " chamber (National Scienti-
fic Research Center, 1966 : French patent NR : P.V.85030).
This chamber records simultaneously several microphoto-
graphs corresponding to different planes or optical cuts of
the object.

How does the chamber operate : the main beam emer-
ging from the lens 2 is divided into four secondary beams by
three semi reflecting surfaces 3a, 3b, 3c – A system of ad-
justable prisms 14a... 14d guides the secondary beams into
optical routes of different and variable lengths. The secon-
dary images A_1 ... D_1 correspond to the planes A to D of the
object. The spacing of these planes is adjustable. The ima-
ges are projected on the film 10 by projection lenses 5a...
5d wich are movable for the tuning of the magnifications. A
reflex view finder 21 allows the framing and the focusing in
the middle plane E. This chamber can fit any modern micros-

cope. It also permits polyplanetic and stereoscopic microcinematography.

We make excellent stereosolids and stereoscopic microphotographs (stereograms) with the photographs obtained by means of the above explained techniques. The stereograms allow fine qualitative and quantitative tridimensional studies. All these techniques can be applied in various field such as : Protistology, Cytology, Histology, Palynology, Micropaleontology etc.....

COUDERC H.; GORENFLOT R. Développements de la photo-stéréosynthèse en micrographie – Revue de Cytol.et Biol. végétale 28,p.261 (1965).
COUDERC H. Techniques d'étude polyplanétique des objets microscopiques.D.E.S.Faculté d'Orsay (publication in course of issue).
LOCQUIN M. Microphotostéréosynthèses et reconstructions photographiques aux grossissements élevés. Bull.Soc. Linéenne de Lyon, 18 (1945)
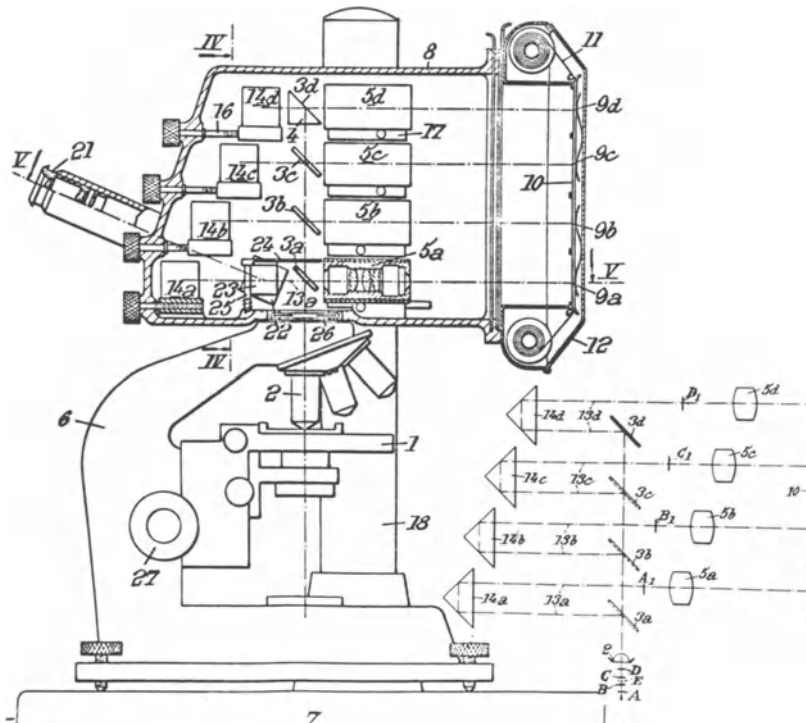
THE SYNTHALYZER FOR OPTICAL RECONSTRUCTION
AND DISSECTION OF STRUCTURES IN
THREE DIMENSIONS

ROGER LANNES DE MONTEBELLO

RLM Research Corporation, Yonkers, New York

Usual means of reconstruction fall into categories such as
physical stacking, mental extrapolation (Kleinerman, Postle-
thwait), microscope vibration (Gregory), and dynamic dis-
plays (Hirsch, Marks). The new system of dynamic display
here described and in particular the concept and method of
optical sectioning of the reconstruction, are believed to
be distinctly original.

A Synthalyzer (synthesis analyzer) prototype has been built.
The input of this electro-optical device is a set of coor-
dinated serial sections* photographically recorded in reg-
ister on a 16mm film strip. The output is a three-dimen-
sional virtual synthesis which stands in space, visible wi-
thin 360° azimuth and 80° elevation.

In operation, the film strip is mounted on a clear drum
(Fig.1,a) which revolves at about 1200 rpm. High frequency
xenon flash pulses (1,b) in the order of microseconds, are
sprocket-hole triggered to project and to visually "freeze"
the passing frames, on the surfaces of several Archimedes
spiral segments forming the edge of a larger drum (1,c) whose
rate of rotation equals the film's rate divided by the num-
ber of segments. The pulse rate is 2000 cps for 60 conti-
guous frames with a 30 frame gap. Projection is via a 45°
prism, an objective, and three 45° mirrors.

The segments are so
oriented that, during
rotation, their sur-
face is constantly ri-
sing; one film cycle
corresponds to the
travel of one segment
and the flash-projec-
ted frames are succes-
sively "frozen" on suc-
cessively higher levels
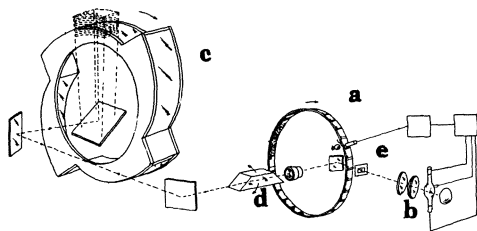of the segments. Since
the cycle is repeated

Fig.1. Schematic diagram

with high frequency, the ob-
server perceives the sequen-
tial projection as a three-
dimensional continuum (Fig.2)
made of fused horizontal lay-
ers simultaneously present in
their natural spatial rela-
tionship. The synthesis is
transparent and can be rota-
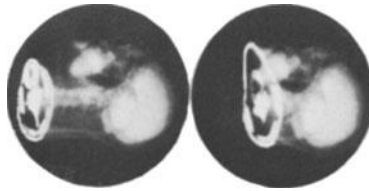ted for inspection, by means
of a dove prism (Fig.1,d).

Fig. 2. Synthesis and
sectioning of a human head

When the specimen is complex, however, as illustrated, one
"does not see the forest, for the trees", and an optical
dissector, capable somehow of "cutting through" the virtual
stack of sections, had to be designed. It is, essentially,
composed of a slide carrier (Fig.1e) transversally movable
via a driving wheel and gear train. The release of a brak-
ing mechanism allows the whole gear train to follow the
wheel, causing a rotation of the carrier and of the mask it
contains; the mask has an opaque zone and a narrow clear
zone. The translating and rotating mask controls the illu-
minance of the film frames. Thus the narrow, brightly ill-
uminated zone on each frame is projected in register with
that of the other frames, and the aggregate forms a thin,
vertical slice (Fig.2,b), containing well defined detail of
the inner structure. Owing to the mask's mobility, the cuts
may be made anywhere in the synthesis and in any azimuth.
The horizontally projected original sections can also be in-
dividually displayed by electro-mechanical controls, adding
to the versatility of this instrument.

Fields of Application: Research and teaching in medical and
natural sciences, engineering, mathematics, etc. A typical
clinical application for cancer detection: display of the
output of the Digital Positron Camera for radioactive tracer
scan (Kenny).

Bibliography: R.L. Gregory, Brit.Med.J. 1960, p. 1722; M.
Hirsch, US 3 077 816; P.J. Kenny, A. Lundy, J. S. Laughlin,
Trans. N.Y. Acad. Sci., Ser. II, Vol. 5, pp. 628-634, March
1966; J. Kleinerman and C. R. Cowdrey,Am. Rev. Resp. Dis.
Vol. 89, No.2, Feb. 1964; A.M. Marks, US 2 543 793; S. N.
Postlethwait, R. Mills, and K.B. Lohmann, Jr., JSMPTE, Vol.
73, pp. 629-31, 1964.

---

*Concrete, or hypothetical (by computer, or hand-drawn).

AN INVESTIGATION INTO HUMAN ENAMEL
STRUCTURE BY AN OPTICAL SECTIONING TECHNIQUE

J. W. OSBORN

Anatomy Department, Guy's Hospital Medical School, London Bridge

The inter-relationship of the 4µ diameter rods of which human enamel is composed has previously been deduced from the appearances of cut surfaces of transverse and longitudinal slices of teeth. These can be very misleading as to the true structure. The basis of the present technique was the 3-dimensional reconstruction and analysis of rod inter-relationships from series of optical sections produced by means of a through focussing technique on thick slices of enamel. Slices of enamel about 120µ thick were prepared in such a way that the rods were approximately perpendicular to the cut faces. The slices were observed with a microscope fitted with a fine focus attachment graduated to record changes of 2µ in the height of the microscope stage. Photographs were taken with a Leitz Orthomat photographic apparatus which automatically winds a 35mm film on for each successive photograph. This obviated any interference with the microscope, camera and slice during the filming and led to a stability of relationship between slice and camera which was an important factor when subsequently locating rods between successive prints. Using a X100 oil immersion lens (N.A. 1·32) the microscope was focussed near the lower border of the section and the first photograph was taken. By lowering the stage 2µ between each photograph a series of optical sections was produced. Each series consisted of between 30 and 70 optical sections. Dust within the optical system of the camera caused a pattern of dust spots to be produced on each of the successive negatives of a series. Comparison of these spots on the first and last prints of a series revealed their constancy of location and in the constructions to be described three were used as reference points.

On the first optical section of a series all the rods were labelled with identifying numbers and the same numbers used to label each rod as it appeared within the subsequent optical sections of the series. Tracings, in which each rod was represented merely by a number situated at its centre, were now made of every third photograph of a series.

308

On each of these tracings the three reference points were indicated.

Two widely separated tracings of the same series were accurately superimposed in relation to their reference points. It could be seen that any given rod occupied a different position in the two tracings. A master tracing was made which joined by a line and indicated by an arrow the distance and direction in which each rod had become displaced (Fig.1). It could frequently be seen that a given rod occupying a particular rod interspace at the beginning of a series had become displaced to an adjacent rod interspace at the end of the series. On a tracing of the first optical section of a series the directions in which each rod had become displaced relative to those originally above it and on its left side were indicated (Fig.2). From a knowledge of the plane of slices with respect to the enamel dentine junction it was possible to reconstruct the angles that each rod made with the enamel dentine junction in the transverse plane of the tooth. These angles were always less than 20°.

On the basis of this investigation it was concluded:
(a) There were only slight changes in direction between adjacent rods (Fig.1).
(b) Horizontal rows of rods crossed at well marked displacement planes (Fig.2).
(c) There was very little crossing of rods on the vertical plane (Fig.2).
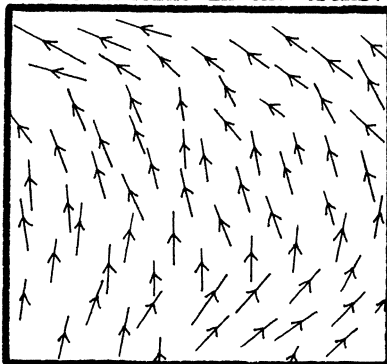(d) Each rod was angled at less than 20° to the surface of the dentine in the transverse plane of the tooth.

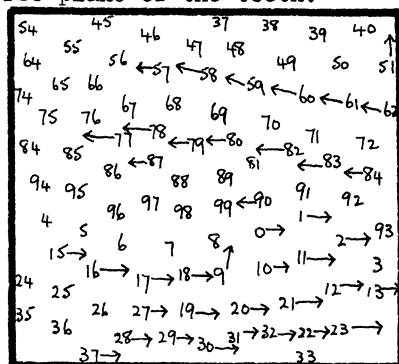Fig.1. There was a 20µ separation between the tracings from which this master tracing was constructed.

Fig.2. There was a 60µ separation between the tracings used for this construction.

309

THREE-DIMENSIONAL RECONSTRUCTION OF NERVOUS TISSUE

C. M. H. PEDLER AND R. TILLY

*Department of Anatomy, Institute of Ophthalmology, Judd Street, London*

To interpret the connections between nerve cells at the electron-microscopic level, it is usually necessary to make tracings of prints from each one of a series of sections. This results in a stack of transparent sheets, each one carrying the outline of interwoven plasma-membrane profiles. Unless each tracing is then cut out of some solid material, and assembled, no sense can be made of the series because the human visual system is incapable of retaining such complex topographic data.

After several attempts to assemble models in this way by making each individual membrane profile from various solid materials, it was found that the easiest method was to make a machine which would construct models directly from electron micrographs with ease and accuracy.

This communication is an account of the technique and some of its applications. A preliminary account of this method has already been published (Pedler & Tilly, 1966).

The device is basically a specially design-ed pantograph constructed of balsa wood and light alloy. A rigid square section arm A is freely suspended from a clamp B. Arms C, D, E and F complete the conventional pantograph arrangement with the difference that the out-put arm, instead of being composed of a single lever and pen, is, in fact, a spring-loaded pair of arms (E and F) with an electrically heated hot wire (I) stretched between them at the output end. The method of operation is as follows:

A profile (H) on an electron micrograph is followed by a pointer (G). This causes the hot wire (I) to describe the same shape and cut out from a sheet of expanded polystyrene (J) an identical profile having first made an entry into the sheet at the point K. The size of the profile cut from the polystyrene sheet is dependent upon the order of magnification given by the pantograph assembly and can be varied between unity and a magnification of six. The thickness of the polystyrene sheet is chosen to be in accord with the thickness of the section from which the electron micrograph was prepared. In this way, by sticking together each profile from the polystyrene sheet, it is possible to assemble a model in depth.
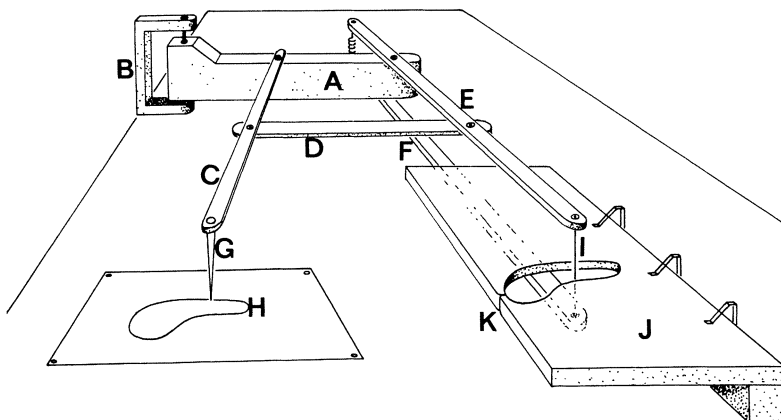
Reference.

Pedler, C. and Tilly, R. (1966). J. roy. micr. Soc. 86, 189-197.

SERIAL   SECTION   CINEMATOGRAPHY

TOPOLOGY AND SERIAL SECTION CINEMATOGRAPHY

EDITOR'S NOTE

As stated in the introduction, serial section cinematography invented by Dr. Hegre and perfected by him and by Dr. Postlethwait is much more than a tool for teaching and embryological, histological and botanical research. It is an important device for topological research. Dr. Rhines, in his lecture on topology as well as Dr. Gurland, Dr. Steel and Drs. Kronsbein and Steele emphasized the necessity of serial sectioning for the determination of topological parameters. They photograph the surface of the remaining block after etching it to create contrast. Drs. Hegre and Postlethwait are going a step further recording the sections on motion picture film, thus being able to re-synthesize the total structure, substituting time for height. While identification of identical structures in serial still photographs is still a laborious process, the motion picture film keeps every spot identified: and the recognition of topologically related parts is neuro-physiologically or psychologically automatic.

The sessions on topology and serial section photography provided an excellent meeting ground where biologists who had used serial section cinematography for the study of anatomical concepts learned how much bearing their work has on topology; and metallurgists learned how useful the motion picture camera could be to their topological studies.

Dr. de Montebello's synthalizer combines all these techniques, creating a transparent, three-dimensional image of complex objects useful for anatomical as well as topological work.

<div align="right">H. E.</div>

SERIAL SECTION CINEMATOGRAPHY

ERLING S. HEGRE

Department of Anatomy, Medical College of Virginia, Richmond, Virginia

THE BASIC TECHNIQUE

The present procedure for serial section cinematography is based upon a rapid method of staining the exposed surface of a specimen embedded in a paraffin block.

The specimen, such as an embryo, is first impregnated with lead acetate. This is done by immersing it in a saturated solution of lead acetate in 95% alcohol for a period of from 4 to 10 hours depending upon the size of the specimen. This represents a significant improvement in the method first described by Hegre and Brashear, (1946). Only the clear supernatant solution is used. The container should be completely filled and well stoppered to exclude all contact with the atmosphere.

Following this treatment, the specimen is passed into absolute alcohol, cleared in zylene or other suitable agent and embedded in paraffin.

Serial slices can then be cut in the usual way except for the significant fact that it is the exposed and intact surface of the block which is stained and photographed in each instance, whereas the prepared slices themselves are discarded.

The staining procedure consists of applying a water solution of sodium sulphide to the block surface. After an interval of from 5 to 10 seconds the solution is wiped off leaving the histologic details visualized by the precipitate of lead sulphide. With no further preparation the surface can be photographed using light transmitted through the paraffin.

APPLICATION TO TEACHING

This technique forms the basis for a simple but
effective laboratory exercise for students of
mammalian embryology (Hegre and Brashear, 1947).
Specimens which have been prepared in the manner
just described are mounted in an exposed position
on individual paraffin blocks (see Figure 1) and
issued to the students. Each student is also
provided with a single-edge safety razor blade
and a small bottle containing a 20% solution of
sodium sulphide in water.

The students prepare both longitudinal and cross
sections. They confine their observations to the
block surface (see Figure 2).

The attractive feature of this exercise is that
the student is able to observe the section or
level in its normal relationship to the remainder
of the specimen. It is felt that this very
materially aids him in developing a three-
dimensional concept of the internal structures.

MECHANICAL SECTIONING AND STAINING

An apparatus has been constructed which operates
automatically to slice, stain and photograph
successive levels through specimens which have
been prepared by the same method. It is essen-
tially a rotating arbor bearing a face plate to
which the paraffin block is attached in an
eccentric position. During one cycle the block
encounters the knife and then passes into a
solution of sodium where staining of the surface
takes place. Then, after an appropriate and
predetermined interval, the mechanism is actuated
and the face plate revolves to carry the block
out of the solution and past a jet of air which
removes any water droplets from the surface. The
block is photographed during the pause which
follows. The cycle is repeated until the desired
series of levels has been recorded.

TEACHING FILMS

The apparatus just described has been used to prepare teaching films of interest to several specialties. The best results have been obtained when using embryonic material (Hegre, 1966). The technical procedure has been to prepare the slices (sections) at intervals of 4 μ and to take 4 photographic exposures of each section or level. The progression through the specimen is therefore at the rate of 1 μ per second when the film is projected at "silent" speed.

If the specimen is to be photographed at a higher magnification, it is necessary to prepare the sections at intervals of 1 or 2 μ. It should be mentioned that the preparation of 1 μ sections presents no special problem since the slices themselves are discarded.

Another tissue that has been studied successfully is the lung. Serial sections through the normal adult lung reveal several features that merit further study.

Cinematography of the spinal cord has also been accomplished with interesting results, but it is too early to predict whether it will be possible to make observations which cannot better be made by routine methods.

CINEMATOGRAPHY IN RESEARCH

A study has been made of the conduction system of the human heart (Reed, Hegre and Russi, 1953). As a part of this investigation a cinematographic record has been made of serial sections through the atrioventricular bundle.

THE MAKING OF RECONSTRUCTIONS

The same technique of staining the block surface has been used as the basis for making reconstructions of embryos as a whole or in part. For this purpose, the photographs of the sections are taken at a higher initial magnification.

The model shown in Figure 3 is of a 9 mm pig embryo. The slices were cut at 16 μ and one photograph was prepared of each. The photographic paper (Translite) averaged 160 μ in thickness. The overall magnification is 16 times.

This model has been so helpful to both students and instructors that a printed edition is now being prepared (Hegre 1967).

REFERENCES

Hegre, E.S. and A.D. Brashear, Stain Technology, 21(4), 161-164, 1946, Block-surface staining.

Hegre, E.S. and A.D. Brashear, Anat. Rec., 97(1), 21-28, 1947, The block-surface method of staining, as applied to the study of embryology.

Hegre, E.S., 1966, The anatomy of the 9 mm pig embryo as seen in serial sections. Distributed by Commonwealth Motion Pictures, Richmond, Va. (16 mm educational film in color.)

Read, J.L., E.S. Hegre and S. Russi, Circulation, VII(1), Jan., 1952, Reaffirmation of the auriculoventricular conduction system in man. The introduction of a unique technic for its serial motion picture reconstruction.

Hegre, E.S., Medical College of Va. (In Press), 1967, A Model Atlas of the 10 mm Pig.

Fig. 1.   Prepared embryo mounted on a paraffin
          block.

Fig. 2. Section through the embedded specimen
         stained to show the histologic details.

Fig. 3. A photographic reconstruction of a 9 mm
         pig embryo.

AN AUTOMATED DEVICE FOR CINEMATOGRAPHY OF SEQUENTIAL MICROSCOPE SECTIONS*

S. N. POSTLETHWAIT AND ROY MILLS

Purdue University, Lafayette, Indiana

Attempts to photograph sequential sections through a specimen so the images could be viewed using a movie projector extend back to the early part of the twentieth century (Bush, 1952; Michaelis, 1955; Reicher, 1907). Most efforts have involved making prepared slides of the sections and superimposing the successive images by judging the alignment while viewing the specimen through the microscope or by photographing projected images from the microscope slides. The major difficulties of these systems include the determination of points of reference within the specimen for superimposition, excessive time consumption and labor and obtaining uniform material the successive sections of which are superimposable. Some recent efforts (Postlethwait, 1963; Zimmermann, 1965) involving staining and photographing the specimen surface prior to removal of each section have met with reasonable success. The techniques, developed independently, have been used in both research and in the production of loop films for use in the teaching of biology. This approach was the basis for a NSF grant received by the senior author to build an automated device to stain, photograph and section specimens and to produce thirteen selected botanical films. The junior author designed and built the machine used in this project.

Several films have been produced of plant specimens including seeds, stems, roots and flowers. As the viewer observes the projected images with a movie projector, he obtains the impression of motion as he progressively views successively lower levels in the specimen. Films prepared which involve transverse sectioning and longitudinal sectioning truly add an additional dimension to student understanding of the structure of a specimen. This is especially true where specimens are ramified by coalescing and anastomosing tissues such as vascular bundles and other highly differentiated tissue. Our work provides good evidence as to the effectiveness of this tool for stereology. Films thus produced can be used for direct study, a basis for structuring three dimensional models and as source material for computer analysis of the quantitative aspects of a great variety of complicated forms and specimens ramified with irregularly-shaped interstices or inclusions.

REFERENCES

Bush, V. Science. 115:649. 1952

Gasteiger, E. Personal communication. 1967

Michaelis, Anthony R. Academic Press, Inc., 1955

Postlethwait, S. N. Proc. First International Congress for Stereology 37a/1. 1963

Reicher, K. Neurol. Zbl. 26:496. 1907

Zimmermann, M. H., and P. B. Tomlinson. Jour. Arnold Arbor. 46:160-178. 1948

DEMONSTRATIONS

Several of the demonstrations were set up to illustrate papers presented from the platform.

Since the text for them was identical with that of the spoken communication, this text will not be repeated here.

DEMONSTRATION OF THE RELATIONSHIP BETWEEN CRYSTAL ORIENTATION AND OCTAHEDRAL TRACES

RALPH A. ATKINSON

Guest Scientist, Stevens Institute of Technology, Hoboken, New Jersey

A model used for the demonstration consists of an octahedron mounted in such a way that its vertical or Z axis can be tilted through a known angle ω in a vertical plane which makes an angle $\emptyset$ with the plane containing the X and Z axes. Starting with the Z axis in a vertical position (zero tilt) it can then be placed in the position corresponding to any given orientation by tilting in the appropriate vertical plane with the help of two graduated quadrants incorporated in the model. The octahedral traces corresponding to this orientation can be obtained by proceeding as follows: A sheet of white paper is placed on the table or other horizontal surface under the model and lines are drawn where the faces of the octahedron would intersect the paper if extended. These intersection lines and the angles between them correspond to octahedral traces and trace angles, respectively, for the given orientation.

BIO-PHOTOGRAMMETRY (DEMONSTRATIONS)

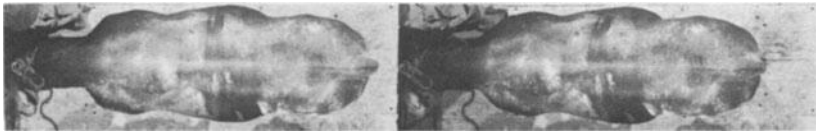WALTER LEYDOLPH, ULF ROSENOW, AND HELMUT JANKE

Universität Göttingen, Göttingen

Various applications of X-ray and normal Stereophoto-
grammetry are given, of which only three can be dis-
played here:(Figures (a) can in each case be viewed
stereoscopically.)
Fig.1: Evaluation of a bull for purpose of selection
b)iso-altitude lines,c)cross-section of back and loin
Fig.2:Measurements of the volume of coronary arteries
of a human heart (a) by means of X-ray Stereophoto-
grammetry. (b),(c) and (d) give the front, side and
basic views of the arteries respectively.
Fig.3: Determination of the position of an intraute-
rine radium applicator and of pelvic lymph nodes for
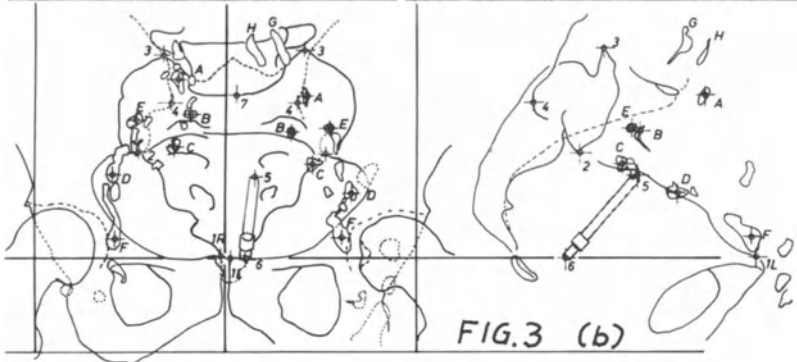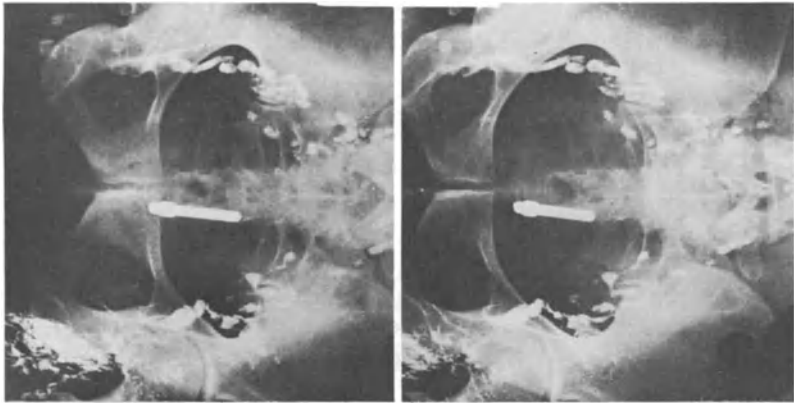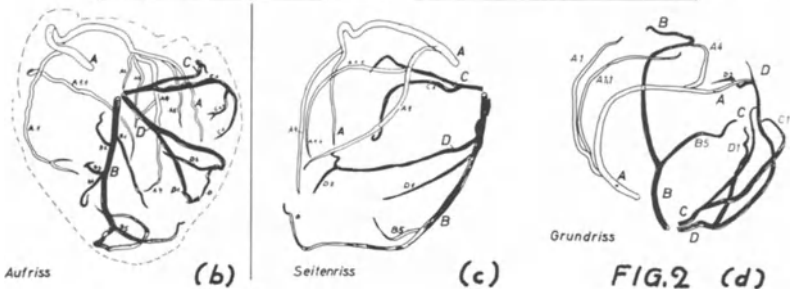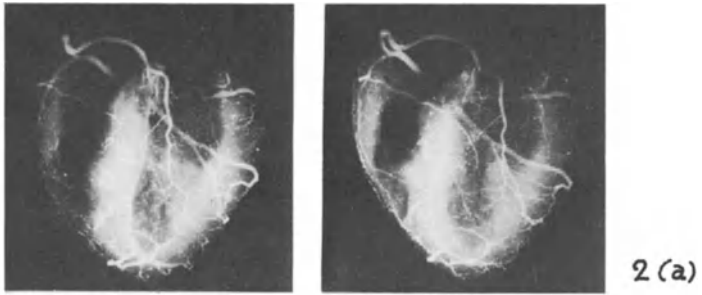dose calculations in radio-therapy.
(b) Evaluation of front and side view.

1 (b)

FIG.1 (C)

BULLE 1005 (OBEN)

1015/66

Aufriss (b)   Seitenriss (c)   Grundriss   FIG.2 (d)

FIG.3 (b)
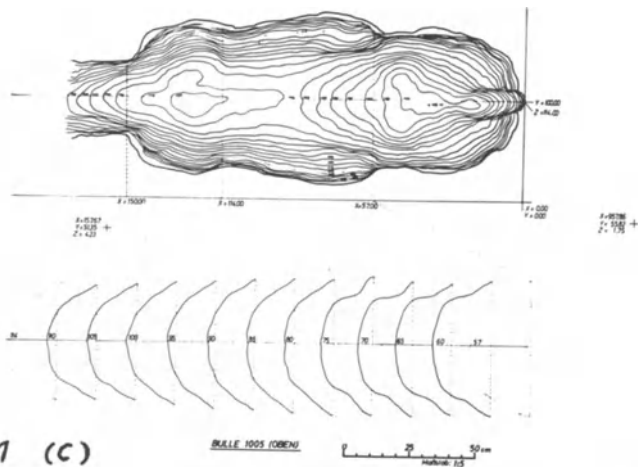
AUTOMATIC SAMPLING STAGE MICROSCOPE AND DATA PRINT-OUT UNIT

EWALD R. WEIBEL

Department of Anatomy, University of Bern, Bern

In order to facilitate and accelerate stereologic work some routine steps in the general procedure which leads from a specimen to morphometric data have been automated (1). It has been our aim to obtain a set of instruments which were (a) reliable, versatile, and thus adaptable to many problems, as well as (b) simple, more or less foolproof, and not too expensive. We thought primarly of the (research) pathologist as a potential user of these devices, since he will often have to process a relatively ample material.

1. <u>Automatic sampling stage for optical microscope.</u> Selection of microscope fields for analysis is prone to be biased unless it is performed mechanically. In this device, an electronically controlled motor-drive displaces the specimen by preset distances and thus allows systematic sampling which is random with respect to the specimen. The length of steps can be varied from 25 μ to 2 cm. A nomogram has been developed to allow proper setting of step distance controls: section size is determined by fitting of circles; with a pre-fixed number of required samples the adequate distance selector setting is directly read off. It is also possible to obtain complete section coverage with appropriate square screens. The standard settings for edge-to-edge fitting of test systems vary with magnification and are indicated on the nomogram. Complete section coverage is particularly useful in studying small objects. This stage was technically developed in collaboration with and is being manufactured by WILD HEERBRUGG INSTRUMENTS INC., Switzerland. For additional features of this instrument and illustration see R. Gander (2).

2. <u>An automatic data recorder</u> (Fig. 1) accumulates
primary classified counts in ten three-digit coun-
ters which can be coupled with either of two to-
talizers or with none. At the end of each sample
evaluation a push-button control triggers automa-
tic printing of the data onto a table; the coun-
ters are cleared for the next sample. A card pun-
cher can be fed automatically with the same data.
This unit was technically developed in collabo-
ration with FISTRONIC AG. Zürich, and is manufac-
tured by this firm.

3. <u>An adaptable general purpose computer program</u>
for varied stereologic problems has been develo-
ped by Mr. H.R. Gnägi, Bern. It will shortly be
available in FORTRAN lay-out.

This system is so conceived as to permit a step
by step build-up in order to include additional
possibilities.

<u>References:</u>
(1) E.R. Weibel: A semi-automatic system for ste-
    reologic work in light and electron micros-
    cope (this volume).
(2) R.H. Gander: A morphometric microscope with
    automatic sampling stage (this volume).
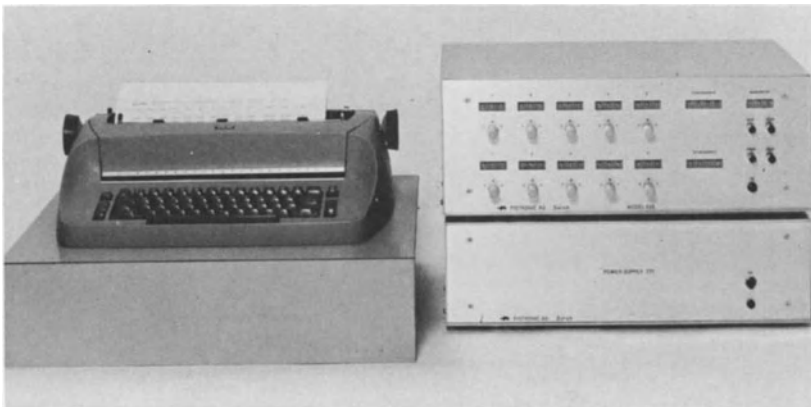

<u>Fig. 1:</u> Data accumulator and print-out unit
         (FISTRONIC)

"STEREOSCAN" SCANNING ELECTRON MICROSCOPE

FRANCO ROSSI

Engis Equipment Company, Morton Grove, Illinois

Based on principles developed by Prof. C.W. Oatley
and colleagues at the Engineering Laboratories of
Cambridge University,Cambridge,England,the Stereoscan
scanning electron microscope is commercially manufactur-
ed by Cambridge Inst.Co.,Ltd.,Cambridge,England,and is
marketed in the U.S. by Engis Equipment Co.,Morton
Grove,Ill.

The instrument consists of three basic assemblies:
1- the electron optical column with the specimen
chamber mounted on a cabinet enclosing the vacuum
system;
2- the main console housing all the electronic
controls and display units for operation;
3- the power supply racks usually located at some
distance from the main assembly.

The Stereoscan has been called the instrument which
"sees around corners" because of its very impressive
depth of focus which exceeds the depth of focus of a
light microscope of at least 300x.

Because of its versatility and virtually unlimited
applications,the Stereoscan has a unique place in both
scientific research and industrial quality control.
Moreover,it has opened new fields of investigation, such
as microelectronics.

The Stereoscan is provided with full facilities for
routine work and can be easily adapted to more
sophisticated disciplines because of its modular basis
construction with all interchangeable electronic and
electron-optical components.This permits the accomodation
of modifications,taking account of the latest develop-
ments and requirements of modern research.The chamber
itself has been built with a considerable capacity,and
access ports are furnished to accomodate extra apparatus.

The preparation required for the specimens can be
reduced to one step only:the provision of conductivity to
earth.This is accomplished by using colloidal dispersions

in the case of conductive specimens,and by coating with
metallic films non-conductive specimens.While the metal
coating furnishes the conductivity to earth,it also
enriches the coefficient of secondary emission.Coating
films of 200 Au of thickness are too thin to obscure
details,and specimens thus coated are more reliable than
replicas.

Metals used for coatings vary from specimen to
specimen.Some of them are:aluminum,gold,gold-palladium
alloy,chromium,platinum,platinum-palladium,etc.Excellent
results have been obtained using gold-carbon,and metal
oxides;for instance,uranium oxide.

The stage,which houses the collector,a wide range of
mechanical movements to permit any translation of the
specimen under observation.On a plane normal to the
optical axis,the X movement offers a translation of 16mm,
and the Y movement offers a translation of 13mm.Alomg the
optical axis the Z movement offers a translation of 15mm.
About the axis perpendicular to the beam, the tilting
movement offers a translation from 0 to 90 degrees,and
about the axis of the specimen holder the rotating move-
ment offers a continuous circular translation.

The specimens are mounted on a flat stub which plugs
into the stage,and,although there a limitation in size
of 12mm in diameter and 3mm in thickness,larger specimens
can be examined at the expense of one or more movements,
depending on the size of the specimen.

The range of magnification values obtainable which
goes from 20x to 200,000x by steps of 2,5,10 can be read
directly together with the allowance values for varia-
tions of working distance on a meter mounted on the scan
amplifier panel.The maximum useful magnification is nor-
mally between 40,000 and 50,000x,and can be better de-
pending on the specimen.It is not necessary to refocus
the image when changing from one magnification to
another.

The resolution of the Stereoscan theoretically ap-
proaches the minimum size of the electron probe,very
close to 80 Au.
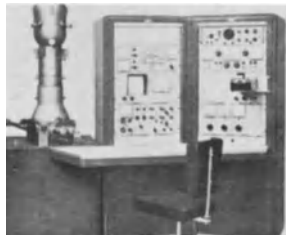
AUTHOR INDEX

A

Abrahamson, Dean E.
    279–280
Atkinson, Ralph H.
    228–230, 327

B

Bach, Günter
    174–186
Bartley, M.H.
    68–69
Blümcke, Sigurd
    112–113
Bockstiegel, G.
    193–194
Briese, Franklin W.
    133–134

C

Carpenter, Anna–Mary
    133–134, 189–190
Couderc, Henri
    304–305

D

DeHoff, Robert T.
    95–105, 119–130
Dörfler, Gerhard
    231–232, 277–278

E

Ebbesson, Sven O.
    131–132

Eichner, Dietrich
    287–288
Elias, Hans
    VII, IX, 77–78,
    149–159, 315

F

Fischer, Wolfgang M.
    70–71
Fischmeister, Hellmut F.
    263–274
Fisher, Colin
    285–286
Flinn, John E.
    110–111
Fuller, R. Buckminster
    27–29

G

Gander, Ralph H.
    289–290
Giger, Hans
    257–258
Gorenflot, Robert
    304–305
Gurland, Joseph
    250–251

H

Haug, Herbert
    66–67, 199–210
Hegre, Erling S.
    316–322

335

Hennig, August
  83-94, 259-260
Hilliard, John E.
  195-196, 211-215,
  219-227
Hires, Clara S.
  106-109

J

Janke, Helmut
  328-329
Jee, W.S.S.
  68-69

K

Kolodny, Steven
  77-78
Krieg, Wendell J.S.
  293-301
Kronsbein, J.
  252-253

L

Lazarow, Arnold
  189-190, 279-280
Leydolph, Walter K.
  65, 141-142,
  328-329
Loud, Alden V.
  72-73

M

Martino, Luigi
  139-140, 145-146
Merckx, Kenneth R.
  191-192
Millhouse, Edward W.
  302-303
Mills, Roy
  323-324

Montebello de, Roger L.
  306-307
Moore, George A.
  281-284
Morgenroth, Konrad M.
  143-144
Müller, Gerhard A.
  70-71
Myers, Edward J.
  187-188

N

Nicholson, Wesley L.
  191-192

O

Ohta, Yoshikuni
  302-303
Osborn, Jeffrey W.
  308-309

P

Pedler, Christopher M.
  310-311
Philofsky, Elliot M.
  110-111
Postlethwait, Samuel N.
  323-324
Pysh, Joseph J.
  61-62

R

Rhines, Frederick N.
  235-249
Rosenow, Ulf F.
  65, 141-142, 328-
  329
Rossi, Franco
  114-115, 332-333

S

Saltikov, Sarkis A.
  63-64
Schwartz, David
  77-78
Seamans, S.
  68-69
Smith, Cyril S.
  33-46
Steele, James H. Jr.
  74-76, 252-253

T

Tang, Douglas B.
  131-132
Targonski, S.
  68-69
Tilly, R.
  310-311

U

Underwood, Ervin E.
  49-60, 79-80

W

Weibel, Ewald R.
  15-26, 275-276, 330-
  331
Wernicke, Eckart H.
  70-71
Wolff, Joachim R.
  135-136